EXPLOITING DIVERSITY ACROSS SPACE, TIME AND FREQUENCY FOR HIGH-RATE COMMUNICATIONS

by

Jinsong Wu

A thesis submitted to the
Department of Electrical and Computer Engineering
in conformity with the requirements
for the degree of Doctor of Philosophy

Queen's University
Kingston, Ontario, Canada
September 2006

Abstract

High data-rate and high reliability are two long-term objectives in digital communications theory and practice. This thesis discusses new approaches enabling communications systems to have both high spectral efficiency and high reliability without the need of having channel state information in the transmitters.

This thesis introduces the concept and structure of linear dispersion codes (LDC). This thesis proposes and analyzes a class of rectangular information lossless linear dispersion codes, which is termed uniform linear dispersion codes (U-LDC) and can be used for 2-dimensional channels with a number of advantages.

This thesis proposes and analyzes linear dispersion coded orthogonal frequency division multiplexing (LDC-OFDM) and linear dispersion coded single carrier modulation division multiplexing (LDC-SCM) for jointly exploiting time and frequency diversity in time varying frequency selective channels. Both LDC-OFDM and LDC-SCM may be applied to both wireline and wireless communications. Lower complexity approaches, double linear transformation coded OFDM and linear transformation coded SCM, are also proposed.

This thesis proposes and analyzes high-rate diversity approaches over space, time, and frequency dimensions for MIMO-OFDM systems. The proposed coded systems

include linear dispersion space-time-frequency codes (LD-STFC), double linear dispersion space-time-frequency codes (DLD-STFC), and multiple-input multiple-output LDC-OFDM (MIMO-LDC-OFDM). This thesis introduces two diversity concepts for 3-dimensional codes: per dimension diversity order and per dimension symbol-wise diversity order, and provides a sufficient condition for DLD-STFC to achieve full symbol-wise diversity order in spite of the order of the two CDC stages. This thesis also investigates how much gain can be obtained using the combination of CDC and forward error correction (FEC) for STFC designs.

This thesis proposes coordinate-interleaving as a general principle for high-rate block-based space-time code design, i.e., space-time coordinate interleaving linear dispersion codes (ST-CILDC). This thesis shows that ST-CILDC maintains the same upper bound diversity order as the corresponding conventional ST-LDC, and ST-CILDC may double the statistical diversity order over the corresponding ST-LDC with high probability. ST-CILDC systems may show either almost doubled upper bound average diversity order or extra coding advantage in time varying channels.

Acknowledgments

I would first like to thank my advisor and mentor, Dr. Steven D. Blostein, who has provided me with excellent guidance, insight, and freedom to create. His consistent encouragement, generous support, and beneficial advice has allowed me to smoothly proceed my research progress, improve my writing skills, and develop my academic interests.

I am grateful to my other thesis committee members, Dr. Tim N. Davidson from McMaster University University, Dr. Saeed Gazor and Dr. Alois P. Freundorfer from Department of Electrical and Computer Engineering, Dr. Fady Alajaji from Department of Mathematics and Statistics, for their taking time to review my thesis and for their comments and suggestions with respect to this thesis. I would like to especially thank Dr. Tim N. Davidson for his extremely careful reading and providing detailed and sharp comments to examine and enabling me to further improve my thesis.

It has been a great pleasure for me to collaborate and discuss research with Dr. Saeed Gazor and Dr. Hamidreza Saligheh Rad during my PhD study. Sincere thanks to many bright students at Queen's, especially my colleagues in Information Processing and Communications Laboratory, for their friendship and assistance.

Finally, I would like to thank my wife, Jie Zheng, who has supported me with encouragement, love, and delicious food, my parents, who invested their whole life in

loving, caring and educating us, my younger brother, Haosun Wu, who provided me unselfish support and encouragement.

This work has been made possible by the financial sponsors of Natural Sciences and Engineering Research Council, Samsung Electronics, Bell Mobility, Communications and Information Technology Ontario, Association of Universities and Colleges of Canada through their Canadian Cable Telecommunications Research Fellowship, and Queen's University. I also would like to thank IEEE Communications Society in 2004 and Information Theory Society in 2006 for their travel awards to support my traveling to the conferences for presenting papers.

Contents

List of Tables

List of Figures

Acronyms

AEP	average error probability
AFDE	approximate frequency-domain equalization
AILL	asymptotic-information-lossless
AWGN	additive white Gaussian noise
BER	bit error rate
QPSK	quadrature phase shift keying
CDC	complex diversity coding
CCI	channel change interval
CFO	carrier frequency offsets
CI	coordinate interleaving or component interleaving
CP	cyclic prefix
CSI	channel state information
CSIT	channel state information at transmitter
DAB	digital audio broadcasting
DVB	digital video broadcasting
DFT	discrete Fourier transform
EUB	error union bound
FDE	frequency-domain equalization
FEC	forward error correction

FFT	fast Fourier transform
FTC	frequency time codes
FIR	finite impulse response
FSR	frequency synchronization rate
IDFT	inverse discrete fourier transform
IBI	inter-block interference
IFFT	inverse fast Fourier transform
i.i.d.	independent and identically-distributed
ISI	inter-symbol interference
LCP	linear constellation precoding
LDC	linear dispersion codes
LTC	linear transformation codes
LDC-OFDM	linear dispersion coded OFDM
DLT-OFDM	double linear transformation coded OFDM
LDC-SCM	linear dispersion coded single carrier modulation
LTC-SCM	linear transformation coded single carrier modulation
LD-STFC	linear dispersion space-time-frequency codes
DLD-STFC	double linear dispersion space-time-frequency codes
LS	least squares
MIMO	multiple-input multiple-output, which refers to multiple transmit multiple receive antenna based wireless communications systems
MLD	maximum-likelihood decoding
MCM	multicarrier modulation
MMSE	minimum mean-square error

OFDM	orthogonal frequency division multiplexing
OSTBC	orthogonal space time block codes
PAPR	peak-to-average power ratio
PEP	pairwise error probability
P/S	parallel-to-serial
QoS	quality of service
RS	Reed Solomon
SCM	single carrier modulation, which refers single carrier block communications in this thesis
SD	sphere decoding
SFC	space frequency codes
SINR	signal to interference plus noise ratio
SISO	single-input single-output
SNR	signal-to-noise ratio
S/P	serial-to-parallel
STC	space time codes
STFC	space-time-frequency codes
STTC	space time trellis codes
SVD	singular value decomposition
TDE	time-domain equalization
V-BLAST	vertical Bell laboratories layered space-time
ZF	zero-forcing
ZP	zero-padding

List of Important Symbols

$C^{A\times B}$	A complex matrix with dimensions $A \times B$
$\delta(x)$	Kronecker delta
$\det(\cdot)$	Determinant of a matrix
$diag(\mathbf{x})$	Diagonal matrix with diagonal entries given by $\mathbf{x}$
$\mathbb{E}\{\cdot\}$	Expectation of random variable or matrix
$\mathbb{E}_{\alpha}\{\cdot\}$	Expectation of random variable or matrix conditioned on α
$\exp(\cdot)$	Exponential function
$\mathbf{F}_M$	Denote the discrete Fourier transform (DFT) matrix representing the M-point FFT with elements, $[\mathbf{F}_M]_{a,b} = \left(1/\sqrt{M}\right)\exp(-j2\pi(a-1)(b-1)/M)$
$\mathbf{I}_K$	$K \times K$ identity matrix
$\mathrm{Im}(\cdot)$	Imaginary part of a complex number or matrix
j	Square root of -1
N_C	Number of subcarriers in one OFDM block or data symbols in one SCM block
N_T	Number of transmit antennas
N_R	Number of receive antennas
$\Pr(\cdot)$	Probability of
$\mathrm{Re}(\cdot)$	Real part of a complex number or matrix

$Tr(\cdot)$	Trace of a matrix
$vec\,(\mathbf{X})$	$vec\,(\mathbf{X}) = \left[\left[\mathbf{X}\right]_{:,1}\right]^{\mathcal{T}}, ..., \left[\left[\mathbf{X}\right]_{:,N}\right]^{\mathcal{T}}\Big]^{\mathcal{T}}$, where matrix $\mathbf{X}$ is of size $M \times N$
$\lvert x \rvert$	Absolute value (modulus) of the scalar x
$\lVert \mathbf{x} \rVert$	A norm of a vector $\mathbf{x}$
$\lVert \mathbf{x} \rVert_2$	2-norm of a vector $\mathbf{x} : \lVert \mathbf{x} \rVert_2 = (\mathbf{x}^{\mathcal{H}}\mathbf{x})^{1/2}$
$\mathbf{X} \otimes \mathbf{Y}$	Kronecker (tensor) product of matrices of $\mathbf{X}$ and $\mathbf{Y}$
$\mathbf{X} \odot \mathbf{Y}$	Hardmard product of matrices of $\mathbf{X}$ and $\mathbf{Y}$
$\mathbf{0}_{M \times N}$	Zero matrix of size $M \times N$,
$(\cdot)^{\mathcal{T}}$	Matrix or vector transpose
$(\cdot)^*$	Complex conjugate
$(\cdot)^{\mathcal{H}}$	Matrix or vector conjugate transpose
$(\cdot)^{\dagger}$	Matrix Moore-Penrose pseudo-inverse
$[\cdot]_m$	m-th entry of a vector
$[\cdot]_{m,n}$	(m, n)-th entry of a matrix
$[\cdot]_{m,:}$	m-th row of a matrix
$[\cdot]_{:,n}$	n-th column of a matrix

Chapter 1

Introduction

1.1 Critical concerns in future communications systems

1.1.1 High rate of communications

Since Shannon introduced information theory in 1948 [93], obtaining high data-rate and approaching capacity have been a long-term goal in communication system designs. In the recent decade, both wireline and wireless broadband communications have been growing at explosive rates, stimulated by a host of important high-data-rate demand applications [25, 80]. One solution to improving the spectrum efficiency is through the use of multiple antenna technology, especially multiple transmit and multiple receive antenna based multiple-input multiple-output technology (MIMO) [31, 35, 103, 120]. The core idea behind MIMO is that signals at both ends are "combined" in such a way that they create effective multiple parallel spatial data pipes (increasing therefore the data rate). Another class of spectral efficiency enabling techniques are multicarrier communications, especially orthogonal frequency division

multiplexing (OFDM) [5,14,20,48,87,115,134], which may be applied in both wireline and wireless channels. Another key issue to realize high bandwidth efficiency is to have the coding rate as high as possible [29, 70, 118].

1.1.2 High reliability of communications

There exist fundamental barriers of the communications channels, such as propagation loss, time variation, noise, interference and multi-path fading, which create difficulties in high data-rate communications. These barriers are common to the channels of either conventional SISO (single transmit and single receive element) [65, 84, 86] and SIMO (single transmit and multiple receive elements) [9, 24, 119] or newly promising MISO (multiple transmit and single receive element) [3, 11, 39, 56, 125, 128] and MIMO (multiple transmit and multiple receive elements) [31, 36, 81, 103, 120] communication systems. Compared with SISO and SIMO, on one hand, MIMO experiences more challenging channel impairments due to increasing channel dimensions. On the other hand, MIMO provides more possibilities to handle hostile channel environments. Quality of service (QoS) is important for reliability of real-time communications, such as multimedia communications. Two main performance measures of QoS are bit error probability (BER) and transmission latency (delay) [38, 50, 121].

For given signal structures and physical configurations of transmitters and receivers, such as antenna configurations, developing sophisticated receiver algorithms or channel estimation, signal estimation and detection algorithms is certainly critical in improving transmission quality, and this issue will be of consideration in this thesis. However, more important and fundamental approaches to improve transmission quality are to use proper coding and signaling structures and physical configurations of transmitters and receivers, to reach maximum reliability or diversity. Properly

designed diversity may provide desirable system performance with acceptable computational complexity.

1.2 Motivation

Diversity represents a class of techniques that exploit the random nature of independent channels to improve communication performance. In past, diversity methods for SIMO, i.e., receiver diversity methods, have been well established at both theoretical and practical levels [9, 24]. Conventional receiver diversity, such as maximal ratio combining, equal gain combining, and selection combining, utilize multiple paths of multiple receiver antennas [9, 24]. In recent years, the research community has become increasingly interested in diversity methods for multiple transmit antenna systems [3, 32, 33, 39, 102, 127]. A thorough discussion and overview on the impact of spatial diversity in wireless networks can be found in [19].

Although it has been noticed that several research efforts have been related to designing diversity approaches using channel state information (CSI) available at transmitters [45,91,133], this thesis will solely consider communication systems, where CSI is only available at receivers and not at transmitters. Although physical structures, such as MIMO and OFDM, provide high capacity potential, the capacity cannot be achieved without proper error protection methods due to independent parallel fading channels [6, 31, 68, 72, 103]. Transmit diversity approaches are primarily considered to achieve high reliability communications in this thesis. There are various types of diversity used in communication systems over fading channels, such as space diversity [3,39,102], frequency diversity [72], time diversity [63], polarization diversity [67], and multipath diversity [61]. In this thesis, diversity is generally defined as

Definition 1 *Diversity is a kind of mechanism by which information data in communications channels may exploit statistical independent randomness over one or more physical dimensions to improve communications reliability.*

Note that Diggavi et. al. generally defined diversity as the method of conveying information through multiple independent instantiations of these random attenuations [19]. The difference between Definition 1 and the definition of Diggavi is that Definition 1 emphasizes the "one or more physical dimensions", which reflects not only the effects of statistical nature of one random variable but also the joint effects of statistical nature of multiple random variables. Note that multiple random dimensions may come from not only a single user but also multiple users. Recently, diversity is discussed in an information theory perspective, and two relations,

1) diversity and multiplexing tradeoff [132],

2) throughput and reliability tradeoff [4],

are discussed.

In [132], the authors in the earlier part of the paper claimed that their definition of diversity gain is based on actual error probability of the code. However, from their whole analysis [4, 132], it is clear that their definition of diversity gain is actually based on outage probability of capacity instead of actual error probability in system performance. This is the difference between the definition in [4,132] and the definition in this thesis. The concept of diversity in [4, 132] is in the context of a capacity limit. However, The concept of diversity in this thesis is in context of actual system performance under available diversity freedom in physical dimensions. Note that is is not clear whether or not the slope of outage capacity curve is equal to the available diversity freedom in physical dimensions over any SNR regions.

Definition 1 is the basis of new diversity proposals contained this thesis. Conventionally, communications reliability is achieved at transmitters using forward error correction with the sacrifice of bandwidth efficiency [29, 70, 118]. The central concern in this thesis is how to obtain desirable diversity performance with high bandwidth efficiency. Unlike traditional SIMO diversity, MIMO systems provide many more new possibilities to utilize physical dimensions, which motivate more profound and effective approaches to realize communications with both high data rates and desirable communications quality.

1.3 Thesis overview

This thesis investigates the transmit diversity approaches for SISO and MIMO communications. The following introduces the basic organization of this thesis.

Chapter 2 introduces related background, including fading channels, performance measures, multicarrier and space-time MIMO communications, and a tight bound for performance analysis of transmit diversity. Chapter 3 introduces the definition, matrix formulation and decoding of linear dispersion codes (LDC). Chapter 3 also provides the definition of symbol coding rate of LDC.

In Chapter 4, a new class of rate-one rectangular LDC dispersion codes of arbitrary size, uniform linear dispersion codes (U-LDC), are proposed, and their properties are analyzed. It is shown that U-LDC are capacity-optimal and satisfy sub-optimal constraints for rapid fading channels, which ensures that U-LDC based systems approximately minimize an error union bound, as well as meet a traceless minimal non-orthogonality criterion. The encoding matrix of U-LDC is unitary. Thus, U-LDC are suitable for multi-stage receiver designs and can be efficiently applied across

space-time-frequency dimensions. Although U-LDC may not attain full diversity, it is shown that U-LDC achieve maximal symbolwise diversity order.

In Chapters 5 and 6, the scenarios considered are single input single output (SISO) communications in frequency selective channels. In Chapter 5, LDC across time and frequency are proposed to improve the performance of orthogonal frequency division multiplexing (OFDM), known as LDC-OFDM, while, in Chapter 6, LDC are proposed to support high-rate joint frequency and time diversity for SISO block transmission, known as LDC-SCM. To overcome the requirement of constant channel gains over an entire LDC time interval, a new decoding strategy, called two-step-estimation (TSE) is proposed. In the TSE procedure, the receiver first estimates the multiple LDC codewords, and second decodes multiple LDC codewords individually. With the advantage of layered processing, TSE procedure is applied to both LDC-OFDM and LDC-SCM. The design criterion of full diversity frequency-time block design for LDC-OFDM and LDC-SCM are discussed in Chapters 5 and 6, respectively. Chapter 5 shows that rate-one LDC-OFDM outperforms uncoded OFDM without increasing the peak-to-average power ratio (PAPR). Through simulations, Chapter 5 investigates two performance related factors: (1) imperfect channel estimation for LDC cyclic-prefix OFDM (LDC-CP-OFDM), (2) low complexity receiver for LDC zero-padding OFDM (LDC-ZP-OFDM). Chapter 6 shows that LDC-CP-SCM may outperform CP-SCM even under carrier frequency offset (CFO) effects. Chapter 6 shows that LDC zero-padding SCM (LDC-ZP-SCM) can be effectively employed with low-complexity minimum mean-squared error (MMSE) equalizers.

In Chapters 7 and 8, the scenarios considered are multiple antenna based MIMO-OFDM communications in frequency selective channels. In Chapter 7, two new

classes of high-rate space, time, and frequency codes (STFC) are proposed, linear dispersion space-time-frequency Codes (LD-STFC) and double linear dispersion space-time-frequency codes (DLD-STFC). DLD-STFC is compared with an extension of a recently proposed LDC-OFDM to MIMO systems, called MIMO-LDC-OFDM. Chapters 7 analyzes diversity properties of STF block based designs under arbitrary channel correlation. Based on error union bound analysis, Chapter 7 discuss new LDC code design criteria for complex input symbols. Using the general terms of complex diversity coding (CDC) and channel codes, Chapter 8 proposes to generally classify STFC into seven categories. Chapter 8 investigates two issues related to the performance improvement of high-rate STFCs. First, Chapter 8 shows that the two CDC stages of DLD-STFC can be exchanged. Chapter 8 introduces two diversity concepts for 3-dimensional codes: per dimension diversity order and per dimension symbol-wise diversity order, and provides a sufficient condition for DLD-STFC to achieve full symbol-wise diversity order in spite of the sequence of the two CDC stages. Second, Chapter 8 investigates how much gain can be obtained using the combination of CDC and forward error correction (FEC) for STFC designs.

In Chapter 9, the scenario considered is multiple antenna based MIMO communications in flat fading channels. The coordinate-interleaving or component interleaving is originally proposed as an alternative to bit interleaving for SISO communications. Chapter 9 proposes a general coordinate-interleaving method for block-based space-time codes or linear dispersion codes, called space-time coordinate interleaving linear dispersion codes (ST-CILDC), which enables not only symbol-level diversity but also coordinate-level diversity for high-rate block-based space-time code design. Chapter 9 shows that ST-CILDC maintains the same upper bound diversity order as the

corresponding conventional ST-LDC, and ST-CILDC may double the statistical diversity order over the corresponding ST-LDC with high probability. Compared with conventional ST-LDC systems, ST-CILDC systems may show either almost doubled average diversity order or extra coding advantage in time varying channels. With trivial extra complexity over ST-LDC systems, ST-CILDC systems maintain the diversity performance in quasi-static block fading channels, and significantly improve the diversity performance in rapid fading channels.

1.4 Summary of contributions

The primary contributions of this thesis are summarized as follows.

1) A new class of rate-one rectangular LDC dispersion codes of arbitrary 2-D matrix sizes, uniform linear dispersion codes (U-LDC), are proposed, and the properties of these codes are analyzed.

2) LDC-OFDM are proposed to improve the time-frequency diversity performance of OFDM, while, LDC-SCM are proposed to primarily support time diversity for single stream SCM block transmission. Both LDC-OFDM and LDC-SCM allow all arbitrary symbol rates, and highest symbol rates are one, i.e., without symbol-rate loss. The proposed two-step-estimation (TSE) enables both LDC-OFDM and LDC-SCM to have a layered structure and allow channel gains to vary over different channel uses. Design criteria of full joint frequency-time diversity block design for both LDC-OFDM and LDC-SCM are offered. Double linear transformation coded OFDM (DLT-OFDM) and linear transformation coded SCM (LTC-SCM) are proposed as low complexity designs of LDC-OFDM and LDC-SCM, respectively.

3) Two new classes of high-rate STFC, LD-STFC and DLD-STFC, are proposed. DLD-STFC systems, based on flexible three-layer structure with reduced complexity, show superior performance. Diversity properties of STF block based designs are analyzed under arbitrary channel correlation. An error union bound (EUB) analysis provides more specific LDC code design criteria for complex input sequences. This thesis introduces two new diversity concepts for 3-dimensional codes: per dimension diversity order and per dimension symbol-wise diversity order, and provides a sufficient condition for DLD-STFC to achieve full symbol-wise diversity order in spite of the sequence of the two complex diversity coding (CDC) stages. Through simulations, this thesis shows that STFC based on the combination of CDC and FEC may outperform STFC purely based on FEC, and STFCs based on the combination of DLD-STFC and FEC outperform STFC based on the combination of one 2-dimensional CDC and FEC, especially in spatially correlated channels. Further, the choice of mapping from FEC to DLD-STFC may significantly impact system performance.

4) This thesis proposes a general coordinate-interleaving method for block-based space-time codes or linear dispersion codes, called space-time coordinate interleaving linear dispersion codes (ST-CILDC), which enables not only symbol-level diversity but also coordinate-level diversity for high rate block-based space-time code design. This thesis introduces two new diversity concepts, statistical diversity order and average diversity order. Compared with conventional ST-LDC systems, ST-CILDC systems may show either almost doubled average diversity order or extra coding advantage in time varying channels.

Chapter 2

Background

2.1 Fading channels

2.1.1 Fading classification

Fading is a process of random fluctuations of the signal level due to channel environments between signal transmitter and receiver. Time-variation is the most important feature of fading. There are two sources of signal attenuation, modeled through the time-varying channel impulse response [65, 84, 86].

1) Large scale fading

   a. Propagation path loss - This is determined by the distance between the transmitter and the receiver, whose randomness is only due to the position of the mobile terminal. The channel changes due to path loss are very limited for practical systems over time intervals of interest.

   b. Shadowing - This incurs due to the presence of obstacles in the signal path and due to the relative position of the mobile unit with respect to the base station. The channel changes due to path loss can be expressed as a slow

process and is commonly modeled using log-normal statistics.

2) Small-scale fading is rapid fluctuation of the amplitude of a signal over a short period of time or travel distance, caused by constructive and destructive interference between two or more versions of the same signal. Small-scale fading may be corrected by adaptive equalizers or by robust modulation and error correction. The main causes of small-scale fading are the mobile moving with surrounding scattering and the existence of several propagation paths between transmitter and receiver. Two manifestations of channel time variations are delay spread and Doppler-frequency spread. A fading-channel classification can be based on these two parameters.

   a. Delay spread : The multipath signals with different delays combine to produce a distorted version of the transmitted signal. To describe it by a single constant, a delay spread is defined as the difference between the largest and the smallest among these delays. This delay spread could result in time dispersion and frequency-selective fading.

   b. Doppler spread : When the receiver and the transmitter are in the constant relative speed of the motion, the received signal is subject to a constant frequency shift (the Doppler shift) proportional to this speed and to the carrier frequency. This Doppler effect, along with multipath propagation, causes frequency dispersion and time-selective fading.

2.1.2 Simple time varying model

To simplify the simulations, this thesis uses simple time varying models to approximate time varying fading channels. The channels are assumed to be constant over

different integer numbers of channel uses, and independent identically-distributed (i.i.d.) between blocks. We term this integer number of the intervals as the channel change interval (CCI). The definition of one channel use is different for the different channel models employed in this thesis.

1) For OFDM block communications, one channel use is referred to as one OFDM block.

2) For singe carrier modulation (SCM) block communications as discussed in Chapter 6, one channel use is referred to as one SCM block.

3) For space time codes in flat fading channels as discussed in Chapter 9, one channel use is referred to as one channel symbol over one symbol time slot.

The following lists several remarks for these simple models.

1) These simple models are used only in simulations. In all the diversity analysis, channel correlation is assumed to be arbitrary across space, time, and frequency dimensions

2) These simple models, which are suitable for testing performance for code design in rapid fading channels, are extensively used in the literature.

3) Even if channel initiations over short time periods are not i.i.d, channels symbols within a codeword can be interleaved over a long period, so that channel coefficients can be approximately considered as i.i.d.

In the majority of this thesis, frequency selective channels are considered. When the frequency selective channel models choose exponential power delay profile, the rate of decay is set to 1.

In digital transmission over frequency-selective Rayleigh fading, the channel may be simply modeled with a tapped-delay-line [21]. The outputs of the different taps are generated by a flat Rayleigh fading simulator, are combined by weighted gains. This information is in the form of the delay and the attenuation associated to each of these taps. In correlated frequency-selective channels, it is important to recognize that in a scenario of multi-path delays, the gains for the different delays are independent from one another [21]. Rather, the dependency among different channel gains comes from the correlation among corresponding tap-gains on different channels. This way, the correlation coefficient between each pair of tap-gains could be modeled to be the same.

Note that, although this thesis assumes multiple taps of the same transmit and receive path to be uncorrelated, non-zero spatial correlation are considered in the simulations of quite a few diversity approaches.

2.2 Performance measures

This thesis considers the communications quality. Quality of service (QoS) is critical concern for real-time communications, such as multimedia communications. Two main performance measures are error probability and transmission latency (delay). This section summarizes several important performance measures, which may not include all the performance measures used in this thesis. However, a majority of them are introduced here and the rest will be detailed in the later chapters. The error measure can be in units of bits, symbols (which may embrace multiple bits), and blocks or framess (which may embrace multiple symbols).

2.2.1 Exact average error probability

Exact average error probabilities reflect the actual performance of communications systems in given channels. The average bit [117], symbol [77], and block error probability at the average SNR $\overline{\gamma}$ are, respectively, given by

1)

$$P_s(\overline{\gamma}) = \int_0^\infty P_s(\gamma) p(\gamma|\overline{\gamma}) d\gamma, \tag{2.1}$$

2)

$$P_b(\overline{\gamma}) = \int_0^\infty P_b(\gamma) p(\gamma|\overline{\gamma}) d\gamma, \tag{2.2}$$

3)

$$P_\Omega(\overline{\gamma}) = \int_0^\infty P_\Omega(\gamma) p(\gamma|\overline{\gamma}) d\gamma, \tag{2.3}$$

where γ is the instantaneous SNR at the receiver, $P_b(\gamma)$, $P_s(\gamma)$, and $P_\Omega(\gamma)$ are the instantaneous bit, symbol, and block error probability, and $p(\gamma|\overline{\gamma})$ is the probability density function of γ at the average SNR $\overline{\gamma}$.

2.2.2 Error union bound

The error union bound (EUB), an upper bound on the average error probability, is an average of the pairwise error probabilities between all pairs of codewords. The EUB is related to the union of events via

$$\Pr\left(A_1 \cup ..., A_N\right) \leqslant \sum_{a=1}^{N} \Pr\left(A_a\right).$$

This thesis mainly considers block based communications. The bit [27], symbol, and block [88] based EUB for block based communications are respectively given by

1)

$$\mathrm{P}_b \leqslant \frac{1}{N_X^{(b)}} \sum_{a=1}^{N} \sum_{c \neq a}^{N} \phi_b(X_a, X_c) \Pr(X_a) \Pr(X_a \to X_c), \tag{2.4}$$

2)

$$\mathrm{P}_s \leqslant \frac{1}{N_X^{(s)}} \sum_{a=1}^{N} \sum_{c \neq a}^{N} \phi_s(X_a, X_c) \Pr(X_a) \Pr(X_a \to X_c), \tag{2.5}$$

3)

$$\mathrm{P}_\Omega \leqslant \sum_{a=1}^{N} \sum_{c \neq a}^{N} \Pr(X_a) \Pr(X_a \to X_c), \tag{2.6}$$

where $\Pr(X_a)$ is the a priori probability that the block X_a was transmitted, $\Pr(X_a \to X_c)$ is the probability that receiver decides X_c when X_a is actually transmitted, $\phi_b(X_a, X_c)$ and $\phi_s(X_a, X_c)$ are the number of bit and symbol errors, respectively, occurring when X_a is transmitted and X_c is chosen by the decoder, $N_X^{(b)}$ is the total number of bits per X block, $N_X^{(s)}$ is the total number of symbols per X block, and N is the code book size of the block.

2.2.3 Signal to interference plus noise ratio (SINR)

SINR is an alternative performance measure to signal to noise ratio at communication receivers under the impact of interference. In this thesis, the SINR is referred to the decision SINR at receivers.

The instantaneous decision SINR at the instantaneous SNR γ under the average SNR $\overline{\gamma}$ can be defined by

$$SINR(\gamma|\overline{\gamma}) = \frac{\|c_s(\gamma|\overline{\gamma})\|^2}{\|c_i(\gamma|\overline{\gamma})\|^2 + \|c_n(\gamma|\overline{\gamma})\|^2}, \tag{2.7}$$

where $c_s(\gamma|\overline{\gamma})$, $c_i(\gamma|\overline{\gamma})$, and $c_n(\gamma|\overline{\gamma})$ are the elements at the instantaneous SNR γ under the average SNR $\overline{\gamma}$ referred to complex source, interference, and noise signals, respectively.

The average decision SINR can be defined by

$$SINR(\overline{\gamma}) = \int_0^\infty SINR(\gamma|\overline{\gamma})\, p(\gamma|\overline{\gamma})\, d\gamma, \tag{2.8}$$

where $p(\gamma|\overline{\gamma})$ is the probability density function of the SNR γ under the average SNR $\overline{\gamma}$.

2.3 Multicarrier and space-time MIMO communications

2.3.1 Multicarrier (OFDM) communications

2.3.1.1 Introduction

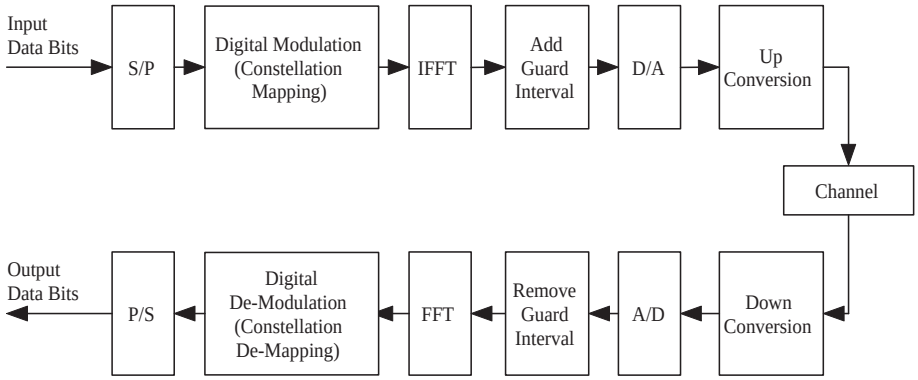

Figure 2.1. OFDM system model

Multicarrier modulation (MCM) [12], usually realized as orthogonal frequency division multiplexing (OFDM), is a powerful modulation technique that has two key

features. In OFDM, as shown in Figure 2.1, the transmitter first converts the input data from a serial to parallel streams or data sets. Each set of data contains one symbol for each sub-carrier. Before performing the Inverse Fast Fourier Transform (IFFT), this example data set is arranged on the horizontal axis in the frequency domain. An inverse Fourier transform converts the frequency domain data set into samples of the corresponding time domain representation of this data, and a cyclic-prefix is added to the transmitted OFDM block. Then, the parallel to serial block creates the OFDM signal by sequentially outputting the time domain samples. The receiver performs the inverse of the transmitter. First, the OFDM data are split from a serial stream into parallel sets, and the a cyclic-prefix is removed from the received OFDM block. The Fast Fourier Transform (FFT) converts the time domain samples back into a frequency domain representation. The magnitudes of the frequency components correspond to the original data. Finally, the parallel to serial block converts this parallel data into a serial stream to recover the original input data.

In OFDM, each subchannel can be assumed to be flat and the intersymbol interference is negligible due to the channel partitioning of the transmission bandwidth into many narrowband subchannels if the inter-block interferences (IBI) are combated by using enough long guard interval and channel coefficients are constant over one OFDM block. In general, MCM methods are especially suitable to data transmission in the channels with moderate or severe ISI. A key feature of MCM is the possibility to maximize the mutual information [15] between transmitter and receiver due to the possibility of adaptive spectral shaping, also called adaptive loading, at the transmitter. Although MCM has been successfully employed in the form of discrete multi-tone in wireline communications, several performance issues arise in wireless systems. In

particular, the practical implementation of spectral shaping at the transmitter is difficult because of the time-varying nature of cellular channels, which makes channel estimation very inaccurate. Also, wireless channels with Rayleigh fading experience very-low signal-to-noise ratio (SNR) at least over a fraction of the transmitted time for some subchannels. This means that the information transmitted in these subbands will be lost. A technique to mitigate this is through the use of error-correcting codes across all subchannels.

2.3.1.2 PAPR problem

The complex envelope of the OFDM signal, consisting of N_C carriers is given [78] by

$$S_{total}(t) = \sum_{k=-\infty}^{\infty} \sum_{n=0}^{N_C-1} a_{n,k}.g(t-kT)e^{jn\frac{2\pi}{T}t}, \tag{2.9}$$

where $g(t)$ is rectangular pulse of duration T and T is OFDM symbol duration. The peak to average power ratio (PAPR) is defined by

$$PAPR = \frac{\max\limits_{t\in[0,T]} |S(t)|^2}{\mathbb{E}\left\{|S(t)|^2\right\}}. \tag{2.10}$$

The PAPR for a discrete-time OFDM signal $x_n[k]$ is defined in a time interval [n, n+N-1] by the following formula:

$$PAPR = \frac{\max\limits_{k} |x_n[k]|^2}{E\left\{|x_n[k]|^2\right\}}. \tag{2.11}$$

In OFDM, PAPR increases with N_C [41], while single-carrier modulations usually avoids the high PAPR problem associated with multi-carrier schemes, which results in the requirement of larger linear range of RF amplifiers. Lowering PAPR enables cheaper and more efficient power amplifiers may be used. The amplitude of a multicarrier signal has a Rayleigh distribution, while the power distribution becomes a

central chi-square distribution with two degrees of freedom. The cumulative distribution function (CDF) of the amplitude, $z \geqslant 0$, of a signal sample is given by [41]

$$\mathcal{F}(z) = 1 - \exp(-z). \tag{2.12}$$

Assuming the samples to be mutually uncorrelated, the complementary cumulative distribution function for the peak power per OFDM symbol or OFDM block is given by [41]

$$\Pr(PAPR > z) = 1 - (1 - \exp(-z))^{N_C}, \tag{2.13}$$

From (2.13), it is seen that large PAPR is possible but occurs only infrequently.

2.3.2 Space-time MIMO communications

2.3.2.1 Introduction

When multiple antenna elements are also added on both sides of an antenna system to form a MIMO (N_T input antennas, N_R output antennas) link, the conventional diversity benefits of smart antennas may be still retained. However, MIMO links offer additional advantages that go far beyond those of smart antennas. Multiple antennas at both the transmitter and the receiver create a matrix channel (of size equal to the product of the number of receive antennas and the number of transmit antennas). One of the key advantages of MIMO lies in the ability to transmit different data over several spatial modes of the matrix channel within the same time-frequency slot. The benefits that space-time processing and especially MIMO systems can provide to wireless communications are enormous: improved data-rate throughout the cell, increased coverage area and improved network capacity.

2.3.2.2 MIMO capacity

A space time MIMO system with N_T transmit antennas and N_R transmit antennas is modeled as

$$\mathbf{r} = \sqrt{\frac{SNR}{N_T}}\mathbf{H}\mathbf{s} + \mathbf{n}, \tag{2.14}$$

where source signal vector is $\mathbf{s} \in C^{N_T}$, the received signal vector $\mathbf{r} \in C^{N_R}$, MIMO flat fading channel matrix $\mathbf{H} \in C^{N_R \times N_T}$, complex Gaussian noise vector $\mathbf{n} \in C^{N_R}$.

Let $\mathbf{R}_s$ denote the covariance matrix of $\mathbf{s}$, then the capacity of the system 2.14 is given by [103]

$$C = \log_2 \left(\det \left(\mathbf{I}_{N_R} + \mathbf{H}\mathbf{R}_s\mathbf{H}^{\mathcal{H}} \right) \right). \tag{2.15}$$

2.3.2.3 Spatial multiplexing

Spatial multiplexing (SM) techniques [30] use MIMO channels to provide parallel spatial channels, if the path gains between individual transmit-receive antenna pair fade independently, the channel matrix is well-conditioned with high probability. V-BLAST [30, 120], one of effective spatial multiplexing algorithms, implements Zero Forcing (ZF) detection combined with symbol cancelation to improve the performance [35]. SM combines the signals from all the receive antennas simultaneously, first extracting the strongest sub-stream from the received signals, then proceeding with the remaining weaker signals, which are easier to recover once the strongest signals have been removed as a source of interference. When symbol cancelation is used, the order in which the sub-streams are detected becomes important for the overall performance of the system. In fact, the transmitted symbol with the smallest post-detection SNR will dominate the error performance of the system. Post detection SNR

is determined by ordering. An optimal ordering is based on choosing the best post-detection SNR at each stage of the detection process and leads to the maximization of the worst SNR over all possible orderings.

2.3.2.4 Spatial coding

Spatial coding permits the efficiently use of correlation in space , time, and/or frequency among transmitted signals to improve information protection while the goal of SM is to increase data rate. One of important advantages of spatial coding is that channel state information is not required at transmitters. The most well-known space time coding techniques are space time trellis codes (STTC) [102] and orthogonal space time block codes (OSTBC) [3, 101]. STTC transmits one input symbol at a time, producing a sequence of vector symbols whose length represents antennas. STTC provides both coding gain and full diversity gain, which will be defined in Section 2.4.1. The design of STTC is difficult and, and the main disadvantage of it is to generally require very high complexity encoders and decoders [102].

OSTBC [3, 101] operates on a block of input symbols, producing a matrix output whose columns represent time and rows represent antennas. The main desirable trait of OSTBC is the provision of full diversity with a very simple decoding scheme. The disadvantage of OSTBC is that

1) it does not generally provide coding gain, unless concatenated with an outer code,

2) it cannot reach capacity if $\min\{N_T, N_R\} \geqslant 2$.

By employing space-time coding concepts in OFDM-based broadband systems, space-frequency coding was investigated through coding across OFDM tones [7].

Bolcskei and Paulraj found that space-time codes designed to achieve full spatial diversity in the narrowband case will in general not achieve full space-frequency diversity. In addition these authors point out that the Alamouti scheme across tones fails to exploit frequency diversity [7].

In recent years, to achieve rate close to capacity, quite a few high-rate (generally non-orthogonal) space time code designs have appeared [16, 42, 76, 129], where high complexity maximum likelihood decoding and sphere decoding (SD) are primarily considered. Maximum likelihood decoding/detection (MLD) of digital messages in general requires joint detection of an entire block of symbols [57]. MLD can be implemented efficiently, such as using the Viterbi algorithm, only for the problems of certain structure. In general, however, when no exploitable structure is at hand, MLD is very computationally intensive. This kind of hard problem with exponential complexity also occurs in optimal multiuser detection of code division multiple access systems [112]. Consequently, there has recently been a growing interest in sphere decoding for ML detection in digital communications [113]. Sphere decoding, or the Fincke-Pohst algorithm [17, 113], offers large reductions in average computational complexity for the class of computationally hard combinatorial problems in MLD. In [28], it is shown that the complexity of sphere decoding, under certain assumptions, is polynomial in the problem size, meaning that there is a polynomial function that bounds the problem size. The assumptions in [28] were, however, made in another context and are not generally applicable to the ML detection problem encountered in digital communications [44]. As shown in [44], the expected complexity of the sphere decoder is dependent both on the size and the signal-to-noise ratio (SNR). On the other hand, the worst case complexity of SD is exponential.

2.4 Diversity gain (advantage or order), coding gain (advantage or order), and multiplexing gain

2.4.1 PEP based definitions

We model a flat-fading MIMO channel as one when the channel matrix contains i.i.d. Gaussian elements. Note that the following discussions can be easily generalized for correlated fading, and other fading distributions.

The MIMO system can be modeled as

$$\mathbf{y}(k) = \mathbf{H}(k)\mathbf{x}(k) + \mathbf{z}(k), \tag{2.16}$$

where transmit signal vector is $\mathbf{x}(k) \in C^{N_T}$, MIMO channel matrix is $\mathbf{H}(k) \in C^{N_R \times N_T}$, complex Gaussian noise vector is $\mathbf{z}(k) \in C^{N_R}$, and receive signal vector is $\mathbf{y}(k) \in C^{N_R}$.

Consider a codeword sequence $\mathbf{x} = \left[[\mathbf{x}(0)]^{\mathcal{T}}, ..., [\mathbf{x}(N-1)]^{\mathcal{T}}\right]$, where $\mathbf{x}(k) = [\mathbf{x}_1(k), ..., \mathbf{x}_{N_T}(k)]^{\mathcal{T}}$ as defined in (2.16). In the case when the receiver has perfect channel state information, the pairwise error probability (PEP), $\Pr(\mathbf{c} \to \mathbf{e})$, between two codeword sequences $\mathbf{x}$ and $\mathbf{e}$ can be bounded as follows [102].:

$$\Pr(\mathbf{x} \to \mathbf{e}) \leqslant \prod_{a=1}^{N_R} \left(\prod_{b=1}^{N_T} \frac{1}{1 + \frac{E_s}{4N_0}\lambda_b} \exp\left(\frac{K_{a,b}\frac{E_s}{4N_0}\lambda_b}{1 + \frac{E_s}{4N_0}\lambda_b} \right) \right), \tag{2.17}$$

where $K_{a,b}$ is the Ricean coefficient, P is transmit power constraint, $E_s = P/N_T$ is the power per transmitted symbol, λ_b are the eigenvalues of the matrix $\mathbf{A}(\mathbf{x}, \mathbf{e}) =$

$[\mathbf{B}(\mathbf{x},\mathbf{e})]^{\mathcal{H}}\mathbf{B}(\mathbf{x},\mathbf{e})$, and

$$\mathbf{B}(\mathbf{x},\mathbf{e}) = \begin{bmatrix} \mathbf{x}_1(0)-\mathbf{e}_1(0) & \cdots & \mathbf{x}_{N_T}(0)-\mathbf{e}_{N_T}(0) \\ \vdots & \ddots & \vdots \\ \mathbf{x}_1(N-1)-\mathbf{e}_1(N-1) & \cdots & \mathbf{x}_{N_T}(N-1)-\mathbf{e}_{N_T}(N-1) \end{bmatrix}.$$

For the Rayleigh fading channel, PEP can be bounded by [102]

$$\Pr(\mathbf{x}\to\mathbf{e}) \leqslant \left(\prod_{b=1}^{N_T}\left(1+\frac{E_s}{4N_0}\lambda_b\right)\right)^{-N_R}. \tag{2.18}$$

If q denotes the rank of $\mathbf{A}(\mathbf{x},\mathbf{e})$, (i.e., the number of nonzero eigenvalues) then we can bound (2.18) as [102]

$$\Pr(\mathbf{x}\to\mathbf{e}) \leqslant \left(\prod_{b=1}^{N_T}\lambda_b\right)^{-N_R}\left(\frac{E_s}{4N_0}\lambda_b\right)^{-qN_R}. \tag{2.19}$$

The diversity advantage (gain or order) based on PEP is the power of SNR in the denominator in (2.19) [102]. The coding advantage (gain) based on PEP is an approximate measure of the gain over an uncoded system operating with the same advantage [102].

Full diversity can be defined in different contexts throughout this thesis. In the context of rank based diversity order, full diversity code is achieved if rank of $\mathbf{A}(\mathbf{x},\mathbf{e})$ is full rank over any possible codeword pair $\mathbf{x}$ and $\mathbf{e}$.

2.4.2 Definitions based on infinite SNR

The ergodic capacity (b/s/Hz) of the MIMO channel,

$$C(SNR) = \mathbb{E}\left\{\log\det\left(\mathbf{I}+\frac{SNR}{N_T}\mathbf{H}\left[\mathbf{H}\right]^{\mathcal{H}}\right)\right\}. \tag{2.20}$$

Consider a scheme as a family of codes $\{C(SNR)\}$ of block length l. Let $R(SNR)$ (b/symbol) be the rate of the code $\{C(SNR)\}$, and let the average error probability of

the code system be $P_e(SNR)$. The following are the definitions of spatial multiplexing gain and diversity gain based on asymptotically high SNR [4, 132].

Definition 2 *A coding scheme* $\{C(SNR)\}$ *is said to achieve spatial multiplexing gain* r *and diversity gain* d*, respectively, if*

$$\lim_{SNR\to\infty} \frac{R(SNR)}{\log SNR} = r \tag{2.21}$$

and

$$\lim_{SNR\to\infty} \frac{\log P_e(SNR)}{\log SNR} = -d. \tag{2.22}$$

2.5 Design criteria of linear block based space time codes

This thesis mainly focuses on block based codes. Relevant background on several design criteria of linear block based space time codes is introduced here. Note that orthogonality may have to be sacrificed to obtain high rate block based space time codes. The code matrix can be expanded as

$$\mathbf{C} = \sum_{k=1}^{K} \mathbf{C}_k(z_k), \tag{2.23}$$

where $\mathbf{C}_k(z_k)$ are K matrices of dimension $T \times N_T$ that are linear functions of the individual symbols z_k and their complex conjugates. The Hermitian square of

$$\mathbf{C}^{\mathcal{H}}\mathbf{C} = \sum_{k=1}^{K} \mathbf{C}_k^{\mathcal{H}}\mathbf{C}_k + \sum_{i<k} \left(\mathbf{C}_i^{\mathcal{H}}\mathbf{C}_k + \mathbf{C}_k^{\mathcal{H}}\mathbf{C}_i\right). \tag{2.24}$$

2.5.1 Rank, determinant, and trace

In the literature, design criteria for space-time codes was based on the codeword difference matrix $\mathbf{D}^{(ce)} = \mathbf{C}^{(c)} - \mathbf{C}^{(e)}$. Minimizing the pairwise error probability of

deciding in favor of $\mathbf{C}^{(c)}$ when transmitting $\mathbf{C}^{(e)}$ leads to the well known rank [39] and determinant [102] criteria. Ionescu introduces a trace criterion [51], which is less well-known but important for designing non-orthogonal space-time block codes.

Criterion 1 *[51] In Rayleigh fading, C should be optimally designed so that the eigenvalues of* $\left[\mathbf{D}^{(ce)}\right]^{\mathcal{H}}\mathbf{D}^{(ce)}$ *are as close as possible to each other and to* $\frac{Tr\ \left[\mathbf{D}^{(ce)}\right]^{\mathcal{H}}\mathbf{D}^{(ce)}}{N_T}$, *and for which the row-wise sum of the absolute values of the elements off the main diagonal is as small as possible. Moreover,* $Tr\left(\left[\mathbf{D}^{(ce)}\right]^{\mathcal{H}}\mathbf{D}^{(ce)}\right)$ *plays the role of Euclidean distance between codeword pairs.*

In the context of the linearity of the codes, the codeword difference matrix is linear in the symbol differences $\Delta_k = z_k^{(c)} - z_k^{(e)}$,

$$\mathbf{D}^{(ce)} = \sum_{k=1}^{K} \mathbf{C}_k(\Delta_k) \equiv \sum_{k=1}^{K} \mathbf{D}_k. \tag{2.25}$$

Thus, $\mathbf{D}^{(ce)}$ is a linear combination of the matrices $\mathbf{D}_k = \mathbf{C}_k(\Delta_k)$ on k. The distance matrix (the Hermitian square of the codeword difference matrix), is given by

$$\left[\mathbf{D}^{(ce)}\right]^{\mathcal{H}}\mathbf{D}^{(ce)} = \mathcal{D} + \mathcal{N}, \tag{2.26}$$

where

$$\mathcal{D} = \sum_{k=1}^{K} \left(|\Delta_k|^2\, \mathbf{D}_k^{\mathcal{H}}\mathbf{D}_k\right)$$

and

$$\mathcal{N} = \sum_{i<k} \left(\mathbf{D}_i^{\mathcal{H}}\mathbf{D}_k + \mathbf{D}_k^{\mathcal{H}}\mathbf{D}_i\right).$$

2.5.2 Minimal non-orthogonality

The principle of minimal non-orthogonality is introduced in [107, 109].

Criterion 2 *[107, 109] The average ratio of the norms of $\mathcal{N}$ and $\mathcal{D}$ in (2.26) should be minimized, which minimizes the inter-symbol-interference directly caused by the non-orthogonality of the code.*

Minimal non-orthogonality can be explained more clearly as follows. The orthogonality situation occurs when $\left[\mathbf{D}^{(ce)}\right]^{\mathcal{H}} \mathbf{D}^{(ce)} = \sum_{k=1}^{K} \left(|\Delta_k|^2 \mathbf{I}\right)$ and thus $\mathcal{N} = \mathbf{0}$. Note that $\mathcal{N}$ stands for inter-symbol-interference, and it is desirable to minimize inter-symbol-interference, which leads to minimize non-orthogonality.

2.5.3 Maximal symbolwise diversity

Note that the Euclidean distance squared $Tr\left(\left[\mathbf{D}^{(ce)}\right]^{\mathcal{H}} \mathbf{D}^{(ce)}\right)$ is a real valued positive semidefinite quadratic function of the symbol differences Δ_k (and their complex conjugates). It is desirable to design codes such that the Euclidean distance is a monotonically increasing function of the number of bit-errors in a codeword pair. Preferably, the Euclidean distance squared is proportional to a sum of the symbolwise Euclidean distances squared, $|\Delta_k|^2$. Next, from the linearity of the code it is clear that if the code does not provide full diversity protection against one symbol error, it cannot provide full diversity protection against multiple-symbol errors.

The requirement of maximal symbolwise diversity (MSD) [108, 109] is that in a non-orthogonal case, the individual code matrices $\mathbf{C}_k$ should be unitary matrices with $\mathbf{C}_k^{\mathcal{H}} \mathbf{C}_k = |z_k|^2 \mathbf{I}$. For a maximal symbolwise diversity code, the distance matrix is $\left[\mathbf{D}^{(ce)}\right]^{\mathcal{H}} \mathbf{D}^{(ce)} = \sum_{k=1}^{K} \left(|\Delta_k|^2 \mathbf{I}\right) + \mathcal{N}$.

We remark that maximal symbolwise diversity can be defined more generally than that in [108, 109] such that for $\forall k$, $rank(\mathbf{C}_k) = \min\{T, N_T\}$.

2.5.4 Traceless non-orthogonality

If maximal symbolwise diversity is satisfied, the C_k should be designed so that the non-orthogonality matrix $\mathcal{N}$ is traceless [108, 109], i.e.,

$$Tr\left(\mathcal{N}\right) = 0. \tag{2.27}$$

2.5.5 Frobenius orthogonality

Frobenius orthogonality is also called traceless self-interference [110].

Theorem 1 *[110] For a linear matrix modulation with a Frobenius orthogonal basis, i.e.,*

$$Tr\left(\mathbf{C}_i^{\mathcal{H}}\mathbf{C}_k + \mathbf{C}_k^{\mathcal{H}}\mathbf{C}_i\right) = 0, \tag{2.28}$$

the union bound on the pairwise error probabilities increases with increasing self-interference at any SNR.

Note that Frobenius orthogonality supports minimizing the union bound [110].

2.5.6 Capacity optimality

The space time channel model is

$$\mathbf{Y} = \sqrt{E_s}\sum_{n=0}^{N-1}\mathbf{H}\mathbf{M}_n s_n + \mathbf{V}, \tag{2.29}$$

where $\mathbf{M}_n$ is of size $N_T \times T$, $\mathbf{H}$ is a MIMO channel matrix of size $N_R \times N_T$, $s_n, n = 0, ..., N-1$ are data source symbols, $\mathbf{V}$ is a $N_R \times T$ matrix whose columns represent realizations of an i.i.d. circular complex additive white Gaussian noise (AWGN) process with distribution $\mathcal{CN}(\mathbf{0}, N_0\mathbf{I}_{N_R})$. Note that $\mathbf{C}_k\left(s_k\right) = \mathbf{M}_k s_k$ determines $\mathbf{C}_k$ as a linear code.

The model (2.30) can also be written as [47]

$$\mathbf{y} = \sqrt{E_s}\mathcal{H}\mathcal{X}\mathbf{s} + \mathbf{v}, \tag{2.30}$$

where

$$\mathcal{X} = \left[vec(\mathbf{M}_0), ..., vec(\mathbf{M}_{N-1})\right],$$

$\mathcal{H} = \mathbf{I}_T \otimes \mathbf{H}$, $\mathbf{y} = vec(\mathbf{Y})$, $\mathbf{v} = vec(\mathbf{V})$, and $\mathbf{s} = [s_0, ..., s_{N-1}]^{\mathcal{T}}$.

Assume $R_{\mathbf{s}} = \mathbb{E}_{\mathbf{s}}\left(\mathbf{s}\mathbf{s}^{\mathcal{H}}\right) = \mathbf{I}_N$. Then the ergodic capacity of the AWGN system with Rayleigh fading for capacity-optimum complex LDCs is given by [47]

$$C_c = \max_{Tr(\mathcal{X}\mathcal{X}^{\mathcal{H}}) \leqslant N_T T} \frac{1}{T}\mathbb{E}_{\mathbf{H}}\left[\log\det\left(\mathbf{I}_{N_T T} + \mathcal{H}\mathcal{X}\mathcal{X}^{\mathcal{H}}\mathcal{H}^{\mathcal{H}}\right)\right] \tag{2.31}$$

Then, the following is a design criterion based on optimal capacity.

Theorem 2 *[47] Let $N = N_T T$. Any $\mathcal{X}$ such that $\mathcal{X}\mathcal{X}^{\mathcal{H}} = \frac{1}{N_T}\mathbf{I}_{N_T T}$ is a capacity-optimal linear dispersion code (LDC).*

The concept of LDC will be introduced in Chapter 3.

2.6 A tight bound for performance analysis of transmit diversity

Recently, Siwamogsatham, Fitz, and Grimm have derived a tight bound for performance analysis of transmit diversity approaches in in correlated Rayleigh fading [96]. This bound, extensively used in this thesis, is introduced in this section.

2.6.1 System model

The space-time communication system has L_t antennas at the transmitter and L_r antennas at the receiver. The channel between a transmit and a receive antenna is

modeled as a frequency nonselective flat Rayleigh-fading process. At a given receive antenna, a vector of matched filter output is formulated as [96]

$$\mathbf{Q}_i = \sqrt{E_b}\mathbf{D}\mathbf{C}_i + \mathbf{N}_i, \tag{2.32}$$

where $i = 1, ..., L_r$, E_b defines the bit energy per receive antenna, $\mathbf{D}$ is an $N_C \times N_C L_t$ transmitted codeword matrix formed as

$$\mathbf{D} = [\mathbf{D}_1, ..., \mathbf{D}_{L_t}],$$

where $\mathbf{D}_k = diag[D_k(1), ..., D_k(N_C)]$ is an $N_C \times N_C$ diagonal matrix of the signals transmitted from the k-th transmit antenna with $D_k(a)$ being the symbol transmitted at time a, $\mathbf{C}_i = diag\left[\mathbf{C}_{1i}^{\mathcal{T}}, ..., \mathbf{C}_{L_t i}^{\mathcal{T}}\right]^{\mathcal{T}}$ is an $N_C L_t \times 1$ channel vector in which $\mathbf{C}_{ki}^{\mathcal{T}} = diag[C_{ki}(1), ..., C_{ki}(N_C)]^{\mathcal{T}}$ is an $N_C \times 1$ vector of channel distortions between the i-th receive antenna and the k-th transmit antenna with $C_{ki}(a)$ being the complex path gain at time a, and $\mathbf{N}_i$ is additive white Gaussian noise (AWGN) with a covariance matrix $N_0\mathbf{I}_{N_C}$. The channel distortion coefficients are random variables with variance $2\sigma_C^2$, and hence the SNR per receive antenna can be computed as $2\sigma_C^2 E_b/N_0$.

The overall system description can be simply generated by sequentially stacking the $N_C \times 1$ matched filter output vector for each receive antenna to form a larger $N_C L_r \times 1$ observation vector and accordingly defining the corresponding $N_C \times N_C L_t L_r$ symbol matrix $\mathbf{D}$ and $N_C L_t L_r \times 1$ channel vector $\mathbf{C}_i$ [96]. The length of the stacked matched filter output vector shall be defined as $N = N_C L_r$.

2.6.2 Pairwise error probability

The pairwise error probability (PEP) is a common performance measure for digital communication receivers [96]. In the case of a coherent maximum-likelihood (ML) receiver to which perfect channel state information (CSI) is available, the optimum

rule for deciding between two possible transmitted data sequences, $\mathbf{D} = \mathbf{d}_\alpha$ and $\mathbf{D} = \mathbf{d}_\beta$, when the channel distortion is known to have the value $\mathbf{C} = \mathbf{c}$ and the observations $\mathbf{Q} = \mathbf{q}$, is [96]

$$(\mathbf{q} - \mathbf{d}_\alpha \mathbf{c})^{\mathcal{H}} (\mathbf{q} - \mathbf{d}_\alpha \mathbf{c}) \overset{\mathbf{d}_\alpha}{<} (\mathbf{q} - \mathbf{d}_\beta \mathbf{c})^{\mathcal{H}} (\mathbf{q} - \mathbf{d}_\beta \mathbf{c}) \tag{2.33}$$

or

$$(\mathbf{q} - \mathbf{d}_\alpha \mathbf{c})^{\mathcal{H}} (\mathbf{q} - \mathbf{d}_\alpha \mathbf{c}) \overset{\mathbf{d}_\beta}{>} (\mathbf{q} - \mathbf{d}_\beta \mathbf{c})^{\mathcal{H}} (\mathbf{q} - \mathbf{d}_\beta \mathbf{c}) . \tag{2.34}$$

The PEP is [96]

$$P(\alpha, \beta) = P\left(\|\mathbf{Q} - \mathbf{d}_\alpha \mathbf{C}\|^2 > \|\mathbf{Q} - \mathbf{d}_\beta \mathbf{C}\|^2 \, | \mathbf{d}_\alpha sent \right) . \tag{2.35}$$

Denote

$$\mathbf{C}_s = (\mathbf{d}_\alpha - \mathbf{d}_\beta) \, \mathbf{C}_C \, (\mathbf{d}_\alpha - \mathbf{d}_\beta)^{\mathcal{H}} ,$$

where $\mathbf{C}_C$ denotes the covariance matrix of $\mathbf{C}$, and $\lambda_k^{(s)}$ denotes the k-th eigenvalue of $\mathbf{C}_s$ and $\Delta_H(s)$ denoting the number of nonzero eigenvalues of the signal matrix $\mathbf{C}_s$ or, equivalently, the rank of $\mathbf{C}_s$. Then an asymptotic upper bound of PEP is provided in a simple product form. This bound is asymptotically tighter than the standard Chernoff bound [96]. This asymptotic upper bound is given by [96]

$$P(\alpha, \beta) \leqslant \frac{\begin{pmatrix} 2\Delta_H(s) - 1 \\ \Delta_H(s) - 1 \end{pmatrix} (N_0)^{\Delta_H(s)}}{\prod_{k=1}^{\Delta_H(s)} \lambda_k^{(s)}} . \tag{2.36}$$

Chapter 3

Linear dispersion codes

3.1 Introduction

Hassibi and Hochwald have proposed linear dispersion codes (LDC) as a general framework for arbitrary complex space time codes (STC) for block flat-fading channels [42]. LDC possess symbol coding rates of up to one (the definition of symbol coding rate will be discussed in Section 3.3.1), and can support arbitrary configuration of transmit and receive antennas. In LDC design, minimizing average pairwise error probability (PEP) is shown to be numerically difficult for high rate systems [42]. Rather, LDC design was achieved by formulating a power-constrained optimization problem based on mutual information [42]. Later, Heath and Paulraj proposed a frame-theory-based LDC design to optimize both ergodic capacity and error probability [47]. Although LDC were proposed as STC, we treat LDC in a more general complex symbol matrix coding framework to allow the application of LDC to different system models. Note that

1) LDC also embrace conventional block error control coding (BECC), which work on binary or integer domains, as subclasses, such as product codes;

2) the design criteria of LDC are different from those of BECC;

3) the coding rate of BECC can never be one.

3.2 Definition of LDC

Assume that an uncorrelated data sequence has been modulated using complex-valued source data symbols chosen from an arbitrary, e.g. r_c-PSK or r_c-QAM, constellation.

A $T \times M$ LDC matrix codeword, $\mathbf{S}_{LDC}$, is transmitted from M transmit channels and occupies T channel uses and encodes Q source data symbols. LDC was originally proposed as a complex space-time matrix coding framework [42]. The matrix codeword $\mathbf{S}_{LDC}$ is expressed as

$$\mathbf{S}_{LDC} = \sum_{q=1}^{Q} \alpha_q \mathbf{A}_q + j\beta_q \mathbf{B}_q, \tag{3.1}$$

where $\mathbf{S}_{LDC} \in C^{T\times M}$, and $\mathbf{A}_q \in C^{T\times M}, \mathbf{B}_q \in C^{T\times M}, q = 1, ..., Q$ are called dispersion matrices. The constellation data symbols are defined by

$$s_q = \alpha_q + j\beta_q, q = 1, ..., Q. \tag{3.2}$$

Note that there is another LDC definition with different dispersion matrices, $\mathbf{C}_q$ and $\mathbf{D}_q$, as follows [42],

$$\mathbf{S}_{LDC} = \sum_{q=1}^{Q} s_q \mathbf{C}_q + s_q^* \mathbf{D}_q, \tag{3.3}$$

where $\mathbf{C}_q = \frac{1}{2}(\mathbf{A}_q + \mathbf{B}_q)$ and $\mathbf{D}_q = \frac{1}{2}(\mathbf{A}_q - \mathbf{B}_q)$, $q = 1, ..., Q$. In this thesis, $\mathbf{A}_q$ and $\mathbf{B}_q$ are chosen as dispersion matrices.

The basic LDC system was originally formulated as follows [42]:

$$\mathbf{X} = \sqrt{\frac{\rho}{M}} \sum_{q=1}^{Q} (\alpha_q \mathbf{A}_q + j\beta_q \mathbf{B}_q)\mathbf{H} + \mathbf{V} \tag{3.4}$$

where space time MIMO channel matrix is $\mathbf{H} \in C^{M\times N}$, received signal matrix $\mathbf{X} \in C^{T\times N}$ and complex white Gaussian noise $\mathbf{V} \in C^{T\times N}$, the normalizaton $\sqrt{\frac{\rho}{M}}$ ensures that the signal-to-noise-ratio (SNR) at each receive antenna ρ is independent of M. A matrix format of (3.4) can be written as

$$\mathbf{x} = \sqrt{\frac{\rho}{M}}\mathcal{H}\theta + \mathbf{v}, \tag{3.5}$$

where

$$\theta = [\alpha_1, \beta_1, ..., \alpha_Q, \beta_Q]^{\mathcal{T}},$$
$$\mathbf{x} = \left[\mathrm{Re}\left([\mathbf{X}]_{:,1}\right), \mathrm{Im}\left([\mathbf{X}]_{:,1}\right), ..., \mathrm{Re}\left([\mathbf{X}]_{:,N}\right), \mathrm{Im}\left([\mathbf{X}]_{:,N}\right)\right]^{\mathcal{T}},$$
$$\mathbf{v} = \left[\mathrm{Re}\left([\mathbf{V}]_{:,1}\right), \mathrm{Im}\left([\mathbf{V}]_{:,1}\right), ..., \mathrm{Re}\left([\mathbf{V}]_{:,N}\right), \mathrm{Im}\left([\mathbf{V}]_{:,N}\right)\right]^{\mathcal{T}},$$

and

$$\mathcal{H} = \begin{bmatrix} \mathcal{A}_1\underline{\mathbf{h}}_1 & \mathcal{B}_1\underline{\mathbf{h}}_1 & \cdots & \mathcal{A}_Q\underline{\mathbf{h}}_N & \mathcal{B}_Q\underline{\mathbf{h}}_N \\ \vdots & \vdots & \ddots & \vdots & \vdots \\ \mathcal{A}_1\underline{\mathbf{h}}_N & \mathcal{B}_1\underline{\mathbf{h}}_N & \cdots & \mathcal{A}_Q\underline{\mathbf{h}}_N & \mathcal{B}_Q\underline{\mathbf{h}}_N \end{bmatrix}, \tag{3.6}$$

where

$$\mathcal{A}_q = \begin{bmatrix} \mathrm{Re}\left(\mathbf{A}_q\right) & -\mathrm{Im}\left(\mathbf{A}_q\right) \\ \mathrm{Im}\left(\mathbf{A}_q\right) & \mathrm{Re}\left(\mathbf{A}_q\right) \end{bmatrix},$$
$$\mathcal{B}_q = \begin{bmatrix} -\mathrm{Im}\left(\mathbf{B}_q\right) & -\mathrm{Re}\left(\mathbf{B}_q\right) \\ \mathrm{Re}\left(\mathbf{B}_q\right) & -\mathrm{Im}\left(\mathbf{B}_q\right) \end{bmatrix},$$

and

$$\underline{\mathbf{h}}_n = \begin{bmatrix} \mathrm{Re}\left([\mathbf{H}]_{:,n}\right) \\ \mathrm{Im}\left([\mathbf{H}]_{:,n}\right) \end{bmatrix}.$$

The following remarks are in order:

1) The above LDC system model (3.4) requires $(M \times N)$ MIMO block fading channels that are valid only when the channel is constant for at least T channel uses.

2) The matrix model (3.5) is the same as Eq. (23) in [42] except for different notation. It can be observed that (3.4) and (3.5) leads to LDC decoding that requires block fading channel knowledge.

3.3 Coding rate of LDC

3.3.1 Coding rate of LDC defined by Hassibi and Hochwald

Hassibi and Hochwald have defined the coding rate with the unit of bits of LDC as

$$R = \frac{Q}{T} \log_2 r, \tag{3.7}$$

where r is the size of constellation [42]. This definition may be proper for multiple antenna based MIMO wireless channels. However, this definition may not be proper if LDC are applied into other communications channels, such as frequency-time (FT) channels. In FT channels, the calculated rate is using (3.7) is less than the actual data rate, since a FT channels is a SISO channel. In addition, from only the rate calculated using (3.7), one cannot clearly determine the symbol rate that the LDC achieves, and finally (3.7) does not agree with the conventional definition of error control coding rate.

3.3.2 Symbol coding rate of LDC

This thesis uses the term data symbol coding rate in the units of symbols of LDC, which is defined as

$$R_{LDC}^{sym} = \frac{Q}{MT} \tag{3.8}$$

When $Q = MT$, we therefore refer to the coding rate of LDC as "rate-one".

In this thesis, we avoid using the term "full rate", which may be confused with terminology from the block-based space-time coding literature. For example, while "full rate" commonly refers to a data symbol coding rate of $\frac{Q}{T}$, such "full rate" codes, however, are not information lossless codes if the minimum of the number of transmit and receive antennas, denoted by N_T and N_R, respectively, is larger than one [46,98]. Another use of the term "full rate" refers to information lossless codes if N_T is not larger than N_R [76,129]. We remark that in space-time channels, if $\min\{N_T, N_R\} > 1$, the symbol coding rate may be alternatively be defined as

$$R_{LDC}^{sym} = \frac{Q}{T \min\{N_T, N_R\}}, \tag{3.9}$$

which may be appropriate for linear estimation and detection.

The definition (3.8) is also general enough to denote symbol coding rates of complex-valued matrix codes in frequency-time channels [122]. In the rest of this thesis, we employ the definition (3.8) for LDC, using M rather than N_T, to apply to both space-time and frequency-time channels.

3.3.3 Symbol coding rate one of LDC

The most interested case using (3.8) or (3.9) of symbol coding rate one of LDC is rate-one. This can be explained using the concept of asymptotic-information-lossless (AILL) codes [94]. AILL is a necessary and sufficient condition of achieving the optimal diversity-multiplexing tradeoff, and rate-one based on (3.9) is the necessary condition to be AILL [94].

3.4 Matrix form LDC encoding

3.4.1 A special subclass of LDC

In this thesis, we primarily consider a special subclass of dispersion matrices with the constraints

$$\mathbf{A}_q = \mathbf{B}_q, q = 1, ..., Q. \tag{3.10}$$

Substituting (3.2) and (3.10) into (3.1),

$$\mathbf{S}_{LDC} = \sum_{q=1}^{Q} s_q \mathbf{A}_q. \tag{3.11}$$

Using of the *vec* operation, we transform (3.11) into matrix form. Reordering $\mathbf{S}_{LDC}$ and each matrix $\mathbf{A}_q$ into a $TM \times 1$ column vector, respectively, by $vec(\mathbf{S}_{LDC})$ and $vec(\mathbf{A}_q)$, we obtain

$$vec(\mathbf{S}_{LDC}) = \begin{bmatrix} vec(\mathbf{A}_1) & ... & vec(\mathbf{A}_Q) \end{bmatrix} \begin{bmatrix} s_1 \\ \vdots \\ s_Q \end{bmatrix}. \tag{3.12}$$

An example of that special class of LDC codes is shown as follows. The group of square dispersion matrices of this code, which we call HH Square LDC, satisfies the constraint of (3.10) [42], which is

$$\mathbf{A}_{M(k-1)+l} = \mathbf{B}_{M(k-1)+l} = \frac{1}{\sqrt{M}} \mathbf{D}^{k-1} \mathbf{\Pi}^{l-1}, \tag{3.13}$$

where $k = 1, ..., M$, $l = 1, ..., M$,

$$\mathbf{D} = \begin{bmatrix} 1 & 0 & ... & 0 \\ 0 & e^{j\frac{2\pi}{M}} & ... & 0 \\ \vdots & \vdots & \ddots & \vdots \\ 0 & 0 & ... & e^{j\frac{2\pi(M-1)}{M}} \end{bmatrix},$$

and

$$\mathbf{\Pi} = \begin{bmatrix} 0 & 0 & \cdots & 0 & 0 & 1 \\ 1 & 0 & \cdots & 0 & 0 & 0 \\ 0 & 1 & \cdots & 0 & 0 & 0 \\ 0 & 0 & \cdots & 0 & 0 & 0 \\ \vdots & \vdots & \ddots & \vdots & \vdots & \vdots \\ 0 & 0 & \cdots & 0 & 1 & 0 \end{bmatrix}.$$

Using the above matrices, the data symbol coding rate of LDC is one.

A possible zero-forcing method to estimate the data symbol vector in (3.12) is to calculate the Moore-Penrose pseudo-inverse of LDC encoding matrix

$$\mathbf{G}_{LDC} = [vec(\mathbf{A}_1), ..., vec(\mathbf{A}_Q)] \tag{3.14}$$

offline and store the result.

3.4.2 General matrix form

Denote

$$\mathbf{A}_{vec} = \begin{bmatrix} vec(\mathbf{A}_1^{\mathcal{T}}) & vec(\mathbf{A}_2^{\mathcal{T}}) & ... & vec(\mathbf{A}_Q^{\mathcal{T}}) \end{bmatrix}, \tag{3.15}$$

$$\mathbf{B}_{vec} = \begin{bmatrix} vec(\mathbf{B}_1^{\mathcal{T}}) & vec(\mathbf{B}_2^{\mathcal{T}}) & ... & vec(\mathbf{B}_Q^{\mathcal{T}}) \end{bmatrix}, \tag{3.16}$$

$$\alpha_{vec} = \begin{bmatrix} \alpha_1 & \alpha_2 & ... & \alpha_Q \end{bmatrix}^{\mathcal{T}}, \tag{3.17}$$

$$\beta_{vec} = \begin{bmatrix} \beta_1 & \beta_2 & ... & \beta_Q \end{bmatrix}^{\mathcal{T}}, \tag{3.18}$$

$$\theta_{vec} = \begin{bmatrix} \alpha_{vec}^{\mathcal{T}} & \beta_{vec}^{\mathcal{T}} \end{bmatrix}^{\mathcal{T}}, \tag{3.19}$$

$$\mathbf{G}_{vec} = \begin{bmatrix} \mathbf{A}_{vec} & j\mathbf{B}_{vec} \end{bmatrix}, \tag{3.20}$$

$$\mathbf{s}_{vec} = \begin{bmatrix} s_1 & \cdots & s_Q \end{bmatrix}^{\mathcal{T}}. \tag{3.21}$$

In this general case, we have

$$vec\left(\mathbf{S}_{LD}^{\mathcal{T}}\right) = \mathbf{G}_{vec}\theta_{vec}. \tag{3.22}$$

With the constraint in (3.10), we have

$$vec(\mathbf{S}_{LD}^{\mathcal{T}}) = \mathbf{A}_{vec}\mathbf{s}_{vec}. \tag{3.23}$$

In this special case, the length of the estimated signal vector is only half that of the general case.

Note that (3.12) and (3.23) are used primarily in Chapter 9. There is a slight difference between $\mathbf{A}_{vec}$ in (3.15) and $\mathbf{G}_{LDC}$ in (3.14), i.e., the transpose operations, and both $\mathbf{A}_{vec}$ and $\mathbf{G}_{LDC}$ can encode LDC in different contexts, respectively. In this thesis, we only call $\mathbf{G}_{LDC}$ LDC encoding matrix under the constraint (3.10).

3.5 LDC decoding

3.5.1 MLD and MLD-like decoding

Conventionally, high complexity decoding, maximum likelihood decoding (MLD) [83, 92] and MLD-like decoding, such as sphere decoding (SD) [17,43,53,113], are primarily considered in literature. Note that the worst case of complexity of both MLD and SD is exponential, which may be prohibitively expensive for practical applications.

3.5.2 Low complexity decoding

Without loss of generality, low complexity linear decoding is employed for performance comparisons via simulations in this thesis. However, the gains offered by the new LDC approaches proposed in this thesis are also applicable to more complex optimal decoders.

3.5.2.1 One step decoding

Based on the equivalent channels, such as (3.6), LDC can be decoded in one-step low-complexity non-linear decoding, such as decision feedback decoding, or linear decoding methods, such as zero-forcing (ZF) and linear minimum mean-square error. One step decoding is a class of decoding approaches, which do not perform the step of channel symbol (LDC coded symbol) estimation but perform data source symbol estimation in one step. One example of this will be shown in Section 5.4. A concurrent approach in one step decoding is also described in [34].

3.5.2.2 Multiple step decoding

In multiple step decoding approaches proposed in this thesis, the first step is channel symbol (LDC coded symbol) estimation, which can be done non-linearly, such as using decision feedback estimation, or linearly, such as using ZF and linear MMSE. The following step is to decode LDC, which may also be done linearly or non-linearly, to estimate source data symbols. After the channel symbol estimation, To estimate the source signal vector, we may use pre-computed zero-forcing (ZF) or Moore-Penrose pseudo-inverse of $\mathbf{G}_{LDC}$, $\mathbf{G}_{vec}$, or $\mathbf{A}_{vec}$ as the decoding matrix. Linear ZF LDC decoding may work well if

1) the designed decoding matrix has full column rank, which depends on proper

code design,

2) the channel symbols (LDC coded symbols) are estimated in good quality.

Note that the above LDC decoding requires channel symbols (LDC coded symbols) to first be estimated. After the channel symbol estimation, linear MMSE LDC decoding may also be used with the added complexity in calculating the variance of residual noise of channel symbols. Moreover, if the first step estimation is biased, the residual noise is non-Gaussian, the degraded MMSE approach may not be worth the increased complexity.

3.5.3 Complexity level

Assume that the LDC is of size $T \times M$, and one LDC codeword encodes Q source data symbols, and the constellation size of each data symbol is r_c. Assume that this LDC is a full diversity code, then the codebook size of this LDC is ${r_c}^Q$. The complex level is discussed as follows.

1) Assume that the worst case complexity of MLD or MLD-like LDC decoding is K_M, and then $\ln(K_M)$ has complexity of in the level $O({r_c}^Q)$.

2) Let $y = \max\{T, M\}$. The channel symbols (LDC coded symbols) are estimated using linear MMSE, and LDC is linearly decoded using the multiplication of an matrix, pre-computed ZF decoding matrix and an estimated signal vector. The complexity of this linear LDC decoding is $O\left((\max\{T, M\})^3\right) + O(Q)$.

Chapter 4

Rectangular asymptotic information lossless linear dispersion codes

4.1 Introduction

Recently, Shashidhar, Rajan, Sundar, and Kumar introduces the concept of asymptotic-information-lossless(AILL) [94]. A key problem is to design asymptotic information lossless LDC with arbitrary dimensions algebraically. In the literature, there are the only two known classes of LDCs based on algebraically designed LDC that accommodate variable matrix sizes. Hassibi and Hochwald have proposed a class of rate-one square LDC matrices of size $M \times M$ as in Eq. (31) of [42], which we denote as HH square LDC as shown in (3.10). However, in some applications, rectangular rate-one LDC are desirable, e.g., to new approaches that employ LDC across combinations of space, time and frequency dimensions, such as double linear dispersion space-time-frequency-coding (DLD-STFC) [123, 124]. Zhang et. al. propose a class of rate-one rectangular LDC of size $T \times M$ [129]. However, their design requires $T = KM$, where K is a positive integer [129].

As an extension of HH square LDC [42], this chapter proposes a new class of

algebraically designed rate-one rectangular linear dispersion codes of arbitrary size $T \times M$, called uniform linear dispersion codes (U-LDC). When used with double linear dispersion space-time-frequency-coding (DLD-STFC), which will be described later, these systems significantly outperform uncoded MIMO-OFDM systems [123, 124]. Note that, although HH square LDC have been proposed in [42] and shown to have superior performance even in frequency-time channels [122], several important analyses for HH square LDC have not appeared in literature. This chapter provides an analysis of U-LDC (including HH square LDC). This chapter shows that U-LDC (1) meet sub-optimal constraints for both block fading and rapid fading channels, which enables U-LDC to approximately minimize the error union bound [88,89,108–110], (2) are capacity optimal and suitable for multistage receiver design, (3) reach maximal symbolwise diversity [108, 109].

The chapter is organized as follows. The design of rectangular rate-one U-LDC is proposed in Section 4.2. The properties of U-LDC are analyzed in Section 4.3. Detailed proofs are provided in appendices.

4.2 Proposed construction of uniform linear dispersion codes

4.2.1 The case of $T \leq M$

Denote

$$\mathbf{D} = \begin{bmatrix} 1 & 0 & \cdots & 0 \\ 0 & e^{j\frac{2\pi}{T}} & \cdots & 0 \\ \vdots & \vdots & \ddots & \vdots \\ 0 & 0 & \ddots & e^{j\frac{2\pi(T-1)}{T}} \end{bmatrix}, \mathbf{\Pi} = \begin{bmatrix} 0 & 0 & \cdots & 0 & 1 \\ 1 & 0 & \cdots & 0 & 0 \\ 0 & 1 & \ddots & \cdots & 0 \\ \vdots & \vdots & \ddots & \ddots & \vdots \\ 0 & 0 & \cdots & 1 & 0 \end{bmatrix},$$

$$\mathbf{\Gamma} = \begin{bmatrix} 1 & 0 & \cdots & \cdots & 0 & \cdots & 0 \\ 0 & 1 & \ddots & \cdots & 0 & \cdots & 0 \\ \vdots & \ddots & \ddots & \ddots & \cdots & \vdots & \vdots \\ 0 & 0 & \ddots & 1 & 0 & \cdots & 0 \\ 0 & 0 & \cdots & 0 & 1 & \cdots & 0 \end{bmatrix},$$

where $\mathbf{D}$ is of size $T \times T$, $\mathbf{\Pi}$ is of size $M \times M$, and $\mathbf{\Gamma}$ is of size $T \times M$.

The $T \times M$ LDC dispersion matrices are:

$$\mathbf{A}_{M(k-1)+l} = \mathbf{B}_{M(k-1)+l} = \frac{1}{\sqrt{T}} \mathbf{D}^{k-1} \mathbf{\Gamma} \mathbf{\Pi}^{l-1}, \tag{4.1}$$

where $k = 1, ..., T$ and $l = 1, ..., M$.

4.2.2 The case of $T > M$

Denote

$$\mathbf{D} = \begin{bmatrix} 1 & 0 & \cdots & 0 \\ 0 & e^{j\frac{2\pi}{M}} & \cdots & 0 \\ \vdots & \vdots & \ddots & \vdots \\ 0 & 0 & \ddots & e^{j\frac{2\pi(M-1)}{M}} \end{bmatrix}, \mathbf{\Gamma} = \begin{bmatrix} 1 & 0 & \cdots & 0 & 0 \\ 0 & 1 & \ddots & 0 & 0 \\ \vdots & \ddots & \ddots & \ddots & \vdots \\ 0 & 0 & \ddots & 1 & 0 \\ 0 & 0 & \cdots & 0 & 1 \\ \vdots & \vdots & \vdots & \vdots & \vdots \\ 0 & 0 & \cdots & 0 & 0 \end{bmatrix},$$

where $\mathbf{D}$ is of size $M \times M$, $\mathbf{\Pi}$, defined earlier, is of size $T \times T$, and $\mathbf{\Gamma}$ is of size $T \times M$.

The $T \times M$ LDC dispersion matrices are:

$$\mathbf{A}_{M(k-1)+l} = \mathbf{B}_{M(k-1)+l} = \frac{1}{\sqrt{M}} \mathbf{\Pi}^{k-1} \mathbf{\Gamma} \mathbf{D}^{l-1}, \tag{4.2}$$

where $k = 1, ..., T$ and $l = 1, ..., M$.

4.3 Properties of uniform linear dispersion codes

4.3.1 Entries of U-LDC dispersion matrices

To derive and prove the following properties of U-LDC, it is useful to obtain expressions for the entries of U-LDC dispersion matrices, which are provided in Appendix A.1.

4.3.2 Encoding matrix of U-LDC is unitary

Property 1 *For uniform linear dispersion codes with arbitrary size $T \times M$ dispersion matrices $\mathbf{A}_q, q = 1, ..., TM$, the encoding matrix $\mathbf{G}_{LDC} = [vec(\mathbf{A}_1), ..., vec(\mathbf{A}_{TM})]$ is*

unitary.

Proof: See Appendix A.2.

With regard to Property 1, we have the following remarks.

1) According to Theorem 1 of [47], as shown in Section 2.5.6, the unitary property, $\mathbf{G}_{LDC}\left[\mathbf{G}_{LDC}\right]^{\mathcal{H}} = \mathbf{I}_{TM}$, ensures that U-LDC is capacity optimal in block-fading space-time channels.

2) According to the condition shown in [94], the unitary property of $\mathbf{G}_{LDC}$ ensures U-LDC AILL.

3) The unitary matrix $\mathbf{G}_{LDC}$ ensures the uncorrelatedness of U-LDC coded symbols for uncorrelated data source symbols. This enables computationally simpler multi-stage receivers to perform without significant loss in comparison to single-stage receivers as shown in Chapter 7 and 8.

4.3.3 U-LDC optimality

In the proofs of our results of this subsection, we need to derive expressions for $\mathbf{A}_{q_1}\left[\mathbf{A}_{q_2}\right]^{\mathcal{H}}$ and $\left[\left[\mathbf{A}_{q_1}\right]^{\mathcal{H}}\mathbf{A}_{q_2}\right]$, where $q_1 = M(k_1-1)+l_1$, $q_2 = M(k_2-1)+l_2$, $k_1, k_2 = 1, ..., T, l_1, l_2 = 1, ..., M$, $\mathbf{A}^{(k_1,l_1)} = \mathbf{A}_{q_1}$, and $\mathbf{A}^{(k_2,l_2)} = \mathbf{A}_{q_2}$, which are provided in Appendix A.3.

Property 2 *Uniform linear dispersion codes of arbitrary size $T \times M$ dispersion matrices $\mathbf{A}_q, q = 1, ..., TM$ meet the optimal energy constraint under capacity optimization [42], i.e.,*

$$Tr\left[\left[\mathbf{A}_q\right]^{\mathcal{H}}\mathbf{A}_q\right] = \frac{TM}{Q} = 1, \tag{4.3}$$

where $Q = TM$. If $T \geq M$, U-LDC meets the more restrictive constraint

$$[\mathbf{A}_q]^{\mathcal{H}} \mathbf{A}_q = \frac{1}{M} \mathbf{I}_M \tag{4.4}$$

Proof: See Appendix A.4.

Property 3 *For uniform linear dispersion codes with arbitrary size $T \times M$ dispersion matrices $\mathbf{A}_q, q = 1, ..., TM$, the following constraint minimizes the error union bound in the absence of correlation among rapid fading transmit channels:*

$$Tr\left[vec(\mathbf{A}_p)\left[vec(\mathbf{A}_q)\right]^{\mathcal{H}}\right] = 0. \tag{4.5}$$

In the presence of correlation, however, the above constraint is suboptimum and is only able to minimize the component of the EUB arising from inter-symbol-interference (see Section 7.5 and Appendix D.2).

Proof: See Appendix A.5.

Property 4 *Uniform linear dispersion codes with arbitrary size $T \times M$ dispersion matrices $\mathbf{A}_q, q = 1, ..., TM$ meet the traceless minimal non-orthogonality criterion for block quasi-static fading channels [108, 109],*

$$Tr\left[[\mathbf{A}_{q_1}]^{\mathcal{H}} \mathbf{A}_{q_2}\right] = Tr\left[\mathbf{A}_{q_1}[\mathbf{A}_{q_2}]^{\mathcal{H}}\right] = 0 \tag{4.6}$$

for any $1 \leq q_1 \neq q_2 \leq TM$.

Proof: See Appendix A.6.

We remark that

1) Error union bound (EUB) is an upper bound on the average error probability, and as such is an average of the pairwise error probabilities between all pairs of

codewords. The system performance in terms of average bit error rate (BER) is not only related to pairwise error probabilities but also to the EUB, an indicator of average system performance.

2) Property 3 states that U-LDC approximately minimize EUB in 2-D (e.g. space-time) time-varying channels. In Section 7.5 and Appendix D.2, it is proven that (4.5) is a criterion for minimizing the dominant inter-symbol-interferences for rapid fading channels, if the auto-correlation of channel elements in the 2-D channel dominates the cross-correlation of any two different channel elements in 2-D channels.

3) Property 4 is called the traceless minimal non-orthogonality criterion in [108, 109], which is related to the error union bound (EUB) [88, 89, 110]. In [110], Tirkkonen and Kokkonen have more recently proven that (4.6) minimizes the dominant self-interference related to EUB, referred to as the Frobenius orthogonality criterion or traceless self-interference.

Thus, U-LDC based systems may achieve low average bit error rate (BER) in both rapid and block fading channels.

4.3.4 Symbolwise diversity order of U-LDC

Symbolwise diversity, first defined in [108], is a special case of full diversity in that protection against single-symbol errors is a necessary condition for full diversity protection against multiple-symbol errors. In a well-designed code, the number of bit-errors in a codeword is a monotonically increasing with the reduction of the squared Euclidean distance. Specifically, the squared Euclidean distance is proportional to a

sum of the squared symbolwise Euclidean distances, which is essentially the significance of symbolwise diversity [108, 109].

Although U-LDC may not be full diversity codes, U-LDC achieves maximal symbolwise diversity in space-time block fading channels.

Property 5 *Uniform linear dispersion codes of arbitrary size $T \times M$ dispersion matrices $\mathbf{A}_q, q = 1, ..., TM$ achieve symbolwise diversity order $r = \min\{M, T\}$*

Proof: See Appendix A.7.

4.4 Conclusion

In summary, this chapter proposes and analyzes a new class of rate-one AILL rectangular linear dispersion codes of arbitrary size, termed uniform linear dispersion codes (U-LDC), which support high performance and lower complexity though multiple stage decoding when applied to space-time-frequency coding design [123]. Although it has not been proven that U-LDC are full diversity codes, U-LDC has been shown to achieve maximal symbolwise diversity order in space time block fading channels. This chapter also shows that U-LDC of arbitrary size possess several important and attractive properties, including

1) the satisfaction of error union bound constraints for both rapid and block fading channels which ensures low average bit error rates;

2) suitability for low complexity multi-stage receiver designs;

3) capacity optimality for space-time channels.

Chapter 5

Linear dispersion over time and frequency

5.1 Introduction

In recent years, multicarrier communications systems, especially those employing orthogonal frequency division multiplexing (OFDM) [5], have received increasing attention for high-data-rate communications in frequency selective fading environments [48]. In fact, OFDM has been accepted as a component of multiple industrial standards for high-data-rate communications [23, 48, 87, 106]. By serial-to-parallel (S/P) conversion, OFDM transforms a single wideband multipath channel into multiple parallel narrowband flat fading channels, enabling simple equalization.

In practical OFDM system design, it is important to notice that uncoded OFDM cannot provide the same order of diversity as uncoded single-carrier systems in severe frequency-selective fading environments, since the frequency responses of channel space branches differ from one another. One technique to mitigate the above problem is the combination of interleaving and forward error correction across all subchannels at the price of reduced bandwidth efficiency, i.e., coded OFDM (COFDM) [49, 60, 64, 69, 95, 134].

A critical issue related to bandwidth efficiency for high-data-rate transmission is the coding rate. In conventional COFDM, the coding rate usually is less than one, and thus achieving appropriate trade-offs between coding rate and error probability are critical design criteria. Recently, as an alternative to error control coding , linear precoding has been combined with OFDM to exploit or maximally exploit frequency diversity [71, 114]. To further improve performance, linear constellation precoding [126] was more recently proposed to combine with OFDM, known as LCP-OFDM, to maximize not only frequency diversity gain but also coding gain [72]. However, LCP-OFDM is not able to exploit time diversity over different OFDM blocks in the channels.

The contributions and organization of this chapter is discussed as follows.

1) This chapter proposes a high-rate (rate up to unity) linear dispersion coded OFDM (LDC-OFDM) system that improves BER performance and exploits diversity across both multiple subcarrier channels and multiple OFDM blocks. By considering guard intervals, cyclic prefix (CP) and zero-padding (ZP), we propose LDC-CP-OFDM and LDC-ZP-OFDM, respectively. We show that LDC-OFDM outperforms LCP-OFDM in dynamic frequency-selective fading channels.

2) One LDC-OFDM block consists of T OFDM blocks. The basic signal detection strategy of LDC-OFDM proposed in this chapter involves a layered, complexity-reduced, backward- compatible two-step-estimation (TSE) procedure: first, the receiver estimates channel symbols per OFDM block; second, the receiver estimates complex data symbols from the whole LDC-OFDM block. Data bits are then detected.

3) For comparison purposes, this chapter also formulates a one-step-estimation (OSE) system procedure and system equations for LDC-OFDM, which treats LDC-OFDM as a single linear system acting over multiple OFDM blocks and which also may facilitate LDC-OFDM system analysis.

4) This chapter analytically shows that a properly designed LDC-OFDM may fully utilize available time and frequency diversity, and provides a design criterion for full-diversity frequency-time block codes.

5) Through simulations, this chapter investigates two performance related factors:

   a. imperfect channel estimation for LDC-CP-OFDM,

   b. low complexity receivers for LDC-ZP-OFDM.

This chapter is organized as follows. In Section 5.2, the construction of an LDC-OFDM block is proposed. The proposed TSE based LDC-OFDM system is discussed in Section 5.3, and the proposed receiver structure is illustrated. In Section 5.4, the system equations of OSE based LDC-OFDM are established. An analytical discussion of diversity properties of LDC-OFDM is given in Section 5.5. Performance analysis and comparison of LDC-OFDM is presented in Section 5.6.

5.2 Proposed LDC-OFDM block construction

Let there be N_C subcarriers in one OFDM block. One LDC-OFDM block, illustrated in Figure 5.1, consists of T adjacent OFDM blocks. An LDC-OFDM system includes D LDC codewords, each with LDC matrices occupying $N_{F(i)}$ subcarriers and T OFDM blocks $\in C^{T\times N_{F(i)}}, i = 1, ..., D$, with $\sum_{i=1}^{D} N_{F(i)} = N_C$. In OFDM systems, since the

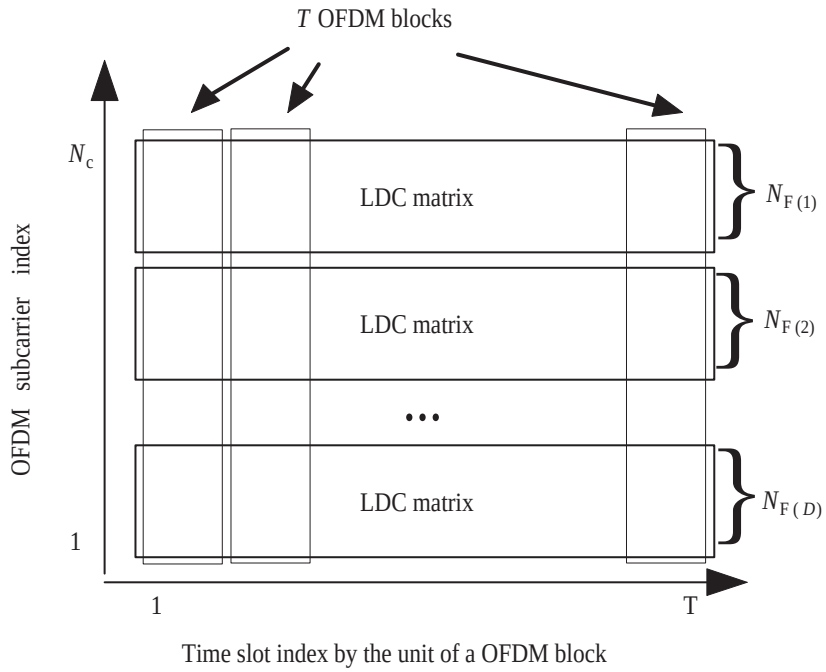

Figure 5.1. LDC-OFDM blocks in the time-frequency plane

number of subcarriers is typically much higher than the number of antennas in space-time MIMO systems, LDC has more freedom to choose larger dispersion matrices. In addition, the low correlation across subcarriers in OFDM serves as an advantage for LDC-OFDM.

One LDC-OFDM block is organized into the $T \times N_C$ matrix:

$$\mathbf{S}_{LDC-OFDM-block} = \begin{bmatrix} \left(\mathbf{s}_{OFDM}^{(1)}\right)^{\mathcal{T}} \\ \ldots \\ \left(\mathbf{s}_{OFDM}^{(T)}\right)^{\mathcal{T}} \end{bmatrix} \tag{5.1}$$

where $\mathbf{S}_{LDC-OFDM-block} \in C^{T \times N_C}$ and $\mathbf{s}_{OFDM}^{(k)}$ is the k-th OFDM block symbol vector of size $1 \times N_C$, and represents the transmitted complex symbol vector before the inverse Fourier tranformation in the transmitter for the k^{th} OFDM transmitted block. $\mathbf{s}_{OFDM}^{(k)}$ consists of all the D row vectors $\mathbf{S}_{LDC(k,.)}^{(i)}, i = 1, ..., D$, where $\mathbf{S}_{LDC(k,.)}^{(i)} \in C^{1 \times N_{F(i)}}$ is

the k-th row of the i-th LDC matrix codeword $\mathbf{S}_{LDC}^{(i)}$ in a single LDC-OFDM block. $S_{LDC(k,.)}^{(i)}$ occupies $N_{F(i)}$ subcarriers, and it is not necessary that the $N_{F(i)}$ subcarriers are spectrally adjacent.

5.3 TSE based LDC-OFDM

5.3.1 Two step estimation and its necessary condition for LDC decoding

Maximum-likelihood (ML) or MLD-like sphere decoding (SD) for LDC decoding methods have been studied extensively [42, 47], and both are with high computational complexity. Further, channel symbol estimation and LDC decoding is not separated, which results in channel knowledge dependency for LDC decoding and the large symbol size decoding block [42]. To remove *direct channel knowledge dependency* and reduce complexity, we propose the concept of two step estimation (TSE). The basic idea of layered decoding has also been discussed in Section 3.5.2.

The TSE procedure may be applied to LDC-OFDM to permit the channel coefficients to change per each OFDM block instead of per T OFDM blocks. This enables an LDC decoding layer to be independent of the specific equalizers used and enables wide applicability for enhancing different standards. A possible zero-forcing method to estimate the data symbol vector in (3.12) is to calculate the Moore-Penrose pseudo-inverse of LDC encoding matrix $\mathbf{G}_{LDC}$ offline and store the result. If $\mathbf{G}_{LDC}$ has full column rank, we obtain the least squares solution

$$\left[\mathbf{G}_{LDC}^{(i)}\right]^{\dagger} = \left[\left[\mathbf{G}_{LDC}^{(i)}\right]^{\mathcal{H}} \mathbf{G}_{LDC}^{(i)}\right]^{-1} \left[\mathbf{G}_{LDC}^{(i)}\right]^{\mathcal{H}}. \tag{5.2}$$

To remove the direct dependency of LDC decoding on channel symbol estimation,

LDC designs need to meet the following:

Correlation criterion: Denote the correlation matrix of $vec\left([\mathbf{S}_{LDC}]^{\mathcal{T}}\right)$ as $\mathbf{R}_{vec\left([\mathbf{S}_{LDC}]^{\mathcal{T}}\right)}$. For the case that channel symbols per channel use or per row of $\mathbf{S}_{LDC}$ are block-wise estimated, $\mathbf{S}_{LDC}$ needs to be row-wise uncorrelated. In other words, $\mathbf{R}_{vec\left([\mathbf{S}_{LDC}]^{\mathcal{T}}\right)}$ has block diagonal form,

$$\mathbf{R}_{vec\left([\mathbf{S}_{LDC}]^{\mathcal{T}}\right)} = \begin{bmatrix} \mathbf{R}_{\mathbf{S}_{LDC(1,.)}} & \cdots & \mathbf{0} \\ \vdots & \ddots & \vdots \\ \mathbf{0} & \cdots & \mathbf{R}_{\mathbf{S}_{LDC(T,.)}} \end{bmatrix} \tag{5.3}$$

where $\mathbf{R}_{\mathbf{S}_{LDC(k,.)}} \in C^{M\times M}, k = 1..., T$ is the correlation matrix of the k-th row vector of $\mathbf{S}_{LDC}$, and $\mathbf{0}$s are $M \times M$ zero matrices. For the case that channel symbols are estimated per channel symbol or per element of $\mathbf{S}_{LDC}$, $\mathbf{S}_{LDC}$ needs to be element-wise uncorrelated. In other words, $\mathbf{R}_{vec\left([\mathbf{S}_{LDC}]^{\mathcal{T}}\right)}$, needs to be diagonal, and more restrictive constraints are applied.

The two steps are:

1) *Signal estimation per channel use:*

   Signals in each of T channel uses are estimated. No immediate signal detection is performed (In different channel uses, channel matrices may be different);

2) *Data symbol estimation and detection per LDC block:*

   The data symbols corresponding to one LDC codeword are estimated (In this step, channel knowledge is not required). Bit detection is then performed.

Note that unlike conventional iterative estimation methods, each TSE step operates on different physical dimensions of signals, which could have different sized symbol blocks. LDC encoding and decoding only requires matrix-vector multiplication. The per-data-symbol complexity of encoding and decoding is constant and

proportional to the data symbol coding rate of LDC.

5.3.2 TSE based LDC-OFDM system

5.3.2.1 Wideband OFDM model

The OFDM system has been introduced in Section 2.3.1. During transmission, for the k-th block of N_C IFFT transformed complex symbols, a block of P symbols (a OFDM block and its guard interval) undergoes order L frequency selective, time flat Rayleigh fading channel with coefficients $\mathbf{h}^{(k)} = \left[h_0^{(k)}, ..., h_L^{(k)}\right]^{\mathcal{T}}$. Choosing $P \geq N_C + L$, the inter-block interference due to the previous transmitted block is eliminated by a guard interval of size $(P - N_C)$.

Denote $s_{OFDM(p)}^{(k)}, p = 1..., N_C$ as the channel symbol transmitted on the p-th subcarrier during the k-th OFDM block. The receiver experiences additive complex Gaussian noise. Before transmission, a guard interval (cyclic prefix (CP)) is added to each OFDM block. After FFT processing, the received symbol is

$$x_p^{(k)} = \sqrt{\rho} H_p^{(k)} s_{OFDM(p)}^{(k)} + v_p^{(k)}, p = 1, ..., N_c \tag{5.4}$$

where $H_p^{(k)}$ is the p-th subcarrier channel gain during the k-th OFDM block, and

$$H_p^{(k)} = \sum_{l=o}^{L} h_l^{(k)} e^{-j(2\pi/N_c)l(p-1)},$$

or

$$H_p^{(k)} = \left[\mathbf{w}_p\right]^{\mathcal{T}} \mathbf{h}^{(k)}, \tag{5.5}$$

where

$$\mathbf{w}_p = \left[1, \omega^{p-1}, \omega^{2(p-1)}, \cdots, \omega^{L(p-1)}\right]^{\mathcal{T}}$$

and

$$\omega = e^{-j(2\pi/N_c)}.$$

The additive noise is circularly symmetric, zero-mean, complex Gaussian with variance N_0. Assume additive noise is statistically independent for different k, and ρ is the normalized signal to noise ratio (SNR).

The CP-OFDM system may also be written in block matrix form,

$$\mathbf{x}^{(k)} = \sqrt{\rho}\mathbf{D}_{\mathbf{H}}^{(k)}\mathbf{s}_{OFDM}^{(k)} + \mathbf{v}^{(k)} \tag{5.6}$$

where $\mathbf{x}^{(k)}$ and $\mathbf{v}^{(k)}$ are the frequency domain received signal and noise vector, respectively, $\mathbf{D}_{\mathbf{H}}^{(k)} = \mathbf{F}_{N_C}\mathbf{H}^{(k)}\left[\mathbf{F}_{N_C}\right]^{\mathcal{H}} = diag(H_1^{(k)}, ..., H_{N_C}^{(k)})$,

$$\left[\mathbf{F}_{N_C}\right]_{m,n} = \frac{1}{\sqrt{N_C}}e^{-j2\pi(m-1)(n-1)/N_C} \tag{5.7}$$

and

$$\left[\mathbf{H}^{(k)}\right]_{m,n} = h_{((m-n) \bmod N_C}^{(k)}. \tag{5.8}$$

When zero-padding (ZP) is consider as the OFDM guard interval, orthogonality is destroyed, and the system model does not have n simple frequency domain element form as shown in (5.4). However, the ZP-OFDM system model can be written as block matrix form in the time domain,

$$\begin{aligned}&\mathbf{x}_{ZP\_OFDM}^{(k)} = \\ &\sqrt{\rho}\mathbf{H}_0^{(k)}\left[\mathbf{F}_{N_C}\right]^{\mathcal{H}}\mathbf{s}_{OFDM}^{(k)} + \mathbf{v}_{ZP\_OFDM}^{(k)}\end{aligned}, \tag{5.9}$$

with the k-th received ZP-OFDM block $\mathbf{x}_{ZP\_OFDM}^{(k)} \in C^{P\times 1}$, and the frequency selective channel matrix $\mathbf{H}_0^{(k)} \in C^{P\times N_C}$ corresponding to the k-th OFDM block. The Toeplitz channel matrix $\mathbf{H}_0^{(k)}$ is always guaranteed to be invertible, regardless of the channel zero locations [66]. Zero-mean white additive complex Gaussian noise vector is represented by $\mathbf{v}_{ZP\_OFDM}^{(k)}$.

5.3.2.2 TSE based LDC-OFDM system

The proposed TSE LDC decoding procedure in Section 5.3.1 is applied to the wide-band OFDM channel described above.

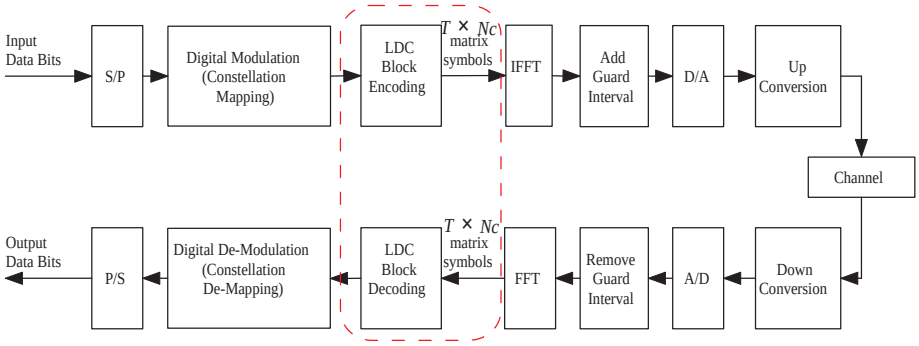

Figure 5.2. Proposed TSE based LDC-OFDM system (the dashed lines indicate the enhancement parts over conventional OFDM system)

The differences between conventional OFDM and the proposed TSE based LDC-OFDM are indicated by the dashed lines in Figure 5.2. Note that the block size used in the proposed system differs from that of the conventional OFDM system.

5.3.2.3 LDC-OFDM receiver

The receiver for LDC-OFDM, illustrated in Figure 5.4, first estimates the signals in T OFDM blocks. Second, the estimated $S_{LDC-OFDM-block}$ is reorganized into D LDC blocks. The D LDC demodulators operate in parallel, followed by data bit detection. Denote the LDC encoding matrix of the i-th LDC matrix codeword $\mathbf{S}_{LDC}^{(i)} \in C^{T \times N_{F(i)}}$ as $\mathbf{G}_{LDC}^{(i)}$, which encodes source data symbol vector with zero mean, unit variance, $\mathbf{s}^{(i)} = \left[s_1^{(i)}, ..., s_{Q_i}^{(i)}\right]$, Q_i is the number of source data symbols in $\mathbf{s}^{(i)}$. If $\mathbf{G}_{LDC}^{(i)} = \mathbf{G}_{LDC}, i = 1, ..., D$ are unitary matrices, the correlation matrices of $\mathbf{s}_{OFDM}^{(k)}, k = 1, ..., T$ are identity matrices. Note that, in general, unitariness is not

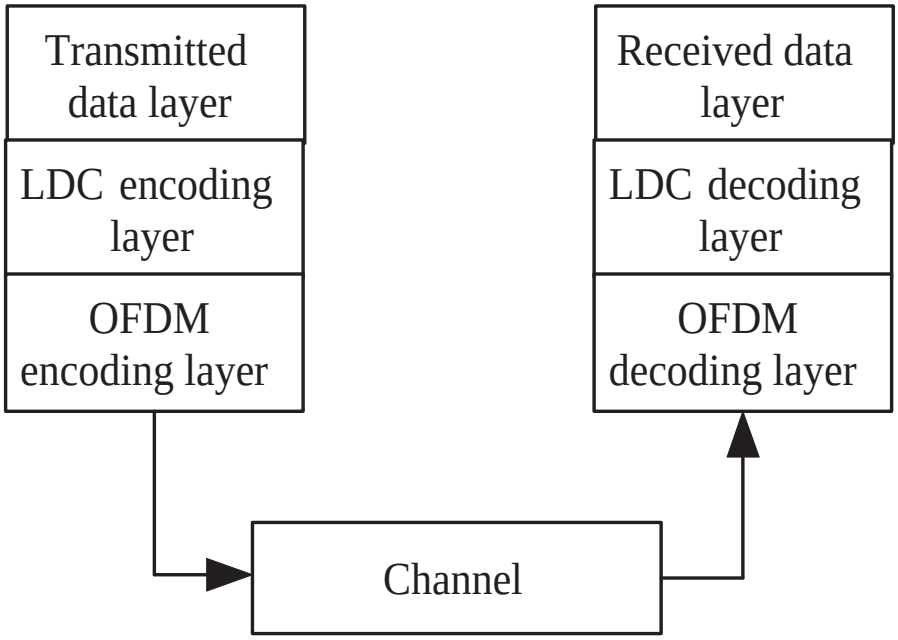

Figure 5.3. Layered structure of TSE based LDC-OFDM communications.

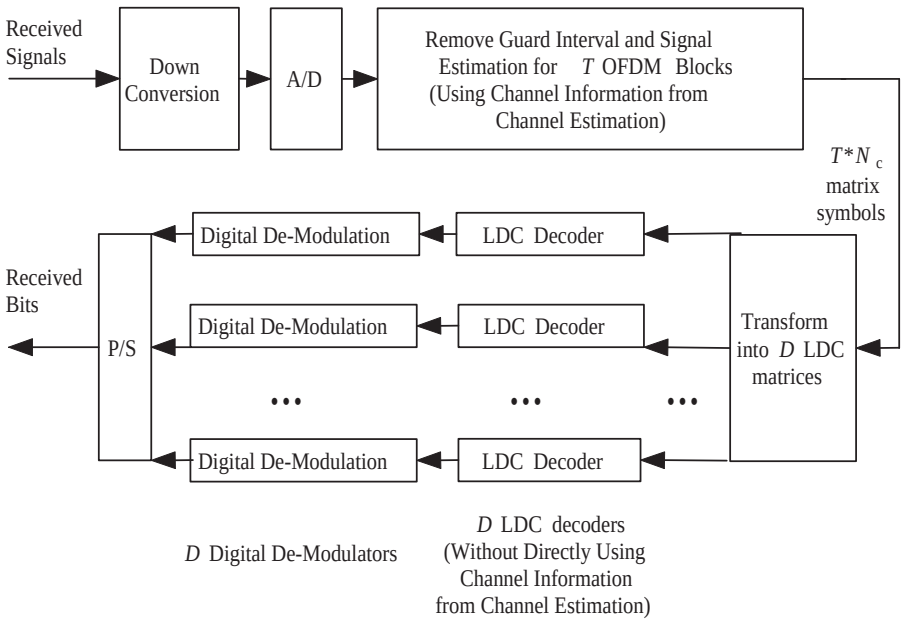

Figure 5.4. Proposed TSE based LDC-OFDM receiver structure.

a necessary condition for $\mathbf{G}_{LDC}^{(i)}$.

Due to the independence of the two estimation steps, TSE LDC-OFDM systems possess the layered structure shown in Figure 5.3, which provides flexible choices for system design and communications error control.

5.3.2.3.1 First estimation step - OFDM Demodulation In the proposed TSE based LDC decoding strategy, LDC decoding is independent of OFDM signal estimation. Thus the proposed TSE based LDC-OFDM system could be made backwards-compatible with conventional OFDM systems.

In Section 5.6, minimum-mean-squared-error MMSE equalizers are chosen to investigate error performance. Assuming that OFDM symbols are normalized with unit variance, the respective equalizers are given by [66]

1) case of CP-OFDM

$$\begin{aligned}\mathbf{G}_{OFDM\_CP\_MMSE}^{(k)} &= \sqrt{\rho}\mathbf{C}_{\mathbf{s}_{OFDM}^{(k)}}\left(\mathbf{D}_{\mathbf{H}}^{(k)}\right)^{\mathcal{H}}\cdot \\ &\left(\mathbf{I}_{N_C}+\rho\mathbf{D}_{\mathbf{H}}^{(k)}\mathbf{C}_{\mathbf{s}_{OFDM}^{(k)}}\left(\mathbf{D}_{\mathbf{H}}^{(k)}\right)^{\mathcal{H}}\right)^{-1}\end{aligned} \tag{5.10}$$

and

$$\widehat{\mathbf{s}_{OFDM}^{(k)}} = \mathbf{G}_{OFDM\_CP\_MMSE}^{(k)}\mathbf{x}^{(k)}, \tag{5.11}$$

2) case of ZP-OFDM

$$\begin{aligned}\mathbf{G}_{OFDM\_ZP\_MMSE}^{(k)} &= \sqrt{\rho}\mathbf{F}_{N_C}\mathbf{C}_{\mathbf{s}_{OFDM}^{(k)}}\left(\mathbf{H}_0^{(k)}\right)^{\mathcal{H}}\cdot \\ &\left(\mathbf{I}_P+\rho\mathbf{H}_0^{(k)}\left[\mathbf{F}_{N_C}\right]^{\mathcal{H}}\mathbf{C}_{\mathbf{s}_{OFDM}^{(k)}}\mathbf{F}_{N_C}\left(\mathbf{H}_0^{(k)}\right)^{\mathcal{H}}\right)^{-1}\end{aligned} \tag{5.12}$$

and

$$\widehat{\mathbf{s}_{OFDM}^{(k)}} = \mathbf{G}_{OFDM\_ZP\_MMSE}^{(k)}\mathbf{x}_{ZP\_OFDM}^{(k)}, \tag{5.13}$$

where $k = 1, ..., T$, $\mathbf{C}_{\mathbf{s}_{OFDM}^{(k)}}$ is the covariance matrix of the k-th OFDM block symbols, $\mathbf{C}_{\mathbf{s}_{OFDM}^{(k)}}$ can be derived using $\mathbf{G}_{LDC}^{(i)}, i = 1, ..., D$.

When $\mathbf{G}_{LDC}^{(i)}, i = 1, ..., D$ is unitary, the equalizers could be written as

1) case of CP-OFDM

$$\mathbf{G}_{OFDM\_CP\_MMSE}^{(k)} = \sqrt{\rho}\left(\mathbf{D}_{\mathbf{H}}^{(k)}\right)^{\mathcal{H}}\left(\mathbf{I}_{N_C} + \rho\mathbf{D}_{\mathbf{H}}^{(k)}\left(\mathbf{D}_{\mathbf{H}}^{(k)}\right)^{\mathcal{H}}\right)^{-1} \tag{5.14}$$

2) case of ZP-OFDM

$$\mathbf{G}_{OFDM\_ZP\_MMSE}^{(k)} = \sqrt{\rho}\mathbf{F}_{N_C}\left(\mathbf{H}_0^{(k)}\right)^{\mathcal{H}}\left(\mathbf{I}_P + \rho\mathbf{H}_0^{(k)}\left(\mathbf{H}_0^{(k)}\right)^{\mathcal{H}}\right)^{-1}. \tag{5.15}$$

It is easy to show that if $\mathbf{G}_{LDC}^{(i)}, i = 1, ..., D$ is unitary, (5.15) is much more complex than (5.14) when matrix dimensions are high, since $\mathbf{D}_{\mathbf{H}}^{(k)}$ is diagonal, and the matrix inversion operation (5.10) may be simplified to element-wise inversion operations. Based on the layer-independent design principle of TSE based LDC-OFDM, a lower complexity solution for ZP-OFDM may be found. A possible solution is via a ZP-OFDM-FAST-MMSE approach [66]: Denote

$$\mathbf{F}_{ZP} = \begin{bmatrix} \mathbf{F}_{N_C} & \mathbf{0}_{(P-N_C)\times N_C} \end{bmatrix}^{\mathcal{H}}$$

$$\mathbf{U} = \left[\mathbf{F}_P\mathbf{F}_{ZP}\right]^{\dagger},$$

$$D_{\mathbf{H}_P^{(k)}} = \mathbf{F}_P C_P^{(\mathbf{h}^{(k)})}\left[\mathbf{F}_P\right]^{\mathcal{H}},$$

where $C_P^{(\mathbf{h}^{(k)})}$ is a $P \times P$ circulant matrix, and $C_P^{(\mathbf{h}^{(k)})} = Circ(h_0^{(k)}, 0, ..., h_L^{(k)}, ..., h_1^{(k)})$. Then the low complexity MMSE ZP-OFDM equalizer corresponding to (5.15) is given as

$$\mathbf{G}_{OFDM\_ZP\_FAST\_MMSE}^{(k)} = \mathbf{U}\left[D_{\mathbf{H}_P^{(k)}}\right]^{\mathcal{H}}\left[\frac{P}{N_C}\mathbf{I}_P + \rho D_{\mathbf{H}_P^{(k)}}\left[D_{\mathbf{H}_P^{(k)}}\right]^{\mathcal{H}}\right]^{-1} \tag{5.16}$$

Note that $\mathbf{U}$ could be precomputed; $D_{\mathbf{H}_P^{(k)}}$ is diagonal, simplifying the matrix inversion operation.

5.3.2.3.2 Second estimation step - LDC-OFDM Block Demodulation Re-organizing the estimation results of the first estimation step into D estimated LDC matrix codewords, $\widehat{\mathbf{S}_{LDC}^{(i)}}, i = 1, ..., D$, the estimated data symbol vectors corresponding to D LDC blocks are

$$\widehat{\mathbf{s}^{(i)}} = \left[\mathbf{G}_{LDC}^{(i)}\right]^{\dagger} vec\left(\widehat{\mathbf{S}_{LDC}^{(i)}}\right). \tag{5.17}$$

5.4 OSE based LDC-OFDM

This section discusses one-step-estimation (OSE) system strategy of LDC-OFDM. Basically, OSE LDC decoding strategy is to integrate LDC decoding and channel symbol estimation, that is to say this procedure processes one LDC codeword together with channel knowledge, thus OSE strategy with high complexity, especially in the case of using maximum-likelihood or MLD-like sphere decoding. Although we start to use the term OSE, actually OSE strategy has been applied to LDC decoding in space time channels and chosen by primary LDC research community [42, 47], in addition, existing work assume channel coefficients constant over time during one LDC codeword. This section proposes to use an OSE strategy for LDC in frequency time channels, and assumes channel coefficients may vary over time during one LDC codeword.

5.4.1 LDC coding matrix for OSE system

Recall $\mathbf{G}_{LDC}$ and $\mathbf{A}_{vec}$ have been defined in (3.14) and (3.15), where

$$\mathbf{G}_{LDC} = [vec(\mathbf{A}_1), ..., vec(\mathbf{A}_Q)]$$

and

$$\mathbf{A}_{vec} = \left[\begin{array}{cccc} vec(\mathbf{A}_1^{\mathcal{T}}) & vec(\mathbf{A}_2^{\mathcal{T}}) & ... & vec(\mathbf{A}_Q^{\mathcal{T}}) \end{array} \right].$$

There is a permutation relation between $\mathbf{A}_{vec}$ and $\mathbf{G}_{LDC}$,

$$\mathbf{A}_{vec} = \mathbf{P}\mathbf{G}_{LDC}, \tag{5.18}$$

where $\mathbf{P}$ is a permutation matrix,

$$\mathbf{P} = \left[\begin{array}{c} \mathbf{I}_M \otimes \mathbf{a}_{T(1)} \\ \mathbf{I}_M \otimes \mathbf{a}_{T(2)} \\ \vdots \\ \mathbf{I}_M \otimes \mathbf{a}_{T(T)} \end{array} \right] \tag{5.19}$$

where $\mathbf{a}_{T(k)}, k = 1, ..., T$ is a row vector with size $1 \times T$, and with a one in the k-th entry and with zero in all the other entries

We choose $\mathbf{A}_{vec}$ for LDC encoding to facilitate establishing one-step system equations.

5.4.2 OSE LDC-OFDM system model

5.4.2.1 Component matrices

The receiver signal vector of OSE LDC-OFDM is

1) case of LDC-CP-OFDM

$$\mathbf{x}_{LDC\_CP\_OFDM} = \left[\left[\mathbf{x}^{(1)} \right]^{\mathcal{T}}, ..., \left[\mathbf{x}^{(T)} \right]^{\mathcal{T}} \right]^{\mathcal{T}}, \tag{5.20}$$

2) case of LDC-ZP-OFDM

$$\mathbf{x}_{LDC\_ZP\_OFDM} = \left[\left[\mathbf{x}_{ZP\_OFDM}^{(1)} \right]^{\mathcal{T}}, ..., \left[\mathbf{x}_{ZP\_OFDM}^{(T)} \right]^{\mathcal{T}} \right]^{\mathcal{T}}, \tag{5.21}$$

where frequency domain $\mathbf{x}^{(k)} \in C^{N_C \times 1}$ and time domain $\mathbf{x}^{(k)}_{ZP\_OFDM} \in C^{P \times 1}$, $k = 1..., T$ are the receiving vectors corresponding to the k-th OFDM block in a single LDC-CP-OFDM or LDC-ZP-OFDM block respectively.

The system channel matrix is

1) case of LDC-CP-OFDM

$$\mathbf{H}_{CP} = \begin{bmatrix} \mathbf{H}^{(1)} & \cdots & \mathbf{0}_{N_C \times N_C} \\ \vdots & \ddots & \vdots \\ \mathbf{0}_{N_C \times N_C} & \cdots & \mathbf{H}^{(T)} \end{bmatrix}, \tag{5.22}$$

2) case of LDC-ZP-OFDM

$$\mathbf{H}_{ZP} = \begin{bmatrix} \mathbf{H}_0^{(1)} & \cdots & \mathbf{0}_{P \times N_C} \\ \vdots & \ddots & \vdots \\ \mathbf{0}_{P \times N_C} & \cdots & \mathbf{H}_0^{(T)} \end{bmatrix}, \tag{5.23}$$

where $\mathbf{H}^{(k)} \in C^{N_C \times N_C}$ and $\mathbf{H}_0^{(k)} \in C^{P \times N_C}$, $k = 1, ..., T$ are frequency selective channel matrix corresponding to the k-th OFDM block in a single LDC-CP-OFDM and LDC-ZP-OFDM block respectively.

The block-diagonal discrete Fourier transform system matrix for T blocks is

$$\mathbf{F} = \begin{bmatrix} \mathbf{F}_{N_C} & \cdots & \mathbf{0}_{N_C \times N_C} \\ \vdots & \ddots & \vdots \\ \mathbf{0}_{N_C \times N_C} & \cdots & \mathbf{F}_{N_C} \end{bmatrix}, \tag{5.24}$$

where $\mathbf{F}_{N_C} \in C^{N_C \times N_C}$, defined in (5.7), is an N_C-point FFT matrix.

The complex Gaussian noise vector is

1) case of LDC-CP-OFDM

$$\mathbf{v}_{LDC\_CP\_OFDM} = \left[\left[\mathbf{v}^{(1)} \right]^{\mathcal{T}}, ..., \left[\mathbf{v}^{(T)} \right]^{\mathcal{T}} \right]^{\mathcal{T}}, \tag{5.25}$$

2) case of LDC-ZP-OFDM

$$\mathbf{v}_{LDC\_ZP\_OFDM} = \left[\left[\mathbf{v}_{ZP\_OFDM}^{(1)} \right]^{\mathcal{T}}, ..., \left[\mathbf{v}_{ZP\_OFDM}^{(T)} \right]^{\mathcal{T}} \right]^{\mathcal{T}}, \tag{5.26}$$

where frequency domain $\mathbf{v}^{(k)} \in C^{N_C \times 1}$ and time domain $\mathbf{v}_{ZP\_OFDM}^{(k)} \in C^{P \times 1}$, $k = 1..., T$ are the additive noise vectors corresponding to the k-th OFDM block in a single LDC-CP-OFDM or LDC-ZP-OFDM block respectively.

The system complex symbol vector before inverse FFT processing at transmitter is

$$\mathbf{s}_{OFDM} = \left[\left[\mathbf{s}_{OFDM}^{(1)} \right]^{\mathcal{T}}, ..., \left[\mathbf{s}_{OFDM}^{(T)} \right]^{\mathcal{T}} \right]^{\mathcal{T}} \tag{5.27}$$

where $\mathbf{s}_{OFDM}^{(k)} \in C^{N_C \times 1}, k = 1..., T$ are the complex valued symbol vectors to be operated upon with inverse fast Fourier transform ${F_N}^{\mathcal{H}}$ corresponding to each of T OFDM blocks in a single LDC-OFDM block.

5.4.2.2 LDC-OFDM block system model

The OSE LDC-OFDM system of equations over T OFDM blocks could be written as

1) case of LDC-CP-OFDM

$$\mathbf{x}_{LDC\_CP\_OFDM} = \sqrt{\rho}\mathbf{F}\mathbf{H}_{CP}\mathbf{F}^{\mathcal{H}}\mathbf{s}_{OFDM} + \mathbf{v}_{LDC\_CP\_OFDM} \tag{5.28}$$

2) case of LDC-ZP-OFDM

$$\mathbf{x}_{LDC\_ZP\_OFDM} = \sqrt{\rho}\mathbf{H}_{ZP}\mathbf{F}^{\mathcal{H}}\mathbf{s}_{OFDM} + \mathbf{v}_{LDC\_ZP\_OFDM} \tag{5.29}$$

Let $\mathbf{D} = \mathbf{F}\mathbf{H}_{CP}\mathbf{F}^{\mathcal{H}}$, the OSE system equation of LDC-CP-OFDM, (5.28), can be rewritten as

$$\mathbf{x}_{LDC\_CP\_OFDM} = \sqrt{\rho}\mathbf{D}\mathbf{s}_{OFDM} + \mathbf{v}_{LDC\_CP\_OFDM} \tag{5.30}$$

5.4.2.3 Construction of LDC-OFDM codeword vector

The system channel complex symbol vector of OSE based LDC-OFDM actually is a permutation of D LDC codeword symbols. We could write $\mathbf{s}_{OFDM} = \mathbf{T}\mathbf{s}$, where $\mathbf{s} = \left[\left[\mathbf{s}^{(1)}\right]^{\mathcal{T}}, ..., \left[\mathbf{s}^{(D)}\right]^{\mathcal{T}}\right]^{\mathcal{T}}$, and $\mathbf{s}^{(i)} = \left[s_1^{(i)}, ..., s_{Q_i}^{(i)}\right]^{\mathcal{T}}$ is the data source symbol vector for the i-th LDC codeword within one LDC-OFDM block. The transformation matrix $\mathbf{T}$ could be written as

$$\mathbf{T} = \begin{bmatrix} \mathbf{\Omega} & \cdots & \mathbf{0}_{N_C \times N_C} \\ \vdots & \ddots & \vdots \\ \mathbf{0}_{N_C \times N_C} & \cdots & \mathbf{\Omega} \end{bmatrix} \mathbf{\Psi} \begin{bmatrix} \mathbf{P}^{(1)}\mathbf{G}_{LDC}^{(1)} & \cdots & \mathbf{0}_{TN_{F(1)} \times Q_D} \\ \vdots & \ddots & \vdots \\ \mathbf{0}_{TN_{F(D)} \times Q_1} & \cdots & \mathbf{P}^{(D)}\mathbf{G}_{LDC}^{(D)} \end{bmatrix} \tag{5.31}$$

where $\mathbf{\Psi}$ initially maps the k-th rows D LDC codewords to a vector, say $\widetilde{\mathbf{s}_{OFDM}^{(k)}}$, which just connects all the k-th rows for the k-th OFDM block. $\mathbf{\Omega}$ of size $N_C \times N_C$ is the permutation matrix of determining the mappings from $\widetilde{\mathbf{s}_{OFDM}^{(k)}}$ to actual OFDM subcarriers $\mathbf{s}_{OFDM}^{(k)}$ in the k-th OFDM block, and $\mathbf{\Omega}$ is the same for all OFDM blocks. $\mathbf{P}^{(i)}, i = 1, ..., D$ has been defined in (5.19).

Without loss of generality, for simplicity, we consider the case $N_{F(i)} = N_F, i = 1, .., D$ and $Q_i = Q, i = 1, ..., D$, all the LDC codewords use the same encoding matrix $\mathbf{U} = \mathbf{P}\mathbf{G}_{LDC} \in C^{TN_F \times Q}$, and for all T OFDM blocks, the rows of LDC codewords

follow the same rules of mapping to OFDM subcarriers, the we could write

$$\mathbf{\Psi} = \begin{bmatrix} \mathbf{I}_D \otimes \mathbf{\Theta}_{(1)} \\ \mathbf{I}_D \otimes \mathbf{\Theta}_{(2)} \\ \vdots \\ \mathbf{I}_D \otimes \mathbf{\Theta}_{(T)} \end{bmatrix},$$

where $\mathbf{\Theta}_{(k)}$ is a permutation matrix of size $N_F \times N_F T$, $\mathbf{\Theta}_{(k)} = \mathbf{c}_{T(k)} \otimes \mathbf{I}_{N_F}$, and $\mathbf{c}_{T(k)}$ is a row vector of size $1 \times T$, and with 1 in the k-th entry and with 0 in all the other entries.

5.4.3 Full system model for OSE based LDC-OFDM system and its receiver

The full form of proposed linear system equations of OSE based LDC-OFDM (5.30) and (5.29) can be written as

1) case of LDC-CP-OFDM

$$\mathbf{x}_{LDC\_CP\_OFDM} = \sqrt{\rho}\mathbf{D}\mathbf{T}s + \mathbf{v}_{LDC\_CP\_OFDM} \tag{5.32}$$

2) case of LDC-ZP-OFDM

$$\mathbf{x}_{LDC\_ZP\_OFDM} = \sqrt{\rho}\mathbf{H}_{ZP}\mathbf{F}^{\mathcal{H}}\mathbf{T}s + \mathbf{v}_{LDC\_ZP\_OFDM} \tag{5.33}$$

Letting $\mathbf{Z}_{CP} = \mathbf{D}\mathbf{T}$ and $\mathbf{Z}_{ZP} = \mathbf{H}_{ZP}\mathbf{F}^{\mathcal{H}}\mathbf{T}$, we rewrite Eq. (5.32) and (5.33) as

1) case of LDC-CP-OFDM

$$\mathbf{x}_{LDC\_CP\_OFDM} = \sqrt{\rho}\mathbf{Z}_{CP}s + \mathbf{v}_{LDC\_CP\_OFDM} \tag{5.34}$$

2) case of LDC-ZP-OFDM

$$\mathbf{x}_{LDC\_ZP\_OFDM} = \sqrt{\rho}\mathbf{Z}_{ZP}s + \mathbf{v}_{LDC\_ZP\_OFDM}. \tag{5.35}$$

Note that the estimation operation unit of OSE based LDC-OFDM is a LDC-OFDM block instead of a OFDM block. Thus the estimation matrix is much larger than that of TSE case. From the above equation, different receiver designs are possible. Minimum mean-squared error (MMSE) equalizers will be used for OSE LDC-OFDM systems in simulations.

In this section, assume the covariance matrices of $\mathbf{s}$ and $\mathbf{v}$ hold $C_{\mathbf{s}} = \mathbf{I}_{TN_C}$ and $C_{\mathbf{v}} = \mathbf{I}_{TN_C}$ respectively.

The MMSE equalizer is

1) case of LDC-CP-OFDM

$$\mathbf{G}_{LDC-CP-OFDM\_MMSE} = \sqrt{\rho}\left[\mathbf{Z}_{CP}\right]^{\mathcal{H}}\left(\mathbf{I}_{TN_C} + \rho\mathbf{Z}_{CP}\left[\mathbf{Z}_{CP}\right]^{\mathcal{H}}\right)^{-1}, \tag{5.36}$$

2) case of LDC-ZP-OFDM

$$\mathbf{G}_{LDC-ZP-OFDM\_MMSE} = \sqrt{\rho}\left[\mathbf{Z}_{ZP}\right]^{\mathcal{H}}\left(\mathbf{I}_{TP} + \rho\mathbf{Z}_{ZP}\left[\mathbf{Z}_{ZP}\right]^{\mathcal{H}}\right)^{-1}. \tag{5.37}$$

Unlike the TSE system, for OSE systems, it is convenient to obtain the corresponding decision signal-to-interference-plus-noise ratio or SINR as [2]

$$SINR_i = \frac{1}{\left[\mathbf{C}_{\mathbf{s}|\mathbf{x}}\right]_{ii}} - 1, \tag{5.38}$$

where $\mathbf{C}_{\mathbf{s}|\mathbf{x}}$ is calculated as

1) case of LDC-CP-OFDM

$$\mathbf{C}_{\mathbf{s}|\mathbf{x}} = \mathbf{I}_{TN_C} - \rho\left[\mathbf{Z}_{CP}\right]^{\mathcal{H}}\left(\mathbf{I}_{TN_C} + \rho\mathbf{Z}_{CP}\left[\mathbf{Z}_{CP}\right]^{\mathcal{H}}\right)^{-1}\mathbf{Z}_{CP}, \tag{5.39}$$

2) case of LDC-ZP-OFDM

$$\mathbf{C}_{\mathbf{s}|\mathbf{x}} = \mathbf{I}_{TN_C} - \rho \left[\mathbf{Z}_{ZP}\right]^{\mathcal{H}} \left(\mathbf{I}_{TN_C} + \rho \mathbf{Z}_{ZP} \left[\mathbf{Z}_{ZP}\right]^{\mathcal{H}}\right)^{-1} \mathbf{Z}_{ZP}. \tag{5.40}$$

Note that in SINR, the signal is referred to the source data symbol (after LDC decoding) instead of channel symbol (before LDC decoding).

5.5 Diversity analysis of LDC-OFDM

The orthogonality property of CP-OFDM makes analysis of LDC-CP-OFDM convenient. In this section, LDC-OFDM is referred to as LDC-CP-OFDM.

Since LDC-OFDM includes all LDC coding properties within the time-frequency (TF) $T \times N_{F(i)}$ block in a LDC-OFDM codeword, in the following analysis, we consider a single $T \times N_{F(i)}$ block $\mathbf{C}^{(i)}, i = 1, ..., D$ in a LDC-OFDM codeword. The block $\mathbf{C}^{(i)}$ is created after encoding all the i-th LDC codewords within a LDC-OFDM codeword.

Denote subcarrier indexes chosen for TF block $\mathbf{C}^{(i)}, i = 1, ..., D$ as $\{p^{(k)}_{n_{F(i)}}, n_{F(i)} = 1, ..., N_{F(i)}, i = 1, ..., D, k = 1, ..., T\}$. Denote the block $\mathbf{C}^{(i)}$ as the matrix form

$$\mathbf{C}^{(i)} = \begin{bmatrix} c^{(1)}_{p_{1_{(i)}}} & c^{(1)}_{p_{2_{(i)}}} & \cdots & c^{(1)}_{p_{N_{F(i)}}} \\ c^{(2)}_{p_{1_{(i)}}} & c^{(2)}_{p_{2_{(i)}}} & \cdots & c^{(2)}_{p_{N_{F(i)}}} \\ \vdots & \vdots & \ddots & \vdots \\ c^{(T)}_{p_{1_{(i)}}} & c^{(T)}_{p_{2_{(i)}}} & \cdots & c^{(T)}_{p_{N_{F(i)}}} \end{bmatrix}.$$

We may express the system equation for block $\mathbf{C}^{(i)}$ as

$$\mathbf{R}^{(i)} = \sqrt{\rho}\mathbf{M}^{(i)}\mathbf{H}^{(i)} + \mathbf{V}^{(i)}, \tag{5.41}$$

where received signal vector $\mathbf{R}^{(i)}$ and noise vector $\mathbf{V}^{(i)}$ are of size $N_{F(i)}T \times 1$, the i-th LDC coded channel symbol matrix is of size $N_{F(i)}T \times N_{F(i)}T$, $\mathbf{M}^{(i)}$ is of size

$N_{F(i)}T \times N_{F(i)}T$, $c^{(k)}_{p_{n_{F(i)}}}, n_{F(i)} = 1, ..., N_{F(i)}$, is the channel symbol of the k-th OFDM block, the $p_{n_{F(i)}}$-th subcarrier in the i-th LDC codeword, and

$$\mathbf{M}^{(i)} = diag(c^{(1)}_{p_{1_{(i)}}}, ..., c^{(1)}_{p_{N_{F(i)}}}, ..., c^{(T)}_{p_{1_{(i)}}}, ..., c^{(T)}_{p_{N_{F(i)}}}), \tag{5.42}$$

where $i = 1, ..., D$.

The channel $\mathbf{H}^{(i)}$ is of size $N_{F(i)}T \times 1$, and

$$\mathbf{H}^{(i)} = \left[\begin{array}{c} H^{(1)}_{p_{1(i)}}, H^{(1)}_{p_{2(i)}}, ..., H^{(1)}_{p_{N_{F(i)}}}, ..., H^{(T)}_{p_{1(i)}}, H^{(T)}_{p_{2(i)}}, ..., H^{(T)}_{p_{N_{F(i)}}} \end{array} \right]^{\mathcal{T}} \tag{5.43}$$

and $H^{(k)}_{p_{n_{F(i)}}}$ is the path gain of of k-th OFDM block , the $p_{n_{F(i)}}$-th subcarrier for block $\mathbf{C}^{(i)}$. Thus

$$H^{(k)}_{p_{n_{F(i)}}} = \left[\mathbf{w}_{p_{n_{F(i)}}}\right]^{\mathcal{T}} \mathbf{h}^{(k)}, \tag{5.44}$$

where $\mathbf{w}_p$ and $\mathbf{h}^{(k)}$ have been defined in Section 5.3.2.1.

Consider a pair of matrices $\mathbf{M}^{(i)}$ and $\tilde{\mathbf{M}}^{(i)}$ corresponding to two different time-frequency (TF) blocks $C^{(i)}$ and $\tilde{C}^{(i)}$. Then the upper bound pairwise error probability [96] between $\mathbf{M}^{(i)}$ and $\tilde{\mathbf{M}}^{(i)}$ is

$$\Pr\left(\mathbf{M}^{(i)} \rightarrow \tilde{\mathbf{M}}^{(i)}\right) \leq \left(\begin{array}{c} 2r-1 \\ r \end{array} \right) \left(\prod_{a=1}^{r} \gamma_a\right)^{-1} (\rho)^{-r} \tag{5.45}$$

where r is the rank of

$$\left(\mathbf{M}^{(i)} - \tilde{\mathbf{M}}^{(i)}\right) \mathbf{R}_{\mathbf{H}^{(i)}} \left(\mathbf{M}^{(i)} - \tilde{\mathbf{M}}^{(i)}\right)^{\mathcal{H}},$$

and $\mathbf{R}_{\mathbf{H}^{(i)}} = \mathbb{E}\left\{\mathbf{H}^{(i)} \left[\mathbf{H}^{(i)}\right]^{\mathcal{H}}\right\}$ is the correlation matrix of vector $\mathbf{H}^{(i)}$, $\gamma_a, a = 1, ..., r$ are the non-zero eigenvalues of

$$\left(\mathbf{M}^{(i)} - \tilde{\mathbf{M}}^{(i)}\right) \mathbf{R}_{\mathbf{H}^{(i)}} \left(\mathbf{M}^{(i)} - \tilde{\mathbf{M}}^{(i)}\right)^{\mathcal{H}}.$$

Then the corresponding rank and product criteria are

1) Rank criterion: the minimum rank of

$$\left(\mathbf{M}^{(i)} - \tilde{\mathbf{M}}^{(i)}\right) \mathbf{R}_{\mathbf{H}^{(i)}} \left(\mathbf{M}^{(i)} - \tilde{\mathbf{M}}^{(i)}\right)^{\mathcal{H}}$$

over all pairs of different matrices $\mathbf{M}^{(i)}$ and $\tilde{\mathbf{M}}^{(i)}$ and should be as large as possible.

2) Product criterion: the minimum value of the product $\prod_{a=1}^{r} \gamma_a$ over all pairs of different $\mathbf{M}^{(i)}$ and $\tilde{\mathbf{M}}^{(i)}$ should be maximized.

For simplicity, denote

$$\mathbf{\Lambda}^{(i)} = \left(\mathbf{M}^{(i)} - \tilde{\mathbf{M}}^{(i)}\right) \mathbf{R}_{\mathbf{H}^{(i)}} \left(\mathbf{M}^{(i)} - \tilde{\mathbf{M}}^{(i)}\right)^{\mathcal{H}}.$$

Now we need to derive the matrix form of $\mathbf{R}_{\mathbf{H}^{(i)}}$. Denote

$$\mathbf{W}^{(i)} = \left[\mathbf{w}_{p_{1(i)}}, \cdots, \mathbf{w}_{p_{N_{F(i)}}}\right]^{\mathcal{T}} \tag{5.46}$$

and

$$\mathbf{h} = \left[\left[\mathbf{h}^{(1)}\right]^{\mathcal{T}}, \cdots, \left[\mathbf{h}^{(T)}\right]^{\mathcal{T}}\right]. \tag{5.47}$$

Thus

$$\mathbf{H}^{(i)} = \left(\mathbf{I}_T \otimes \mathbf{W}^{(i)}\right) \mathbf{h}. \tag{5.48}$$

Then, we have

$$\begin{aligned} \mathbf{R}_{\mathbf{H}^{(i)}} &= \mathbb{E}\left\{\left(\mathbf{I}_T \otimes \mathbf{W}^{(i)}\right) \mathbf{h} \left[\left(\mathbf{I}_T \otimes \mathbf{W}^{(i)}\right) \mathbf{h}\right]^{\mathcal{H}}\right\} \\ &= \left[\mathbf{I}_T \otimes \mathbf{W}^{(i)}\right] E\left\{\mathbf{h}\left[\mathbf{h}\right]^{\mathcal{H}}\right\} \left[\mathbf{I}_T \otimes \left[\mathbf{W}^{(i)}\right]^{\mathcal{H}}\right] \quad , \\ &= \left[\mathbf{I}_T \otimes \mathbf{W}^{(i)}\right] \mathbf{\Phi} \left[\mathbf{I}_T \otimes \left[\mathbf{W}^{(i)}\right]^{\mathcal{H}}\right] \end{aligned} \tag{5.49}$$

where $\mathbf{\Phi} = E\left\{\mathbf{h}\left[\mathbf{h}\right]^{\mathcal{H}}\right\}$.

Using the well-known property,

$$rank\left(\mathbf{AB}\right) \leq \min\left\{rank\left(\mathbf{A}\right), rank\left(\mathbf{B}\right)\right\}, \tag{5.50}$$

$$rank\left(\mathbf{\Lambda}^{(i)}\right) \leq \min\left\{rank\left(\mathbf{M}^{(i)} - \tilde{\mathbf{M}}^{(i)}\right), rank\left(\mathbf{R}_{\mathbf{H}^{(i)}}\right)\right\}. \tag{5.51}$$

It is desired to maximize

$$\min\left\{rank\left(\mathbf{M}^{(i)} - \tilde{\mathbf{M}}^{(i)}\right), rank\left(\mathbf{R}_{\mathbf{H}^{(i)}}\right)\right\}.$$

We know the maximum of rank of $\mathbf{\Phi}$ is $T(L+1)$. To maximize the rank of $\mathbf{R}_{H^{(i)}}$, we need to maximize the rank of matrix $\mathbf{W}^{(i)}$ of size $N_{F(i)} \times (L+1)$. Thus we need to choose $N_{F(i)} \geq L+1$. When $p_{n_F}^{(i)} = p_1^{(i)} + b(n_F - 1), n_F = 1, ..., N_{F(i)}, N_{F(i)} \geq L+1$, where $p_{n_F}^{(i)} \leq N_C$ and b is a positive integer, $\mathbf{W}^{(i)}$ could achieve maximum rank $L+1$. Then $\mathbf{R}_{H^{(i)}}$ has the potential to achieve the maximum rank of $T(L+1)$, only if $Rank(\mathbf{\Phi}) = T(L+1)$. That is to say, channels need to be full rank jointly in frequency and time domains. The choice of interval b depends on the type of power delay profile of the frequency selective channel, and a detailed discussion can be found in [72] and [98].

Since $\mathbf{M}^{(i)} - \tilde{\mathbf{M}}^{(i)}$ is of size $N_{F(i)}T \times N_{F(i)}T$,

$$rank\left(\mathbf{M}^{(i)} - \tilde{\mathbf{M}}^{(i)}\right) \leq N_{F(i)}T, \tag{5.52}$$

and $N_{F(i)} \geq L+1$.

Note that $\mathbf{M}^{(i)} - \tilde{\mathbf{M}}^{(i)}$ is a diagonal matrix. Thus, the necessary and sufficient condition for maximizing the rank of $\mathbf{M}^{(i)} - \tilde{\mathbf{M}}^{(i)}$ is that all the diagonal elements are non-zero, which can be summarized as

Theorem 3 *1) If the correlation matrix $\mathbf{R}_{\mathbf{H}^{(i)}}$ of channel vector $\mathbf{H}^{(i)}$ is full rank $T(L+1)$, the necessary condition that the frequency-time (FT) block $\mathbf{C}^{(i)}$ of*

LDC-OFDM achieves full joint frequency-time diversity order, i.e. $rank(\mathbf{\Lambda}_{(i)}) = T(L+1)$*, is that the frequency dimension size of the FT block* $\mathbf{C}^{(i)}$ *satisfies*

$$N_{F(i)} \geq L + 1. \tag{5.53}$$

2) The sufficient condition that the frequency-time (FT) block $\mathbf{C}^{(i)}$ *of LDC-OFDM achieves available joint frequency-time diversity order,* $rank(\mathbf{R}_{\mathbf{H}^{(i)}})$*, is that any two elements* $c^{(k)}_{p_{n_{F(i)}}}$ *and* $\widetilde{c^{(k)}_{p_{n_{F(i)}}}}$*, of any two different blocks,* $\mathbf{C}^{(i)}$ *and* $\widetilde{\mathbf{C}^{(i)}}$ *are different. Mathematically, the sufficient condition is*

$$c^{(k)}_{p_{n_{F(i)}}} - \widetilde{c^{(k)}_{p_{n_{F(i)}}}} \neq 0, \tag{5.54}$$

where $n_{F(i)} = 1, ..., N_{F(i)}, k = 1, ..., T$*;*

3) If both $N_{F(i)} = L + 1$ *and* $rank(\mathbf{R}_{\mathbf{H}^{(i)}}) = T(L+1)$ *are satisfied, the condition (5.54) is the necessary and sufficient condition that the frequency-time (FT) block* $\mathbf{C}^{(i)}$ *of LDC-OFDM achieves joint full frequency-time diversity order,* $rank(\mathbf{\Lambda}_{(i)}) = T(L+1)$*;*

4) The related product criterion of design is that the minimum of products

$$\prod_{k=1}^{T} \prod_{a=1}^{N_{F(i)}} \left| c^{(k)}_{p_{a(i)}} - \widetilde{c^{(k)}_{p_{a(i)}}} \right|^2$$

taken over distinct FT block $\mathbf{C}^{(i)}$ *and* $\widetilde{\mathbf{C}^{(i)}}$ *must be maximized.* ■

A detailed proof is provided in Appendix B.

The result of Theorem 3 is somewhat surprising. The criterion provided in Theorem 3 is different from the design criterion for space-time rapid fading channels [102]. If $c^{(k)}_{p_{n_{F(i)}}}, n_{F(i)} = 1, ..., N_{F(i)}$ were space-time code signals, $n_{F(i)}$ would refer to the indices of transmit antennas, then the design criterion (distance criterion) would be

$$c^{(k)}_{p_{1(i)}} c^{(k)}_{p_{2(i)}} ... c^{(k)}_{p_{N_{F(i)}}} \neq \widetilde{c^{(k)}_{p_{1(i)}}}\, \widetilde{c^{(k)}_{p_{2(i)}}} ... \widetilde{c^{(k)}_{p_{N_{F(i)}}}}.$$

Denote

$$\left| c_{(i)}^{k} - \widetilde{c_{(i)}^{k}} \right|^2 = \sum_{a=1}^{N_{F(i)}} \left[c_{p_{a(i)}}^{(k)} - \widetilde{c_{p_{a(i)}}^{(k)}} \right]^2$$

and the corresponding product criterion for the space-time codes would be that the minimum of products

$$\prod_{k=1}^{T} \left| c_{(i)}^{k} - \widetilde{c_{(i)}^{k}} \right|^2$$

taken over distinct codewords $\mathbf{C}^{(i)}$ and $\widetilde{\mathbf{C}^{(i)}}$ be maximized.

Clearly there are differences between the design criteria of frequency-time code and space-time code for 2-D rapid fading channels. The reason for the differences is that the received signals at each receive antenna of space-time channel communications are superpositions of parallel signals from multiple transmit antennas, while there is no additive operation of parallel channel signals at the receivers of frequency-time communications. The differences between design criteria could lead to different designs of matrix codewords between frequency-time and space-time channels, which implies that the best code design for 2-D space-time rapid fading channels is not necessarily to the best code design for 2-D frequency-time rapid fading channels.

This above analysis has revealed that instead of using all available subcarriers, a proper frequency-time (FT) block design usually uses a much smaller block, and could achieve diversity order up to $T(L+1)$. The necessary condition that FT block design achieves a certain diversity order is that the rank of the channel correlation matrix is equal to the diversity order of the FT block. However, in practice, the diversity order achieved is based on the specific LDC design chosen. Originally, Hassibi and Hochwald did not consider diversity order as a design criterion [42]. Heath and Paulraj considered both capacity and error probability as criteria [47], but they only consider channel coefficients that are constant over time within an entire LDC codeword. This chapter provides a more general analysis that considers correlation across parallel

frequency channels (OFDM subcarriers) as well as across time channel uses (OFDM blocks).

An important special case for FT-block design is $T = 1$, and the corresponding upper bound diversity order $L + 1$, which is known as LCP-OFDM [72]. Hence, the diversity order of LCP-OFDM is always equal to or less than that of full frequency-time diversity LDC-OFDM (of order $T(L + 1)$ with $T > 1$) in dynamic frequency-selective fading channels.

5.6 Performance Analysis and Comparison

5.6.1 Simulation setup

Perfect channel state information (CSI), including amplitude and phase, is assumed to be known at the receiver but not at the transmitter. In the simulations, Eq. (31) of [42] defines the dispersion matrices in all LDC codewords. Note that the corresponding LDC encoding matrices $\mathbf{G}_{LDC}$, defined in (3.14), of the above codes are unitary, as proven in Appendix A. Thus this code meets the correlation criterion in Section 5.3.1. The D LDC demodulators each decode $T \times N_{F(i)}$ LDC matrices. In particular, we set

$$N_{F(i)} = N_F = T, i = 1, ..., D. \tag{5.55}$$

In all simulations, the mapping used from LDC to OFDM subcarriers is an evenly spaced LDC subcarrier mapping (ES-LDC-SM), in which the subcarriers used within one LDC codeword are evenly and maximally spaced with respect to the subcarrier indices. Using this mapping, $\mathbf{W}^{(i)}$ defined in (5.46) is guaranteed full rank, which is a necessary condition to achieve full diversity.

To assess performance as a function of LDC matrix size, N_C is fixed while D is varied. Data symbols use QPSK modulation. The frequency selective Rayleigh fading channel has $(L+1)$ paths with exponential power delay profile. The channel is assumed to be constant over different integer numbers of OFDM blocks, and independent identically-distributed (i.i.d.) between blocks. We term this integer number of the intervals as the channel change interval (CCI).

5.6.2 Performance Analysis and Comparison for TSE based LDC-OFDM

In this performance analysis of TSE LDC-OFDM systems, the number of subcarriers of OFDM, N_C, is set to 64.

5.6.2.1 Comparison of LDC-OFDM and OFDM

Figures 5.5 shows the Bit Error Rate (BER) performance vs. receiver input average symbol SNR of the LDC-ZP-OFDM and LDC-CP-OFDM system respectively. Various combinations of N_F with MMSE equalizers are used, and compared to uncoded ZP-OFDM and CP-OFDM systems, respectively. The channel order used in this case was set to $L = 12$.

It can be seen that both LDC-ZP-OFDM and LDC-CP-OFDM are very effective in frequency selective Rayleigh fading channels. With MMSE equalizers, both LDC-ZP-OFDM and LDC-CP-OFDM systems significantly outperform ZP-OFDM and CP-OFDM systems. The larger the dispersion matrices used, the greater the performance improvement achieved, at a cost of increased decoding delay. Despite LDC's increased delay in decoding, we note that a symbol coding rate of one is used, resulting in no bandwidth expansion. The higher SNR, the more diversity gains are achieved for

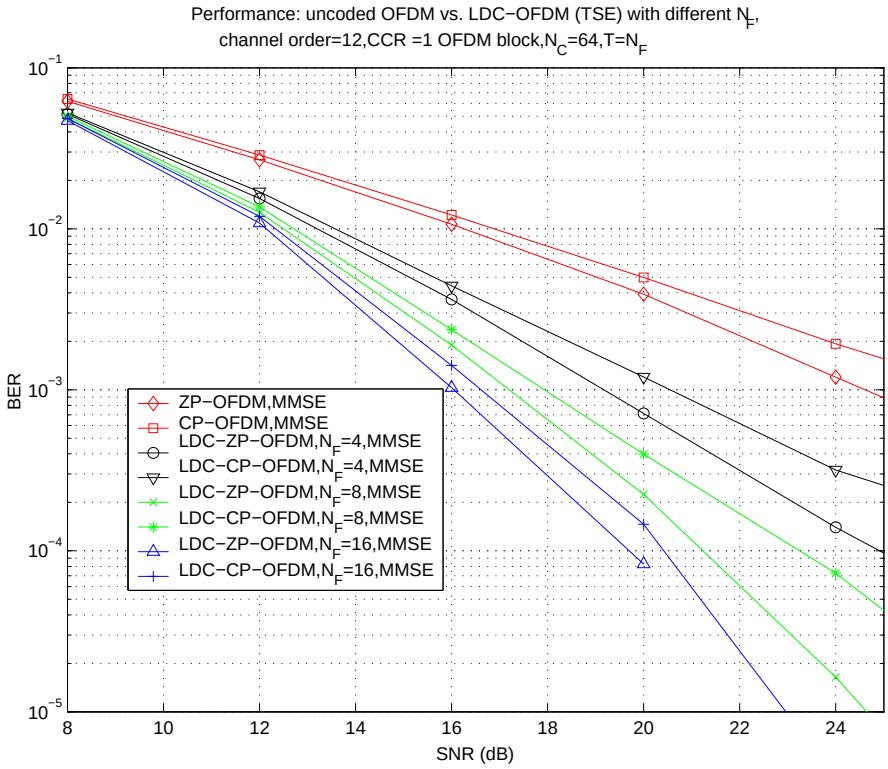

Figure 5.5. BER Performance of OFDM vs. LDC-OFDM, channel order 12, $CCI = 1$ OFDM block, $N_C = 64$, $T = N_F$

both LDC-ZP-OFDM and LDC-CP-OFDM.

5.6.2.2 LDC-OFDM under different channel dynamics

Figure 5.7 shows a performance comparison of BER vs. SNR of LDC-ZP-OFDM and LDC-CP-OFDM under various different CCIs. The channel order used in this case was set $L = 7$. Note that different CCIs arise from for different degrees of channel correlation over time. As discussed in Section 5.5, the diversity order of LDC-OFDM is achievable only if the channel provides corresponding diversity.

As shown, the performance of both LDC-ZP-OFDM and LDC-CP-OFDM is notably influenced by channel dynamics or time correlation, which are represented by different CCIs. At high SNRs, the faster the channel changes, the better the performance. This indicates that both LDC-ZP-OFDM and LDC-CP-OFDM effectively exploit available temporal diversity across multiple OFDM blocks. In the future, testing on a more accurate model of channel dynamics is needed to obtain a more accurate assessment.

Note that, although the time diversity advantage is notable in Figure 5.7, the time diversity gain is small. The reason for the above observation is not the usage of linear decoding but the usage of a code that does not possess full temporal diversity. However, in Section 6.5.5, LDC-OFDM shows a significant time diversity gain in time varying channels, when the code that possesses full temporal diversity is chosen.

5.6.2.3 Comparison of LDC-OFDM and LCP-OFDM

Recently, linear constellation precoded OFDM (LCP-OFDM) with subcarrier grouping was proposed as a non-redundancy approach to improve BER performance [72]. However, although LCP-OFDM achieves both maximum frequency selective diversity

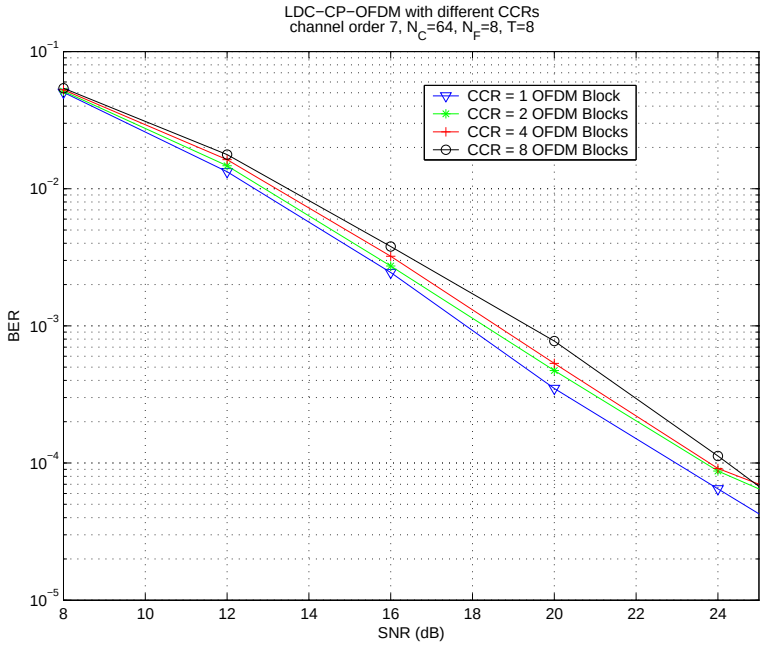

(a) Performance of LDC-CP-OFDM,channel order 7, $N_C = 64$, $N_F = 8$, $T = 8$

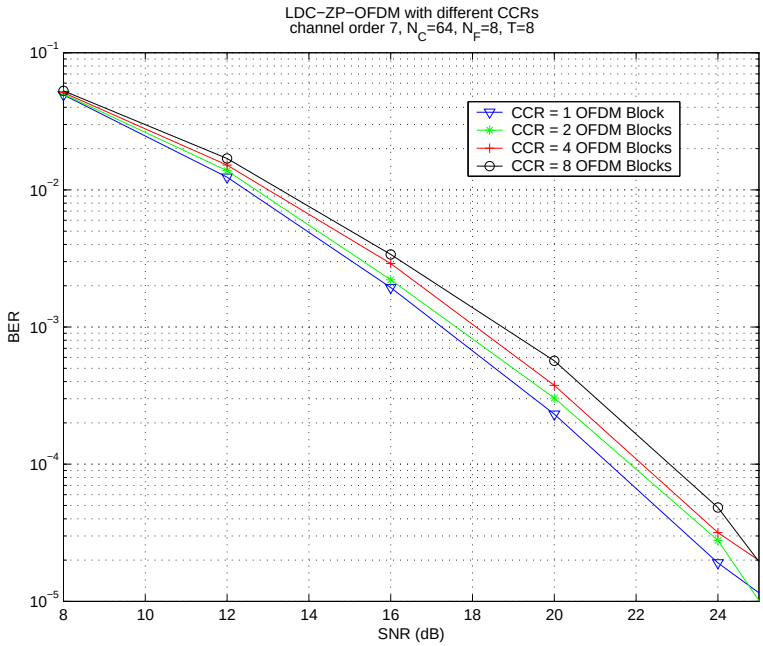

(b) Performance of LDC-ZP-OFDM,channel order 7, $N_C = 64$, $N_F = 8$, $T = 8$

Figure 5.6. BER Performance of LDC-OFDM under different channel dynamics

gain and coding gain, LCP-OFDM cannot exploit time diversity over OFDM blocks. We have compared LCP-OFDM with our proposed LDC-OFDM under both cyclic prefix and zero-padding cases. In the simulations, the OFDM block length was also set to $N_C = 64$, and the channel order L was set to 7. The LCP uses the construction LCP-A shown in Table I of [72], thus LCP-OFDM may approach both maximum frequency selective diversity and coding gains. For a fair comparison, all the settings of LCP-OFDM were the same as those of LDC-OFDM. Thus the diversity available is the same for both LDC-OFDM and LCP-OFDM.

Note that, to date, linear constellation precoded ZP-OFDM has not been studied previously to our knowledge, while LCP with CP-OFDM has been analyzed in [72].

It is not surprising that in Figures 5.7(a) and 5.7(b), both LCP-ZP-OFDM and LCP-CP-OFDM systems perform similarly under $CCI = 1$ and $CCI = 8$. LDC-ZP-OFDM and LDC-CP-OFDM systems perform similarly to LCP-ZP-OFDM and LCP-CP-OFDM under $CCI = 8$, respectively. That is to say, when channels have full correlation over time (OFDM blocks), properly designed LDC-OFDM could potentially achieve both maximum frequency selective diversity gain and coding gain. Further, LDC-ZP-OFDM and LDC-CP-OFDM outperform LCP-ZP-OFDM and LCP-CP-OFDM under $CCI = 1$, respectively. That is to say, when channels have no correlation over time (OFDM blocks), properly designed LDC-OFDM can exploit time independence or diversity, while LCP-OFDM cannot, which agrees to the analysis in Section 5.5. Thus, LDC-OFDM systems show noticeable advantages over LCP-OFDM systems in channel environments that vary over OFDM blocks.

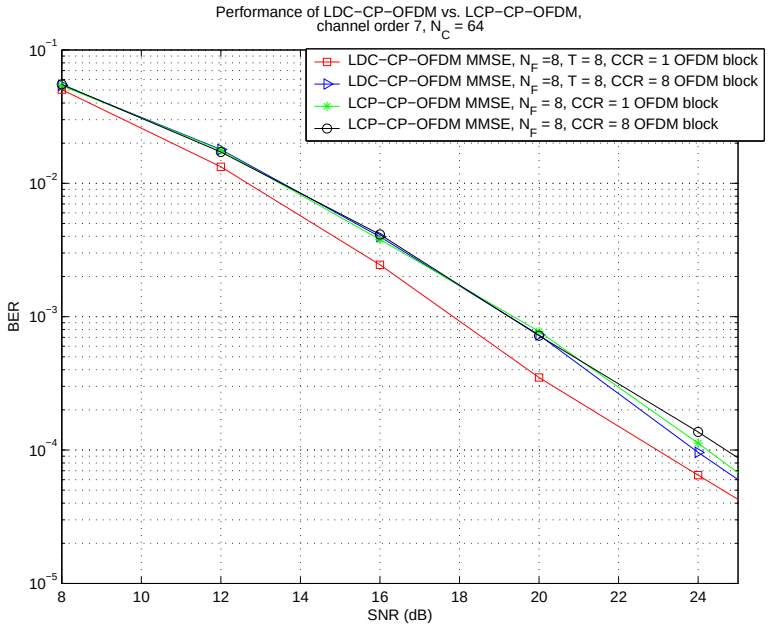

(a) Performance of LDC-CP-OFDM vs. LCP-CP-OFDM,channel order 7, $N_C = 64$

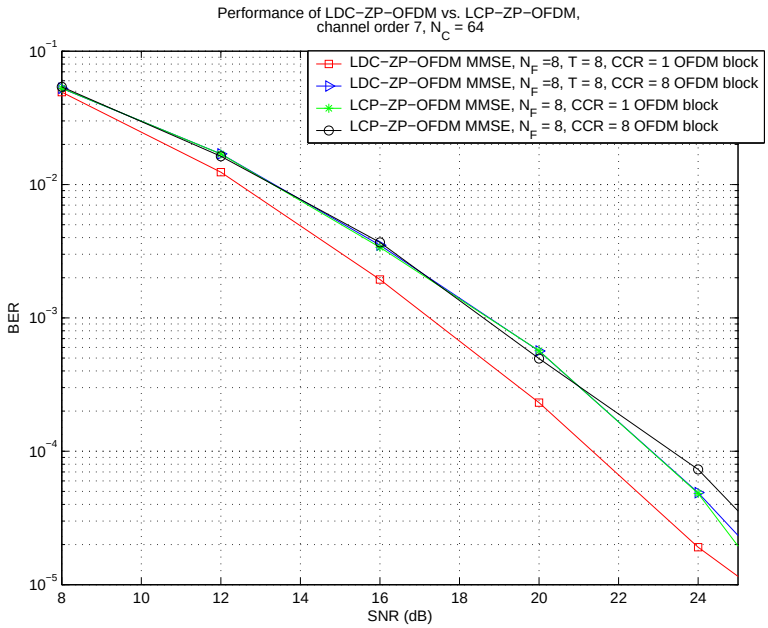

(b) Performance of LDC-ZP-OFDM vs. LCP-ZP-OFDM,channel order 7, $N_C = 64$

Figure 5.7. BER Performance of LCP-OFDM vs. LDC-OFDM

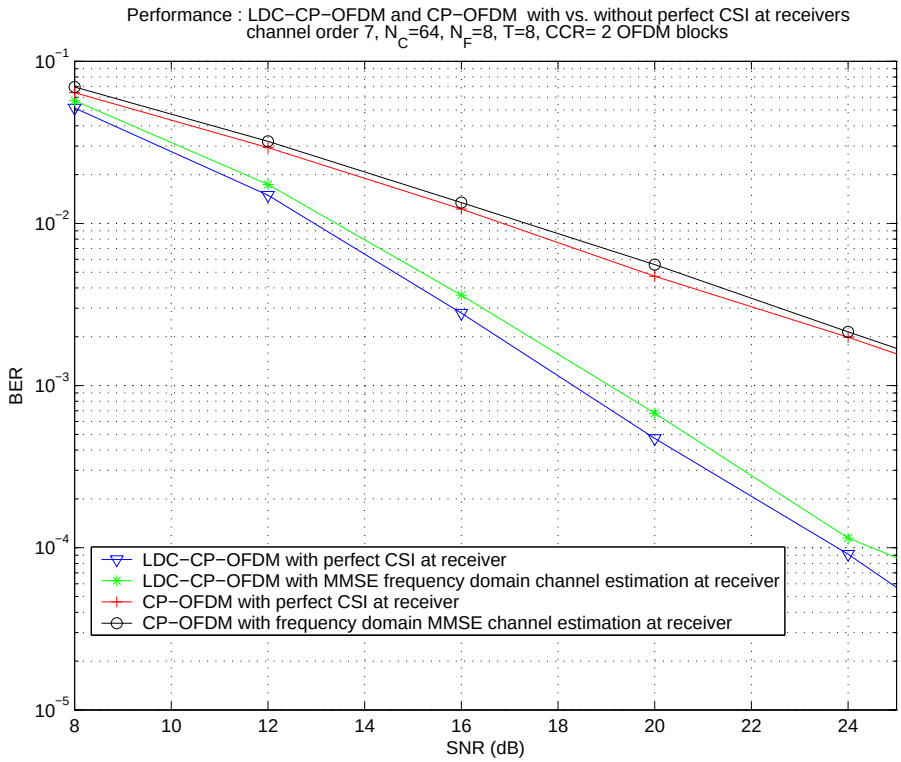

Figure 5.8. Effects of LDC-CP-OFDM under estimated channel information, channel order 7, $N_C = 64$, $N_F = 8$, $T = 8$, $CCI = 2$ OFDM blocks

5.6.2.4 Comparison of LDC-CP-OFDM under perfect CSI vs. estimated channel information

To consider a more realistic scenario in terms of effects of imperfect channel state information (CSI) at receiver, Figure 5.8 shows a performance comparison of BER performance of LDC-CP-OFDM under perfect CSI vs. estimated channel information. The estimated channel information is obtained through pilot-based standard MMSE channel estimation [22].

It can be observed that the performance of both LDC-CP-OFDM and uncoded CP-OFDM degrades under estimated channel information. For instance, at a BER of 10^{-2}, compared with the case of perfect CSI, the performances of LDC-CP-OFDM and uncoded CP-OFDM degrade by 0.31dB and 0.22dB, respectively. LDC-CP-OFDM is more sensitive to channel estimation errors than CP-OFDM. However, although the performance loss of LDC-CP-OFDM under estimated channel information is higher that of CP-OFDM, LDC-CP-OFDM under MMSE channel estimation outperforms CP-OFDM under MMSE channel estimation, since the high diversity gain of LDC-OFDM compensate for performance loss due to channel estimation errors.

5.6.2.5 Comparison of LDC-ZP-OFDM under MMSE vs. low complexity MMSE receivers

In Section 5.3, a layered structure of TSE LDC-OFDM has been discussed. This is demonstrated by the comparison of LDC-ZP-OFDM under MMSE vs. low complexity MMSE equalizers in Figure 5.9. The low complexity MMSE equalizer is given in (5.16) in Section 5.3.2.3. The ZP-OFDM-FAST-MMSE approach was designed by approximation [66], which may degrade performance compared with that of standard MMSE equalizer.

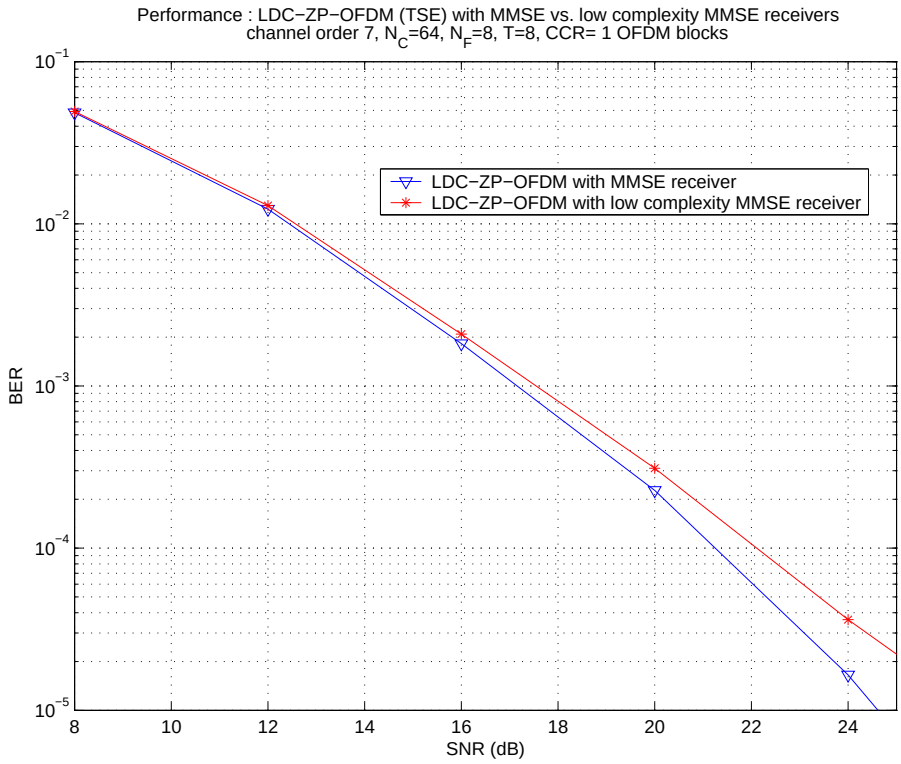

Figure 5.9. BER Performance of LDC-ZP-OFDM (TSE) under MMSE vs. low complexity MMSE receivers, channel order 7, $N_C = 64$, $N_F = 8$, $T = 8$, $CCI = 1$ OFDM block

From Figure 5.9, it can be seen that in the range of low to medium SNR, the performance of LDC-ZP-OFDM under MMSE vs. low complexity MMSE equalizers is quite close. At BER of 10^{-3}, compared with the case of under MMSE equalizer, the performance of LDC-ZP-OFDM under low complexity MMSE equalizer degrades by only 0.4dB. In other words, almost the same high diversity gain is maintained for both equalizers. With an increase of SNR, the performance loss due to using a low complexity approach becomes more significant. At a BER of 10^{-4}, the performance loss of LDC-ZP-OFDM under low complexity MMSE equalizer is 0.8dB.

This comparison represents just one example of the flexibility of layered structure flexibility using different equalizers. OFDM systems have been developed about 40 years, and extensive research work have been conducted for OFDM signal estimation, which may be applied in TSE LDC-OFDM systems.

5.6.3 Performance Analysis and Comparison of OSE based LDC-OFDM

In this performance analysis of OSE LDC-OFDM systems, two performance measures used are bit error probability (BER) and decision-point SINR. To evaluate SINR performance, we propose to determine the probability that the instantaneous SINR is larger than a threshold, i.e. $\Pr(SINR > SINR_0)$, which we call SINR distribution. This method is inspired by investigation of OFDM Peak-to-Average Power Ratio (PAPR).

The BER and SINR performance results were obtained through Monte Carlo simulation and calculation respectively, with channel order $L = 7$ and exponential power delay profile, and random channel coefficients with Rayleigh fading. Uncorrelated

QPSK modulated source data symbols were used throughout. The number of sub-carriers in an OFDM block was set to $N_C = 32$. Channel change interval was set to $CCI = 1$

5.6.3.1 BER Comparison

Fig. 5.10 shows BER performance vs. receiver input average symbol SNR of OFDM and OSE/TSE LDC-OFDM.

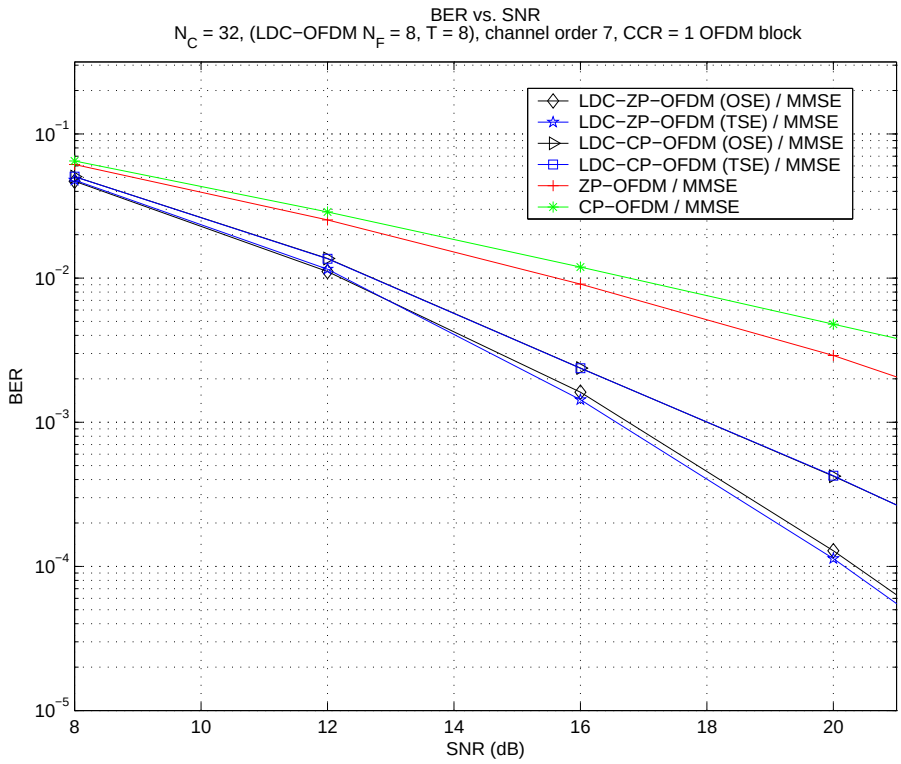

Figure 5.10. BER Performance of OFDM vs. LDC-OFDM (OSE) vs. LDC-OFDM (TSE),$N_C = 32$, (LDC-OFDM $N_F = 8$, $T = 8$), channel order 7, $CCI = 1$ OFDM block

It can be seen that the performance of the OSE and TSE cases for both LDC-ZP-OFDM and LDC-CP-OFDM are quite close. We reiterate that the LDC encoding

matrices chosen $\mathbf{G}_{LDC}^{(k)}, k = 1, ..., T$ corresponding to the LDC code (Eq. (31) of [42]) are unitary matrices, which result in uncorrelated LDC-coded symbols. It appears that TSE actually consists of two decoupled estimation stages. In other words, it is possible that by using special LDC coding matrices, two-step-estimation with much lower complexity could produce performance close to that of one-step-estimation.

Further, it appears that the two estimation stages are not completely uncorrelated for LDC-ZP-OFDM case. The two estimation stage of LDC-CP-OFDM shows better decorrelation, possibly because of the maintenance of orthogonality of CP-OFDM.

5.6.3.2 SINR Comparison

The SINR results shown in this part were generated through Monte Carlo calculation, using (5.38), where frequency selective Rayleigh fading channel coefficients were randomly produced .

From Fig. 5.11, it is found the average SINR of OFDM is at least 5 dB higher than that of LDC-ZP-OFDM for each SNR. This point is somewhat surprising, which tells us that LDC-ZP-OFDM systems do not provide an average SINR gain. On the contrary, a large average SINR loss results. Average SINR, however, does not provide insights of LDC-OFDM.

To explain the above performance improvement, we investigate instantaneous SINR performance of the one-step system. In multipath fading channels, signals may experience deep fading. In OFDM systems, wideband channels are transformed into parallel narrowband channels. This reduces deep fading effects generally, but there usually exist some subcarriers that experience deep fading, which is a main source of bit errors. The probability distribution of being in a low SINR region, say from 0 to 5dB, determines overall performance. Thus Figure 5.12(b) for $SNR = 8dB$,

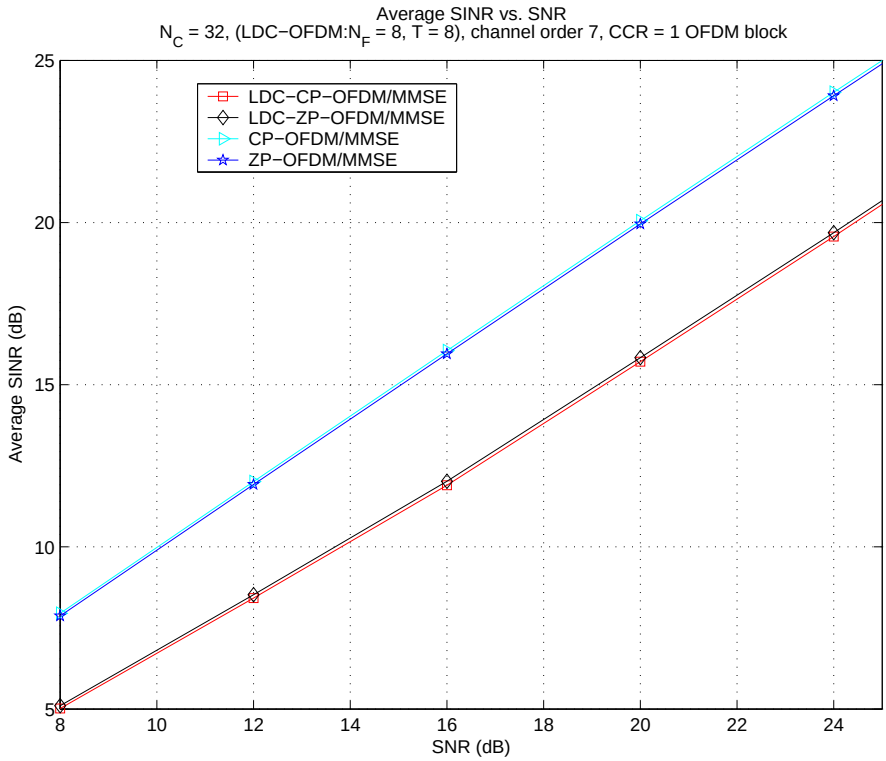

Figure 5.11. Average SINR vs. SNR between OFDM and LDC-OFDM, $N_C = 32$, (LDC-OFDM $N_F = 8$, $T = 8$), channel order 7, $CCI = 1$ OFDM block

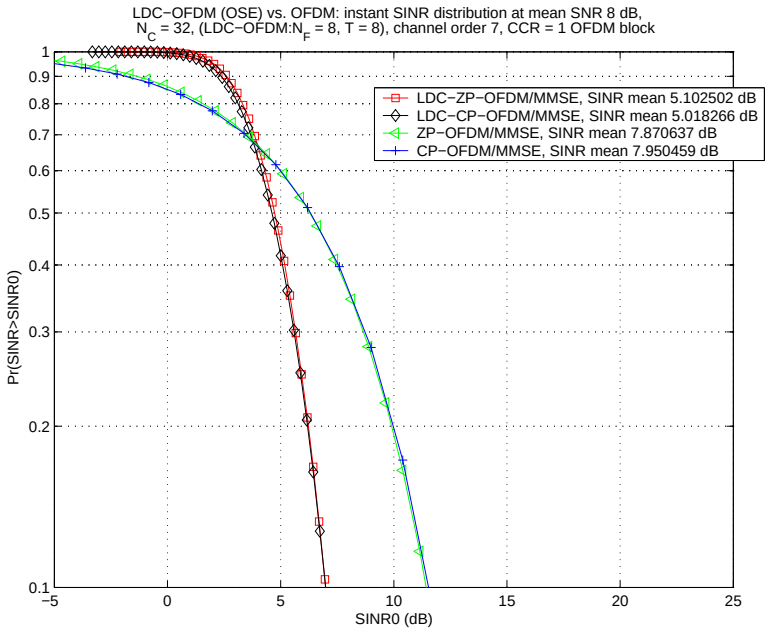

(a) $Pr(SINR > SINR_0) \geq 0.1$

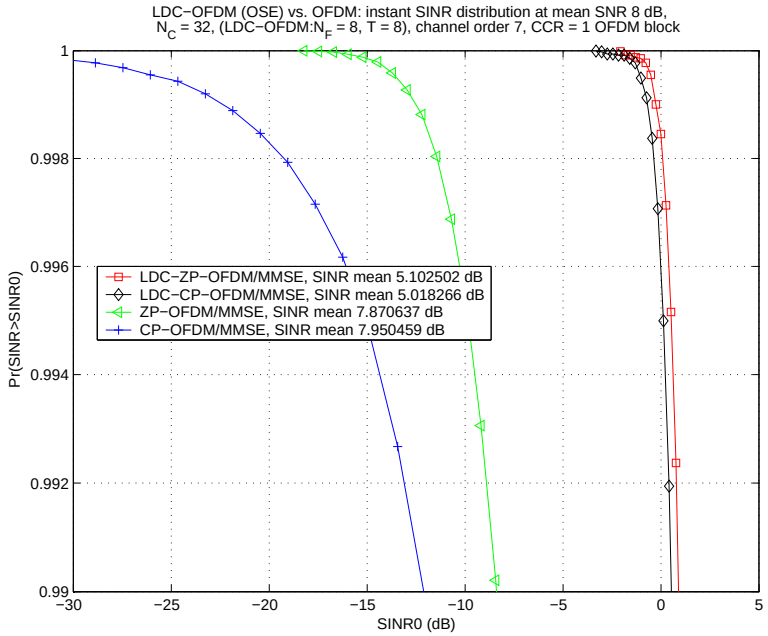

(b) $Pr(SINR > SINR_0) \geq 0.99$

Figure 5.12. SINR Distribution at $SNR = 8dB$, $N_C = 32, N_F = T = 8$,

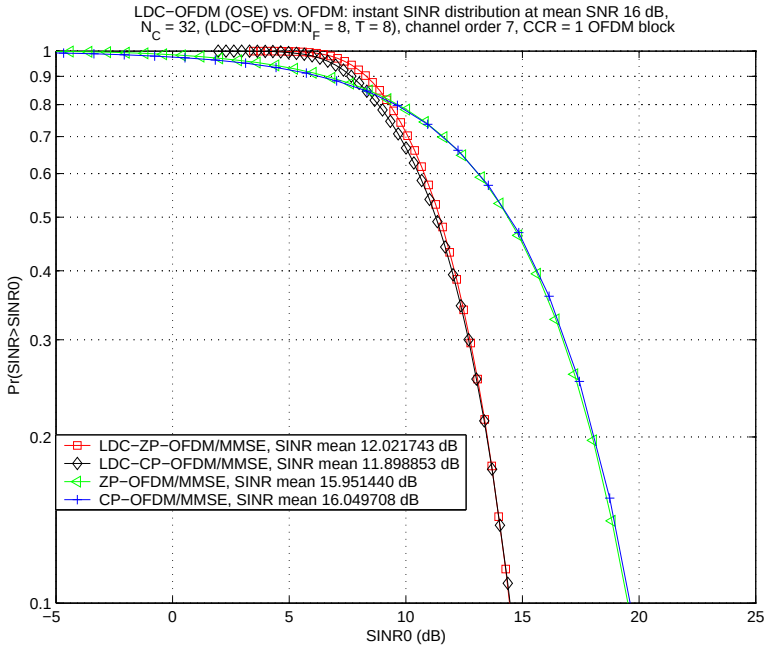

(a) $Pr(SINR > SINR_0) \geq 0.1$

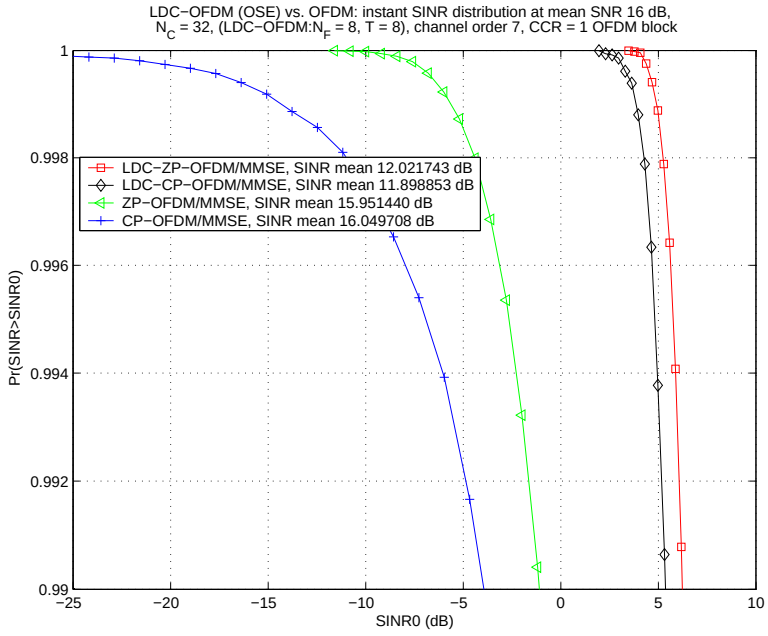

(b) $Pr(SINR > SINR_0) \geq 0.99$

Figure 5.13. SINR Distribution at $SNR = 16dB$, $N_C = 32, N_F = T = 8$,

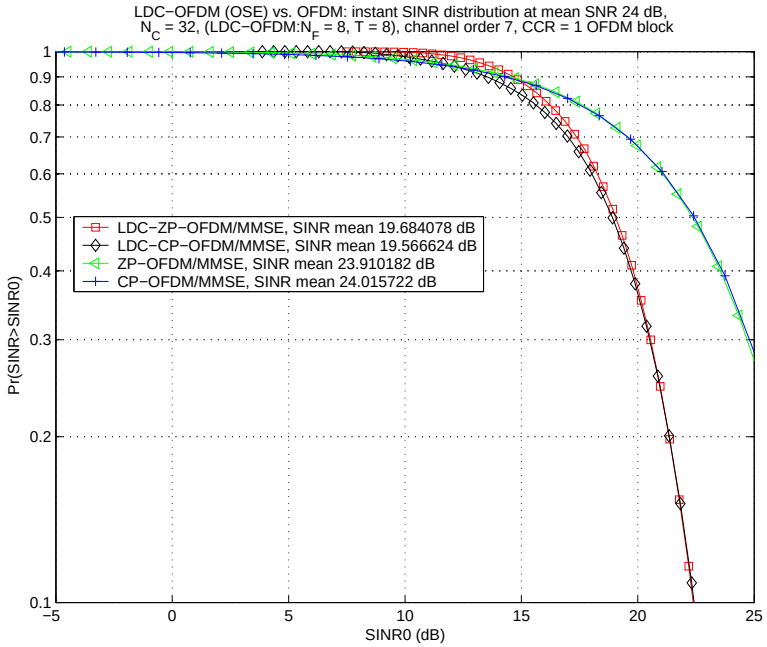

(a) $Pr(SINR > SINR_0) \geq 0.1$

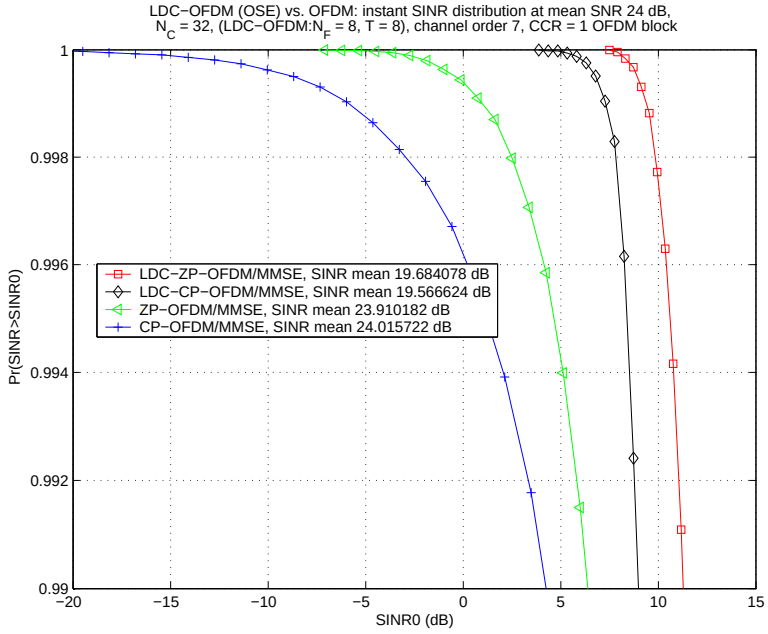

(b) $Pr(SINR > SINR_0) \geq 0.99$

Figure 5.14. SINR Distribution at $SNR = 24dB$, $N_C = 32, N_F = T = 8$,

Figure 5.13(b) for $SNR = 16dB$, and Figure 5.14(b) for $SNR = 24dB$ are more important than Figure 5.12(a) for $SNR = 8dB$, Figure 5.13(a) for $SNR = 16dB$, and Figure 5.14(a) for $SNR = 24dB$, respectively, in terms of depicting the critical low SINR region for investigating error performance. From Figures 5.12(a), 5.13(a), and 5.14(a), the reason why OFDM has much better average SINR than LDC-OFDM becomes clear. In high $SNR = 16dB$ and $SNR = 24dB$ and low SINR regions, the added diversity offered by LDC results in clear improvement. At an $SNR = 8dB$, the MMSE receivers of LDC-ZP-OFDM and LDC-CP-OFDM have better SINRs than those of ZP-OFDM only when the SINR is less than $3.5dB$, where bit errors are highly likely, which is the reason that the performance improvement of LDC-OFDM over OFDM is not that significant, as is shown in Figure 5.10. Observing Figures 5.12(b), 5.13(b), and 5.14(b), the more SNR increases, the more the gap in SINR performance between LDC-ZP-OFDM and LDC-CP-OFDM, which leads to an increase in corresponding BER performance gap, as is shown in Figure 5.10.

5.6.4 Peak-to-average power ratio comparison

The concept of PAPR has been introduced in Section 2.3.1.2. Here, the number of subcarriers of OFDM, N_C, is set to 64. Simulation results in Figure 5.15 show the PAPRs of LDC-OFDM systems and OFDM systems are similar. Thus, LDC-OFDM systems may improve BER without increasing PAPR. We remark that, the unitary G_{LDC} chosen is a possible reason for the results of simulations. We conjecture that properly chosen linear dispersion matrices could reduce the PAPR of LDC-OFDM further over that of OFDM.

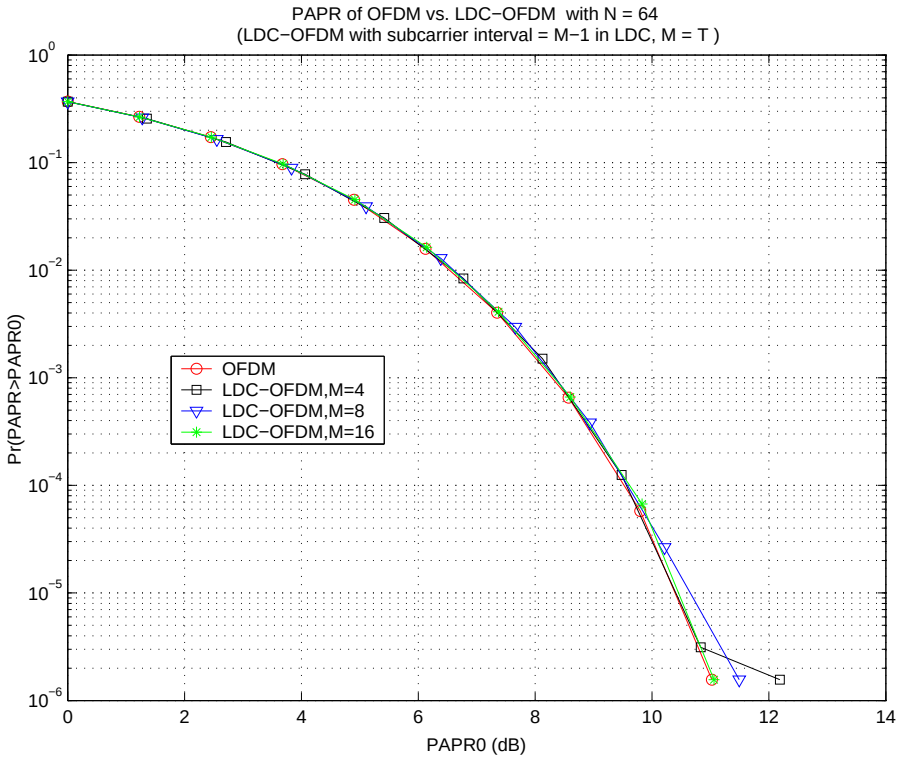

Figure 5.15. PAPR performance of OFDM vs. LDC-OFDM

5.7 Conclusion

Inspired by a technique proposed for space-time processing, we have applied linear dispersion codes to improve OFDM performance in multipath fading channels. The attractive LD codes can be advantageously combined with OFDM transmission to enable simple decoding. Recently, we note that an concurrent work with this topic is published recently [82], and unlike their work, we provide a thorough diversity analysis for this topic. A novel LDC decoding strategy, two step estimation (TSE), is proposed for a special subclass of LDC matrices with the constraint (3.10), which eliminates the direct dependency between LDC decoding and channel knowledge. At a cost of increased decoding delay, the proposed LDC decoder can support channels that change across OFDM blocks. Exploiting both frequency and time diversity available in frequency selective wideband OFDM channels, the performance of the proposed LDC-OFDM has high transmission bandwidth efficiency and improved BER. For instance, as shown in Figure 5.5, LDC-ZP-OFDM across 8 subcarriers per LDC codeword obtains 3.5 dB and 7.3 dB gains over ZP-OFDM observed at BERs of 10^{-2} and 10^{-3}, respectively. With lower complexity, the performance of TSE LDC-OFDM systems is close to that of OSE LDC-OFDM systems.

Motivated by the significant performance gain of LDC-OFDM as observed in Section 5.3, we analyze performance by formulating a single linear system of equations. Although higher complexity, the single-step receiver is mathematically tractable. This chapter also introduces a new performance analysis method for diversity systems involving the instantaneous SINR probability distribution.

This chapter analytically provides the upper bound diversity order that LDC-OFDM can achieve, which gives insights of linear dispersion over time and frequency. A properly designed LDC-OFDM could potentially utilize full available time and

frequency diversity in a given communication channel. This chapter also provides a design criterion of full diversity frequency-time block for LDC-OFDM, which may direct new LDC-OFDM design in the future.

Through simulations, this chapter shows that LDC-OFDM systems have the potential to maintain good performance even with imperfect channel estimation and low complexity receivers.

Chapter 6

Linear dispersion for single-carrier communications in frequency selective channels

6.1 Introduction

With the increases in data rate, broadband communication signals often experience frequency selective fading, increasing the problem of inter-symbol interference (ISI). Recently, cyclic-prefix single-carrier modulation (CP-SCM) with frequency-domain equalization (FDE) has attracted a lot of attention. Similar to orthogonal frequency-division multiplexing (OFDM) [48], CP-SCM FDE provides much lower computational complexity than conventional time-domain equalization techniques, especially for long impulse response tail channels [26]. Unlike OFDM, CP-SCM does not suffer high peak-to-average power ratio (PAPR) as well as sensitivity to frequency and phase offsets (carrier-frequency offsets, or CFO) [48], and nonlinear distortions [10]. CP-SCM FDE has been recommended for fixed wireless broadband standard IEEE 802.16 [1]. The complexity of CP-SCM-FDE transmitter is simpler than that of

OFDM, due to lack of Fast Fourier Transform (FFT) components, and [26] encourages the use of CP-SCM in the uplink and OFDM in the downlink in order to reduce the processing complexity at the terminal.

In Chapter 5, high-rate linear dispersion codes have been employed to obtain joint frequency and time diversity in OFDM, known as LDC-OFDM. Although LDC has been applied to multicarrier communications, it has not been investigated for application in single stream single carrier communications. This chapter investigates the application of LDC to achieve joint frequency-time diversity in CP-SCM for frequency selective channels.

This chapter proposes to apply linear dispersion codes to single-carrier block communications (SCBC). Two types of SCBC are considered: cyclic-prefix single-carrier modulation (CP-SCM) and zero-padded single-carrier modulation (ZP-SCM). CP-SCM utilizes frequency-domain equalization (FDE) with lower complexity, due to its use of the computationally-efficient fast Fourier transform (FFT). Note that the complexity of time-domain equalization using Viterbi algorithms (TDE) grows exponentially with channel memory and spectral efficiency (trellis-based schemes) or requires very long FIR filters to achieve satisfactory performance (e.g., decision feedback equalizers) [26]. This chapter shows that ZP-SCM may perform with lower complexity using approximate frequency-domain equalization (AFDE). Both CP-SCM and ZP-SCM enjoy lower PAPR and are more robust to CFO [26, 116]. Unlike LDC-OFDM, in which LDC significantly exploits both frequency and time diversity available in the channels, simulations reveal that LDC primarily improves time diversity in LDC-SCM.

6.2 Single-carrier communications model

Assume the communications channel experiences frequency-selective fading, and the channel for the k-th SCM block is modeled as an L th-order FIR filter with impulse response $\mathbf{h}^{(k)} = \left[h_0^{(k)}, ..., h_L^{(k)}\right]^{\mathcal{T}}$. Channel coefficients are constant within one SCM block but change statistically independently across different SCM blocks. Each SCM block is of size $P = N_C + N_g$, including a data symbol block of size N_C and a guard interval of size $N_g \geq L$ to avoid inter-block interference.

Denote $\mathbf{x}_{SC}^{(k)}$ as the channel data symbol vector transmitted during the k-th SCM block of size $N_C \times 1$, and $\mathbf{x}_{SC}^{(k)} = \left[x_{SC(1)}^{(k)}, ..., x_{SC(N_C)}^{(k)}\right]^{\mathcal{T}}$, where $x_{SC(p)}^{(k)}, p = 1, ..., N_C$ is the p-th data symbol of the k-th SCM block in sequence. Each receive antenna experiences additive white complex Gaussian noise. The system signal-to-noise-ratio (SNR) is denoted by ρ.

6.2.1 CP-SCM case

Before transmission, a cyclic prefix (CP) guard interval is appended to each CP-SCM block. The CP is then removed at the receiver. The effective channel of the k-th SCM block is a circulant matrix $\mathbf{H}_{CP\_SC}^{(k)}$ with elements $\left[\mathbf{H}_{CP\_SC}^{(k)}\right]_{a,b} = h_{((a-b) \bmod N_C)}^{(k)}$. Hence, the CP-SCM block system can be modeled as

$$\mathbf{r}_{CP\_SC}^{(k)} = \sqrt{\rho}\mathbf{H}_{CP\_SC}^{(k)}\mathbf{x}_{SC}^{(k)} + \mathbf{v}_{CP\_SC}^{(k)} \tag{6.1}$$

where $\mathbf{r}_{CP\_SC}^{(k)}$ is the received block after CP removal, and $\mathbf{v}_{CP\_SC}^{(k)}$ is the corresponding noise vector.

At the receiver, the received block $\mathbf{r}_{CP\_SC}^{(k)}$ is first processed by an FFT to generate block $\mathbf{y}_{CP\_SC}^{(k)} = \mathbf{F}_{N_C}\mathbf{r}_{CP\_SC}^{(k)}$.

Due to the circulant property of $\mathbf{H}_{CP\_SC}^{(k)}$, can be decomposed as

$$\mathbf{H}_{CP\_SC}^{(k)} = [\mathbf{F}_{N_C}]^{\mathcal{H}} \mathbf{D}_{CP\_SC}^{(k)} \mathbf{F}_{N_C},$$

where $\mathbf{D}_{CP\_SC}^{(k)}$ is diagonal with

$$\left[\mathbf{D}_{CP\_SC}^{(k)}\right]_{pp} = \sum_{l=0}^{L} h_l^{(k)} \exp\left(-j2\pi l(p-1)/N_C\right).$$

Thus, the frequency domain system equation is

$$\mathbf{y}_{CP\_SC}^{(k)} = \sqrt{\rho}\mathbf{D}_{CP\_SC}^{(k)}\mathbf{F}_{N_C}\mathbf{x}_{SC}^{(k)} + \mathbf{F}_{N_C}\mathbf{v}_{CP\_SC}^{(k)}. \tag{6.2}$$

6.2.2 ZP-SCM case

Due to zero padding, the ZP-SC system model does not have a simple frequency domain format shown in (6.2). However, the ZP-SCM system model can be written in block matrix form in the time domain as,

$$\mathbf{r}_{ZP\_SC}^{(k)} = \sqrt{\rho}\mathbf{H}_{ZP\_SC}^{(k)}\mathbf{x}_{SC}^{(k)} + \mathbf{v}_{ZP\_SC}^{(k)}, \tag{6.3}$$

where $\mathbf{H}_{ZP\_SC}^{(k)}$ represents a Toeplitz convolution matrix with $\left[\mathbf{H}_{ZP\_SC}^{(k)}\right]_{a,b} = h_{(a-b)}^{(k)}$, where $\mathbf{r}_{ZP\_SC}^{(k)}$ is the received block of size $P \times 1$, and is the corresponding noise vector of size $\mathbf{v}_{ZP\_SC}^{(k)}$. Due to the Toeplitz structure of $\mathbf{H}_{ZP\_SC}^{(k)}$, $\mathbf{H}_{ZP\_SC}^{(k)}$ is guaranteed to be invertible, regardless of the channel zero locations in reality [66].

6.3 Proposed LDC based single-carrier block communications

6.3.1 Proposed system structure

Similar to LDC-OFDM, we adopt a layered approach, shown in Figure 6.1, that utilizes a two-step-estimation (TSE) procedure as discussed in Section 5.3.

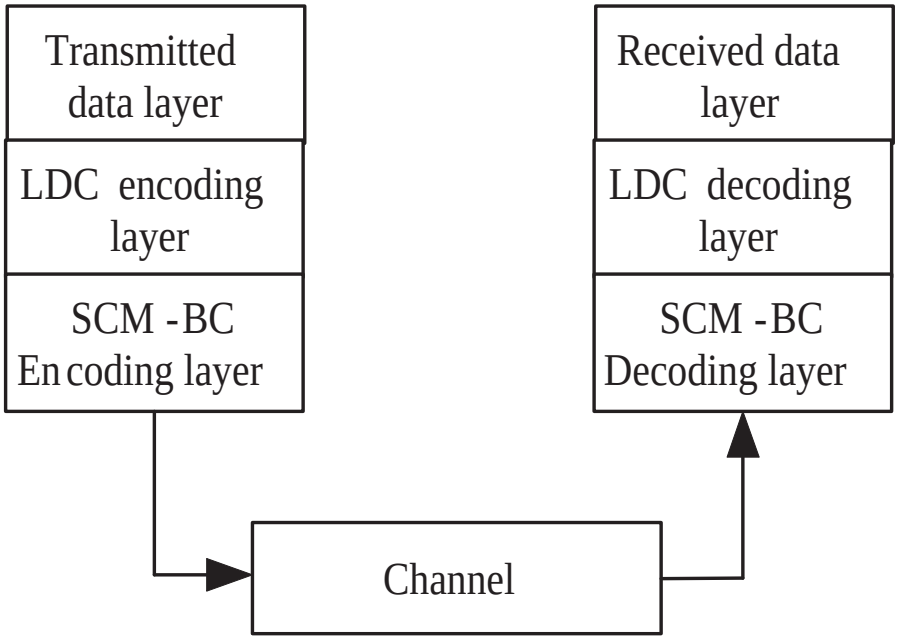

Figure 6.1. Layered structure of linear dispersion coded single-carrier modulation block communications (SCM-BC)

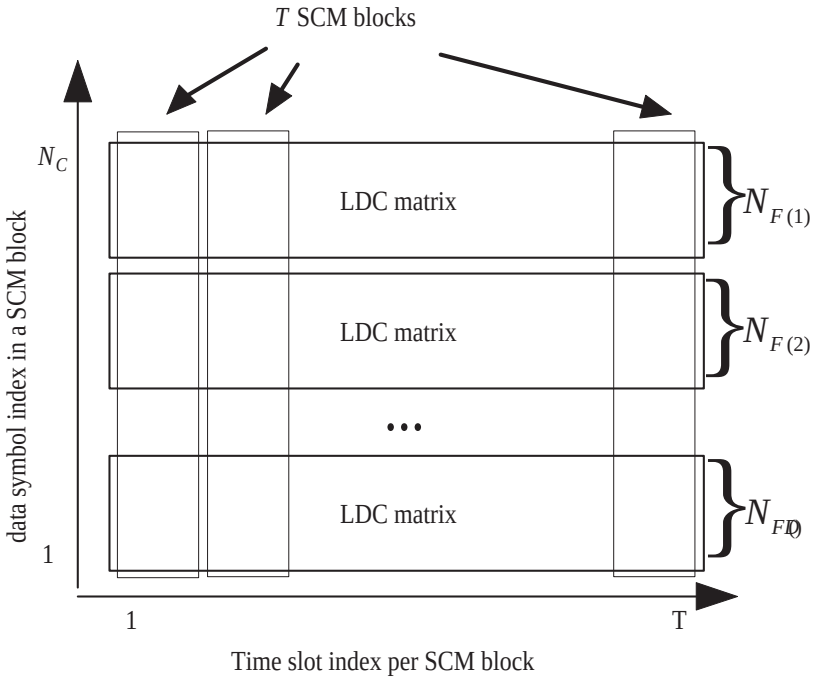

Figure 6.2. LDC-SCM block plane

One LDC-CP-SCM block, as shown in Figure 6.2, consists of T adjacent SCM blocks. In addition, one LDC-SCM block includes D LDC codewords, each of size $T \times N_{F(i)}, i = 1, ..., D$, where $N_{F(i)}$ is the number of channel symbols within one SCM block, which the i-th LDC codeword is across. Thus, the maximal size of one LDC-SCM block is $T \times N_C$.

One LDC-SCM block is transmitted during the period of T SCM blocks, a guard interval (CP or ZP) is added to each SCM block before transmission. After the transmitted channel symbols are corrupted in the channels, the receiver removes the guard interval and performs equalization.

For the LDC-CP-SCM receiver, frequency-domain equalization (FDE) can be applied as shown in Figure 6.3. The received SCM data block arrived is first FFT-processed. Then, the influence of the frequency-selective channel impulse response is

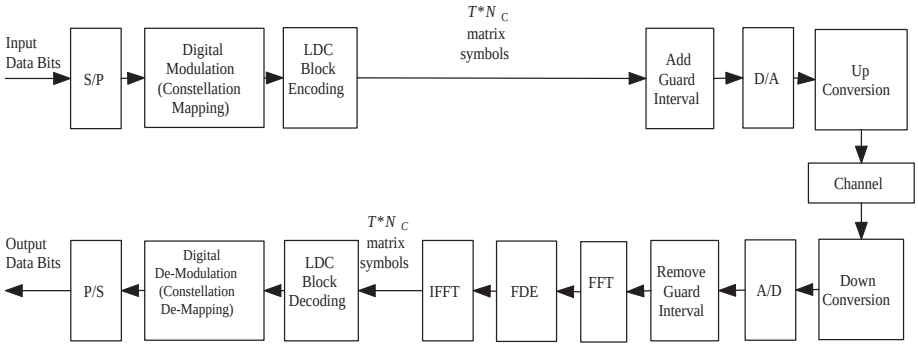

Figure 6.3. Proposed LDC-CP-SCM system model

eliminated by the FDE. The inverse FFT operation returns the equalized signals to the time domain prior to LDC decoding.

6.3.2 LDC-SCM receiver

Denote the LDC encoding matrix of the i-th LDC matrix codeword $\mathbf{S}_{LDC}^{(i)} \in C^{T \times N_{F_{(i)}}}$ as $\mathbf{G}_{LDC}^{(i)}$, which encodes source data symbol vector with zero mean, unit variance, $\mathbf{s}^{(i)} = \begin{bmatrix} s_1^{(i)} & s_1^{(i)} & \dots & s_{Q_i}^{(i)} \end{bmatrix}^{\mathcal{T}}$ into $vec(\mathbf{S}_{LDC}^{(i)})$, where Q_i is the number of source data symbols in $\mathbf{s}^{(i)}$, $i = 1, ..., D$.

6.3.2.1 First estimation step - SCM demodulation

In the proposed LDC decoding algorithm, LDC decoding is independent of SCM signal estimation. Thus, the proposed LDC-SCM system is backwards-compatible to conventional SCM systems.

In Section 8.5, performance is investigated using minimum-mean-squared-error (MMSE) equalization. Assuming that single carrier symbols are normalized to unit variance, the respective frequency and time domain equalizers are given by [83]

1) CP-SCM MMSE-FDE

$$\mathbf{G}_{CP\_SC}^{(k)} = \sqrt{\rho}\mathbf{C}_{\mathbf{x}_{SC}^{(k)}} \left(\mathbf{D}_{CP-SC}^{(k)}\right)^{\mathcal{H}} \cdot \left(\mathbf{I}_{N_C} + \rho\mathbf{D}_{CP-SC}^{(k)}\mathbf{C}_{\mathbf{x}_{SC}^{(k)}} \left(\mathbf{D}_{CP-SC}^{(k)}\right)^{\mathcal{H}}\right)^{-1} \quad (6.4)$$

$$\widehat{\mathbf{x}_{SC}^{(k)}} = \left[\mathbf{F}_{N_C}\right]^{\mathcal{H}} \mathbf{G}_{CP\_SC}^{(k)} \mathbf{y}_{CP\_SC}^{(k)} \quad (6.5)$$

2) ZP-SCM MMSE-TDE

$$\mathbf{G}_{ZP\_SC}^{(k)} = \sqrt{\rho}\mathbf{C}_{\mathbf{x}_{SC}^{(k)}} \left(\mathbf{H}_{ZP-SC}^{(k)}\right)^{\mathcal{H}} \cdot \left(\mathbf{I}_P + \rho\mathbf{H}_{ZP-SC}^{(k)}\mathbf{C}_{\mathbf{x}_{SC}^{(k)}} \left(\mathbf{H}_{ZP-SC}^{(k)}\right)^{\mathcal{H}}\right)^{-1} \quad (6.6)$$

$$\widehat{\mathbf{x}_{SC}^{(k)}} = \mathbf{G}_{ZP\_SC}^{(k)} \mathbf{r}_{ZP\_SC}^{(k)} \quad (6.7)$$

where $k = 1, ..., T$, $\mathbf{C}_{\mathbf{x}_{SC}^{(k)}}$ is the covariance matrix of the k-th SCM block within one LDC-SCM block, which can be calculated using LDC encoding matrices.

In ZP-SCM system, the carrier frequency offset (CFO) acts as multiplicative noise that reduces the useful signal amplitude but does not cause ISI, thus ZP-SCM is more robust against CFO. Although ZP-SCM system does not perform explicit accurate frequency domain equalization (FDE), ZP-SCM could be formulated as an approximate frequency domain equalizer (AFDE).

Denote

$$\mathbf{D}_{\mathbf{H}_P^{(k)}} = \mathbf{F}_P \mathbf{H}_P^{(k)} \left[\mathbf{F}_P\right]^{\mathcal{H}}$$

where $\mathbf{H}_P^{(k)}$ is a is a circulant matrix with $\left[\mathbf{H}_P^{(k)}\right]_{a,b} = h_{((a-b) \bmod N_C)}^{(k)}$. Denote

$$\mathbf{T}_{ZP} = \begin{bmatrix} \mathbf{I}_{N_C} & \mathbf{0}_{(P-N_C)\times N_C} \end{bmatrix}^{\mathcal{T}}$$

and

$$\mathbf{U} = \mathbf{F}_P \mathbf{T}_{ZP}.$$

Thus, we have

$$\mathbf{H}_{ZP\_SC}^{(k)} = [\mathbf{F}_P]^{\mathcal{H}} \mathbf{D}_{\mathbf{H}_P^{(k)}} \mathbf{F}_P \mathbf{T}_{ZP}$$

Consequently, we could rewrite (6.3) in the AFDE form,

$$\mathbf{y}_{ZP\_SC}^{(k)} = \sqrt{\rho} \mathbf{D}_{\mathbf{H}_P^{(k)}} \mathbf{U} \mathbf{x}_{SC}^{(k)} + \mathbf{F}_P \mathbf{v}_{ZP\_SC}^{(k)} \tag{6.8}$$

where

$$\mathbf{y}_{ZP\_SC}^{(k)} = \mathbf{F}_P \mathbf{r}_{ZP\_SC}^{(k)}.$$

The corresponding MMSE-AFDE equalizer

$$\mathbf{G}_{ZP\_SC}^{(k)} = \sqrt{\rho} \mathbf{U} \mathbf{C}_{\mathbf{x}_{SC}^{(k)}} \mathbf{U}^{\mathcal{H}} \left(\mathbf{D}_{\mathbf{H}_P^{(k)}} \right)^{\mathcal{H}} \cdot \left(\mathbf{I}_P + \rho \mathbf{D}_{\mathbf{H}_P^{(k)}} \mathbf{U} \mathbf{C}_{\mathbf{x}_{SC}^{(k)}} \mathbf{U}^{\mathcal{H}} \left(\mathbf{D}_{\mathbf{H}_P^{(k)}} \right)^{\mathcal{H}} \right)^{-1} . \tag{6.9}$$

Note that the matrix inversion of the CP-SCM MMSE-FDE equalizer (6.4) may be performed element-wise if channel data symbols are uncorrelated. However, the matrix inversion of ZP-SCM MMSE time domain equalization (MMSE-TDE) equalizer (6.9) cannot be accurately element-wise performed due to the non-diagonal matrix $\mathbf{U}$. However, if $\mathbf{C}_{\mathbf{x}_{SC}^{(k)}} = \mathbf{I}_{N_C}$, (6.9) can be approximated as

$$\mathbf{G}_{ZP\_SC}^{(k)} = \sqrt{\rho} \left(\mathbf{D}_{\mathbf{H}_P^{(k)}} \right)^{\mathcal{H}} \left(\frac{P}{N_C} \mathbf{I}_P + \rho \mathbf{D}_{\mathbf{H}_P^{(k)}} \left(\mathbf{D}_{\mathbf{H}_P^{(k)}} \right)^{\mathcal{H}} \right)^{-1} , \tag{6.10}$$

which we call MMSE low complexity approximate FDE (MMSE-LC-AFDE). In (6.10), we extend the low complexity MMSE equalizer structure for ZP-OFDM in [66] to ZP-SCM systems.

6.3.2.2 Second estimation step - LDC-SCM block decoding

Reorganizing the results of the first estimation step into D estimated LDC matrix codewords, $\widehat{\mathbf{S}_{LDC}^{(i)}}, i = 1, ..., D$, the estimated data symbol vectors corresponding to D LDC blocks are

$$\widehat{\mathbf{s}^{(i)}} = \left[\mathbf{G}_{LDC}^{(i)} \right]^{\dagger} vec(\widehat{\mathbf{S}_{LDC}^{(i)}}). \tag{6.11}$$

6.3.3 Low complexity approaches - LTC-SCM

Unlike the general class of LDC of codeword size $T \times M$, where $M > 1$, we consider a special class of LDC of codeword size $T \times 1$, which we term linear transformation codes (LTC). Since single-carrier block communications themselves may achieve a certain degree of frequency diversity order, we proposes to apply LTC across multiple SCM blocks, which we call LTC-SCM. LTC-SCM is a class of low complexity approaches to achieve joint frequency and time diversity. Note that frequency diversity is not obtained from this transformation but from inherent properties of single-carrier block communications.

6.3.4 Peak-to-average power ratio (PAPR)

Single-carrier complex matrix codes (SCCMC) are currently proposed as space time block codes in the literature, and usually possess lower PAPR than OFDM. However, the PAPR of SCCMC is often higher than that of conventional constellation-based SCM. Fortunately, designing lower PAPR SCCMC is easier than designing lower PAPR OFDM based systems. Some initial efforts in addressing this issue can be found in [16, 18].

6.3.5 Carrier frequency offsets

Conventional constellation-based SCM have fewer problems with regard to carrier frequency offsets (CFO). We are interested in investigating performance of LDC-CP-SCM under CFO effects. With minor modification, we extend CP-OFDM CFO

system model in [111] to CP-SCM as follows:

$$\begin{aligned}\mathbf{y}_{CP\_SC}^{(k)} &= \sqrt{\rho}\phi(a)\mathbf{U}_{CFO}\mathbf{D}_{CP\_SC}^{(k)}\mathbf{F}_{N_C}\mathbf{x}_{SC}^{(k)} \\ &+\mathbf{F}_{N_C}\mathbf{v}_{CP\_SC}^{(k)}\end{aligned} \tag{6.12}$$

where

1) $\varepsilon = \Delta f T_s N_C$ is normalized CFO, Δf is CFO and T_s is the channel symbol period;

2)

$$\phi(a) = \exp(j2\pi\varepsilon((a-1)P + N_g)/N_C)$$

and

$$a = \begin{cases} k(\mathrm{mod} N_{FS}) \text{ if } k(\mathrm{mod} N_{FS}) \neq 0; \\ N_{FS} \text{ if } k(\mathrm{mod} N_{FS}) = 0; \end{cases}$$

where N_{FS} stands for frequency synchronization rate (FSR) per SCM block. In other words, $(a-1)$ is set to zero every N_{FS} SCM blocks;

3) $\mathbf{U}_{CFO} = \mathbf{F}_{N_C}\mathbf{D}_{CFO}\left[\mathbf{F}_{N_C}\right]^{\mathcal{H}}$, where

$$\mathbf{D}_{CFO} = diag(\exp(j2\pi\varepsilon(1/N_C)), ..., \exp(j2\pi\varepsilon(N_C/N_C))).$$

For comparison purposes, we also consider CP-OFDM under CFO effects, i.e.,

$$\mathbf{y}_{CP\_OFDM}^{(k)} = \sqrt{\rho}\phi(a)\mathbf{U}_{CFO}\mathbf{D}_{CP\_OFDM}^{(k)}\mathbf{x}_{OFDM}^{(k)} + \mathbf{F}_{N_C}\mathbf{v}_{CP\_OFDM}^{(k)} \tag{6.13}$$

Based on models (6.12) and (6.13), a CFO effect comparison through simulations is provided in Section 6.5.4.

6.4 Diversity properties

For simplicity, we only analyze the diversity properties of LDC-CP-SCM. Since it is easier to consider frequency-domain signals in order to study both temporal and frequency diversity, the chosen object to be analyzed is $\mathbf{z}_{CP-SC}^{(k)} = \mathbf{F}_{Nc}\mathbf{x}_{SC}^{(k)}, k = 1, ..., T$. Thus the whole LDC-CP-SCM block with FFT outer processing in each SCM block can expressed as matrix $\mathbf{C}$

$$\mathbf{C} = \begin{bmatrix} c_1^{(1)} & c_2^{(1)} & \cdots & c_{N_C}^{(1)} \\ c_2^{(2)} & c_2^{(2)} & \cdots & c_{N_C}^{(2)} \\ \vdots & \vdots & \ddots & \vdots \\ c_1^{(T)} & c_2^{(T)} & \cdots & c_{N_C}^{(T)} \end{bmatrix},$$

where $c_p^{(k)} = \left[\mathbf{z}_{CP-SC}^{(k)}\right]_{p,1}, p = 1, ..., N_C, k = 1, ...T.$

We write the system equation for the block $\mathbf{C}$ as

$$\mathbf{R} = \sqrt{\rho}\mathbf{M}\mathbf{H} + \mathbf{V}, \tag{6.14}$$

where receive signal vector $\mathbf{R}$ and noise vector $\mathbf{V}$ are of size $N_C T \times 1$. The chosen frequency symbol diagonal matrix $\mathbf{M}$ is of size $N_C T \times N_C T$, and

$$\mathbf{M} = diag(c_1^{(1)}, ..., c_{N_C}^{(1)}, ..., c_1^{(T)}, ..., c_{N_C}^{(T)}) \ .$$

The channel vector $\mathbf{H}$ is of size $N_C T \times 1$, and

$$\mathbf{H} = \left[\ H_1^{(1)}, H_2^{(1)}, ..., H_{N_C}^{(1)}, ..., H_2^{(T)}, H_2^{(T)}, ..., H_{N_C}^{(T)} \ \right]^{\mathcal{T}},$$

where $H_p^{(k)}$ is the p-th subchannel gain of k-th SCM block in $\mathbf{C}$ in the frequency domain. Thus $H_p^{(k)} = [\mathbf{w}_p]^T \mathbf{h}^{(k)}$, where

$$\mathbf{w}_p = \left[1, \omega^{p-1}, \omega^{2(p-1)}, \cdots, \omega^{L(p-1)}\right]^{\mathcal{T}}$$

and

$$\omega = e^{-j(2\pi/N_c)}.$$

With the above frequency domain formulation, the strategy of diversity analysis for LDC-CP-SCM is quite close to that for LDC-CP-OFDM as shown in Section 5.5.

Consider a pair of matrices $\mathbf{M}$ and $\tilde{\mathbf{M}}$ corresponding to two different blocks $\mathbf{C}$ and $\tilde{\mathbf{C}}$. Then the upper bound pairwise error probability between $\mathbf{M}$ and $\tilde{\mathbf{M}}$ is [96]

$$P\left(\mathbf{M} \to \tilde{\mathbf{M}}\right) \leq \left(\begin{array}{c} 2r-1 \\ \\ r \end{array} \right) \left(\prod_{a=1}^{r} \gamma_a\right)^{-1} (\rho)^{-r} \ , \tag{6.15}$$

where r is the rank of $\mathbf{\Lambda} = \left(\mathbf{M} - \tilde{\mathbf{M}}\right) \mathbf{R_H} \left(\mathbf{M} - \tilde{\mathbf{M}}\right)^{\mathcal{H}}$ and $\mathbf{R_H} = \mathbb{E}\left\{\mathbf{H}\left[\mathbf{H}\right]^{\mathcal{H}}\right\}$ is the correlation matrix of $\mathbf{H}$, $\gamma_a, a = 1, \cdots, r$ are the non-zero eigenvalues of $\mathbf{\Lambda}$.

Then the corresponding rank and product criteria are as follows:

1) Rank criterion: The minimum rank of $\mathbf{\Lambda}$ over all pairs of different frequency domain symbol matrices $\mathbf{M}$ and $\tilde{\mathbf{M}}$ should be as large as possible.

2) Product criterion: The minimum value of the product $\prod_{a=1}^{r} \gamma_a$ over all pairs of different frequency domain symbol matrices $\mathbf{M}$ and $\tilde{\mathbf{M}}$ should be maximized.

We remark that we can obtain a sufficient condition for LDC-CP-SCM to achieve full available joint frequency and time diversity in the channels, which is provided in

Theorem 4 *1) The necessary and sufficient condition to ensure rank* $\left(\mathbf{M} - \tilde{\mathbf{M}}\right) = N_C T$ *is*

$$\left[\mathbf{F}_{Nc}\left(\mathbf{x}_{SC}^{(k)} - \widetilde{\mathbf{x}}_{SC}^{(k)}\right)\right]_{p,1} \neq 0, k = 1, ..., T, p = 1, ..., N_C$$

2) In a LDC-CP-SCM system, the rank of $\left(\mathbf{M} - \tilde{\mathbf{M}}\right)$ *satisfies*

$$rank\left(\mathbf{M} - \tilde{\mathbf{M}}\right) = N_C T.$$

a. *The LDC-CP-SCM system achieves full available diversity order in the frequency selective channels, i.e.* $rank\left(\mathbf{\Lambda}\right) = rank\left(\mathbf{R_H}\right)$

b. *The corresponding product design criterion for LDC-CP-SCM block is that the minimum of products*

$$\Delta = \prod_{k=1}^{T}\prod_{p=1}^{N_C}\left|\left[\mathbf{F}_{Nc}\mathbf{x}_{SC}^{(k)}\right]_{p,1} - \left[\mathbf{F}_{Nc}\widetilde{\mathbf{x}}_{SC}^{(k)}\right]_{p,1}\right|^2 \tag{6.16}$$

taken over all pairs of distinct frequency domain symbol matrices $\mathbf{M}$ *and* $\tilde{\mathbf{M}}$ *must be maximized.*

3) *Assume that the frequency selective channel order* L *is constant over time. A condition for LDC-SCM to achieve available full joint frequency and time diversity order* $r_d = rank(\mathbf{R_H})$ *is that there always exist (L+1) indices,* $1 \leqslant p^{(k)} = p_1^{(k)}, ..., p_{L+1}^{(k)} \leqslant N_C$*, for each* $k = 1, ..., T$ *such that*

$$\left[\mathbf{F}_{Nc}\left(\mathbf{x}_{SC}^{(k)} - \widetilde{\mathbf{x}}_{SC}^{(k)}\right)\right]_{p^{(k)},1} \neq 0.$$

Note that this condition is a sufficient and necessary condition for frequency diversity and a sufficient condition for time diversity.

The proof is provided in Appendix C. Note that single-carrier systems are inherently able to achieve some frequency diversity order. However, full frequency diversity order is not guaranteed in conventional uncoded single-carrier communications systems, especially in uncoded CP-SCM systems, and the frequency coding gain may be further improved through careful design [73, 131]. A LDC-SCM block is across multiple SCM blocks in block time varying channels, and the LDC-SCM system has potential to achieve joint frequency-time diversity order up to $T(L+1)$. Although the design strategy of LDC-SCM systems to support a certain order of frequency diversity is different from that of LDC-OFDM, observing both Theorem 3 and 4, we

can obtain the following Corollary on the relation between full joint frequency and time diversity LDC-CP-SCM and LDC-CP-OFDM.

Corollary 1 *Assume that a LDC-CP-OFDM block,* $\mathbf{C}_{LDC\_OFDM}$*, with* N_C *subcarriers and* T *OFDM blocks achieves full joint frequency and time diversity order. Before IFFT, the* k*-th OFDM block within the LDC-CP-OFDM block* $\mathbf{C}_{LDC\_OFDM}$ *is expressed as* $\mathbf{x}_{OFDM}^{(k)}$*, where* $k = 1, ..., T$ *and* $\mathbf{x}_{OFDM}^{(k)} = \left[x_{OFDM(1)}^{(k)}, ..., x_{OFDM(N_C)}^{(k)}\right]^{\mathcal{T}}$.

Then the k*-th SCM block within a LDC-CP-SCM,* $\mathbf{C}_{LDC\_SCM}$*, can be designed as*

$$\mathbf{x}_{SC}^{(k)} = [\mathbf{F}_{Nc}]^{\mathcal{H}} \mathbf{x}_{OFDM}^{(k)}, \tag{6.17}$$

where $k = 1, ..., T$ *and* $\mathbf{x}_{SC}^{(k)} = \left[x_{SC}^{(k)}, ..., x_{SC}^{(k)}\right]^{\mathcal{T}}$. *The consequence is that this LDC-CP-SCM achieves full joint frequency and time diversity order in the time varying frequency selective channel.*

Actually Corollary 1 provides a method on constructing full joint frequency and time diversity LDC-CP-SCM. However, since the IFFT is involved, this LDC-CP-SCM construction is the same as LDC-CP-OFDM with IFFT processing, thus one may be concerned with the related problems, such as high PAPR.

6.5 Performance

6.5.1 Simulation setup

Perfect channel knowledge is assumed at the receiver but not at the transmitter. The number of data symbols per SCM block, N_C, is 32. Two LDC constructions are considered in the simulations

1) HH-LDC - HH square code as shown in (3.10),

2) LCP-LDC - details provided in Appendix G.

One LTC considered in the simulations is linear constellation precoding (LCP) design A [72, 126], termed LCPA.

The LDC or LTC symbol coding rates of the proposed systems used in simulations are all unity. Compared with uncoded CP-SCM systems, no bandwidth is lost unless forward error control is used. The sizes of all LDC codewords are identically $T \times N_F$. An evenly spaced mapping either from LDC to channel data symbol index for LDC-CP-SCM or from LDC to subcarrier index for LDC-CP-OFDM is used in simulations.

The frequency selective channel has $(L+1)$ paths exhibiting an exponential power delay profile, and the guard interval size of each SCM block is set to $N_g = L$. Source data symbols use QPSK modulation in all simulations.

6.5.2 Comparison between LDC-SCM and SCM systems

Figures 6.4 and 6.5 show the diversity performance comparison of bit error rate (BER) vs. SNR between LDC-SCM (LDC-CP-SCM and LDC-ZP-SCM) and uncoded SCM (CP-SCM and ZP-SCM).

When CCI is a multiple of T, i.e. $CCI = 16$, the effects of time diversity in the channels are removed, and it can be observed that the performances of LDC-SCM and SCM are quite similar, which suggests that the LDC-SCM systems using the chosen LDC do not provide notable frequency coding improvement over SCM systems. Note that the chosen LDC is designed for space time block fading channels, which may not be optimal for SCM in frequency selective time varying channels. To obtain frequency diversity improvement, new LDC designs are needed. It is not an easy task to design LDC meeting the design criterion in Theorem 4 as well as maintain desired lower PAPR as in conventional SCM systems, since the new design should consider the

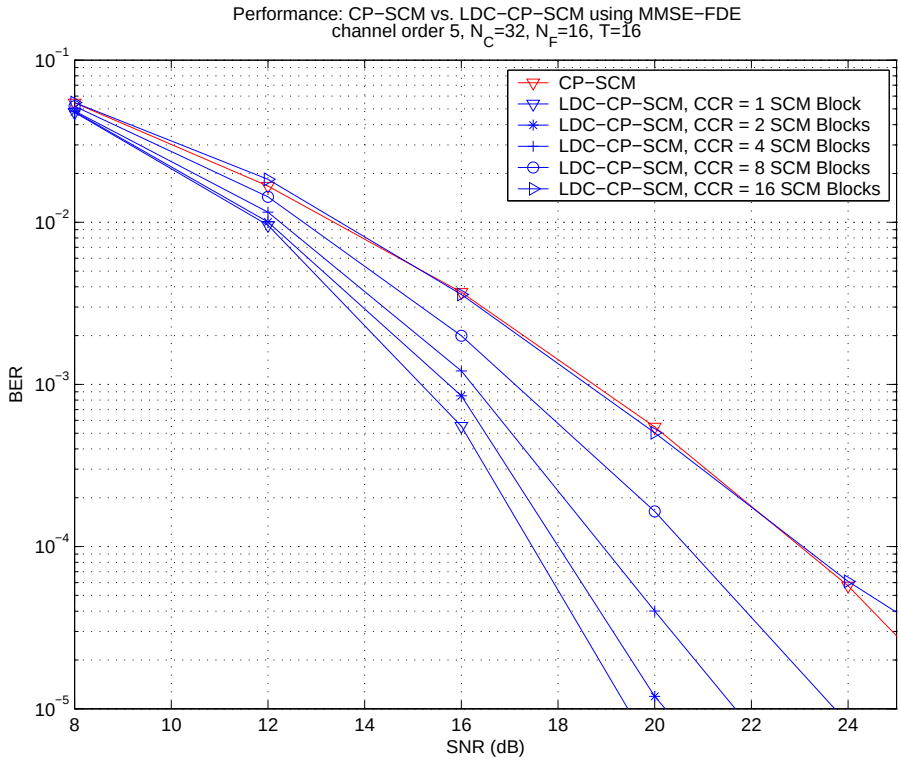

Figure 6.4. BER Performance of LDC-CP-SCM (using HH-LDC) vs. CP-SCM

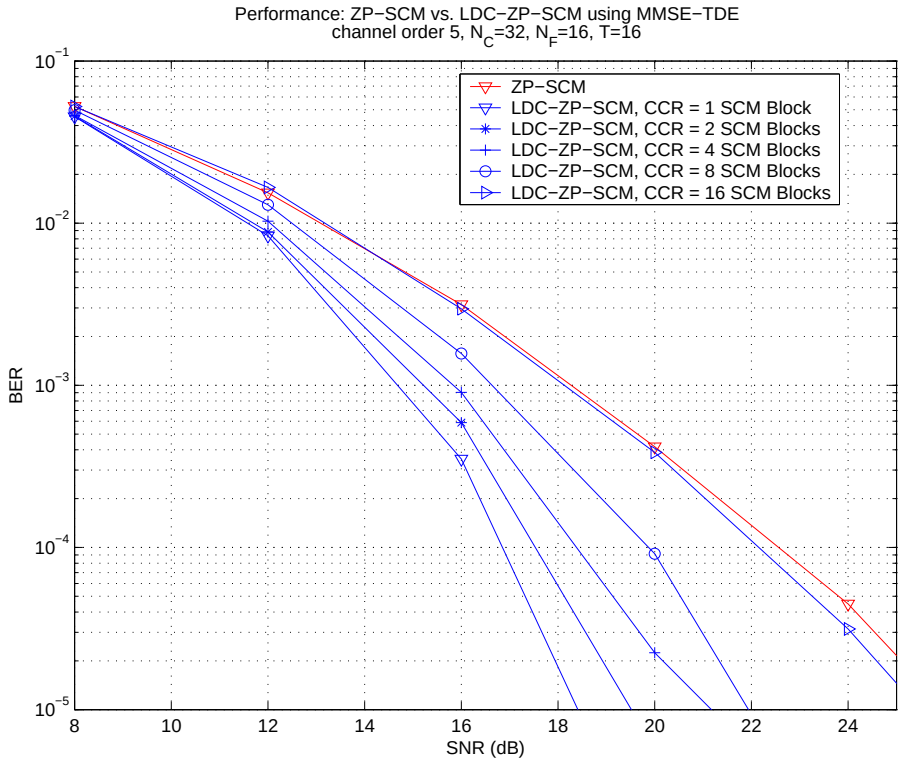

Figure 6.5. BER Performance of LDC-ZP-SCM vs. ZP-SCM

pairwise differences of Fourier transformed coded data symbols instead of coded data symbols themselves, which differ from current existing single-carrier complex matrix code designs.

When CCI is not a multiple of T, i.e. $CCI < 16$, clearly, BER performance of LDC-SCM is remarkably better than that of both uncoded SCM, which is primarily attributed to time diversity. Time diversity order is maximized only if the channel provides block-wise temporal independence. As shown in Figure 6.4, the performance of LDC-SCM systems is significantly influenced by channel dynamics, i.e., time correlation. At high SNRs, the faster the channel changes, the better the performance. This indicates that LDC-SCM effectively exploits available temporal diversity. In the future, testing on a more accurate model of channel dynamics is needed to obtain a more accurate assessment.

6.5.3 Comparison between LDC-CP-SCM and CP-SCM systems using forward error correction

Figure 6.6 shows a diversity performance comparison of BER vs. SNR between LDC-CP-SCM and CP-SCM using forward error correction (FEC). For low latency, Reed Solomon (RS) codes are chosen. In Figure 6.6, $RS(a, b, c)$ denotes RS codes with a coded RS symbols, b information RS symbols, and c bits per symbol. In simulations, shortened RS codes are chosen. For fairness of comparison, in CP-SCM systems, we apply RS codes across the same number of CP-SCM blocks as that in LDC-CP-SCM systems, and each RS symbol is distributed within one CP-SCM block. In this way, RS codes are able to improve time and frequency diversity in CP-SCM systems. In LDC-CP-SCM systems, we partition RS(a,b,c) codewords into $\frac{N_C}{N_F}$ groups, and each group of RS symbols are encoded in one LDC codeword within one LDC-CP-SCM

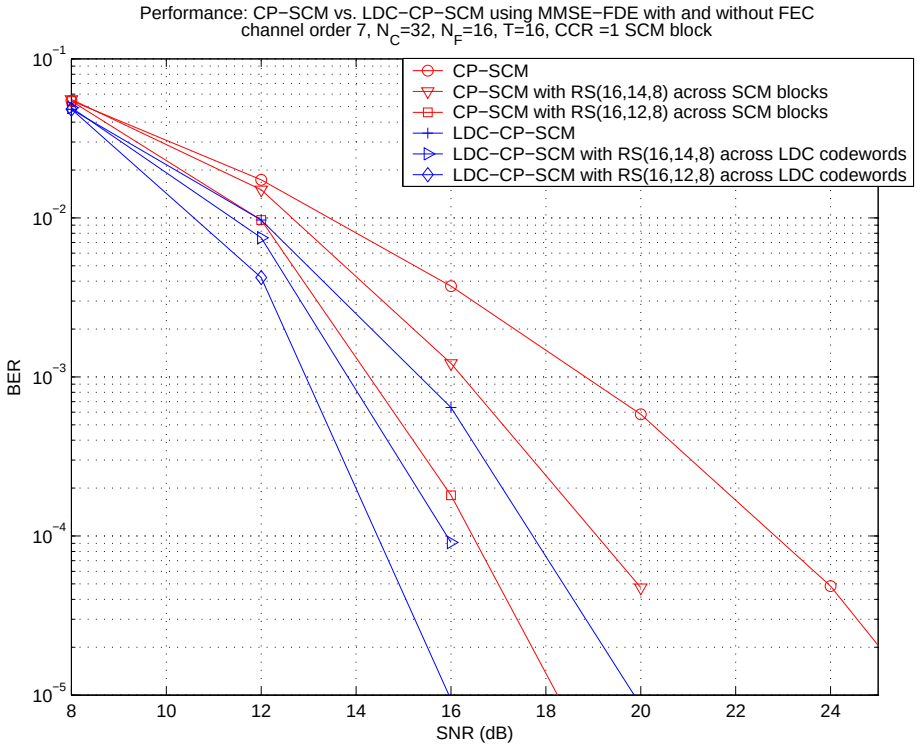

Figure 6.6. BER Performance of LDC-CP-SCM with inter-LDC FEC (using HH-LDC) vs. CP-SCM with inter-block FEC, channel order 7, $N_C = 32$, $N_F = 16$, $T = 16$

block.

It is clear that when using the same RS codes in medium to high SNRs, LDC-CP-SCM with FEC notably outperforms CP-SCM with FEC. For instance, at BER of 10^{-3}, using $RS(16, 12, 8)$, the LDC-CP-OFDM with FEC outperform CP-OFDM with FEC by 2.4 dB. Also note that while CP-SCM with FEC may outperform LDC-CP-SCM without FEC, the data rate of the corresponding CP-SCM with FEC is lower than that of the LDC-CP-SCM without FEC.

6.5.4 Comparison of LDC-ZP-SCM and ZP-SCM under MMSE vs. low complexity MMSE receivers

Figure 6.7 shows the comparison of LDC-ZP-SCM and ZP-SCM using MMSE-TDE and MMSE-LC-ADFE. Due to the layered TSE structure discussed in Section 6.3, it can been seen that, even at low complexity, LDC-ZP-SCM using MMSE-LC-ADFE performs close to that using MMSE TDE over the entire SNR range. At a BER of 10^{-3}, LDC-ZP-SCM using low complexity MMSE equalizer results in only 0.4dB performance degradation.

6.5.5 Comparison between LDC-CP-SCM and LDC-CP-OFDM systems

Figure 6.8 shows a diversity performance comparison of BER vs. SNR between LDC-CP-SCM and LDC-CP-OFDM. In the low range of SNRs, the performances of LDC-CP-SCM and LDC-CP-OFDM are close. However, in medium to high SNRs, especially when CCI is not a multiple of T, i.e. $CCI < 8$, LDC-CP-SCM (using HH-LDC) and LDC-CP-OFDM (using LCPA) significantly outperforms LDC-CP-OFDM

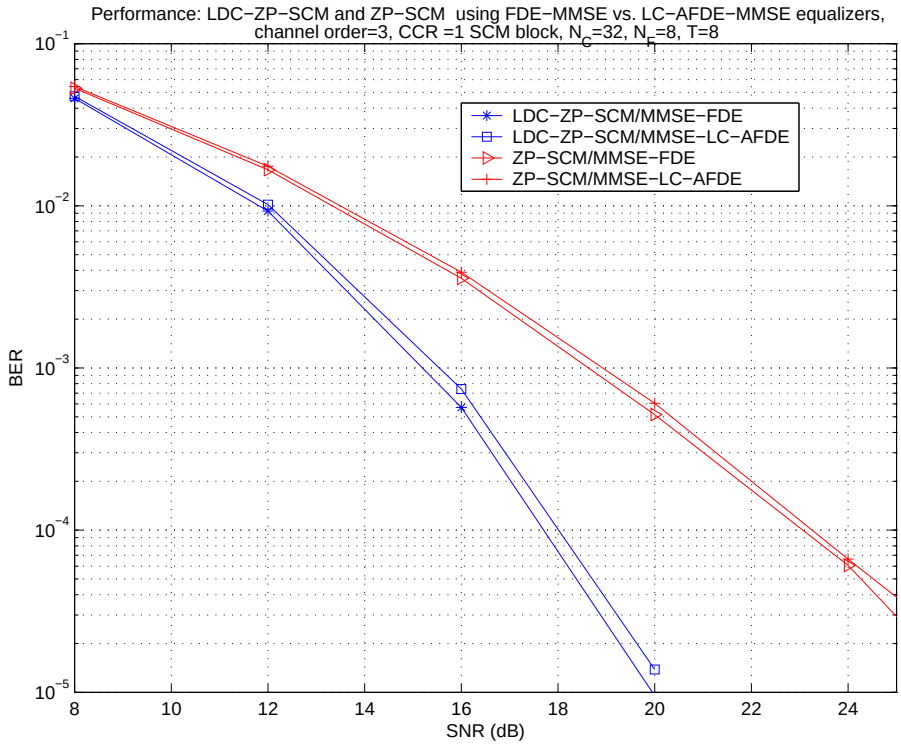

Figure 6.7. BER Performance of LDC-ZP-SCM (using HH-LDC) using MMSE-FDE vs. MMSE-LC-AFDE, channel order= 3, $CCI = 1$ SCM block, $N_C = 32$, $N_F = 8$, $T = 8$

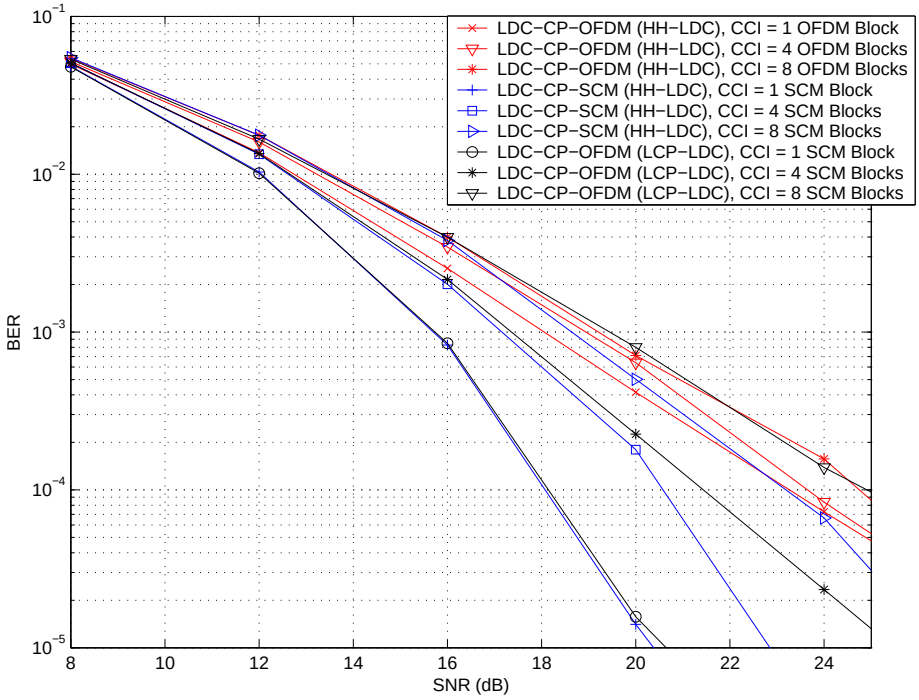

Figure 6.8. BER Performance of LDC-CP-SCM (using HH-LDC, LCP-LDC) vs. LDC-CP-OFDM (using LCP-LDC), channel order 7, $N_C = 32$, $N_F = 8$, $T = 8$

(using HH-LDC), the reason of which is that LDC-CP-OFDM (using HH-LDC) is not full joint frequency-time diversity design. Under $CCI = 8$, LDC-CP-SCM (using HH-LDC) perform similar to LDC-CP-OFDM (using LCPA), which suggests that LDC-CP-SCM (using HH-LDC) is close full joint frequency-time diversity design. In the high SNR region of the cases of under $CCI = 4$ and $CCI = 1$, LDC-CP-SCM (using HH-LDC) perform better than LDC-CP-OFDM (using LCPA), which suggests that LDC-CP-OFDM (using LCPA) do not have uniform diversity properties over the covered channel symbols.

6.5.6 Comparison of cyclic-prefix (CP) based systems under CFO effects

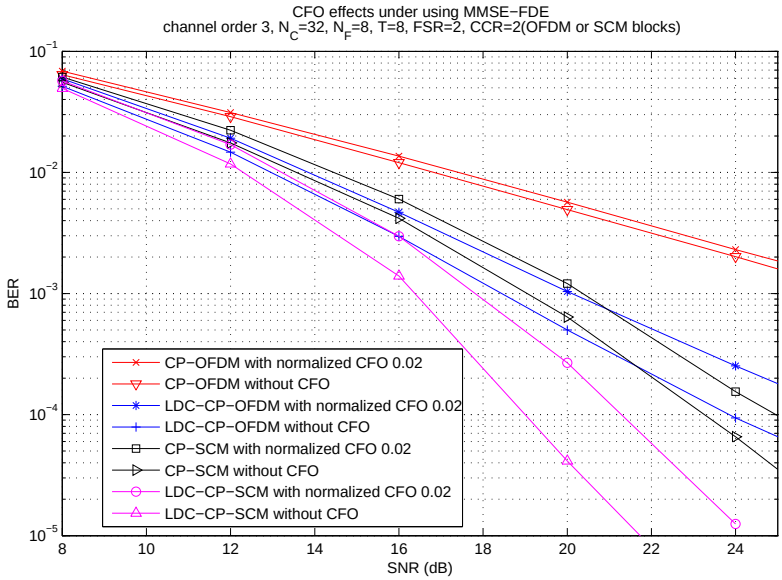

Figure 6.9. BER Performance of CP based systems under CFO effects (using HH-LDC),channel order 3, $N_C = 32$, $N_F = 16$, $T = 16$, $FSR = 2$, $CCI = 2$(OFDM or SCM blocks)

In Figure 6.9, the detrimental effects of CFO are observed. Under the normalized CFO setting of $\varepsilon = 0.02$, CP based systems without CFO outperform those with CFO, especially at higher SNRs. In higher SNRs, the performance loss of LDC-CP based systems due to CFO effects is higher than that of uncoded CP based systems. Although having the highest performance loss under CFO effects, LDC-CP-SCM has the best performance in time varying frequency selective channels.

6.5.7 Comparison between LDC-CP-SCM and LTC-CP-SCM systems

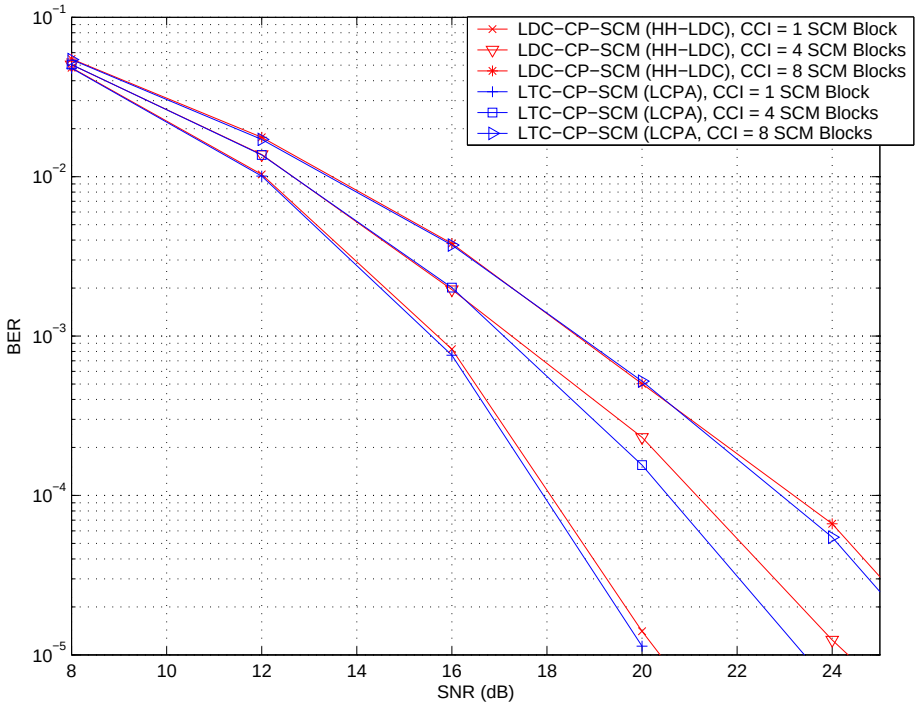

Figure 6.10. BER Performance of LDC-CP-SCM (using HH-LDC) vs. LTC-CP-SCM (using LCPA),channel order 7, $N_C = 32$, $N_F = 8$, $T = 8$

Figure 6.10 shows a diversity performance comparison of BER vs. SNR between

LDC-CP-SCM and LTC-CP-SCM. In all curves shown, LDC-CP-SCM (using HH-LDC) perform similar to LTC-CP-SCM (using LCPA), which suggests that LTC-CP-SCM (using LCPA) is close full joint frequency-time diversity design.

It is deserved to remark that compared to general LDC-SCM, LTC-SCM is only with much small complexity, which agrees with the design principle of SCM-FDE for mobile terminal or uplink transmission.

Further, this result motivates us to propose a new type of LDC-OFDM, which we call double linear transformation coded OFDM (DLT-OFDM).

1) DLT-OFDM may also include multiple frequency-time (FT) blocks, each of which is of size $T \times N_{F(i)}$, $i = 1, ..., K$, where $N_C = \sum_{i=1}^{K} N_{F(i)}$.

2) each $T \times N_{F(i)}$ FT block is constructed by two stages of LTC procedure, frequency-LTC (F-LTC) of size $1 \times N_{F(i)}$ and time-LTC (T-LTC) of size $T \times 1$ in order or T-LTC and F-LTC in order.

3) the LTC chosen of the two stages are not necessary the same.

6.6 Conclusions

This chapter proposes the use of high-rate LDC in single-carrier block communications systems with either cyclic-prefix or zero-padding guard intervals in time-varying frequency selective channels. While performance improvement has been previously obtained for multicarrier systems [122], performance of single-carrier systems may also be improved using high-rate LDC, as is shown in this chapter. In the LDC-SCM design tested, an increase in time diversity resulted in a performance improvement. However, it may be possible for LDC to improve joint frequency and time diversity,

which is a subject of future investigation. This chapter also provides a sufficient condition for LDC-CP-SCM to maximize all available joint frequency and time diversity gain and coding gain. This chapter provides the relation of full joint frequency-time diversity designs between LDC-OFDM and LDC-SCM. Simulations reveal that LDC-SCM may outperform both uncoded SCM in time-varying frequency selective channels, even under CFO effects. Under the normalized CFO setting of $\varepsilon = 0.02$ and $CCI = 2$ OFDM or SCM blocks in Figure 6.9, LDC-CP-SCM with CFO effects outperforms LDC-CP-SCM with CFO effects by 3.8dB at $BER = 10^{-2}$.

Simulations also show that full joint frequency-time diversity designs of both LDC-OFDM and LDC-SCM perform similarly. This chapter also shows that LDC-CP-SCM with forward error correction may outperform CP-SCM with forward error correction over time. LDC-ZP-SCM may be implemented using low complexity MMSE equalizers without significant performance degradation. Finally, this chapter also propose a low complexity LDC-SCM design, LTC-SCM, which is able to perform close to joint frequency-time diversity. Further, as a byproduct of analysis, this chapter proposes a class of low complexity LDC-OFDM designs, DLT-OFDM.

Chapter 7

Linear dispersion over space, time and frequency

7.1 Introduction

Recently, multiple transmit and receive antennas (MIMO) have attracted considerable attention to accommodate broadband wireless communications services. In frequency non-selective fading channels, diversity is available only in space and time domains. The related coding approaches are termed space-time codes (STC) [102]. However, high-data-rate wireless communications often experience wideband frequency-selective fading. In frequency-selective channels, there is additional frequency diversity available due to multipath fading. A challenging problem is to develop new coding and modulation methods to exploit all available diversity across space, time and frequency within reasonable computation complexity limits as well as maintain high bandwidth efficiency.

Multicarrier modulation, especially orthogonal frequency division multiplexing

(OFDM), mitigates frequency selectivity by transforming a wideband multipath channel into multiple parallel narrowband flat fading channels, enabling simple equalization. To obtain frequency diversity in OFDM transmission, space frequency coding (SFC) [7] may be employed, which encodes a source data stream over multiple transmit antennas and OFDM tones. In SFC, codewords lie within one OFDM block period and cannot exploit time diversity over multiple OFDM blocks. Recent coding over three dimensions - space, time and frequency, or STFC, being investigated is summarized as follows. Most existing block-based STFC designs assume constant MIMO channel coefficients over one STFC codeword (comprising multiple OFDM blocks), but may vary over different STFC codewords. In general, existing STFCs are not high-rate codes. For example, in [74], Liu and Giannakis propose a STFC based on a combination of orthogonal space time block codes [3, 101] and linear constellation precoding [126]; Gong and Letaief introduce the use of trellis-based STFC [37], Luo and Wu consider the design of bit-interleaved space-time-frequency block coding (BI-STFBC) [75], and Su and Liu proposes a symbol coding rate $1/\min\{N_T, N_R\}$ STFC using Vandermonde matrix as encoding matrix, where N_T is the number of transmit antennas [99]. We remark that our definition of symbol coding rate is different from that implicitly used in [99]. Symbol coding rate will be formally defined and discussed in Section 7.3.4.

In this chapter, we consider a STFC design with the following features: (1) support of arbitrary numbers of transmit antennas, (2) requirement of constant channel coefficients over only a single OFDM block instead of over a whole STFC codeword, (3) provision of up to rate-one coding, (4) compatibility with non-LDC-coded MIMO-OFDM systems and (5) moderate computation complexity.

The key idea for the proposed STFC designs in this chapter is to employ linear

dispersion codes (LDC), which were pioneered in [42] for use as space time codes for block flat-fading channels. In this chapter, we propose and compare two block-based high-rate STFCs coding procedures with rates up to one - one termed double linear dispersion space-time-frequency-coding (DLD-STFC), and the other termed linear dispersion space-time-frequency-coding (LD-STFC). In these approaches, an STF block is formed only across a subset of subcarrier indices instead of across all subcarriers.

A challenging issue in DLD-STFC design is to apply 2-D LDC in a 3-D code design. In DLD-STFC, two complete LDC stages of encoding are used, which process all complex symbols within one DLD-STFC codeword space. The diversity order for DLD-STFC is determined by the choices of LDC for the two stages. In LD-STFC, only a single LDC procedure is used for one STF block, and to achieve performance comparable to DLD-STFC, LD-STFC uses larger LDC sizes, and may be of higher complexity. This chapter also compares these to a system using a single LDC procedure applied only across frequency and time for MIMO-OFDM, termed MIMO-LDC-OFDM. This chapter analyzes the diversity properties of DLD-STFC and LD-STFC. The error union bound based analysis provides new code design criteria for complex input sequences. Spatial correlation effects for DLD-STFC are considered through simulations.

The chapter is organized as follows: after the MIMO-OFDM system model is described in Section 7.2, the DLD-STFC, LD-STFC and MIMO-LDC-OFDM systems are proposed in Section 7.3. Diversity properties of STF block based designs, related to DLD-STFC and LD-STFC, are discussed in Section 7.4. The LDC design criteria based on error union bound is analyzed in Section 7.5. System performance of DLD-STFC, LD-STFC and MIMO-LDC-OFDM are compared in Section 7.6.

7.2 MIMO-OFDM system model

7.2.1 System model

Consider a MIMO-OFDM system with N_T transmit antennas, N_R receive antennas and a OFDM block of N_C subcarriers per antenna. The channel between the m-th transmit antenna and n-th receive antenna in the k-th OFDM block experiences frequency-selective, temporally flat Rayleigh fading with channel coefficients $\mathbf{h}_{m,n}^{(k)} = \left[h_{m,n(0)}^{(k)}, ..., h_{m,n(L)}^{(k)}\right]^{\mathcal{T}}, m = 1, ..., N_T, n = 1, ..., N_R$, where

$$L = \max\{L_{m,n}, m = 1, ..., N_T, n = 1, ..., N_R\},$$

$L_{m,n}$ is the frequency-selective channel order of the path between the m-th transmit antenna and n-th receive antenna. Note that the above model is based on the fact frequency selective channel between pairs of transmitter and receiver antennas would be different, since different transmitter-receiver channel often experience different physical environments, especially for outdoor communications. We assume channel coefficients that are constant within one OFDM block but statistically independent among different OFDM blocks.

Denote $x_{m,p}^{(k)}$ as the channel symbol transmitted on the p-th subcarrier from the m-th transmit antenna during the k-th OFDM block. The channel symbols $x_{m,p}^{(k)}$, $m = 1, ...N_T$ and $p = 1, ..., N_C$ are transmitted on N_C subcarriers in parallel by N_T transmit antennas.

Each receive antenna signal experiences additive complex Gaussian noise. At the transmitter, a cyclic prefix (CP) guard interval is appended to each OFDM block. After CP is removed, FFT is applied to transform received signals to frequency domain. The received frequency domain channel symbol sample $y_{n,p}^{(k)}$ at the n-th receive

antenna, is

$$y_{n,p}^{(k)} = \sqrt{\frac{\rho}{N_T}} \sum_{m=1}^{N_T} H_{m,n,p}^{(k)} x_{m,p}^{(k)} + v_{n,p}^{(k)}, \quad n = 1, ..., N_R, p = 1, ..., N_c \tag{7.1}$$

where $H_{m,n,p}^{(k)}$ is the p-th subcarrier channel gain from the m-th transmit antenna and n-th receive antenna during the k-th OFDM block,

$$H_{m,n,p}^{(k)} = \sum_{l=o}^{L} h_{m,n(l)}^{(k)} e^{-j(2\pi/N_c)l(p-1)} \tag{7.2}$$

or equivalently

$$H_{m,n,p}^{(k)} = [\mathbf{w}_p]^{\mathcal{T}} \mathbf{h}_{m,n}^{(k)}, \tag{7.3}$$

where

$$\mathbf{w}_p = \left[1, \omega^{p-1}, \omega^{2(p-1)}, \cdots, \omega^{L(p-1)}\right]^{\mathcal{T}}, \tag{7.4}$$

$\omega = e^{-j(2\pi/N_c)}$, and the additive noise is circularly symmetric, zero-mean, complex Gaussian with variance N_0. We assume the additive noise to be statistically independent for different n, p, and k. The normalizaton $\sqrt{\frac{\rho}{N_T}}$ ensures that the signal-to-noise-ratio (SNR) at each receive antenna ρ is independent of N_T.

7.2.2 Matrix form

Denote the transmitted channel symbol vector of the p-th subcarrier during the k-th OFDM block as

$$\mathbf{x}_p^{(k)} = \begin{bmatrix} x_{1,p}^{(k)} & \cdots & x_{N_T,p}^{(k)} \end{bmatrix}^{\mathcal{T}} \in C^{N_T \times 1}, \tag{7.5}$$

the corresponding channel gain matrix of the p-th subcarrier during the k-th OFDM block as

$$\mathbf{H}_p^{(k)} = \begin{bmatrix} H_{1,1,p}^{(k)} & \cdots & H_{N_T,1,p}^{(k)} \\ \vdots & \ddots & \vdots \\ H_{1,N_R,p}^{(k)} & \cdots & H_{N_T,N_R,p}^{(k)} \end{bmatrix}, \tag{7.6}$$

the corresponding noise vector as

$$\mathbf{v}_p^{(k)} = \begin{bmatrix} v_{1,p}^{(k)} & \cdots & v_{N_R,p}^{(k)} \end{bmatrix}^{\mathcal{T}} \in C^{N_R \times 1}, \tag{7.7}$$

and received channel symbol vector of the p-th subcarrier during the k-th OFDM block as

$$\mathbf{y}_p^{(k)} = \begin{bmatrix} y_{1,p}^{(k)} & \cdots & y_{N_R,p}^{(k)} \end{bmatrix}^{\mathcal{T}} \in C^{N_R \times 1}. \tag{7.8}$$

Then, we express the system equation for the p-th subcarrier during the k-th OFDM block as

$$\mathbf{y}_p^{(k)} = \sqrt{\frac{\rho}{N_T}} \mathbf{H}_p^{(k)} \mathbf{x}_p^{(k)} + \mathbf{v}_p^{(k)}, p = 1, ..., N_c. \tag{7.9}$$

7.3 Proposed systems

This section proposes two new constructions of STFC based on linear dispersion codes, referred to as DLD-STFC and LD-STFC, established over the MIMO OFDM model described in Section 7.2. Codeword construction of both DLD-STFC and LD-STFC will be discussed. DLD-STFC is the main focus of this section.

7.3.1 DLD-STFC codeword construction

7.3.1.1 Codeword construction procedure

This is performed in two stages. Each stage is a complete LDC coding procedure itself and processes all complex symbols within the range of one DLD-STFC codeword. The first encoding stage is the frequency-time LDC stage (FT-LDC), in which LDC is performed across frequency (OFDM subcarriers) and time (OFDM blocks), enabling frequency and time diversity. The second encoding stage is the space-time LDC stage

(ST-LDC), in which LDC is performed across space (N_T transmit antennas) and time (T OFDM blocks), enabling space and time diversity.

In the FT-LDC stage, there are D LDC matrix codewords. The d-th matrix codeword is of size $T \times N_F^{(d)}, d = 1, ..., D$, where D is a multiple of N_T. The D LDC matrix codewords are grouped into N_T sub-groups. The m-th subgroup, which is allocated to the m-th antenna, has $D = \sum_{m=1}^{N_T} D_m, m = 1, ..., N_T$ LDC matrix codewords. The i-th LDC codeword of the m-th subgroup in the FT-LDC stage is of size $T \times N_{F(m,i)}, i = 1, ..., D_m, m = 1, ..., N_T$, where $i = d(\mathrm{mod}\ D_m)$. We use $N_{F(i)}$, which differs from $N_F^{(d)}$ in subscript $i = 1, ..., D_m$, as the local index of FT-LDC for each transmit antenna, and superscript $d = 1, ..., D$ which stands for the global index for all D LDC codewords. LDC codewords in the FT-LDC stage are chosen with size constraints

$$N_{F(m,i)} = N_{F(i)}, \tag{7.10}$$

$$\sum_{i=1}^{D_m} N_{F(m,i)} = N_C, \tag{7.11}$$

where $i = 1, ..., D_m, m = 1, ..., N_T$. The size of an DLD-STFC codeword is $N_T N_C T$ symbols. When $D_m = D/N_T,\ m = 1, ..., N_T$ are satisfied, one DLD-STFC codeword consists of D_m STF blocks, each of which is of size $N_T N_{F(i)} T, i = 1, ..., D_m$ and are also constructed through the DLD operation. Constraint (7.10) implies that the i-th LDC codewords of subgroups $m = 1, ..., N_T$, are of the same matrix size. Further, we propose that the i-th LDC codewords of all the m-th subgroups, where $m = 1, ..., N_T$, use the same LDC dispersion matrices and share the same subcarrier mappings, i.e., the same subcarrier indices of OFDM. Thus the FT-LDC coded symbols with the same subcarrier index among different transmit antennas share similar frequency-time diversity properties. The D LDC encoders of FT-LDC encode $Q_d, d = 1, ..., D$

data symbols in parallel. Each codeword is mapped to N_T transmit antennas and T OFDM blocks. Consequently, a three-dimensional array, $\mathbf{U}_{k,m,p}, k = 1, ..., T, m = 1, ..., N_T, p = 1, ...N_c,$, is created. In the FT-LDC stage, LDC symbol coding rate could be less than or equal to one. The FT-LDC blocks are illustrated in Figure 7.1.

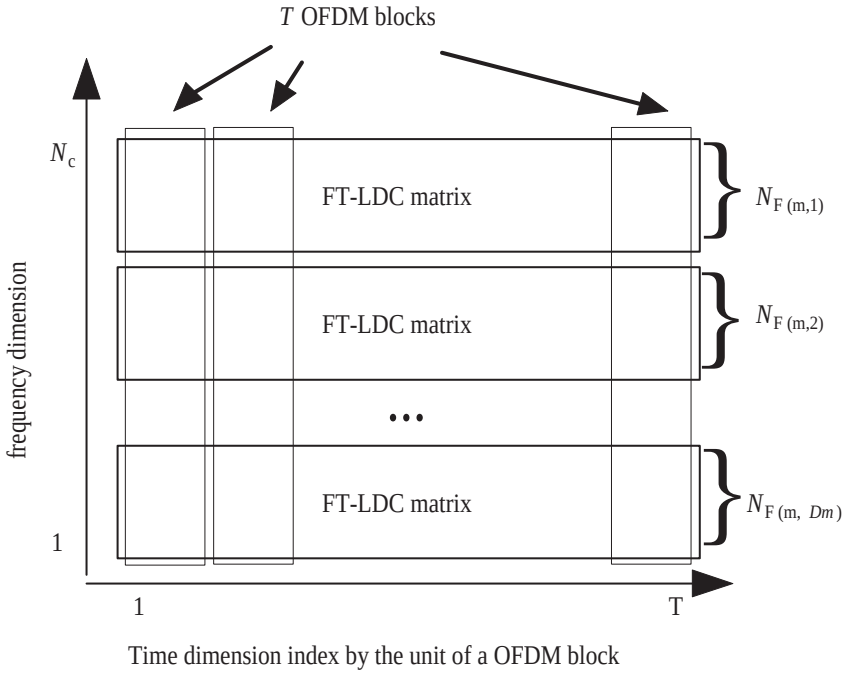

Figure 7.1. FT-LDC blcok in DLD-STFC

In the ST-LDC stage, the signals from the FT-LDC stage are encoded per subcarrier. Thus there are N_C LDC encoders in this stage. Notationally, define the space time symbol matrix having been encoded in FT-LDC stage for the p-th OFDM subcarrier as $\mathbf{U}_p$, and $[\mathbf{U}_p]_{k,m} = \mathbf{U}_{k,m,p}, k = 1, ..., T, m = 1, ..., N_T, p = 1, ...N_C$. The ST-LDC blocks are illustrated in Figure 7.2.

Denote $\mathbf{u_p^{vec}} = \mathbf{vec}(\mathbf{U_p})$, which is the source signal sequence of the p-th LDC codeword to be encoded in the ST-LDC stage, where $p = 1, ...N_C$. This stage further

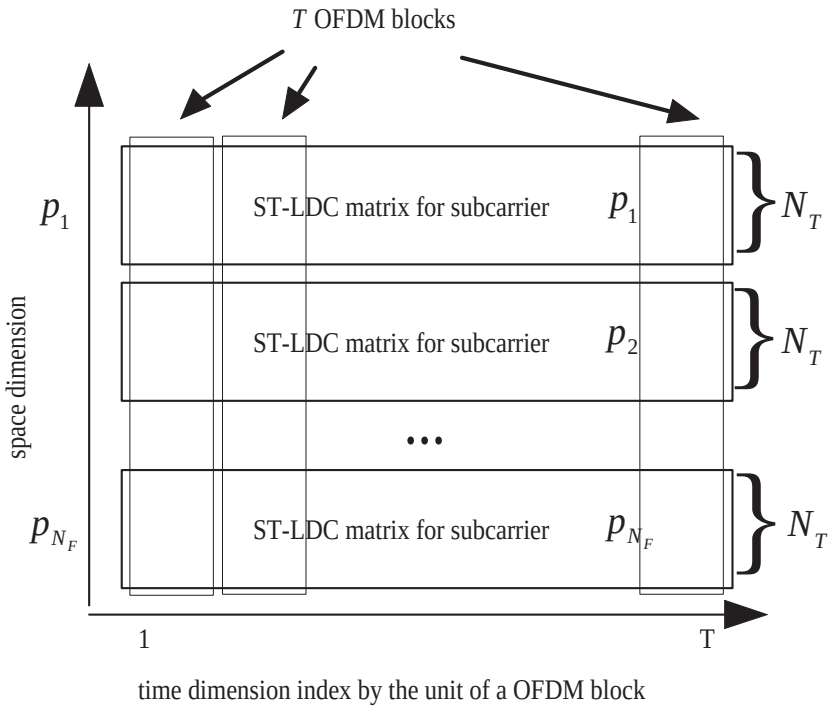

Figure 7.2. ST-LDC blcok in DLD-STFC

establishes the basis of space and time diversity. In this stage, LDC symbol coding rate is required to be one.

7.3.2 LD-STFC codeword construction

This chapter also propose an alternative LDC system with a single combined STFC stage, termed LD-STFC. This comprises only one complete LD coding procedure, and one LDC codeword is applied across multiple OFDM blocks and multiple antennas.

In one LD-STFC codeword, there are D LDC matrix codewords. The i-th matrix codeword is of size $T \times N_{LD}^{(i)}, i = 1, ..., D$, and $N_{LD}^{(i)}$ is a multiple of N_T. One constraint is

$$N_C = \frac{1}{N_T} \sum_{i=1}^{D} N_{LD}^{(i)} \tag{7.12}$$

We partition the i-th LDC codeword into N_T matrix blocks, each of which is of size $T \times N_{LD(i)}^{ant}$, and

$$N_{LD(i)}^{ant} = \frac{1}{N_T} N_{LD}^{(i)}. \tag{7.13}$$

We map each $T \times N_{LD(i)}^{ant}$ block into each transmit antenna, where T denotes the number of OFDM blocks. Each LDC codeword therefore includes multiple antennas (space), OFDM blocks (time) and OFDM subcarriers (frequency). The size of an LD-STFC codeword is $N_T N_C T$ symbols, and one LD-STFC codeword consists of D STF blocks, each with size $N_T \times N_{LD(i)}^{ant} \times T, i = 1, ..., D$.

7.3.3 DLD-STFC system receiver

In a DLD-STFC receiver, signal reception involves three steps. The first step estimates MIMO-OFDM signals for an entire DLD-STFC block, i.e., T OFDM blocks

transmitted from N_T antennas. The second and third steps estimate source symbols of the ST-LDC and FT-LDC encoding stages, respectively. Following this, data bit detection is performed.

Denote the d-th data source symbol vector with zero-mean, unit variance for the d-th LDC codeword of the FT-LDC stage as $\mathbf{s^{(d)}} = \begin{bmatrix} s_1^{(d)} & s_2^{(d)} & \dots & s_{Q_d}^{(d)} \end{bmatrix}$, where $d = 1, ..., D$, and Q_d denote the number of data source symbols encoded in the d-th LDC codeword $\mathbf{S}_{FT\_LDC}^{(d)}$ of the FT-LDC stage and $\widehat{\mathbf{s}^{(d)}}$ is the corresponding estimated data source symbol vector. In addition, denote the estimate of $\mathbf{S}_{FT\_LDC}^{(d)}$ as $\widehat{\mathbf{S}_{FT\_LDC}^{(d)}}$. Further, denote the estimated version of $\mathbf{u}_p^{vec}$ as $\widehat{\mathbf{u}_p^{vec}}$. Also denote estimated $\mathbf{S}_{ST\_LDC}^{(p)}$ as $\widehat{\mathbf{S}_{ST\_LDC}^{(p)}}$. Denote the LDC encoding matrices needed to obtain $\mathbf{S}_{FT\_LDC}^{(d)}$ and $\mathbf{S}_{ST\_LDC}^{(p)}$ as $\mathbf{G}_{FT\_LDC}^{(d)}$ and $\mathbf{G}_{ST\_LDC}^{(p)}$, respectively.

For simplicity of discussion, we consider the case that $\mathbf{G}_{FT\_LDC}^{(d)} = \mathbf{G}_{FT\_LDC}$, $\mathbf{G}_{ST\_LDC}^{(p)} = \mathbf{G}_{ST\_LDC}$, $d = 1, ..., D$, $p = 1, ..., N_C$ are all unitary matrices and $Q_d = Q, d = 1, ..., D$. The covariance matrices of MIMO-OFDM channel symbols are then identity matrices. This can also be generalized to the case of non-identically distributed uncorrelated symbols.

7.3.3.1 Step 1 - MIMO-OFDM signal estimation

In the proposed DLD-STFC decoding algorithm, LDC decoding is independent of MIMO-OFDM signal estimation. Thus the proposed DLD-STFC system could be backwards-compatible with non-LDC-coded MIMO-OFDM systems. An advantage of DLD-STFC decoding is that channel coefficients may vary over multiple OFDM blocks.

Assuming that MIMO-OFDM symbols are normalized to unit variance, based on system equation (7.9), the minimum-mean-squared-error (MMSE) equalizer is given

by

$$\mathbf{G}_{p,(k)}^{MMSE} = \sqrt{\frac{\rho}{N_T}}\mathbf{C}_{\mathbf{x}_p^{(k)}}\left(\mathbf{H}_p^{(k)}\right)^{\mathcal{H}}\left[\mathbf{I}_{N_T} + \frac{\rho}{N_T}\mathbf{H}_p^{(k)}\mathbf{C}_{\mathbf{x}_p^{(k)}}\left(\mathbf{H}_p^{(k)}\right)^{\mathcal{H}}\right]^{-1} \tag{7.14}$$

$$\widehat{\mathbf{x}_p^{(k)}} = \mathbf{G}_{p,(k)}^{MMSE}\mathbf{y}_p^{(k)} \tag{7.15}$$

where $p = 1, ..., N_C, k = 1, ..., T$, $\mathbf{C}_{\mathbf{x}_p^{(k)}}$ is the covariance matrix of $\mathbf{x}_p^{(k)}$, which could be calculated using knowledge of $\mathbf{G}_{FT\_LDC}^{(d)}$ and $\mathbf{G}_{ST\_LDC}^{(p)} = \mathbf{G}_{ST\_LDC}$.

7.3.3.2 Step 2 - ST-LDC block signal estimation

Reorganizing the results of the MIMO OFDM estimation into N_C estimated LDC matrix codewords $\widehat{\mathbf{S}_{ST\_LDC}^{(p)}}$, the estimates are

$$\widehat{\mathbf{u}_p^{vec}} = \left[\mathbf{G}_{ST\_LDC}^{(p)}\right]^{\dagger} vec\left(\widehat{\mathbf{S}_{ST\_LDC}^{(p)}}\right), \tag{7.16}$$

where $p = 1, ..., N_C$.

7.3.3.3 Step 3 - FT-LDC block signal estimation

Reorganizing the results of step 2 into D estimated LDC matrix codewords $\widehat{\mathbf{S}_{FT\_LDC}^{(d)}}$, $d = 1, ..., D$ of the FT-LDC stage, we obtain

$$\widehat{\mathbf{s}^{(d)}} = \left[\mathbf{G}_{FT\_LDC}^{(d)}\right]^{\dagger} vec\left(\widehat{\mathbf{S}_{FT\_LDC}^{(d)}}\right), \tag{7.17}$$

where $d = 1, ..., D$.

7.3.4 Symbol coding rate for DLD-STFC, LD-STFC and MIMO-LDC-OFDM systems

For DLD-STFC, assume that the d-th LDC matrix codeword of the FT-LDC stage is encoded using Q_d complex source symbols. For LD-STFC, assume that the d-th LDC matrix codeword is also encoded using Q_d complex source symbols. We also consider a third system with only a FT-LDC stage (each LDC codeword is not across multiple transmit antennas but transmitted on one antenna), termed MIMO-LDC-OFDM, i.e., straightforwardly applying LDC-OFDM as proposed in [122] to each antenna of a MIMO system.

We define the symbol coding rate of the three systems as

$$R^{sym} = \frac{\sum_{d=1}^{D} Q_d}{\min\{N_T, N_R\} T N_C}. \tag{7.18}$$

7.3.5 Layered system structure and complexity issues

Both DLD-STFC and LD-STFC require coding matrices with the property that STFC codeword symbols are uncorrelated. Hence, the proposed STFC systems could be viewed as having the layered structure as shown in Figure 7.3, which enable the designed STFC systems to be compatible to non-LDC-coded MIMO-OFDM systems. There are at least two advantages of the layered system structure: (1) many existing signal estimation algorithms developed for non-LDC-coded MIMO-OFDM systems are also applicable to DLD-STFC and LD-STFC systems, and (2) reduced complexity. In principle, it is possible to utilize a single STF block across all transmit antennas, subcarriers and OFDM blocks, and a rate-one STFC design would need coding matrices of size $N_T N_C T \times N_T N_C T$, which leads to extremely high computation complexity, since the codebook size for rate-one codes in this case is $[r_c]^{N_T N_C T}$,

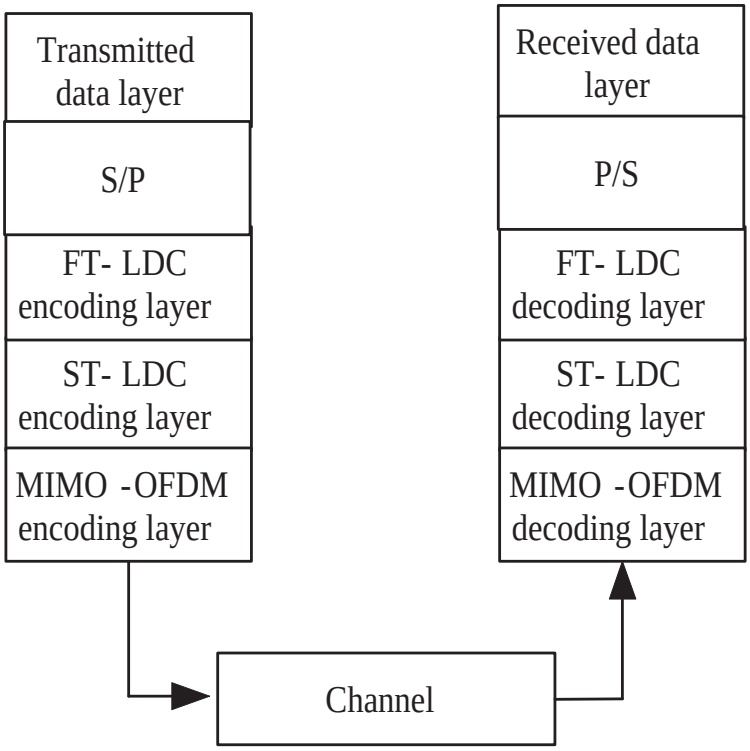

Figure 7.3. Layered structure of DLD-STFC communications

where r_c is the constellation size of source data symbols. Both DLD-STFC and LD-STFC receivers may advantageously employ the lower complexity multiple successive estimation stages instead of single-stage joint signal estimation (maximum likelihood or sphere decoding detectors) and LDC decoding. Due to layered structure, it is clear that the extra complexity of DLD-STFC and LD-STFC beyond MIMO-OFDM signal estimation is the encoding and decoding procedure, and per-data-symbol extra complexity is proportional to the corresponding symbol coding rate.

7.4 Diversity aspects

Both DLD-STFC and LD-STFC are STF block-based designs. Based on the analysis of pairwise error probability, we determine the achievable diversity of these systems.

Since both DLD-STFC and LD-STFC include all LDC coding properties within either a $T \times N_{F(i)}N_T$ block or a $T \times N^{ant}_{LD(i)}N_T$ block, in the following analysis, we consider a single block $C^{(i)}$. The block $C^{(i)}$ is created after encoding all the i-th FT-LDC codewords on all the transmit antennas and encoding the corresponding ST-LDC codewords in the case of DLD-STFC; or, after encoding all of the i-th LDC codewords across all transmit antennas and OFDM blocks in the case of the LD-STFC.

We use the unified notation $N_{freq(i)}$ to represent both $N_{F(i)}$ of DLD-STFC and $N_{LD(m,i)}$ of LD-STFC and unified notation D_{STFB} (the number of STF block) to represent both D_m of DLD-STFC and D of LD-STFC. Thus the block $C^{(i)}, i = 1, ..., D_{STFB}$ is of size $T \times N_{freq(i)}N_T$. For simplicity, in block $C^{(i)}$, consider the case that the subcarrier indices chosen from all the OFDM blocks are the same, and denote subcarrier indexes chosen $\{p^{(m)}_{n_{F(i)}}, n_{F(i)} = 1_{(i)}, ..., N_{freq(i)}, i = 1, ..., D_{STFB}, m =$

$1, ..., N_T\}$. Denote the STF block $C^{(i)}$ in matrix form as

$$\mathbf{C}^{(i)} = \left[\begin{array}{cccc} \left[\mathbf{C}^{(1,i)}\right]^{\mathcal{T}} & \left[\mathbf{C}^{(2,i)}\right]^{\mathcal{T}} & \cdots & \left[\mathbf{C}^{(T,i)}\right]^{\mathcal{T}} \end{array} \right]^{\mathcal{T}},$$

where

$$\mathbf{C}^{(k,i)} = \left[\begin{array}{cccc} c^{(k)}_{p^{(1)}_{1(i)}} & c^{(k)}_{p^{(2)}_{1(i)}} & \cdots & c^{(k)}_{p^{(N_T)}_{1(i)}} \\ c^{(k)}_{p^{(1)}_{2(i)}} & c^{(k)}_{p^{(2)}_{2(i)}} & \cdots & c^{(k)}_{p^{(N_T)}_{2(i)}} \\ \vdots & \vdots & \ddots & \vdots \\ c^{(k)}_{p^{(1)}_{N_{freq(i)}}} & c^{(k)}_{p^{(2)}_{N_{freq(i)}}} & \cdots & c^{(k)}_{p^{(N_T)}_{N_{freq(i)}}} \end{array} \right], \tag{7.19}$$

and $c^{(k)}_{p^{(m)}_{n_{F(i)}}}, n_{F(i)} = 1_{(i)}, ..., N_{freq(i)}, m = 1, ..., N_T$ is the channel symbol of k-th OFDM block in STF block $C^{(i)}$, the $p^{(m)}_{n_{F(i)}}$-th subcarrier from m-th transmit antenna.

Su and Liu [97] recently analyzed the diversity of STFC based on a STF block of size $T \times N_C N_T$. Unlike [97], our analysis deals with only a single STF block of size of $T \times N_{freq(i)} N_T$, where $N_{freq(i)}$ is usually much less than N_C (note that [97] employs a different notation N instead of N_C to express the number of subcarriers in a OFDM block); in addition, the analysis in [97] is based on the assumption that the channel orders of all paths between transmit and receive antennas are the same. However, we assume frequency selective channel with orders that could be different among paths between transmit and receive antennas. Furthermore, the diversity analysis in [97] assumes no spatial correlation among transmit and receive antennas, while our analysis allows for arbitrary channel correlation among space (antennas), time (OFDM blocks) and frequency. In the following, we show that the upper bound diversity order for STF blocks of size $T \times N_{freq(i)} N_T$ could be equal to the upper bound diversity order for STF blocks of size $T \times N_C N_T$. Thus, even with lower complexity, a smaller size STF block-based design is possible to achieve full diversity.

We write the system equation for block $C^{(i)}$ as

$$\mathbf{R}^{(i)} = \sqrt{\frac{\rho}{N_T}}\mathbf{M}^{(i)}\mathbf{H}^{(i)} + \mathbf{V}^{(i)}, \tag{7.20}$$

where receive signal vector $\mathbf{R}^{(i)}$ and noise vector $\mathbf{V}^{(i)}$ are of size $N_{freq(i)}N_RT \times 1$. The coded STF block channel symbol matrix $\mathbf{M}^{(i)}$ is of size $N_{freq(i)}N_RT \times N_{freq(i)}N_TN_RT$, and $\mathbf{M}^{(i)} = I_{N_R} \otimes \left[\mathbf{M}_1^{(i)}, \cdots, \mathbf{M}_{N_T}^{(i)}\right]$, where

$$\mathbf{M}_m^{(i)} = diag\left(c^{(1)}_{m,p^{(m)}_{1(i)}}, \cdots, c^{(1)}_{m,p^{(m)}_{N_{freq(i)}}}, \cdots c^{(T)}_{m,p^{(m)}_{1(i)}}, \cdots, c^{(T)}_{m,p^{(m)}_{N_{freq(i)}}}\right),$$

$i = 1, ..., D_{STFB}, m = 1, ..., N_T$. The channel vector $\mathbf{H}^{(i)}$ is of size $N_{freq(i)}N_TN_RT \times 1$, and

$$\mathbf{H}^{(i)} = \left[\begin{array}{c} \left[\mathbf{H}^{(i)}_{1,1}\right]^{\mathcal{T}}, ..., \left[\mathbf{H}^{(i)}_{N_T,1}\right]^{\mathcal{T}}, ..., \left[\mathbf{H}^{(i)}_{1,2}\right]^{\mathcal{T}}, ..., \left[\mathbf{H}^{(i)}_{N_T,2}\right]^{\mathcal{T}}, \\ ..., \left[\mathbf{H}^{(i)}_{1,N_R}\right]^{\mathcal{T}}, ..., \left[\mathbf{H}^{(i)}_{N_T,N_R}\right]^{\mathcal{T}} \end{array}\right]^{\mathcal{T}}$$

where $\mathbf{H}^{(i)}_{m,n}$ is of size $N_{freq(i)}T \times 1$,

$$\mathbf{H}^{(i)}_{m,n} = \left[\begin{array}{c} H^{(1)}_{m,n,p^{(m)}_{1(i)}}, H^{(1)}_{m,n,p^{(m)}_{2(i)}}, ..., H^{(1)}_{m,n,p^{(m)}_{N_{freq(i)}}}, ..., \\ H^{(T)}_{m,n,p^{(m)}_{1(i)}}, H^{(T)}_{m,n,p^{(m)}_{2(i)}}, ..., H^{(T)}_{m,n,p^{(m)}_{N_{freq(i)}}} \end{array}\right]^{\mathcal{T}}$$

and $H^{(k)}_{m,n,p^{(m)}_{n_{F(i)}}}$ is the path gain of k-th OFDM block , the $p^{(m)}_{n_{F(i)}}$-th subcarrier for block $C^{(i)}$ between the m-th transmit antenna and the n-th receive antenna. Thus, according to (7.3), we get

$$H^{(k)}_{m,n,p^{(m)}_{n_{F(i)}}} = \left[\mathbf{w}_{p^{(m)}_{n_{F(i)}}}\right]^{\mathcal{T}} \mathbf{h}^{(k)}_{m,n}. \tag{7.21}$$

Consider the pair of matrices $\mathbf{M}^{(i)}$ and $\tilde{\mathbf{M}}^{(i)}$ corresponding to two different STF blocks $C^{(i)}$ and $\tilde{C}^{(i)}$. The upper bound pairwise error probability [96] is

$$P\left(\mathbf{M}^{(i)} \to \tilde{\mathbf{M}}^{(i)}\right) \leq \left(\begin{array}{c} 2r-1 \\ r \end{array}\right)\left(\prod_{a=1}^{r}\gamma_a\right)^{-1}\left(\frac{\rho}{M_t}\right)^{-r}, \tag{7.22}$$

where r is the rank of $\left(\mathbf{M}^{(i)} - \tilde{\mathbf{M}}^{(i)}\right) \mathbf{R}_{\mathbf{H}^{(i)}} \left(\mathbf{M}^{(i)} - \tilde{\mathbf{M}}^{(i)}\right)^{\mathcal{H}}$, and $\mathbf{R}_{\mathbf{H}^{(i)}} = E\left\{\mathbf{H}^{(i)} \left[\mathbf{H}^{(i)}\right]^{\mathcal{H}}\right\}$ is the correlation matrix of vector $\mathbf{H}^{(i)}$, $\mathbf{R}_{\mathbf{H}^{(i)}}$ is of size $N_{freq(i)} N_T N_R T \times N_{freq(i)} N_T N_R T$, $\gamma_a, a = 1, ..., r$ are the non-zero eigenvalues of

$$\mathbf{\Lambda}^{(i)} = \left(\mathbf{M}^{(i)} - \tilde{\mathbf{M}}^{(i)}\right) \mathbf{R}_{\mathbf{H}^{(i)}} \left(\mathbf{M}^{(i)} - \tilde{\mathbf{M}}^{(i)}\right)^{\mathcal{H}}.$$

Then the corresponding rank and product criteria are

1) Rank criterion: The minimum rank of $\mathbf{\Lambda}^{(i)}$ over all pairs of different matrices $\mathbf{M}^{(i)}$ and $\tilde{\mathbf{M}}^{(i)}$ should be as large as possible.

2) Product criterion: the minimum value of the product $\prod_{a=1}^{r} \gamma_a$ over all pairs of different $\mathbf{M}^{(i)}$ and $\tilde{\mathbf{M}}^{(i)}$ should be maximized.

To further analyze diversity properties of coded STF blocks, it is helpful to compute $\mathbf{R}_{\mathbf{H}^{(i)}} = E\left\{\mathbf{H}^{(i)} \left[\mathbf{H}^{(i)}\right]^{\mathcal{H}}\right\}$, the correlation matrix of vector $\mathbf{H}^{(i)}$.

The frequency domain channel vector for each transmit and receive antenna path in matrix form is,

$$\mathbf{H}_{m,n}^{(i)} = \left(\mathbf{I}_T \otimes \mathbf{W}^{(m,i)}\right) \mathbf{h}_{m,n}, \tag{7.23}$$

where

$$m = 1, ..., N_T, n = 1, ..., N_R,$$
$$\mathbf{W}^{(m,i)} = \left[\mathbf{w}_{p_{1_{(i)}}^{(m)}}, \cdots, \mathbf{w}_{p_{N_{F(i)}}^{(m)}}\right]^{\mathcal{T}}$$

and

$$\mathbf{h}_{m,n} = \left[\left[\mathbf{h}_{m,n}^{(1)}\right]^{\mathcal{T}}, \cdots, \left[\mathbf{h}_{m,n}^{(T)}\right]^{\mathcal{T}}\right].$$

The frequency domain channel vector for the whole coded STF block is written as,

$$\mathbf{H}^{(i)} = \mathbf{W}^{(i)} \mathbf{h}, \tag{7.24}$$

where

$$\mathbf{W}^{(m,i)} = \left[\mathbf{w}_{p_{1_{(i)}}^{(m)}}, \cdots, \mathbf{w}_{p_{N_{freq(i)}}^{(m)}}\right]^{\mathcal{T}} \tag{7.25}$$

and

$$\mathbf{h} = \left[[\mathbf{h}_{1,1}]^{\mathcal{T}}, ..., [\mathbf{h}_{N_T,1}]^{\mathcal{T}}, ..., [\mathbf{h}_{1,N_R}]^{\mathcal{T}}, ..., [\mathbf{h}_{N_T,N_R}]^{\mathcal{T}}\right]^{\mathcal{T}}.$$

Thus,

$$\begin{aligned} \mathbf{R}_{\mathbf{H}^{(i)}} &= E\left\{\mathbf{W}^{(i)}\mathbf{h}\left[\mathbf{W}^{(i)}\mathbf{h}\right]^{\mathcal{H}}\right\} \\ &= \mathbf{W}^{(i)} E\left\{\mathbf{h}\left[\mathbf{h}\right]^{\mathcal{H}}\right\}\left[\mathbf{W}^{(i)}\right]^{\mathcal{H}} \\ &= \mathbf{W}^{(i)}\mathbf{\Phi}\left[\mathbf{W}^{(i)}\right]^{\mathcal{H}} \end{aligned}, \tag{7.26}$$

where

$$\mathbf{\Phi} = E\left\{\mathbf{h}\left[\mathbf{h}\right]^{\mathcal{H}}\right\}.$$

Note that arbitrary channel correlation among space, time and frequency may occur in $\mathbf{\Phi}$.

In general, for matrices $\mathbf{A}$ and $\mathbf{B}$, we know

$$rank\left(\mathbf{AB}\right) \leq \min\left\{rank\left(\mathbf{A}\right), rank\left(\mathbf{B}\right)\right\}. \tag{7.27}$$

Thus,

$$\begin{aligned} &rank\left(\mathbf{\Lambda}^{(i)}\right) \leq \\ &\min\left\{rank\left(\mathbf{M}^{(i)} - \tilde{\mathbf{M}}^{(i)}\right), rank\left(\mathbf{R}_{\mathbf{H}^{(i)}}\right)\right\} \end{aligned}. \tag{7.28}$$

To maximize the rank of $\mathbf{R}_{H^{(i)}}$, it is sufficient to maximize the rank of $\mathbf{W}^{(i)}$ and the rank $\mathbf{\Phi}$.

To maximize the rank of $\mathbf{W}^{(i)}$, it is sufficient to maximize the ranks of $N_{freq(i)} \times (L+1)$ matrices $\mathbf{W}^{(m,i)}$ respectively, where $m = 1, ..., N_T$. Thus we need to choose

$$N_{freq(i)} \geq L + 1 \geq L_{m,n} + 1. \tag{7.29}$$

When $p^{(m)}_{n_{F(i)}} = p^{(m)}_{1_{(i)}} + b(n_F - 1), n_{F_{(i)}} = 1_{(i)}, ..., N_{freq(i)}, N_{freq(i)} \geq L+1$, where $p^{(i)}_{n_F} \leq N_C$ and b is a positive integer, $\mathbf{W}^{(m,i)}$ could achieve maximum rank $L+1$ (From (7.4) and (7.25), $\mathbf{W}^{(m,i)}$ is a square partition within a FFT matrix. For arbitrary subcarrier indices chosen, $\mathbf{W}^{(m,i)}$ is not generally full rank. For the given subcarrier indices chosen, the square partition is always full rank), then the rank of $\mathbf{W}^{(i)}$ could be maximized to $TN_TN_R(L+1)$. The choice of interval b is discussed in [72] and [98]. It can be shown that the maximal achievable rank of $\mathbf{\Phi}$ is $T\sum_{m=1}^{N_T}\sum_{n=1}^{N_R}(L_{m,n}+1)$. Hence, the maximal achievable rank of $\mathbf{R}_{H^{(i)}}$ is $T\sum_{m=1}^{N_T}\sum_{n=1}^{N_R}(L_{m,n}+1)$. If $L_{m,n} = L$ holds for all $m = 1, ..., N_T, n = 1, ..., N_R$, $\mathbf{R}_{\mathbf{H}^{(i)}}$ can have a maximal achievable rank $N_TN_RT(L+1)$. We know $\mathbf{M}^{(i)} - \tilde{\mathbf{M}}^{(i)}$ is of a size $N_{freq(i)}N_RT \times N_{freq(i)}N_TN_RT$. Thus $rank\left(\mathbf{M}^{(i)} - \tilde{\mathbf{M}}^{(i)}\right) \leq N_{freq(i)}N_RT$.

Consequently, the achievable diversity order of the coded STF block satisfies

$$rank\left(\mathbf{\Lambda}^{(i)}\right) \leq \min\left\{N_{freq(i)}N_RT, T\sum_{m=1}^{N_T}\sum_{n=1}^{N_R}(L_{m,n}+1)\right\}. \tag{7.30}$$

According to [79], when no correlation exists across space, time, and frequency, the STF correlation function can be expressed as

$$\begin{aligned}\rho_{STF}(\Delta f, v) &= \mathbb{E}\left[h_{l,m,n}(t, f_1)\left[h_{l',m',n'}(t+v, f_2)\right]^*\right] \\ &= \mathbf{R}_s((m,n),(m',n'))\mathbf{R}_t(v)\mathbf{R}_f(\Delta f),\end{aligned} \tag{7.31}$$

where $\{l, m, n\}$ and $\{l', m', n'\}$ are a pair of indices of frequency selective channel taps, transmit and receive antennas, t and f are time and frequency parameters, respectively. As a straightforward extension, if the time correlation is independent of the space and frequency correlation,

$$\rho_{STF}(\Delta f, v) = \mathbf{R}_{sf}((m,n,f_1),(m',n',f_2))\mathbf{R}_t(v), \tag{7.32}$$

In this case, we have

$$rank(\mathbf{R}_{\mathbf{H}^{(i)}}) = rank(\mathbf{R}^{(i)}_t)rank(\mathbf{R}^{(i)}_{sf}), \tag{7.33}$$

and the upper bound diversity order in (7.30) becomes

$$\min\left\{N_{freq(i)}N_RT, rank(\mathbf{R}_t^{(i)})\sum_{m=1}^{N_T}\sum_{n=1}^{N_R}(L_{m,n}+1)\right\}, \tag{7.34}$$

where $\mathbf{R}_t^{(i)}$ is a $T \times T$ time correlation matrix, and $N_{freq(i)} \geqslant L+1$.

The above analysis has revealed that it is possible for a properly chosen STF block design of size $T \times N_{freq(i)}N_T$ to achieve a diversity order up to $T\sum_{m=1}^{N_T}\sum_{n=1}^{N_R}(L_{m,n}+1)$, which is more general than the upper bound diversity order $N_RN_TT(L+1)$ provided in [97], since we consider the varying frequency selective channel orders of different transmit-receive antenna paths. The necessary condition that STF block design achieves a certain diversity order is that the rank of the channel correlation matrix be equal to the diversity order of the STF block.

The STF blocks $C^{(i)}, i = 1, ..., D_{STFB}$ of both DLD-STFC and LD-STFC designs are across multiple time-varying OFDM blocks, multiple transmit antennas and multiple subcarriers, and thus have the potential to achieve full diversity order. The smaller block-size STFC design may in fact achieve high performance with lower complexity. However, the actual diversity order achieved is based on the specific LDC design chosen. In [42], diversity order is not optimized. In [47], both capacity and error probability are used as criteria but the diversity analysis is based on quasi-static flat fading space-time channels. The proposed LD-STFC has diversity determined by the a single LDC procedure operating in 3-D STF space. In contrast, DLD-STFC includes two complete LDC procedures, operating over FT and ST 2-D planes. If the FT-LDC and ST-LDC procedures achieve full diversity order, then DLD-STFC can achieve diversity order up to $T\sum_{m=1}^{N_T}\sum_{n=1}^{N_R}(L_{m,n}+1)$, where N_R is independent of specific STFC design. In addition, in DLD-STFC, source symbols for ST-LDC are coded FT-LDC symbols. Thus time dependency is already included, and therefore the upper bound additional maximal diversity order for ST-LDC is N_T instead of N_TT.

DLD-STFC operates on much smaller 2-D FT-LDC and ST-LDC blocks instead of the larger 3-D STF blocks.

7.5 Design criteria based on union bound

The error union bound (EUB) has been defined in Section 2.2.2, and the EUB used in this chapter is block based EUB. Based on EUB, we analyze an LDC coding stage across multiple transmit antennas, i.e., the ST-LDC stage of DLD-STFC and the STF stage of LD-STFC. In [88], space time codes are analyzed based on EUB, where channel gains are assumed constant over time during the entire space time codewords. We provide an EUB analysis for MIMO OFDM channels whose gains may vary over the time duration of an LDC codeword, e.g., over different OFDM blocks. The EUB can be expressed as

$$P_U = \sum_{a=1}^{N_B} p_a \sum_{b \neq a}^{N_B} PEP_{ab} \leq (N_B - 1) \max_{ab} PEP_{ab}, \tag{7.35}$$

where p_a is the probability that LDC codeword $\mathbf{X}^{(a)}$ was transmitted, PEP_{ab} is the probability that receiver decides $\mathbf{X}^{(b)}$ when $\mathbf{X}^{(a)}$ is actually transmitted, and N_B is the LDC code book size.

We write a unified system equation for one STF block as

$$\mathbf{R}_U = \sqrt{\frac{\rho}{N_T}} \mathbf{H}_U \sum_{q=1}^{Q} vec(\mathbf{A}_q) s_q + \mathbf{V}_U, \tag{7.36}$$

where $\mathbf{R}_U$ and $\mathbf{V}_U$ are the received signal and additive noise vectors, respectively, $\mathbf{A}_q, q = 1, ..., Q$ are linear dispersion matrices, $s_q, q = 1, ..., Q$ are source symbols for this LDC coding procedure, and $\mathbf{H}_U$ denotes the channel matrix corresponding to different code mappings.

In the following, the subcarrier indices are the same as that in Section 7.4.

For LD-STFC, $\mathbf{H}_U = \mathbf{H}^{(i)}_{LD\_STFC}$, and

$$\mathbf{H}^{(i)}_{LD\_STFC} = \begin{bmatrix} \mathbf{H}^{(i)}_{LD\_STFC(1,1)} & \cdots & \mathbf{H}^{(i)}_{LD\_STFC(N_T,1)} \\ \vdots & \ddots & \vdots \\ \mathbf{H}^{(i)}_{LD\_STFC(1,N_R)} & \cdots & \mathbf{H}^{(i)}_{LD\_STFC(N_T,N_R)} \end{bmatrix},$$

where

$$\mathbf{H}^{(i)}_{LD\_STFC(m,n)} = diag(H^{(1)}_{m,n,p^{(m)}_{1_{(m,i)}}}, ..., H^{(T)}_{m,n,p^{(m)}_{1_{(m,i)}}}, ..., H^{(1)}_{m,n,p^{(m)}_{N^{ant}_{LD(i)}}}, ..., H^{(T)}_{m,n,p^{(m)}_{N^{ant}_{LD(i)}}})$$

and $p^{(m)}_{n_{F(i)}}, n_{F(i)} = 1_{(i)}, ..., N^{ant}_{LD(i)}$. are the subcarrier indices of the partition of the i-th LDC on the m-th transmit antenna. For the ST-LDC stage of DLD-STFC, $\mathbf{H}_U = \mathbf{H}^{(p_{n_{F(i)}})}_{DLD\_STFC\_ST}$, with

$$\mathbf{H}^{(p_{n_{F(i)}})}_{DLD\_STFC\_ST} = \begin{bmatrix} \mathbf{H}^{(p_{n_{F(i)}})}_{DLD\_STFC\_ST(1,1)} & \cdots & \mathbf{H}^{(p_{n_{F(i)}})}_{DLD\_STFC\_ST(N_T,1)} \\ \vdots & \ddots & \vdots \\ \mathbf{H}^{(p_{n_{F(i)}})}_{DLD\_STFC\_ST(1,N_R)} & \cdots & \mathbf{H}^{(p_{n_{F(i)}})}_{DLD\_STFC\_ST(N_T,N_R)} \end{bmatrix},$$

where

$$\mathbf{H}^{(p_{n_{F(i)}})}_{DLD\_STFC\_ST(m,n)} = diag(H^{(1)}_{m,n,p^{(m)}_{n_{F(i)}}}, \cdots, H^{(T)}_{m,n,p^{(m)}_{n_{F(i)}}}),$$

and $p^{(m)}_{n_{F(i)}}, n_{F(i)} = 1_{(i)}, \cdots, N_{F(i)}$ are the subcarrier indices of the partition of the i-th LDC on the m-th transmit antenna.

Denote the channel-weighted inner product between two dispersion matrices as

$$\begin{aligned} \Omega_{p,q} &= \langle vec\left(\mathbf{A}_p\right), vec\left(\mathbf{A}_q\right)\rangle_{\mathbf{H}_u} \\ &= \frac{1}{2}\begin{pmatrix} Tr\left[[vec(\mathbf{A}_p)]^{\mathcal{H}}\left[\mathbf{H}_U\right]^{\mathcal{H}}\mathbf{H}_U vec(\mathbf{A}_q)\right] + \\ Tr\left[[vec(\mathbf{A}_q)]^{\mathcal{H}}\left[\mathbf{H}_U\right]^{\mathcal{H}}\mathbf{H}_U vec(\mathbf{A}_p)\right] \end{pmatrix} \\ &= Tr\left([vec(\mathbf{A}_p)]^{\mathcal{H}}\left[\mathbf{H}_U\right]^{\mathcal{H}}\mathbf{H}_U vec(\mathbf{A}_q)\right) \\ &= Tr\left(\mathbf{H}_U vec(\mathbf{A}_p)\left[vec(\mathbf{A}_q)\right]^{\mathcal{H}}\left[\mathbf{H}_U\right]^{\mathcal{H}}\right) \end{aligned} \tag{7.37}$$

and

$$\Omega_{q,q} = \|\mathbf{H}_U vec\left(\mathbf{A}_q\right)\|_F^2 \geq 0, \tag{7.38}$$

where p,$q = 1, ..., Q$. Denote squared pairwise Euclidean distance between two received codewords $\mathbf{X}^{(a)}$ and $\mathbf{X}^{(b)}$ and for the given channel $\mathbf{H}_U$ as

$$\begin{aligned}
\mathcal{D}_{a,b} &= \left\|\mathbf{H}_U\left(\mathbf{X}^{(a)} - \mathbf{X}^{(b)}\right)\right\|_F^2 \\
&= \left\|\sum_{q=1}^{Q}\left[\left[\mathbf{H}_U vec\left(\mathbf{A}_q\right)\right]\left(s_q^{(a)} - s_q^{(b)}\right)\right]\right\|_F^2 \\
&= \sum_{q=1}^{Q}\left[\Omega_{q,q}\left|e_q^{(a,b)}\right|^2\right] + 2\,\mathrm{Re}\left\{\sum_{q=1}^{Q}\sum_{p<q}^{Q}\left[\Omega_{p,q}\left[e_p^{(a,b)}\right]^* e_q^{(a,b)}\right]\right\},
\end{aligned} \tag{7.39}$$

where

$$e_q^{(a,b)} = s_q^{(a)} - s_q^{(b)}$$

denotes the difference between source symbol sequences (a) and (b) at the q-th position. Eq. (7.39) is obtained via

$$\begin{aligned}
&Tr\left[vec(\mathbf{A}_p)\right]^H\left[\mathbf{H}_U\right]^H\mathbf{H}_U vec(\mathbf{A}_q)\left[e_p^{(a,b)}\right]^* e_q^{(a,b)} + \\
&Tr\left[vec(\mathbf{A}_q)\right]^H\left[\mathbf{H}_U\right]^H\mathbf{H}_U vec(\mathbf{A}_p)\left[e_q^{(a,b)}\right]^* e_p^{(a,b)} \\
&= 2\,\mathrm{Re}\,Tr\left(\left[vec(\mathbf{A}_p e_p^{(a,b)})\right]^H\left[\mathbf{H}_U\right]^H\mathbf{H}_U vec(\mathbf{A}_q e_q^{(a,b)})\right) \\
&= 2\,\mathrm{Re}\left\{\Omega_{p,q}\left[e_p^{(a,b)}\right]^* e_q^{(a,b)}\right\}.
\end{aligned}$$

The pairwise error probability conditioned on channel $\mathbf{H}_U$ is [84]

$$PEP_{ab|\mathbf{H}_U} = Q\left(\sqrt{\frac{\eta}{2}\mathcal{D}_{ab}}\right), \tag{7.40}$$

where the SNR component is $\eta = \frac{\rho}{N_T}$. The EUB conditioned on channel $\mathbf{H}_U$ is [88]

$$P_{U|\mathbf{H}_U} = \sum_{a=1}^{N_B} p_a \sum_{b\neq a}^{N_B} Q\left(\sqrt{\frac{\eta}{2}\mathcal{D}_{ab}}\right). \tag{7.41}$$

As in [88, 90], denote

$$\Delta_1^{(a,b)} = \frac{\eta}{2} \sum_{q=1}^{Q} \left[\Omega_{q,q} \left| e_q^{(a,b)} \right|^2 \right] \tag{7.42}$$

and

$$\Delta_2^{(a,b)} = \frac{\eta}{2} 2 \sum_{q=1}^{Q} \sum_{p<q}^{Q} \left[\Omega_{p,q} \left[e_p^{(a,b)} \right]^* e_q^{(a,b)} \right]. \tag{7.43}$$

Using (7.37), (7.38), (7.39), (7.41), (7.42) and (7.43), we obtain [88, 90]

$$P_{U|\mathbf{H}_U} = \sum_{a=1}^{N_B} p_a \sum_{b \neq a}^{N_B} Q\left(\sqrt{\Delta_1^{(a,b)} + \Delta_2^{(a,b)}} \right). \tag{7.44}$$

We have the following remarks.

1) The uncorrelated input source symbol sequences above are complex while those in [88, 90], are real-valued. Thus, for QAM constellations for the case of [88, 90], real and imaginary coordinates use different dispersion matrices and the minimum error event is one real output error, i.e., one coordinate in error. However, in the new approach, the minimum error would be one complex symbol.

2) Although (7.41), (7.42), (7.43), (7.44) are similar to expressions in [88, 90], we have redefined $\mathcal{D}_{a,b}$, $\Omega_{p,q}$, $\Delta_1^{(a,b)}$, and $\Delta_2^{(a,b)}$ based on a channel whose coefficients may vary over time within one STFC codeword. The corresponding quantities defined in [88, 90] are only suitable for block-fading channels, i.e., those with constant coefficients over time within one space time matrix codeword.

If all source symbols are equally likely, i.e. $p_a = \frac{1}{N}$ for all a, the following two lemmas apply. Lemma 1 extends Lemma 2 in [90] to complex input sequences. Lemma 2 appears in [90] and applies to both real or complex inputs.

Lemma 1 *For uncorrelated complex input sequences, by carefully selecting terms in (7.44), one can always pair up terms in (7.39) such that their EUB contribution is written as*

$$\theta = \frac{g}{N_B}\left[Q\left(\sqrt{\Delta_1+\Delta_2}\right)+Q\left(\sqrt{\Delta_1-\Delta_2}\right)\right], \tag{7.45}$$

where g is an integer denoting the number of such pairs.

Except the consideration of complex input sequences, the proof of Lemma 1 is similar to that of Lemma 2 in [90]. The outline of the proof of Lemma 1 is provided in Appendix D.1.

Lemma 2 *[88] For a given Δ_1, θ in (7.45) is minimized if and only if $\Delta_2 = 0$.*

For linear dispersion codes in 2-D rapid fading channels with realization $\mathbf{H}_U$, we have the following EUB-based optimal design criterion:

Proposition 1 *For uncorrelated complex source input symbol sequences, consider LDC with $T \times M$ dispersion matrices $\mathbf{A}_q, q = 1, ..., Q$ used for real and imaginary parts of source symbols,*

$$\begin{array}{l} \mathbf{A}_q\left[\mathbf{A}_q\right]^{\mathcal{H}} = I_T, \text{ if } \quad \mathrm{T} \leq \mathrm{M} \\ \left[\mathbf{A}_q\right]^{\mathcal{H}}\mathbf{A}_q = I_M, \text{ if } \quad \mathrm{T} \geq \mathrm{M} \end{array} .$$

Union bound $P_{U|\mathbf{H}_U}$ achieves a minimum in 2-D rapid fading channels iff the matrices satisfy

$$\Omega_{p,q} = Tr\left(\left[vec(\mathbf{A}_p)\right]^{\mathcal{H}}\left[\mathbf{H}_U\right]^{\mathcal{H}}\mathbf{H}_U vec(\mathbf{A}_q)\right) = 0 \tag{7.46}$$

for any $1 \leq p \neq q \leq Q$.

Proposition 1 is equivalent to requiring $vec(\mathbf{A}_p)$ and $vec(\mathbf{A}_p)$ to be pairwise orthogonal for any weighting matrix $\Theta = [\mathbf{H}_U]^{\mathcal{H}} \mathbf{H}_U$. For quasi-static channels, the above result takes the form

$$\Omega_{p,q} = Tr\left([\mathbf{A}_p]^{\mathcal{H}} [\mathbf{H}]^{\mathcal{H}} \mathbf{H}\mathbf{A}_q\right) = 0, \tag{7.47}$$

which is based on real input sequences [88]. The proof of the above Lemma 2 is similar to the proof of Lemma 4 of [90] except for the strategy to deal with complex input sequences shown in Appendix D.1. A further implication of this new result is that (7.47) also ensures that union bound $P_{U|\mathbf{H}_U}$ achieves a minimum in block fading channels.

Based on averaging the channel realizations $\mathbf{H}_U$, we have the following suboptimal criterion for unknown channels at the transmitter.

Theorem 5 *For uncorrelated complex source input symbol sequences, consider LDC with $T \times M$ dispersion matrices and $\mathbf{A}_q, q = 1, ..., Q$ corresponding to real and imaginary parts of source symbols satisfying*

$$\begin{aligned} \mathbf{A}_q [\mathbf{A}_q]^{\mathcal{H}} &= \mathbf{I}_T, \text{ if } \quad T \leq M \\ [\mathbf{A}_q]^{\mathcal{H}} \mathbf{A}_q &= \mathbf{I}_M, \text{ if } \quad T \geq M \end{aligned} .$$

Assume that

1) *the auto-correlation of 2-D channel gains dominates the cross-correlation of any two different channel gains in 2-D channels,*

2) *the auto-correlation of channel gains for each element in the channel matrix are the same.*

The part of the union bound P_U related to the auto-correlation of channel gains in the 2-D channel based on averaged channel realizations is minimized if

$$Tr\left[vec(\mathbf{A}_p) [vec(\mathbf{A}_q)]^{\mathcal{H}}\right] = 0 \tag{7.48}$$

for any $1 \leq p \neq q \leq Q$.

A proof is provided in Appendix D.2.

The correlation between different subcarriers with one OFDM block can be calculated as $\mathcal{R}(a) = \mathbb{E}\left\{H_p \left[H_{p+a}\right]^*\right\} = \sum_{l=0}^{L} \alpha_l \exp\left(j2\pi \frac{la}{N_C}\right)$, and $\mathcal{R}(0) = \mathbb{E}\left\{H_p \left[H_p\right]^*\right\} = \sum_{l=0}^{L} \alpha_l$, where α_l is the variance of the l-th channel tap. Note that the auto-correlation of the subcarriers usually dominates the cross-correlation among different subcarriers, and that the auto-correlation of two channel gains in space-time MIMO channels usually dominates the cross-correlation of two channel gains. Otherwise, the channels would be highly correlated over space and time, and ill-suited for spatial multiplexing. In the above conditions, Theorem 5 may be applied to code design in MIMO-OFDM systems.

Theorem 5 provides a new EUB design criterion for LDC for communications in correlated parallel channels. A class of recently proposed rectangular LDC, termed uniform LDC (U-LDC), meets this union bound criterion, which is shown in Appendix A.

Finally, we conjecture that in a block fading channel, provided that uncorrelated complex source input symbol sequences are used, the part of the union bound P_U related to the auto-correlation of channel gains in the block fading channel based on averaged channel realizations is minimized if

$$Tr\left[\mathbf{A}_p \left[\mathbf{A}_q\right]^H\right] = 0, \tag{7.49}$$

for any $1 \leq p \neq q \leq Q$.

Note that union bound based analysis is most applicable to the system with maximum likelihood decoding or near optimal decoding. However, this analysis may be approximately or asymptotically applied for low complexity decoding, including used

in the later simulation performance study.

7.6 Performance

7.6.1 Simulation setup

Perfect channel knowledge (amplitude and phase) is assumed at the receiver but not at the transmitter. The number of subcarriers per OFDM block, N_C, is 32. In all DLD-STFC, LD-STFC and MIMO-LDC-OFDM system simulations, all LDC codewords are encoded either using HH square code as shown in (3.10) or U-LDC described in Section 4.2.

The symbol coding rates of all systems are unity, so compared with non-LDC-coded MIMO-OFDM systems, no bandwidth is lost. The sizes of all LDC codewords in the FT-LDC stage of DLD-STFC and MIMO-LDC-OFDM are identically $T \times N_F$, as are the sizes of LDC codewords in the ST-LDC stage of DLD-STFC, $T \times N_T$, as are the sizes of LDC codewords in LD-STFC, $T \times N_{LD}$, where $N_{LD} = N_{LD}^{ant} N_T$, and N_{LD}^{ant} is the size of the subcarrier partition on each transmit antenna for an LDC codeword.

An evenly spaced LDC subcarrier mapping (ES-LDC-SM) for the FT-LDC of DLD-STFC and MIMO-LDC-OFDM, as well as LD-STFC, is used in simulations unless indicated otherwise. In ES-LDC-SM, subcarriers chosen within one LDC codeword are evenly spaced by maximum available intervals for all different LDC codewords. We note that ES-LDC-SM ensures $\mathbf{W}^{(m,i)}$, defined in Section 7.4, to be of full rank, to achieve maximum diversity order. For comparison purposes, another subcarrier mapping, called connected LDC subcarrier mapping (C-LDC-SM), is tested for the FT-LDC of DLD-STFC. In C-LDC-SM, subcarriers within one LDC codeword are chosen to be adjacent.

Since the aim of reaching maximal achievable diversity may require non-square FT-LDC or ST-LDC, U-LDC is utilized for DLD-STFC.

The frequency selective channel has $(L+1)$ paths exhibiting an exponential power delay profile, and a channel order of $L = 3$ is chosen. Data symbols use QPSK modulation in all simulations. The number of antennas are set to $N_R = N_T$. Except for Section 7.6.6, no spatial correlation is assumed in simulations. The signal-to-noise-ratio (SNR) reported in all figures is the average symbol SNR per receive antenna.

7.6.2 Performance comparison among DLD-STFC with two different LDC subcarrier mappings and non-LDC-coded MIMO-OFDM

Figure 7.4 shows the performance comparison of Bit Error Rate (BER) vs. SNR among DLD-STFC with two different LDC subcarrier mappings, ES-LDC-SM and C-LDC-SM, and C-LDC-SM, and non-LDC-coded MIMO-OFDM for various combinations of T in two transmit and two receive (2×2) MIMO antennas systems.

Clearly, in frequency-selective Rayleigh fading channels, BER performance of DLD-STFC is notably better than that of non-LDC-coded MIMO-OFDM. The larger the dispersion matrices used, the greater the performance improvement, at a cost of increased decoding delay. The simulations use U-LDC based DLD-STFC. Though we do not claim that U-LDC are full diversity codes, we conjecture that U-LDC based STFC can achieve close to full diversity performance for PSK constellations. This superior performance is also due to U-LDC satisfying the EUB criterion in Section 7.5.

It is clearly observed that the performance of DLD-STFC with ES-LDC-SM is

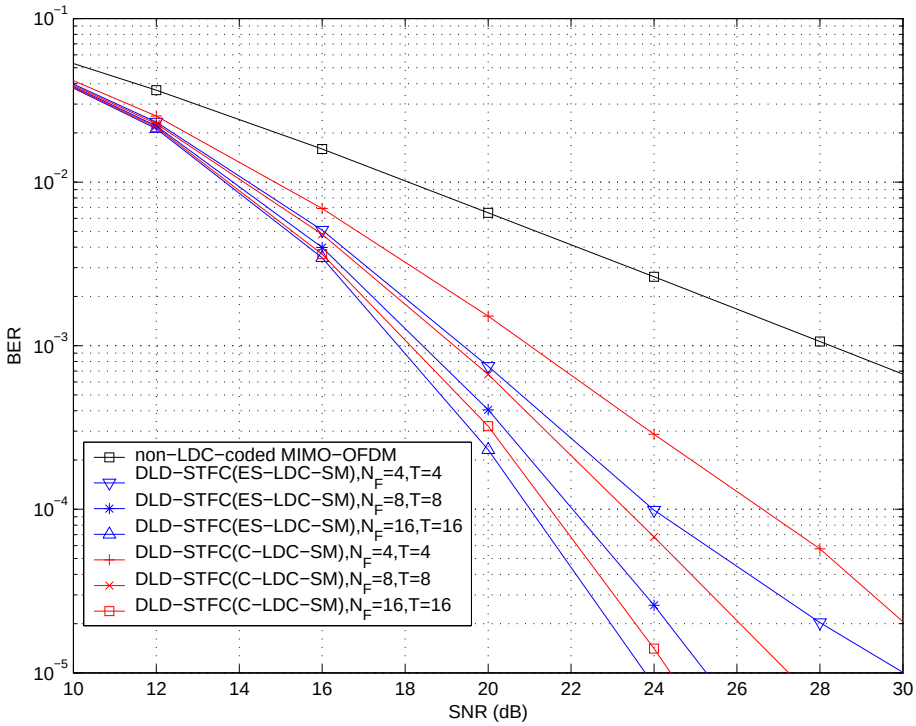

Figure 7.4. BER Performance of MIMO-OFDM vs DLD-STFC with different sizes of dispersion matrices and two different LDC-subcarrier mappings. $L = 3$, $CCI = 1$ OFDM block, $N_T = N_R = 2$, $N_C = 32$.

notably better than that of DLD-STFC with C-LDC-SM. Thus, LDC subcarrier mappings influence the performance of DLD-STFC.

7.6.3 Effect of channel dynamics in DLD-STFC

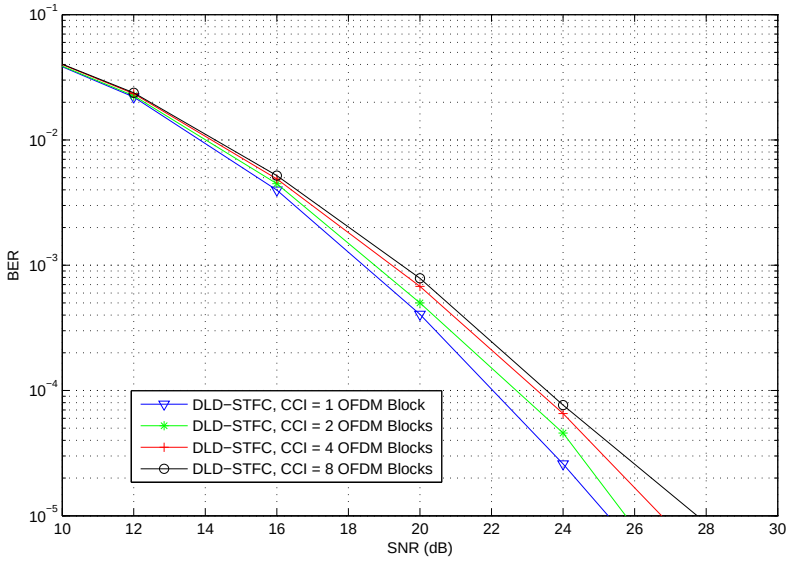

Figure 7.5. BER Performance of DLD-STFC (ES-LDC-SM) under different CCIs, $L = 3$, $N_T = N_R = 2$, $N_C = 32$, $N_F = 8$, $T = 8$.

Figure 7.5 depicts performance of DLD-STFC with ES-LDC-SM under various different rates of channel parameter change in a 2×2 MIMO system. Note that different CCIs roughly correspond to different degrees of temporal channel correlation over OFDM blocks. Two extreme cases were tested: when $CCI = 1$, i.e., channel correlation over time is zero, full time diversity is available in the channel. When $CCI = T$, i.e., channel correlation over time is unity, no time diversity is available in the channel. As discussed in Section 7.4, STFC diversity order is maximized only if the channel provides block-wise temporal independence.

As shown in Figure 7.5, the performance of DLD-STFC is significantly influenced by channel dynamics, i.e., time correlation. At high SNRs, the faster the channel changes, the better the performance. This indicates that DLD-STFC effectively exploits available temporal diversity across multiple OFDM blocks. In the future, testing on a more accurate model of temporal channel dynamics is needed to obtain a more accurate assessment.

7.6.4 Performance comparison between DLD-STFC and MIMO-LDC-OFDM

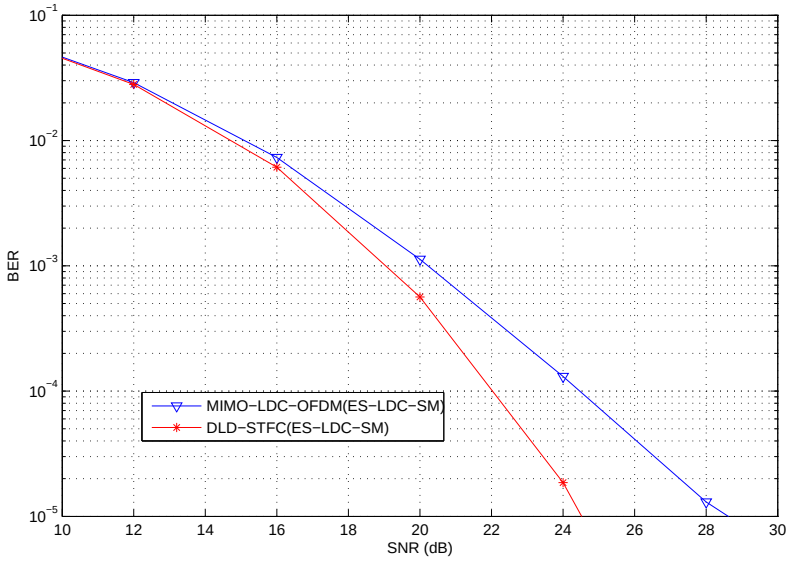

Figure 7.6. BER Performance of MIMO-LDC-OFDM(ES-LDC-SM) vs. DLD-STFC(ES-LDC-SM) with the same size of N_F, $L = 3$, $CCI = 1$ OFDM block, $N_T = N_R = 4$, $N_C = 32$, $N_F = 8$, $T = 8$.

Figure 7.6 compares DLD-STFC to MIMO-LDC-OFDM with same sized FT-LDC codewords in a 4×4 MIMO system. While at low SNRs, the performance

difference between DLD-STFC and MIMO-LDC-OFDM is small, at high SNRs, DLD-STF noticeably outperforms MIMO-LDC-OFDM. The performance gain arises from the increased spatial diversity due to the ST-LDC coding stage of DLD-STFC.

7.6.5 Performance comparison between DLD-STFC and LD-STFC

We compare space and frequency diversity of DLD-STFC with ES-LDC-SM and LD-STFC with ES-LDC-SM in a 2×2 MIMO system, and remove the effects of time diversity in the channels through setting CCI to be a multiple of T.

7.6.5.1 Effects of size of subcarrier group of DLD-STFC and LD-STFC

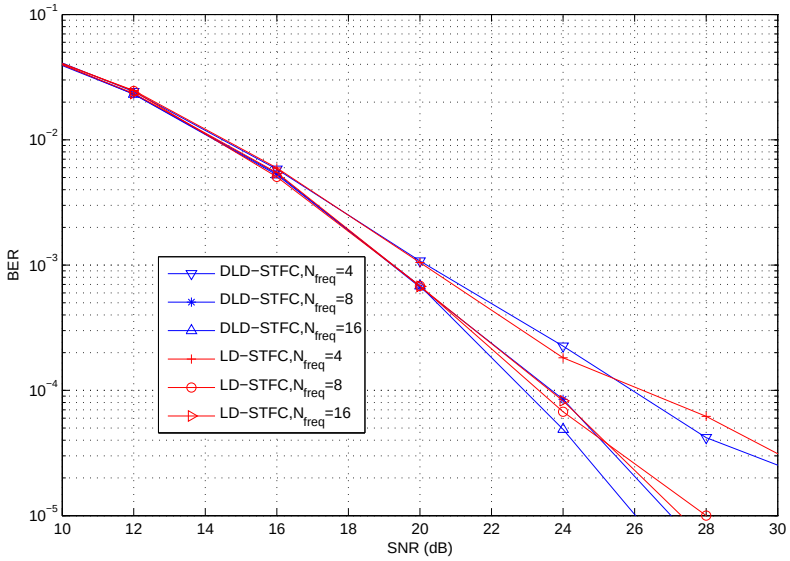

Figure 7.7. BER Performance of LD-STFC(ES-LDC-SM) vs. DLD-STFC(ES-LDC-SM) with different sizes of N_{freq} blocks, $L = 3$, $CCI = 32$ OFDM blocks, $N_T = N_R = 2$, $N_C = 32$, $T = 32$.

The coded STF block design with $N_F = L+1$ could achieve full frequency selective diversity, which we term a *compact frequency diversity design*. We investigate whether the performance of U-LDC based DLD-STFC and LD-STFC is close to compact design through comparison under different sized N_{freq} in a 2×2 MIMO system, as shown in Figure 7.7. In Figure 7.7, the performance of DLD-STFC and LD-STFC with $N_{freq} = 4 = (L+1)$ is worse than that of DLD-STFC and LD-STFC with $N_{freq} = 8 = 2(L+1)$ or $N_{freq} = 16 = 4(L+1)$, which implies $N_{freq} = 4 = (L+1)$ is not enough to efficiently exploit full frequency diversity in the channels. Further the performance of DLD-STFC and LD-STFC with $N_{freq} = 8 = 2(L+1)$ is quite close to that of DLD-STFC and LD-STFC with setting $N_{freq} = 16 = 2N_T(L+1)$, which implies $N_{freq} = 16 = 4(L+1)$ is a saturated or over-length. The results in Figure 7.7 imply that U-LDC based DLD-STFC and LD-STFC designs are not compact frequency diversity designs. Actually, according to our simulation experiences, no matter how the system configurations are set, for example $L = 7$ and $N_T = N_R = 2$, to achieve maximal or saturated frequency selective diversity performance, it is necessary to set N_{freq} to at least $2(L+1)$.

7.6.5.2 Effects of STF block sizes of DLD-STFC and LD-STFC

Figure 7.8 compares DLD-STFC to LD-STFC with different sized $N_T \times T \times N_{freq}$ STF blocks. In Figure 7.8, DLD-STFC with STF block size $2 \times 8 \times 8$ has performance similar to that of LD-STFC with STF block size $2 \times 16 \times 8$, while DLD-STFC with STF block size $2 \times 8 \times 8$ performs better than LD-STFC with STF block size $2 \times 8 \times 8$. The reason is that the diversity order of $T \times M$ U-LDC is no larger than $\min\{T, M\}$ for each matrix dimension. Thus LD-STFC with STF block size $2 \times 16 \times 8$ has the potential to achieve the same space and frequency diversity order as LD-STFC with

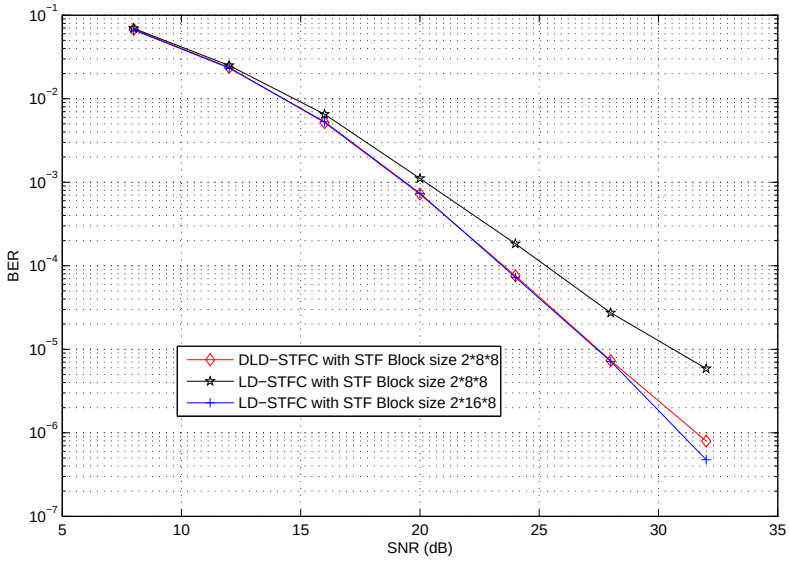

Figure 7.8. BER Performance of LD-STFC(ES-LDC-SM) vs DLD-STFC(ES-LDC-SM) with different sizes of STF blocks, $L = 3$, $CCI = 16$ OFDM blocks, $N_T = N_R = 2$, $N_C = 32$.

STF block size $2 \times 8 \times 8$.

For similar sized STF blocks, DLD-STFC utilizes smaller sized LDC codewords, thus reducing complexity.

7.6.6 Performance of DLD-STFC under spatial transmit channel correlation

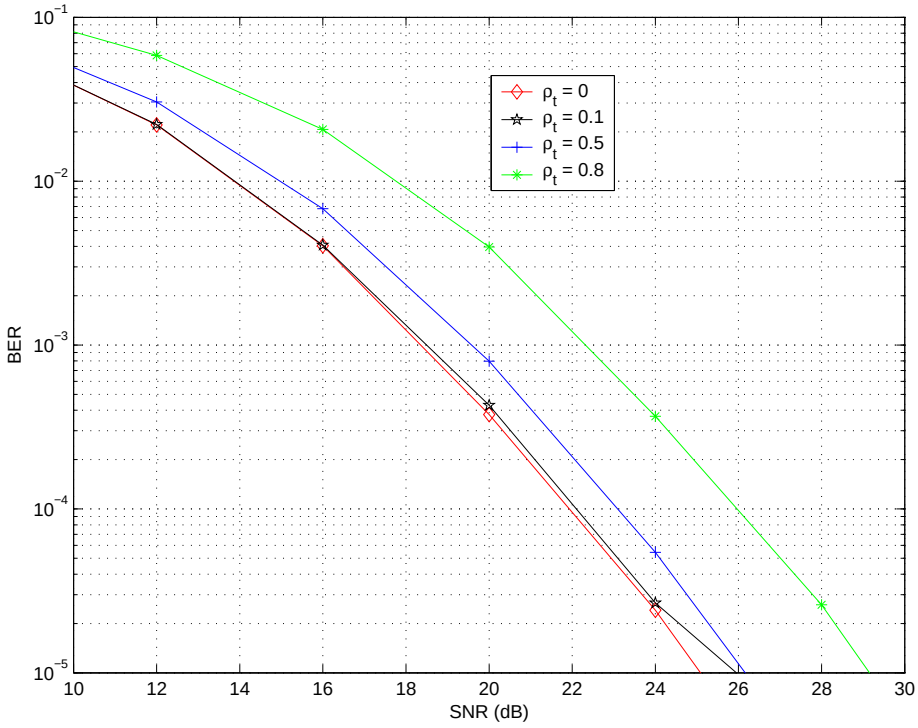

Figure 7.9. BER Performance of DLD-STFC(ES-LDC-SM) under spatial transmit channel correlation coefficients ρ_t, $L = 3$, $CCI = 1$ OFDM block, $N_T = N_R = 2$, $N_C = 32$, $N_F = 8$, $T = 8$.

In previous parts of this section, we considered spatially uncorrelated channels. In multiple antenna systems, spatial correlation must be considered. In order to have spatially correlated frequency-selective channels, it is important to recognize

that in a scenario of multi-ray delays, the gains for different delays of a channel are independent of one another [21]. Thus, the dependency between different channels comes from the correlation between tap-gains corresponding to the taps with the same delay on different spatial channels. Figure 7.9 shows the performance of DLD-STFC with ES-LDC-SM under different spatial transmit channel correlation in a two transmit and two receive antenna system. In the simulations spatial correlation is assumed between transmit antennas (correlation coefficient is denoted by ρ) and not between receive antennas.

As observed in Figure 7.9, spatial transmit correlation indeed degrades DLD-STFC performance. When the correlation is small, e.g., $\rho_t = 0.1$, compared with the spatially uncorrelated case, the performance loss is small. At a BER of 10^{-3}, the performance degrades only 0.2 dB. However, when the correlation is larger, e.g. $\rho_t = 0.5$ and $\rho = 0.8$ cases, compared with the spatially uncorrelated case, the performance loss is significant. At a BER of 10^{-3}, the performance degrades by 1.3 dB and 4.0 dB, respectively. Thus spatial correlation, as expected, may notably affect diversity gain behavior of DLD-STFC when correlation is high.

7.7 Conclusion

High-rate (up to symbol coding rate one) linear dispersion codes significantly improve MIMO-OFDM performance in time varying frequency selective fading channels at the expense of delay. For instance, in Figure 7.4, for a 2×2 MIMO system, $N_F = 8$ and $T = 8$, DLD-STFC with an evenly spaced LDC subcarrier mapping obtains a 9.8 dB gain over non-LDC-coded MIMO-OFDM at a BER of 10^{-3}. At high SNRs, the performance of DLD-STFC is notably better than that of MIMO-LDC-OFDM,

achieving 2.4 dB gain at a BER of 10^{-4} in a 4×4 MIMO system. We reiterate that, due to rate-one codes used, no bandwidth is lost! Both DLD-STFC and LD-STFC systems simultaneously exploit the diversity of space, time, and frequency available in wideband space time multicarrier communications channels. Pairwise error probability based analysis, which allows for arbitrary channel correlation among space (antennas), time (OFDM blocks) and frequency selective channel taps, provides insight into diversity properties of STF block-based STFC systems. From an error union bound analysis, more restrictive LDC code design criteria for complex source symbols are developed. Simulations show that the type of mapping used from LDC to OFDM subcarriers for both LD-STFC and DLD-STFC as well as high spatial transmit channel correlation significantly influences the diversity performance of the proposed STFC systems. In conclusion, the three-stage DLD-STFC technique has a relatively flexible performance/complexity tradeoff.

Chapter 8

Improved high-rate space-time-frequency block codes

8.1 Introduction

Space-time coding (STC) is employed to achieve space and time diversity gains in multiple transmit multiple receive antenna (MIMO) flat-fading channels [100, 101]. However, in frequency-selective channels, STC cannot explore available frequency dimension diversity in MIMO orthogonal frequency division multiplexing (OFDM) systems. Coding over space, time, and frequency, STFC, is therefore needed to exploit all available diversity across three physical dimensions.

Basically, there are two categories of coding approaches which can exploit diversity. Complex coding may be utilized to exploit diversity over physical dimensions, which we refer to as complex diversity coding (CDC). The second category includes conventional channel coding, including block-based or convolutional forward error correction (FEC).

We are interested in high-rate STFC designs. To distinguish among different existing and newly proposed STFCs discussed in this chapter, in terms of different

combinations of CDC and FEC, we may categorize high-rate STFCs into the following seven categories:

1) concatenation of inner 2-dimensional (2-D) channel codes (e.g. SF FEC or ST FEC) and outer 2-D channel codes (e.g. ST FEC or TF FEC) [52],

2) 3-D channel codes,

3) concatenation of inner channel codes and outer 2-D CDC (e.g. over SF or ST) [40],

4) concatenation of inner 2-D CDC and outer 2-D CDC [40, 123] ,

5) 3-D CDC [123, 130],

6) concatenation of first-inner channel codes, second-inner 2-D CDC, and outer 2-D CDC,

7) concatenation of inner channel codes and outer 3-D CDC.

Previously STFCs of Categories 1, 3, 4, and 5 have been proposed. However, there have been no proposals for STFCs of Categories 2, 6, and 7 to date. Note that STFCs of Category 6 and 7 are corresponding to STFCs of Category 4 and 5, respectively, with added channel coding. By extending the concept of linear dispersion coding (LDC) [42], high rate STFCs, known as double linear dispersion space-time-frequency-coding (DLD-STFC) are proposed in [123, 124], which may be classified as Category 4.

This chapter investigates performance improvement of STFCs in Categories 4 and 6, referred to DLD-STFC based approaches. Two issues are discussed in this chapter,

1) investigating the relation of two 2-D CDC for STFC Category 4,

2) investigating STFCs of Category 6.

8.2 MIMO-OFDM system model

The MIMO-OFDM system model used is the same as that in Section 7.2.

8.3 Two stage complex diversity coding of DLD-STFC

Double linear dispersion space-time-frequency-coding (DLD-STFC) [123, 124] is a class of two-stage STFBCs across N_T transmit antennas, N_C subcarriers, and T OFDM blocks. DLD-STFC systems are based on a layered communications structure, which is compatible to non-LDC coded MIMO-OFDM systems. An advantage of DLD-STFC is that the system may obtain 3-D diversity performance for the source data symbols that are only encoded and decoded through 2-D coding, and the complexity advantage may be significant if non-linear decoding methods, e.g. sphere decoding, are involved. Note that [130] claims to have a full diversity STF design. However, the 3-D CDC based STFC design in [130] may have high computational complexity. In this section, we try to improve diversity properties of DLD-STFC through investigating the relationship of the two stages of 2-D CDC of DLD-STFC. We term the originally proposed DLD-STFC as DLD-STFC Type A, which firstly encodes frequency-time LDC (FT-LDC) and secondly encodes space-time LDC (ST-LDC) [123,124]. By exchanging the sequence of the two stages, we propose a modified version of DLD-STFC, termed as DLD-STFC Type B, as follows. The first CDC encoding stage is the ST-LDC, performed across space (transmit antennas) and time

(OFDM blocks), enabling space and time diversity. The second CDC encoding stage is the FT-LDC, performed across frequency (subcarriers) and time (OFDM blocks), enabling frequency and time diversity. The corresponding encoding procedure for the i-th STF block of size $T \times N_{F(i)} \times N_T$ within one DLD-STFC Type B block is that

1) Firstly, the source data signals are encoded through per subcarrier ST-LDC. The p-th ST matrix codeword is of size $T \times N_T$, where $p = p_{1(i)}, ..., p_{N_{F(i)}}$ are subcarrier indices.

2) Secondly, all the m-th space index columns of $N_{F(i)}$ ST-LDC codewords are concatenated in sequence to a vector of size $TN_{F(i)} \times 1$, which is further encoded into the m-th FT-LDC codeword of the i-th STF block. The m-th FT-LDC matrix codeword is of size $T \times N_{F(i)}$. After N_T FT-LDC matrix codewords are created, the i-th STF block is created.

If all subcarriers are used for DLD-STFC and there are in total N_M STF blocks within one DLD-STFC Type B block, the frequency block size relation is $\sum_{i=1}^{N_M} N_{F(i)} = N_C$. The decoding sequence of DLD-STFC Type B is in the reverse order of the encoding procedure.

Note that it is inconvenient to analyze the diversity order of DLD-STFC in general due to the two stages involved. For further analysis, we employ Tirkkonen and Hottinen' concept of symbol-wise diversity order for 2-D codes with dimensions X and Y, $r_{sd(XY)}$ [108, 109]. We extend this concept by introducing a new term, K-symbol-wise diversity order for 2-D codes, $r_d^{(K)}$, for the case that the pair of matrix codewords contain at most K symbol differences, and $r_{d(XY)}^{(K)} = \min \left\{ \begin{array}{l} rank\left(\Phi_{q_1,...,q_K}\right), 1 \leqslant q_i \leqslant Q, \\ q_i \neq q_k, 1 \leqslant \{i,k\} \leqslant K \end{array} \right\}$, where $\mathbf{A}_q, q = 1, ..., Q$ are dispersion matrices,

$\Phi_{q_1,...,q_K} = \mathbf{A}_{q_1}(s_{q_1} - \widetilde{s_{q_1}}) + ... + \mathbf{A}_{q_K}(s_{q_K} - \widetilde{s_{q_K}})$, and $\{s_{q_1}, ..., s_{q_K}\}$ and $\{\widetilde{s_{q_1}}, ..., \widetilde{s_{q_K}}\}$ are a pair of different source symbol sequences with at least one symbol difference. Note that $r_{sd(XY)} = r^{(1)}_{d(XY)}$. Further, we introduce two new concepts of 3-D codes: per dimension diversity order and per dimension symbol-wise diversity order. Symbol-wise diversity order is a subset of full diversity order. The importance of symbol-wise diversity for 2-D codes has been explained in [108, 109], and based on similar reasoning, full symbol-wise diversity for 3-D codes is also important, especially in high SNR regions.

Definition 3 *A pair of 3-D coded blocks* $\mathbf{M}$ *and* $\widetilde{\mathbf{M}}$ *in dimensions* X, Y, *and* Z *are of size* $N_X \times N_Y \times N_Z$. *All possible* $\mathbf{M}$ *and* $\widetilde{\mathbf{M}}$ *comprise the set* $\mathcal{M}$. *Denote* $\mathbf{M}^{(XZ)}_{(a)}$ *and* $\widetilde{\mathbf{M}^{(XZ)}_{(a)}}$ *as a pair of X-Z blocks corresponding to the a-th Y dimension of size* $N_X \times N_Z$ *within* $\mathbf{M}$ *and* $\widetilde{\mathbf{M}}$, *respectively. All possible* $\mathbf{M}^{(XZ)}_{(a)}$ *and* $\widetilde{\mathbf{M}^{(XZ)}_{(a)}}$ *comprise the set* $\mathcal{M}^{(XZ)}_{(a)}$. *Similarly, the sets* $\mathcal{M}^{(YZ)}_{(a)}$ *and* $\mathcal{M}^{(XY)}_{(a)}$ *are defined.*

Denote per dimension diversity order of Y *as* $r_{d(Y)}$, *which is defined as*

$$r_{d(Y)} = \max\left\{r_{d(XY)}, r_{d(ZY)},\right\}, \tag{8.1}$$

where

$$r_{d(XY)} = \min\left\{\begin{array}{l} rank(\mathbf{M}^{(XY)}_{(a)} - \widetilde{\mathbf{M}^{(XY)}_{(a)}}), \\ a = 1, ..., N_Z, \\ \mathbf{M}^{(XY)}_{(a)} \in \mathcal{M}^{(XY)}_{(a)}, \\ \widetilde{\mathbf{M}^{(XY)}_{(a)}} \in \mathcal{M}^{(XY)}_{(a)}, \\ \mathbf{M}^{(XY)}_{(a)} \neq \widetilde{\mathbf{M}^{(XY)}_{(a)}}, \\ \mathbf{M}^{(XY)}_{(a)} \text{within } \mathbf{M} \\ \widetilde{\mathbf{M}^{(XY)}_{(a)}} \text{within } \widetilde{\mathbf{M}} \\ \mathbf{M} \in \mathcal{M}, \widetilde{\mathbf{M}} \in \mathcal{M}, \\ \mathbf{M} \neq \widetilde{\mathbf{M}} \end{array}\right\},$$

$r_{d(ZY)}$ *is defined similarly to* $r_{d(XY)}$ ■

Definition 4 *For a 3-D code, the definition of the per dimension symbol-wise diversity order of* Y *is the same as that of the per dimension diversity order of* Y *except that it is required that the pair of* $\mathbf{M}$ *and* $\widetilde{\mathbf{M}}$ *is different only due to a single source symbol difference, which is denoted as* $\left[\mathbf{M} \neq \widetilde{\mathbf{M}}\right]_{sw}$. *Denote per dimension symbol-wise diversity order of* Y *as* $r_{sd(Y)}$, *which is defined as*

$$r_{sd(Y)} = \max\left\{r_{sd(XY)}, r_{sd(ZY)}\right\}, \tag{8.2}$$

where $r_{sd(XY)}$ *and* $r_{sd(ZY)}$ *are as in Definition 3, except that* $\left[\mathbf{M} \neq \widetilde{\mathbf{M}}\right]_{sw}$ *instead of* $\left[\mathbf{M} \neq \widetilde{\mathbf{M}}\right]$. ■

The above two concepts quantify the fact that in the case of $N_X < N_Y \leq N_Z$, the dimension Y may reach full per dimension (symbol-wise) diversity order N_Y in the Y-Z plane, although Y cannot reach full per dimension (symbol-wise) diversity order in the X-Y plane.

Definition 5 *A 3-D code is called full symbol-wise diversity code if the per dimension symbol-wise diversity orders of* X,Y, *and* Z *satisfy*

$$r_{sd(X)} = N_X,$$

$$r_{sd(Y)} = N_Y,$$

and

$$r_{sd(Z)} = N_Z.$$

■

Note that a full symbol-wise diversity code is achievable only if at least the two largest of N_X, N_Y, and N_Z are equal.

We can show that a properly designed DLD-STFC may achieve full symbol-wise diversity. Let the time dimension be of size T, and space and frequency dimensions be of size either N_X and N_Y, respectively, or, N_Y and N_X, respectively. Without loss of generality, say that dimension X is of size N_X, and dimension Y is of size N_Y. One STF block of size $N_X \times N_Y \times T$ is constructed through a double linear dispersion (DLD) encoding procedure such that the first LDC encoding stage constructs LDCs of size $T \times N_X$ in the X-time planes, and the second LDC encoding stage constructs LDCs of size $T \times N_Y$ in the Y-time planes.

Proposition 2 *Assume that a DLD procedure is with the above notations. Assume that the second LDC encoding stage produces information lossless or rate-one codewords. Assume that all-zero data source elements are allowed for DLD encoding.*

1) In the case of $N_X < N_Y = T$, if each of the two stage LDC encoding procedure enables full diversity in their 2-dimensions, the per dimension diversity orders of Y and time dimensions satisfy

$$r_{d(Time)} = r_{d(Y)} = T = N_Y.$$

2) Assume that the following conditions are satisfied:

a. Each block of Q source data symbols are encoded into each first stage LDC codeword. The first stage LDC encoding procedure enables full symbol-wise diversity in its 2-dimensions, and the second stage LDC encoding procedure enables full K-symbol-wise diversity in its 2-dimensions, where K is the maximum number of non-zero symbols of all the n_X-th time dimensions after the first stage LDC encoding procedure, where $n_X = 1, ..., N_X$.

b. All the encoding matrices of the second stage LDCs are the same. Denote the dispersion matrices of the second stage LDC as $\mathbf{A}_q^{(2)}$*, where* $q = 1, ..., N_Y T$*. Denote*

$$\mathbf{J}_{(a,b)} = \left[\left[\mathbf{A}^{(2)}_{(a-1)T+1} \right]_{:,b}, ..., \left[\mathbf{A}^{(2)}_{aT} \right]_{:,b} \right], \tag{8.3}$$

where $a = 1, ..., N_Y$ *and* $b = 1, ..., N_Y$*. Square matrix* $\mathbf{J}_{(a,b)}$ *is full rank, i.e. invertible, for any* $a = 1, ..., N_Y$ *and* $b = 1, ..., N_Y$*.*

In the cases of both $N_X < N_Y = T$ *and* $N_X = T > N_Y$*, the STF block, constructed using DLD procedure, achieves full symbol-wise diversity order.* ■

The proof of Proposition 2 is provided in Appendix E. We remark that

1) Proposition 2 provides a sufficient condition for full symbol-wise diversity. We call the condition (b) the DLD cooperation criterion (DLDCC). When failing to meeting DLDCC, full symbol-wise diversity cannot be guaranteed. Due to the support of DLDCC, the complex diversity coding design in the second LDC stage is more restrictive than that in the first LDC stage. Note that in [123,124], we have not considered DLDCC as a design criterion,

2) According to Proposition 2, the sequence of ST-LDC and FT-LDC stages can be inter-changed. Properly designed, both DLD-STFC Type A and DLD-STFC Type B are able to achieve full symbol-wise diversity.

8.4 Complex diversity coding based STFC with FEC

The fundamental differences between complex diversity coding (CDC) and FEC is that

1) CDC improves performance through obtaining better effective communication channels for source data signals while channel codes improve performance through correcting errors;

2) CDC operates in the continuous-valued domain, while FEC operates in the discrete-valued domain;

We claim that that CDC and FEC are not mutually exclusive techniques. On the contrary, FEC may cooperate with complex diversity coding to achieve better performance. The practical issue is the amount of gain that can be obtained by combining CDC based STFC and FEC. Recalling our STFC classification, DLD-STFC type A (which satisfies DLDCC) with FEC belongs to Category 6.

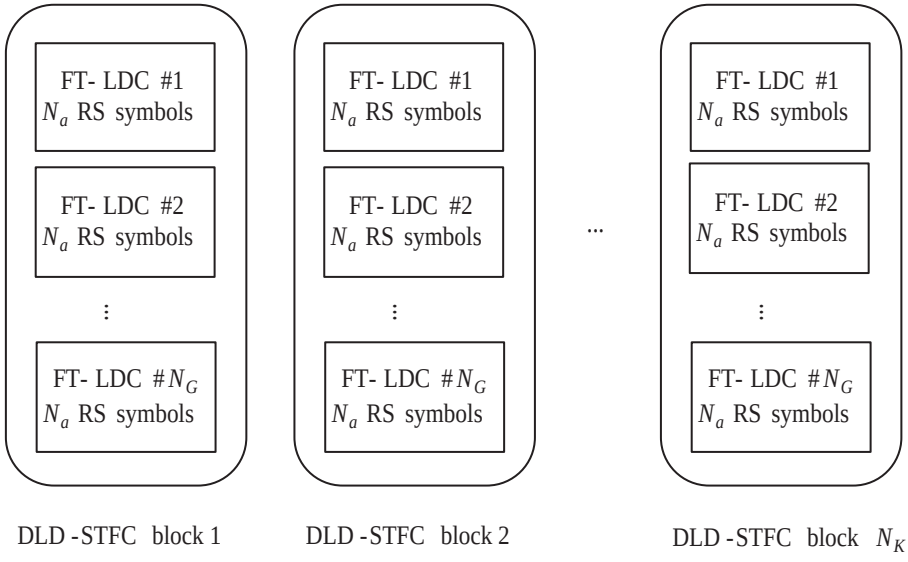

Figure 8.1. FEC mapping to DLD-STFC blocks

Due to the multidimensional structure, there are many possible mappings from FEC to STFC, which might influence system performance. For low latency, Reed Solomon (RS) codes are chosen FEC. The reasons to consider RS codes are listed as

follows.

1) Certainly, other FEC, such as turbo codes, also may be applied. The usage of RS codes is a proof of concept.

2) RS codes are block codes with strong burst error correction ability. If the RS symbols are distributed over different CDC codewords, the burst error correction ability may be efficiently used, since the burst errors may take place within one CDC codeword.

3) RS codes are block based and CDC are also block based, thus the mapping from RS codes to CDCs are convenient.

4) Block codes usually have lower latency than convolutional codes.

In the next section, $RS(a, b, c)$ denotes RS codes with a coded RS symbols, b information RS symbols, and c bits per symbol. As shown in Figure 8.1, we proposes to map one $RS(a, b, c)$ codeword to N_K DLD-STFC blocks, and N_a RS symbols are mapped into each of N_G FT-LDC codewords within each DLD-STFC block, where $a = N_a N_G N_K$. In the case of $N_K > 1$, we call the method inter-CDC-STFC FEC, while in the case of $N_K = 1$, we call the method intra-CDC-STFC FEC. Performance comparison of the combination of DLD-STFC with FEC will be given in Section 8.5.2.

8.5 Performance

Perfect channel knowledge (amplitude and phase) is assumed at the receiver but not at the transmitter. The symbol coding rates of all systems are unity. The sizes of all LDC codewords in the ST-LDC and FT-LDC stage of DLD-STFC are $T \times N_T$ and

$T \times N_F$, respectively. An evenly spaced LDC subcarrier mapping for the FT-LDC of DLD-STFC is used in simulations.

The frequency selective channel has $(L+1)$ paths exhibiting an exponential power delay profile, and a channel order of $L = 3$ is chosen. Data symbols use QPSK modulation in all simulations. Denote the transmit spatial correlation coefficient for 2×2 MIMO systems by ρ_t. The signal-to-noise-ratio (SNR) reported in all figures is the average symbol SNR per receive antenna.

8.5.1 Satisfaction of DLDCC influences the performance of DLD-STFC Type A and Type B

In the previous design of DLD-STFC Type A, FT-LDC and ST-LDC chose HH square code as shown in (3.10) and uniform linear dispersion codes, respectively, as dispersion matrices, both of which support full symbol-wise diversity in 2-dimensions. Note that original U-LDC design in Section 4.2 does not support DLDCC, while the square design Eq. (31) of [42] supports DLDCC. Thus the previous design [123,124] of DLD-STFC Type A does not satisfy DLDCC, and thus does not support full symbol-wise diversity in 3-dimensions. However, our recent results show that by changing index of dispersion matrices such that the sequence of the dispersion matrices $\{\mathbf{A}_1, ..., \mathbf{A}_Q\}$ is modified as $\left\{\mathbf{A}_{\sigma(1)}, ..., \mathbf{A}_{\sigma(Q)}\right\}$, where σ is a special permutation operation, a modified U-LDC is able to support DLDCC, thus DLD-STFC Type A based on the modified U-LDC may achieve full symbol-wise diversity in 3-dimensions. Note that the only situation which the code design should consider is the case of $T > M$. Note that if $T > M$, U-LDC in Section 4.2 is defined as

$$\mathbf{A}_q = \mathbf{B}_q = \mathbf{A}_{M(k-1)+l} = \frac{1}{\sqrt{M}} \mathbf{\Pi}^{k-1} \mathbf{\Gamma} \mathbf{D}^{l-1},$$

where $k = 1, ..., T$ and $l = 1, ..., M$. If $T > M$, the modified U-LDC, which supports DLDCC, is with dispersion matrices as follows,

$$\mathbf{A}_q = \mathbf{B}_q = \mathbf{A}_{T(l-1)+k} = \frac{1}{\sqrt{M}} \mathbf{\Pi}^{k-1} \mathbf{\Gamma} \mathbf{D}^{l-1}, \tag{8.4}$$

where $k = 1, ..., T$ and $l = 1, ..., M$.

We conjecture that the modified DLD-STFC Type A may achieve full K-symbol-wise diversity in 3-dimensions for some $K > 1$, and the performance is close to full diversity performance in 3-dimensions.

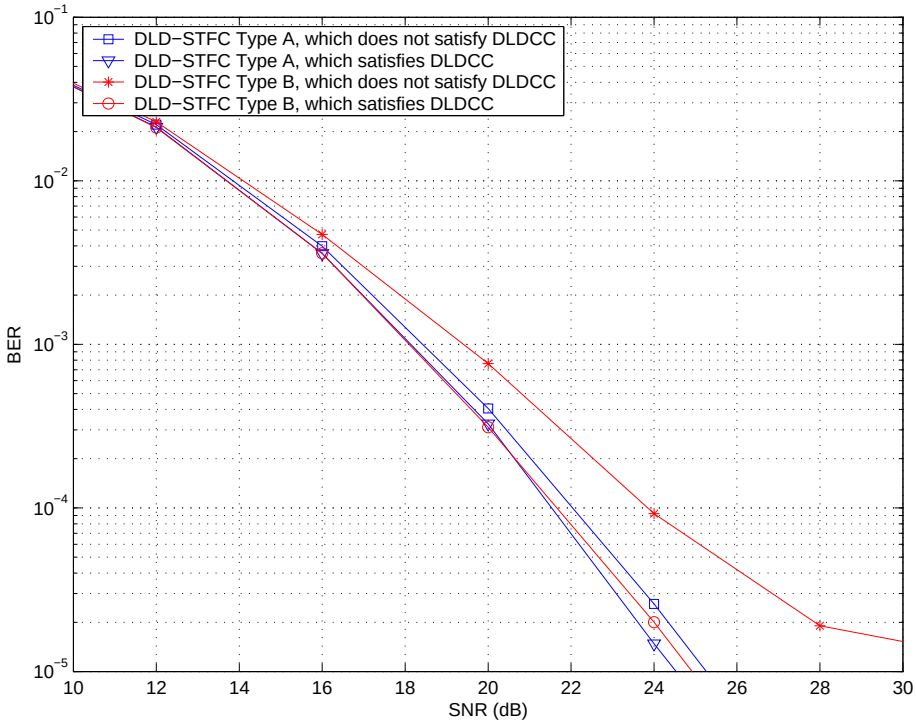

Figure 8.2. BER Performance of DLD-STFC are influenced by the satisfaction of DLDCC, transmit space correlation coefficients ($\rho_t = 0.0$), channel order 3, $CCI = 1$ OFDM block,$N_T = 2$,$N_R = 2$,$N_C = 32$,$N_F = 8$,$T = 8$

Figure 8.2 shows that the performance comparison of Bit Error Rate (BER) vs.

SNR between DLD-STFC Type A and DLD-STFC Type B with and without satisfaction of DLDCC. It is clear that both DLD-STFC Type A and Type B with satisfaction of DLDCC notably outperform both DLD-STFC Type A and Type B without satisfaction of DLDCC. Note that the sensitivity to DLDCC of DLD-STFC Type A is more than that of DLD-STFC Type B, which might be due to the fact that the size of frequency dimension of the codes is larger than that of space dimension of the codes. The performance of DLD-STFC Type A with satisfaction of DLDCC is quite close to that of DLD-STFC Type A with satisfaction of DLDCC. Thus DLD-STFC Type A can achieve similar high diversity performance to DLD-STFC Type B. In the rest of this section, DLD-STFC Type A with satisfaction of DLDCC is chosen.

8.5.2 Performance comparison of RS codes based STFCs

We would like to compare the performance of Category 2 and 3. We compare five $RS(8, 6, 4)$ codes based STFCs:

(1): the combination of DLD-STFC with RS codes with parameters $N_a = 2$, $N_G = 4$, and $N_K = 1$;

(2): the combination of DLD-STFC with RS codes with $N_a = 1$, $N_G = 2$, and $N_K = 4$;

(3): the combination of DLD-STFC with RS codes with $N_a = 1$, $N_G = 1$, and $N_K = 8$;

(4): the combination of linear constellation precoding (LCP) [72, 126] based space-frequency codes with RS codes over $T = 8$ OFDM blocks (Category 2);

(5): using single RS codes across space-time-frequency (Category 3).

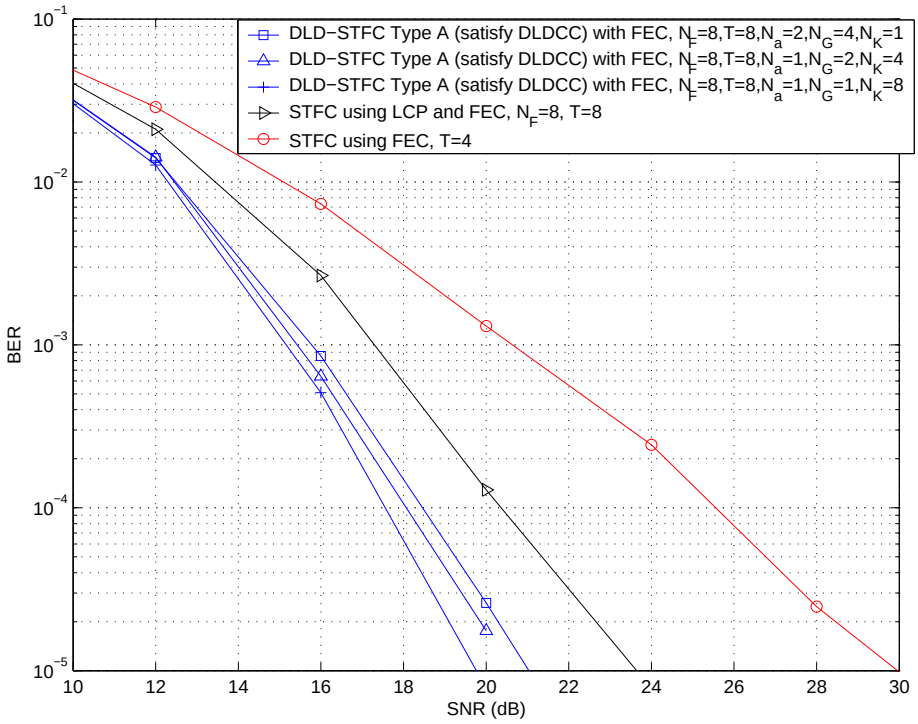

Figure 8.3. BER Performance of FEC based STFCs under transmit correlation $\rho_t = 0$, channel order 3, $CCI = 1$ OFDM block, $N_C = 16$, $N_T = 2$, $N_R = 2$, FEC used is $RS(8, 6, 4)$

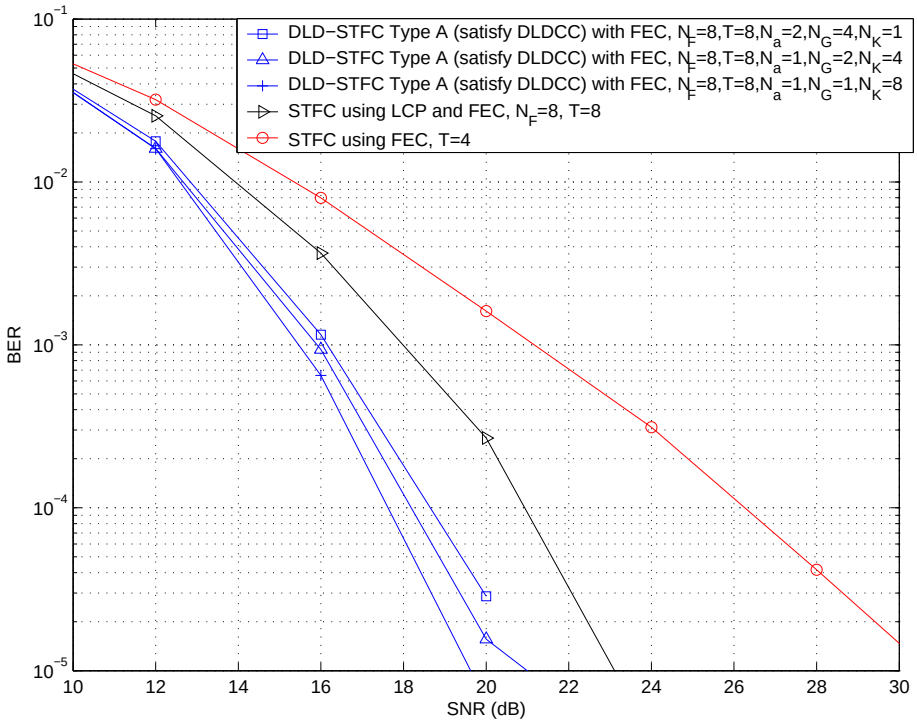

Figure 8.4. BER Performance of FEC based STFCs under transmit correlation $\rho_t = 0.3$, channel order 3, $CCI = 1$ OFDM block, $N_C = 16$, $N_T = 2$, $N_R = 2$, FEC used is $RS(8, 6, 4)$

Figures 8.3 and 8.4 show the performance comparison of FEC based STFCs. Note that LCP used in STFC (4) supports maximal diversity gain and coding gains in supported dimensions. It can observed that using the same FEC, STFCs (1), (2), and (3) significantly outperform STFCs (4) and (5) under transmit spatial correlation $\rho_t = 0$ and $\rho_t = 0.3$, respectively. Thus, STFCs of Category 6 may be the best choices in terms of BER performance. Note that the performance advantage of STFCs (1), (2), and (3) over STFCs (4) and (5) appears more significant with an increase of transmit spatial correlation. According to Figures 8.3 and 8.4, different mappings from FEC to STFC may lead to different BER performance of FEC based DLD-STFCs. Using the same block based FEC, it seems that the larger the number of STFCs that one RS codeword is across, the better the system performance of the STFCs of Category 6, and inter-CDC-STFC FEC systems outperform intra-CDC-STFC FEC ones.

8.6 Conclusion

This chapter introduces two concepts of diversity order for 3-dimensions, per dimension diversity order and per dimension symbol-wise diversity order. These diversity concepts are used to analyze the relation of two stages of complex diversity coding of DLD-STFC. This chapter shows that the two stages of DLD-STFC can be exchanged, and provides a sufficient condition to realize 3-dimensional diversity order for DLD-STFC. This results in notable performance improvement over the originally proposed DLD-STFC codes as shown in simulation results. This chapter also investigates the impact of FEC on performance of DLD-STFC, and shows that the mappings from FEC to DLD-STFC need to be properly designed. Finally, this chapter shows that

STFC based on the combination of DLD-STFC and FEC may significantly outperform STFC based on the combination of LCP SFC and FEC. As in Figure 8.4, at moderate transmit correlation of $\rho_t = 0.3$, DLD-STFC Type A (meeting DLDCC) with FEC outperforms STFC using the combination of LCP and FEC by 2.8dB at the BER of 10^{-3}.

Chapter 9

Coordinate interleaving for space-time linear dispersion

9.1 Introduction

In Chapter 2 and other previous chapters, there are extensive discussions on block based space time code designs. A problem in most existing design criteria of block-based space-time codes, including LDC (which allow different dispersion matrices for real and image parts of coordinates), is that they do not efficiently exploit additional diversity potential in the real and image parts of coordinates of source data constellation symbols. A technique to utilize the diversity potential of real and image parts of coordinates is called coordinate interleaving or component interleaving (CI), which was first proposed for single transmission stream system [8, 54, 55]. Recently, CI has been applied to multiple antennas systems [58,59,62]. Kim and Kaveh have combined CI-OSTBC and constellation rotation [62]. Khan, Rajan, and Lee used CI concepts to design coordinate space-time orthogonal block codes [58, 59]. However, current existing approaches to using CI in block-based space-time codes are low-rate designs using orthogonal space-time block codes or their variation [58, 59, 62].

This chapter proposes coordinate-interleaving as a general principle for high-rate block-based space-time code design, i.e., space-time coordinate interleaving linear dispersion codes (ST-CILDC). This chapter determines the upper bound diversity order, statistical diversity order and average diversity order of ST-CILDC. ST-CILDC maintains the same diversity order as conventional ST-LDC. However, ST-CILDC may show either almost doubled average diversity order or extra coding advantage over conventional ST-LDC in time varying channels. Compared with conventional ST-LDC, ST-CILDC maintains the diversity performance in quasi-static block fading channels, and notably improves the diversity performance in rapid fading channels.

The chapter is organized as follows. In Section 9.2, the channel model and newly proposed space-time inter-LDC coordinate interleaving strategy are presented. Diversity aspects are analyzed in Section 9.3. Performance analysis is discussed in Section 9.4.

9.2 Proposed systems

9.2.1 MIMO system model for LDC in time varying channels

In frequency-flat, time non-selective Rayleigh fading channels whose coefficients may vary per channel symbol time slot or channel use, a multi-antenna communication system is assumed with N_T transmit and N_R receive antennas. Assume that an uncorrelated data sequence has been modulated using complex-valued source data symbols chosen from an arbitrary, e.g. D-PSK or D-QAM, constellation. Each LDC codeword of size $T \times N_T$ is transmitted during every T time channel uses from N_T transmit antennas..

9.2.1.1 Component matrices in system equations

We now introduce several component matrices during the k-th space-time LDC codeword transmission.

The received signal vector $\mathbf{x}_{LDC}^{(k)} = \left[\left[\mathbf{x}_{LDC}^{(k,1)} \right]^{\mathcal{T}}, ..., \left[\mathbf{x}_{LDC}^{(k,T)} \right]^{\mathcal{T}} \right]^{\mathcal{T}}$, where $\mathbf{x}_{LDC}^{(k,t)} \in C^{N_R \times 1}, t = 1..., T$ is the received vector corresponding to the t-th row of the k-th LDC codeword, $\mathbf{S}_{LDC}^{(k)}$.

The system channel matrix is

$$\mathbf{H}_{LDC}^{(k)} = \begin{bmatrix} \mathbf{H}_{LDC}^{(k,1)} & \cdots & \mathbf{0} \\ \vdots & \ddots & \vdots \\ \mathbf{0} & \cdots & \mathbf{H}_{LDC}^{(k,T)} \end{bmatrix}$$

where $\mathbf{H}_{LDC}^{(k,t)} \in C^{N_R \times N_T}, t = 1..., T$ with entries $\left[\mathbf{H}_{LDC}^{(k,t)} \right]_{n,m} = h_{n,m}^{(k,t)}$, $m = 1, ..., N_T$, $n = 1, ..., N_R$, is a complex Gaussian MIMO channel matrix with zero-mean, unit variance entries corresponding to the t-th row of the k-th LDC codeword, $\mathbf{S}_{LDC}^{(k)}$, and $\mathbf{0}$ denotes a zero matrix of size $N_R \times N_T$.

The complex Gaussian noise vector is $\mathbf{v}_{LDC}^{(k)} = \left[\left[\mathbf{v}_{LDC}^{(k,1)} \right]^{\mathcal{T}}, ..., \left[\mathbf{v}_{LDC}^{(k,T)} \right]^{\mathcal{T}} \right]^{\mathcal{T}}$, where $\mathbf{v}_{LDC}^{(k,t)} \in C^{N_R \times 1}, t = 1..., T$ is a complex Gaussian noise vector with zero mean, unit variance entries corresponding to the t-th row of the k-th LDC codeword, $\mathbf{S}_{LDC}^{(k)}$.

The LDC encoded complex symbol vector $\mathbf{s}_{LDC}^{(k)}$ corresponds to the k-th LDC codeword, $\mathbf{S}_{LDC}^{(k)}$, where

$$\mathbf{s}_{LDC}^{(k)} = vec(\left[\mathbf{S}_{LDC}^{(k)} \right]^{\mathcal{T}}). \tag{9.1}$$

9.2.1.2 System model equation

The general system equation for the transmission of the k-th LDC matrix codeword is expressed as

$$\mathbf{x}_{LDC}^{(k)}=\sqrt{\frac{\rho}{N_T}}\mathbf{H}_{LDC}^{(k)}\mathbf{s}_{LDC}^{(k)}+\mathbf{v}_{LDC}^{(k)} \tag{9.2}$$

where ρ is the signal-to-noise ratio (SNR) at each receive antenna, and independent of N_T.

9.2.2 Procedure of space-time inter-LDC coordinate interleaving

We propose a new space-time LDC encoding procedure using inter-LDC CI (ILDC-CI), called space-time coordinate interleaving linear dispersion codes (ST-CILDC) as follows: Consider a pair of source data symbol vectors $\mathbf{s}^{(1)} = \left[s_1^{(1)}, ..., s_Q^{(1)}\right]^{\mathcal{T}}$ and $\mathbf{s}^{(2)} = \left[s_1^{(2)}, ..., s_Q^{(2)}\right]^{\mathcal{T}}$ with the same number, Q of source data symbol symbols, where $s_q^{(i)} = \mathrm{Re}\left(s_q^{(i)}\right) + j\mathrm{Im}\left(s_q^{(i)}\right)$, $i = 1, 2$, and $q = 1, ..., Q$. The transmitter first coordinate-interleaves $\mathbf{s}^{(1)}$ and $\mathbf{s}^{(2)}$ into $\mathbf{s}^{CI(1)} = \left[s_1^{CI(1)}, ..., s_Q^{CI(1)}\right]^{\mathcal{T}}$ and $\mathbf{s}^{CI(2)} = \left[s_1^{CI(2)}, ..., s_Q^{CI(2)}\right]^{\mathcal{T}}$, where

$$s_q^{CI(1)} = \mathrm{Re}\left(s_q^{(1)}\right) + j\mathrm{Im}\left(s_q^{(2)}\right) \tag{9.3}$$

and

$$s_q^{CI(2)} = \mathrm{Re}\left(s_q^{(2)}\right) + j\mathrm{Im}\left(s_q^{(1)}\right). \tag{9.4}$$

Then, using (3.22) or (3.23), $\mathbf{s}^{CI(1)}$ and $\mathbf{s}^{CI(2)}$ are encoded into two LDC codewords of size $T \times N_T$, $\mathbf{S}_{LDC}^{CI(1)}$ and $\mathbf{S}_{LDC}^{CI(2)}$, respectively. Then the transmitter successively sends $\mathbf{S}_{LDC}^{CI(1)}$ and $\mathbf{S}_{LDC}^{CI(2)}$ during two interleaved periods such that channels are less correlated.

We remark that

1) using different permutations, other methods of space-time inter-LDC CI than (9.3) and (9.4) are also possible;

2) The LDC encoding matrices for $\mathbf{S}_{LDC}^{CI(1)}$ and $\mathbf{S}_{LDC}^{CI(2)}$ may not necessarily be the same.

9.2.3 ST-CILDC system structure

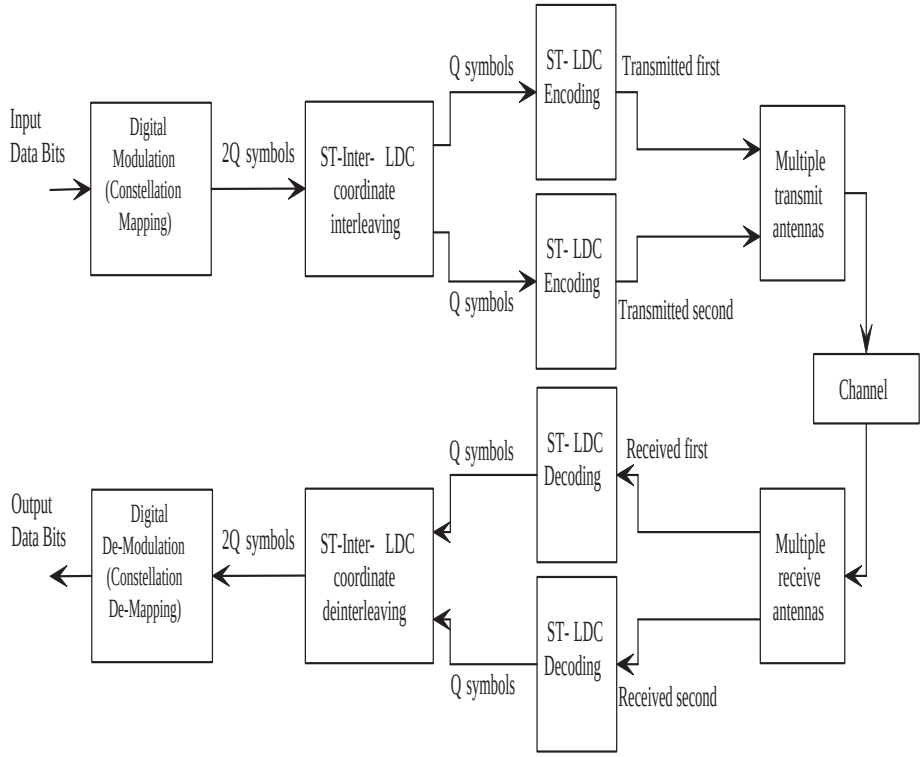

Figure 9.1. Space-time inter-LDC coordinate interleaving system structure

The proposed ST-CILDC system structure is shown in Figure 9.1. The system structure basically consists of three layers : (1) mapping from data bits to constellation points, (2) inter-LDC coordinate interleaving, and (3) LDC coding. Using the

proposed layered structure, the only additional complexity compared with a conventional ST-LDC system is the coordinate interleaving operation. Thus, the ST-CILDC system is computationally efficient. The motivation of ST-CILDC is to render the fading more independent of each coordinate of the source data signals. Note that due to the superposition effects of signals from multiple transmit antennas at the space-time MIMO receivers, existing ST-LDC designs cannot guarantee fading independency of each coordinate of the source data signals. Compared with ST-LDC systems, the result of using ST-CILDC is to introduce coordinate fading diversity at the cost of more decoding delay using a pair of LDC codewords of the same size.

9.3 Diversity analysis

Su and Liu [100] recently analyzed the diversity of space-time modulation over time-correlated Rayleigh fading channels. A modified strategy can be used to investigate the diversity of the proposed ST-CILDC system.

Consider a ST-CILDC block which consists of two ST-LDC codewords of size $T \times N_T$, $\mathbf{S}_{LDC}^{CI(1)}$ and $\mathbf{S}_{LDC}^{CI(2)}$.

The communication model for ST-CILDC can be rewritten in block form

$$\mathbf{Y} = \sqrt{\frac{\rho}{N_T}}\mathbf{M}\mathbf{H} + \mathbf{W}. \tag{9.5}$$

where

1) the noise vector is $\mathbf{W}$,

2) the received signal vector $\mathbf{Y} = \left[\left[\mathbf{Y}^{(1)}\right]^{\mathcal{T}}, \left[\mathbf{Y}^{(2)}\right]^{\mathcal{T}}\right]^{\mathcal{T}}$, where $\mathbf{Y}^{(k)} = \left[\mathbf{Y}_1^{(k)}, ..., \mathbf{Y}_{N_R}^{(k)}\right]^{\mathcal{T}}$, $\mathbf{Y}_n^{(k)} = \left[\left[\mathbf{x}_{LDC}^{(k,1)}\right]_{n,1}, ..., \left[\mathbf{x}_{LDC}^{(k,T)}\right]_{n,1}\right]^{\mathcal{T}}$, $k = 1, 2$ and $n = 1, ..., N_R$.

3) $\mathbf{M}$ is the channel symbol matrix corresponding to the block $\mathbf{C}$, $\mathbf{M} = diag\left(\mathbf{M}^{(1)}, \mathbf{M}^{(2)}\right)$, where $\mathbf{M}^{(1)}$ and $\mathbf{M}^{(2)}$ are the matrices corresponding to the LDC codewords, $\mathbf{S}_{LDC}^{CI(1)}$ and $\mathbf{S}_{LDC}^{CI(2)}$, respectively, $\mathbf{M}^{(k)} = \mathbf{I}_{N_R} \otimes diag\left[\mathbf{M}_1^{(k)}, ..., \mathbf{M}_{N_T}^{(k)}\right]$, $\mathbf{M}_m^{(k)} = diag\left(\left[\mathbf{S}_{LDC}^{CI(k)}\right]_{1,m}, ..., \left[\mathbf{S}_{LDC}^{CI(k)}\right]_{T,m}\right)$, $k = 1, 2$, and $m = 1, ..., N_T$,

4) the channel vector $\mathbf{H} = \left[\left[\mathbf{H}^{(1)}\right]^{\mathcal{T}}, \left[\mathbf{H}^{(2)}\right]^{\mathcal{T}}\right]^{\mathcal{T}}$, where

$$\mathbf{H}^{(k)} = \left[\mathbf{h}_{(k)1,1}^{\mathcal{T}}, ..., \mathbf{h}_{(k)1,N_T}^{\mathcal{T}}, ..., \mathbf{h}_{(k)N_R,1}^{\mathcal{T}}, ..., \mathbf{h}_{(k)N_R,N_T}^{\mathcal{T}}\right]^{\mathcal{T}}$$

and $\mathbf{h}_{(k)n,m} = \left[h_{n,m}^{(k,1)}, ..., h_{n,m}^{(k,T)}\right]^{\mathcal{T}}$.

Consider the directional pair of matrices $\mathbf{M}$ and $\widetilde{\mathbf{M}}$ corresponding to two different ST-LDC blocks C and $\tilde{C}$. Assume that all possible $\mathbf{M}$ and $\widetilde{\mathbf{M}}$ are contained in a set $\mathcal{M}$. The upper bound pairwise error probability [96] is

$$\Pr\left(\mathbf{M} \to \widetilde{\mathbf{M}} \middle| \rho\right) \leqslant \begin{pmatrix} 2r-1 \\ r \end{pmatrix} \left(\prod_{a=1}^{r} \gamma_a\right)^{-1} \left(\frac{\rho}{N_T}\right)^{-r} \tag{9.6}$$

where r is the rank of

$$\mathbf{\Lambda} = \left(\mathbf{M} - \widetilde{\mathbf{M}}\right) \mathbf{R}_{\mathbf{H}} \left(\mathbf{M} - \widetilde{\mathbf{M}}\right)^{\mathcal{H}}, \tag{9.7}$$

and $\mathbf{R}_{\mathbf{H}} = \mathbb{E}\left\{\mathbf{H}\left[\mathbf{H}\right]^{\mathcal{H}}\right\}$ is the correlation matrix of vector $\mathbf{H}$, $\mathbf{R}_{\mathbf{H}}$ is of size $2N_TN_RT \times 2N_TN_RT$, $\gamma_a, a = 1, ..., r$ are the non-zero eigenvalues of $\mathbf{\Lambda}$.

Then the corresponding rank and product criteria are

1) Rank criterion: The minimum rank of $\mathbf{\Lambda}$ over all directional pairs of different matrices $\mathbf{M}$ and $\widetilde{\mathbf{M}}$, i.e., the diversity order, should be as large as possible.

2) Product criterion: the minimum value of the product $\prod_{a=1}^{r} \gamma_a$ over all directional pairs of different $\mathbf{M}$ and $\widetilde{\mathbf{M}}$ should be maximized.

Using commonly accepted definition [100], the diversity order of the ST-CILDC, r_d, is mathematically written as

$$r_d = \min \left\{ rank\left(\mathbf{\Lambda}\right), \mathbf{M} \in \mathcal{M}, \widetilde{\mathbf{M}} \in \mathcal{M}, \mathbf{M} \neq \widetilde{\mathbf{M}} \right\}. \tag{9.8}$$

To maximize the rank of $\mathbf{\Lambda}$, we need to maximize the ranks of both $\mathbf{R_H}$ and $\left(\mathbf{M} - \widetilde{\mathbf{M}}\right)$. Denote

$$\mathbf{\Omega}^{(k)} = \mathbf{M}^{(k)} - \widetilde{\mathbf{M}^{(k)}},$$

where $k = 1, 2$.

By the definition of $\mathbf{M}$ and $\widetilde{\mathbf{M}}$,

$$\begin{aligned} &rank\left(\mathbf{M} - \widetilde{\mathbf{M}}\right) = \\ &rank\left(\mathbf{\Omega}^{(1)}\right) + rank\left(\mathbf{\Omega}^{(2)}\right) \end{aligned} \tag{9.9}$$

Since $\mathbf{\Omega}^{(k)}, k = 1, 2$ are of size $N_R T \times N_T N_R T$, we have

$$rank\left(\mathbf{M}^{(k)} - \widetilde{\mathbf{M}^{(k)}}\right) \leq N_R T. \tag{9.10}$$

From (9.7), (9.9), and (9.10), we have

$$r = rank(\mathbf{\Lambda}) \leq \min\left\{2N_R T, rank\left(\mathbf{R_H}\right)\right\}. \tag{9.11}$$

Assume that all the possible $\mathbf{M}^{(k)}$ and $\widetilde{\mathbf{M}^{(k)}}$ are contained in a set $\mathcal{M}^{(k)}$, i.e., $\left\{\mathbf{M}^{(k)}, \widetilde{\mathbf{M}^{(k)}}\right\} \in \mathcal{M}^{(k)}$, where $k = 1, 2$.

When $\mathbf{M} \neq \widetilde{\mathbf{M}}$, there are three distinct categories of situations,

1) $\mathbf{M}^{(1)} \neq \widetilde{\mathbf{M}^{(1)}}$ and $\mathbf{M}^{(2)} = \widetilde{\mathbf{M}^{(2)}}$,

2) $\mathbf{M}^{(1)} = \widetilde{\mathbf{M}^{(1)}}$ and $\mathbf{M}^{(2)} \neq \widetilde{\mathbf{M}^{(2)}}$,

3) $\mathbf{M}^{(1)} \neq \widetilde{\mathbf{M}^{(1)}}$ and $\mathbf{M}^{(2)} \neq \widetilde{\mathbf{M}^{(2)}}$.

For convenience of the rest of the discussion, denote the situations (1), (2) and (3) as sets $\Upsilon^{(1)}$, $\Upsilon^{(2)}$ and $\Upsilon^{(3)}$, respectively.

Then, we have

$$r_d = \min \left\{ \begin{array}{l} rank\left(\mathbf{\Psi}_1\right), rank\left(\mathbf{\Psi}_2\right), rank\left(\mathbf{\Psi}_3\right), \\ \text{where } \mathbf{\Omega}^{(1)} \neq 0, \mathbf{\Omega}^{(2)} \neq 0, \\ \left\{\mathbf{M}^{(1)}, \widetilde{\mathbf{M}^{(1)}}\right\} \in \mathcal{M}^{(1)}, \left\{\mathbf{M}^{(2)}, \widetilde{\mathbf{M}^{(2)}}\right\} \in \mathcal{M}^{(2)} \end{array} \right\}, \tag{9.12}$$

where

$$\mathbf{\Psi}_1 = \begin{bmatrix} \mathbf{\Omega}^{(1)} & \mathbf{Z} \\ \mathbf{Z} & \mathbf{Z} \end{bmatrix} \mathbf{R_H} \begin{bmatrix} \mathbf{\Omega}^{(1)} & \mathbf{Z} \\ \mathbf{Z} & \mathbf{Z} \end{bmatrix}^{\mathcal{H}},$$

$$\mathbf{\Psi}_2 = \begin{bmatrix} \mathbf{Z} & \mathbf{Z} \\ \mathbf{Z} & \mathbf{\Omega}^{(2)} \end{bmatrix} \mathbf{R_H} \begin{bmatrix} \mathbf{Z} & \mathbf{Z} \\ \mathbf{Z} & \mathbf{\Omega}^{(2)} \end{bmatrix}^{\mathcal{H}},$$

$$\mathbf{\Psi}_3 = \begin{bmatrix} \mathbf{\Omega}^{(1)} & \mathbf{Z} \\ \mathbf{Z} & \mathbf{\Omega}^{(2)} \end{bmatrix} \mathbf{R_H} \begin{bmatrix} \mathbf{\Omega}^{(1)} & \mathbf{Z} \\ \mathbf{Z} & \mathbf{\Omega}^{(2)} \end{bmatrix}^{\mathcal{H}},$$

and $\mathbf{Z} = \mathbf{0}_{N_R T \times N_T N_R T}$.

It is clear that $rank\left(\mathbf{\Psi}_1\right) \leqslant N_R T$, $rank\left(\mathbf{\Psi}_2\right) \leqslant N_R T$, and $rank\left(\mathbf{\Psi}_3\right) \leqslant 2N_R T$. Hence, we have

$$r_d \leqslant N_R T. \tag{9.13}$$

Thus ST-CILDC does not further increase the diversity order over ST-LDC in terms of the conventional definition (9.12). From the above analysis, it is clear that there are situations where coordinate-interleaving may not double the diversity order of OSTBC with constellation rotation. This does not seem to be noted in [62]. However, in partial agreement with [62], ST-CILDC does increase r for the situation (3), which may significantly impact system performance. It is necessary to introduce a new concept to quantify this effect:

Definition 6 *The statistical diversity order, r_{std}, is the rank of $\mathbf{\Lambda}$ achieved with probability α, i.e.,*

$$\Pr\left\{\begin{array}{l} rank\left(\mathbf{\Lambda}\right) \geqslant r_{std}, \\ \mathbf{M} \neq \widetilde{\mathbf{M}}, \\ \left\{\mathbf{M}, \widetilde{\mathbf{M}}\right\} \in \mathcal{M}, \end{array}\right\} = \alpha. \tag{9.14}$$

The above definition may better quantify diversity properties of systems with low diversity order but with high statistical diversity order with high probability.

The diversity order and statistical diversity order of ST-CILDC are quantified as follows.

Theorem 6 *Suppose that a ST-CILDC is constructed through coordinate interleaving across a pair of component LDC codewords. Both component LDC encoders are able to generate different codewords for different input sequences. The diversity orders of the component LDCs are $r_d^{(1)}$ and $r_d^{(2)}$, respectively. Suppose that $\mathbf{R_H}$ is of full rank. Also assume that the codebook sizes (the total number of different codewords) of the two component LDCs are of the same value, N_a.*

1) The diversity order of this ST-CILDC, r_d, is $\min\left\{r_d^{(1)}, r_d^{(2)}\right\}$.

2) Assuming that all directional pairs $\mathbf{M}$ and $\widetilde{\mathbf{M}}$ are equally probable, the statistical diversity order of this ST-CILDC, r_{std}, is $r_d^{(1)} + r_d^{(2)}$ with probability

$$\alpha = \frac{\left(\begin{array}{c} N_a \\ 2 \end{array}\right)\left(\begin{array}{c} N_a \\ 2 \end{array}\right)}{\left(\begin{array}{c} N_a \\ 2 \end{array}\right)\left(\begin{array}{c} N_a \\ 2 \end{array}\right) + N_a \left(\begin{array}{c} N_a \\ 2 \end{array}\right)}. \tag{9.15}$$

The proof of Theorem 6 is provided in Appendix F.1.

A problem of the above analysis is that it is purely based on pairwise error probability, while system performance is normally expressed in terms of average error probability (AEP). We thus introduce a diversity concept based on AEP.

Definition 7 *Denote AEP of a communications system with the codeword block set* $\{\mathbf{M}\}$ *at average receive SNR* ρ *as* $AEP\{\mathbf{M}, \rho\}$. *The AEP may be expressed with respect to different units, e.g., bit, symbol, or block (or frame). Assume that* $AEP\{\mathbf{M}, \rho\}$ *is differentiable at* ρ.

Denote

$$f(\rho) = \log_{10}\left(AEP\{\mathbf{M}, \rho\}\right)$$

and

$$g(\rho) = \log_{10}\rho.$$

The average diversity order, r_{ad}, *at the average SNR of each receive antenna,* ρ, *is defined as the differential*

$$r_{ad} = -\frac{\partial f(\rho)}{\partial g(\rho)}. \tag{9.16}$$

Note that

1) unlike conventional definition of diversity order, which is obtained as SNR goes to infinity, the average diversity order, r_{ad}, is a function of the finite average signal-to-noise ratio (SNR). Average diversity order enables diversity analysis at lower SNRs.

2) the average diversity order r_{ad}, which is defined using AEP, represents the slope of error probability versus SNR on a logarithm - logarithm scale and is related to actual error performance.

In general, AEP cannot be easily computed. Thus we instead propose an analysis of the diversity performance of CI-STLDC based on the error union bound (EUB), an upper bound on the average error probability. The EUB is in fact an average of the pairwise error probabilities between all directional pairs of codewords introduced earlier. The EUB at average signal-to-noise ratio (SNR) of each receive antenna, ρ, is expressed

1) for bit errors as

$$\begin{aligned} &\Pr_{U(bit)}\{\mathbf{M}|\rho\} = \\ &\frac{1}{N_{\mathbf{M}}^{(bit)}} \sum_{a=1}^{N_B} \phi_{bit}(\mathbf{M}_{(a)}, \mathbf{M}_{(b)}) \Pr\left\{\mathbf{M}_{(a)}\right\} \sum_{b\neq a}^{N_B} \Pr\left\{\mathbf{M}_{(a)} \rightarrow \mathbf{M}_{(b)}|\rho\right\}, \end{aligned} \tag{9.17}$$

2) for symbol errors as

$$\begin{aligned} &\Pr_{U(sym)}\{\mathbf{M}|\rho\} = \\ &\frac{1}{N_{\mathbf{M}}^{(sym)}} \sum_{a=1}^{N_B} \phi_{sym}(\mathbf{M}_{(a)}, \mathbf{M}_{(b)}) \Pr\left\{\mathbf{M}_{(a)}\right\} \sum_{b\neq a}^{N_B} \Pr\left\{\mathbf{M}_{(a)} \rightarrow \mathbf{M}_{(b)}|\rho\right\}, \end{aligned} \tag{9.18}$$

3) for block (or frame) errors as

$$\Pr_{U(blk)}\{\mathbf{M}|\rho\} = \sum_{a=1}^{N_B} \Pr\left\{\mathbf{M}_{(a)}\right\} \sum_{b\neq a}^{N_B} \Pr\left\{\mathbf{M}_{(a)} \rightarrow \mathbf{M}_{(b)}|\rho\right\}, \tag{9.19}$$

where $\Pr\left\{\mathbf{M}_{(a)}\right\}$ is the a priori probability that codeword $\mathbf{M}_{(a)}$ was transmitted, $\Pr\left\{\mathbf{M}_{(a)} \rightarrow \mathbf{M}_{(b)}|\rho\right\}$ is the probability that receiver decides $\mathbf{M}_{(b)}$ when $\mathbf{M}_{(a)}$ is actually transmitted at average signal-to-noise ratio (SNR) per receive antenna, ρ, $\phi_{bit}(\mathbf{M}_{(a)}, \mathbf{M}_{(b)})$ and $\phi_{sym}(\mathbf{M}_{(a)}, \mathbf{M}_{(b)})$ are the number of bit and symbol errors, respectively, occurring when $\mathbf{M}_{(a)}$ is transmitted and $\mathbf{M}_{(b)}$ is chosen by the decoder, $N_{\mathbf{M}}^{(bit)}$ is the total number of bits per $\mathbf{M}$ block, $N_{\mathbf{M}}^{(sym)}$ is the total number of symbols per $\mathbf{M}$ block, and N_B is the code book size.

Note that we may analyze the logarithm domain slope of EUB polynomials in order to analyze of average diversity order. As an important basis of analysis, we introduce the following Theorem.

Theorem 7 *Assume that*

1) $p_i(x)$, *where* $i = 1, ..., L$ *and* $L \geqslant 2$, *represent* L *differentiable positive real functions with single positive real variable* $x > 1$,

2) $\frac{\partial p_i(x)}{\partial x}\Big|_{x=x_0} < 0$, *and denote* $q_i(x) = -\frac{\partial(\log_a p_i(x))}{\partial(\log_a x)} > 0$, *where* $0 < q_1(x) \leqslant ... \leqslant q_L(x) < +\infty$.

Denote $w(x) = -\frac{\partial\left[\log_a\left[\sum_{i=1}^{L} p_i(x)\right]\right]}{\partial(\log_a(x))}$, *where* $a > 1$.

Then, the following statements hold.

1) If $q_1(x) \neq q_L(x)$,

$$q_1(x) < w(x) < q_L(x). \tag{9.20}$$

The closeness between $q_1(x)$ *and* $w(x)$ *is quantified by*

$$\left|\frac{w(x) - q_1(x)}{q_1(x)}\right| = \left|\sum_{k=2}^{L}\left(\frac{1 - \frac{q_k(x)}{q_1(x)}}{\frac{1}{p_k(x)}\sum_{i=1}^{L} p_i(x)}\right)\right|,$$

and the closeness between $q_L(x)$ *and* $w(x)$ *is quantified by*

$$\left|\frac{w(x) - q_L(x)}{q_L(x)}\right| = \left|\sum_{k=1}^{L-1}\left(\frac{1 - \frac{q_k(x)}{q_L(x)}}{\frac{1}{p_k(x)}\sum_{i=1}^{L} p_i(x)}\right)\right|.$$

2) If $q_1(x) = q_L(x)$, $q_1(x) = w(x) = q_L(x)$.

3) If

a. $\lim_{x\to+\infty} p_i(x) = 0$, *where* $i = 1, ..., L$, *and* $\lim_{x\to+\infty}\left(\frac{p_k(x)}{p_1(x)}\right) = 0$, *where* $k = 2, ..., L$,

b. $\exists k, 1 < \lim_{x\to+\infty} \frac{q_k(x)}{q_1(x)} < +\infty$, *where* $k = 2, ..., L$,

$$\lim_{x\to+\infty}\left|\frac{w(x) - q_1(x)}{q_1(x)}\right| = 0.$$

The proof of Theorem 7 is provided in Appendix F.2.

Since EUB is the summation of the pairwise error probabilities for all the directional pairs of $\mathbf{M}$ and $\widetilde{\mathbf{M}}$ in $\Upsilon^{(1)}$, $\Upsilon^{(2)}$, and $\Upsilon^{(3)}$, as a unified form, the EUB at average receive SNR ρ can be written as follows,

$$\begin{aligned}
&\Pr_{U(unit)}\{\mathbf{M}|\rho\} \\
&= \frac{1}{N_{\mathbf{M}}^{(unit)}} \sum_{a=1}^{N_B} \phi_{unit}(\mathbf{M}_{(a)}, \mathbf{M}_{(b)}) \Pr\left\{\mathbf{M}_{(a)}\right\} \sum_{b\neq a}^{N_B} \Pr\left\{\mathbf{M}_{(a)} \to \mathbf{M}_{(b)}|\rho\right\} \qquad (9.21)\\
&= \frac{1}{N_{\mathbf{M}}^{(unit)}} \sum_{i=1}^{3} \zeta^{(i)},
\end{aligned}$$

where $unit = bit, sym, blk$ and $\phi_{blk}(\mathbf{M}_{(a)}, \mathbf{M}_{(b)}) = 1$, the EUB component related to $\Upsilon^{(i)}$ is

$$\zeta_\rho^{(i)} = \frac{1}{N_{\mathbf{M}}^{(unit)}} \sum_{\substack{a=1,\\ \{\mathbf{M}_{(a)},\mathbf{M}_{(b)}\}\in\Upsilon^{(i)}}}^{N_B} \left\{ \begin{array}{l} \phi_{unit}(\mathbf{M}_{(a)}, \mathbf{M}_{(b)}) \Pr\left\{\mathbf{M}_{(a)}\right\} \cdot \\ \sum\limits_{\substack{b\neq a,\\ \{\mathbf{M}_{(a)},\mathbf{M}_{(b)}\}\in\Upsilon^{(i)}}}^{N_B} \Pr\left\{\mathbf{M}_{(a)} \to \mathbf{M}_{(b)}|\rho\right\} \end{array} \right\}. \qquad (9.22)$$

Denote $f_1(\rho) = \log_{10} \Pr_{U(unit)}\{\mathbf{M}|\rho\}$ and $g(\rho) = \log_{10}\rho$,. Using (9.16) and (9.21), r_{ad} can be approximated by

$$r_{ad} = -\frac{\partial f(\rho)}{\partial g(\rho)} \approx -\frac{\partial f_1(\rho)}{\partial g(\rho)}, \qquad (9.23)$$

where the $\approx$ is based on the fact that EUB normally is considered as a good approximation of AEP.

Denote $r^{(i)} = rank\left(\mathbf{\Lambda}, \left\{\mathbf{M} \to \widetilde{\mathbf{M}}\right\} \in \Upsilon^{(i)}\right)$ and $r_{\min}^{(i)} = \min\left\{r^{(i)}\right\}$ and $r_{\max}^{(i)} = \max\left\{r^{(i)}\right\}$, where $i = 1, 2, 3$. Note that $r_{\min}^{(1)} = r_d^{(1)}$ and $r_{\min}^{(2)} = r_d^{(2)}$ and $r_{\min}^{(3)} = r_d^{(1)} + r_d^{(2)}$. Clearly, $r_{\min}^{(i)} \leqslant r^{(i)} \leqslant r_{\max}^{(i)}$. According to Theorem 7, using (9.6) and (9.22), we have

1)

$$r_{\min}^{(i)} \leqslant -\frac{\partial \log_{10} \zeta_\rho^{(i)}}{\partial \log_{10} \rho} \leqslant r_{\max}^{(i)}, \tag{9.24}$$

2)

$$\min\left\{r_d^{(1)}, r_d^{(2)}\right\} \leqslant -\frac{\partial\left[\log_{10} \underset{U(unit)}{\Pr}\{\mathbf{M}|\rho\}\right]}{\partial \log_{10} \rho} \leqslant \max\left\{r_{\max}^{(i)}, i = 1, 2, 3\right\}. \tag{9.25}$$

From (9.25), the advantage of ST-CILDC can not be clearly illustrated. Now, we consider the following assumptions

1) $r_d^{(i)} = r_{\max}^{(i)}$, where $i = 1, 2$, which we call uniform rank in the set $\Upsilon^{(i)}$,

2) $r_d^{(1)} = r_d^{(2)}$ (thus $r_{\min}^{(3)} = r_d^{(1)} + r_d^{(2)} = r_{\max}^{(3)}$),

and then

$$r_d^{(1)} = r_d^{(2)} < -\frac{\partial\left[\log_{10} \underset{U(unit)}{\Pr}\{\mathbf{M}|\rho\}\right]}{\partial \log_{10} \rho} < r_d^{(1)} + r_d^{(2)}, \tag{9.26}$$

where the two $<$ are due to $r_d^{(1)} = r_d^{(2)} < r_d^{(1)} + r_d^{(2)}$. This case shows a sufficient (not necessary) condition of average diversity order improvement in ST-CILDC systems. According to Theorem 7, we can approximately quantify this closeness between average diversity order and $r_d^{(1)} = r_d^{(2)}$ as

$$\left|\frac{-\frac{\partial \log_{10} \underset{U(unit)}{\Pr}\{\mathbf{M}|\rho\}}{\partial \log_{10} \rho} - r_d^{(1)}}{r_d^{(1)}}\right| = \left|\frac{\zeta_\rho^{(3)}(1 - \frac{2r_d^{(1)}}{r_d^{(1)}})}{\underset{U(unit)}{\Pr}\{\mathbf{M}|\rho\}}\right| = \left|\frac{\zeta_\rho^{(3)}}{\sum_{i=1}^{3} \zeta_\rho^{(i)}}\right|. \tag{9.27}$$

Similarly, we can approximately quantify this closeness between average diversity order and $r_d^{(1)} + r_d^{(2)}$ as

$$\begin{aligned}\left|\frac{-\frac{\partial \log_{10} \Pr_{U(unit)}\{\mathbf{M}|\rho\}}{\partial \log_{10}\rho} - r_d^{(1)}+r_d^{(2)}}{r_d^{(1)}+r_d^{(2)}}\right| &= \left|\frac{\zeta_\rho^{(1)}+\zeta_\rho^{(2)} \quad (1-\frac{r_d^{(1)}}{2r_d^{(1)}})}{\Pr_{U(unit)}\{\mathbf{M}|\rho\}}\right| \\ &= \left|\frac{\zeta_\rho^{(1)}+\zeta_\rho^{(2)}}{2\sum_{i=1}^{3}\zeta_\rho^{(i)}}\right|.\end{aligned} \tag{9.28}$$

Note that according to Theorem 7, the range of average diversity order is determined by the dominance of $\zeta_\rho^{(i)}$, in other words, approximately by the the dominance of the relative number of elements and pairwise probabilities in the sets $\Upsilon^{(i)}$, where $i = 1, 2, 3$. To show this approximation, assume that

1) the pairwise probability of all directional pairs $\mathbf{M}$ and $\widetilde{\mathbf{M}}$ within the set $\Upsilon^{(i)}$ are equally probable, which is denoted as

$$p_\rho^{(a,b,i)} = \Pr\left\{\mathbf{M}_{(a)} \to \mathbf{M}_{(b)}|\rho, \left\{\mathbf{M}_{(a)}, \mathbf{M}_{(b)}\right\} \in \Upsilon^{(i)}\right\} = p_\rho^{(i)},$$

2) all the $\mathbf{M}$ are equally probable with probability $\frac{1}{N_B}$,

for block (frame) based EUB, the closeness expressions (9.27) and (9.28) are rewritten as

$$\begin{aligned}\left|\frac{-\frac{\partial \log_{10} \Pr_{U(unit)}\{\mathbf{M}|\rho\}}{\partial \log_{10}\rho} - r_d^{(1)}}{r_d^{(1)}}\right| &= \left|\frac{\frac{1}{N_B}N_2 p_\rho^{(3)}}{\frac{1}{N_B}\left(N_1\left(p_\rho^{(1)}+p_\rho^{(2)}\right)+N_2 p_\rho^{(3)}\right)}\right| \\ &= \left|\frac{p_\rho^{(3)}}{\beta\left(p_\rho^{(1)}+p_\rho^{(2)}\right)+p_\rho^{(3)}}\right|\end{aligned} \tag{9.29}$$

and

$$\begin{aligned}\left|\frac{-\frac{\partial \log_{10} \Pr_{U(unit)}\{\mathbf{M}|\rho\}}{\partial \log_{10}\rho} - \left(r_d^{(1)}+r_d^{(2)}\right)}{r_d^{(1)}+r_d^{(2)}}\right| &= \left|\frac{\frac{1}{N_B}N_1\left(p_\rho^{(1)}+p_\rho^{(2)}\right)}{\frac{1}{N_B}\left(N_1\left(p_\rho^{(1)}+p_\rho^{(2)}\right)+N_2 p_\rho^{(3)}\right)}\right| \\ &= \left|\frac{\beta\left(p_\rho^{(1)}+p_\rho^{(2)}\right)}{\beta\left(p_\rho^{(1)}+p_\rho^{(2)}\right)+p_\rho^{(3)}}\right|,\end{aligned} \tag{9.30}$$

respectively, where N_1 and N_2 are defined in Appendix F.1, and $\beta = \frac{N_1}{N_2}$.

The block (frame) based EUB can be written as

$$\begin{aligned} &\Pr_{U(blk)}\{\mathbf{M}|\rho\} = \tfrac{1}{N_B}\left\{N_1\left(p_\rho^{(1)} + p_\rho^{(2)}\right) + N_2 p_\rho^{(3)}\right\} \\ &= \tfrac{N_2}{N_B}\left\{\beta\left(p_\rho^{(1)} + p_\rho^{(2)}\right) + p_\rho^{(3)}\right\} \\ &= \alpha\left\{\beta\left(p_\rho^{(1)} + p_\rho^{(2)}\right) + p_\rho^{(3)}\right\}, \end{aligned} \tag{9.31}$$

where α is defined as in (9.15), and $N_B = 2N_1 + N_2$.

According to (9.29), in enough high SNR, the average diversity order approaches $r_d^{(1)} = r_d^{(2)}$, while, if $p_\rho^{(1)} = p_\rho^{(2)}$, the merit of CI is still approximately maintained as extra coding advantage $2\alpha\beta = \frac{2N_1}{2N_1+N_2}$, which is clear through observing (9.31).

Observing (9.6), $p_\rho^{(a,b,i)}$ can be written in the following form

$$\begin{aligned} p_\rho^{(a,b,i)} &= \Pr\left\{\mathbf{M}_{(a)} \to \mathbf{M}_{(b)}|\rho, \left\{\mathbf{M}_{(a)}, \mathbf{M}_{(b)}\right\} \in \Upsilon^{(i)}\right\} \\ &= u(r^{(a,b,i)})\left(\tfrac{1}{N_T}\right)^{-r^{(a,b,i)}} (\rho)^{-r^{(a,b,i)}}, \end{aligned} \tag{9.32}$$

where $i = 1, 2, 3$, $u(r^{(a,b,i)})$, independent of ρ, is a function of $r^{(a,b,i)}$, where $r^{(a,b,i)}$ is the exponent corresponding to $p_\rho^{(a,b,i)}$. Using the third statement of Theorem 7, it is clear that, when ρ approaches infinity, the average diversity order reaches $\min\left\{r_d^{(1)}, r_d^{(2)}\right\} = \min\left\{r^{(a,b,i)}, \forall\,(a,b,i)\right\}$.

(Q, D, N_T, N_R, T)	N_a
(2,4,2,2,2)	16
(12,4,4,2,4)	16777216
(16,4,4,2,4)	4.295×10^9

Table 9.1. System configurations and corresponding codebook size of component LDCs

An illustration of the relation among α, $1-\alpha$, β, and 2β versus the codebook size of component LDCs N_a, which determines diversity properties of the ST-CILDC

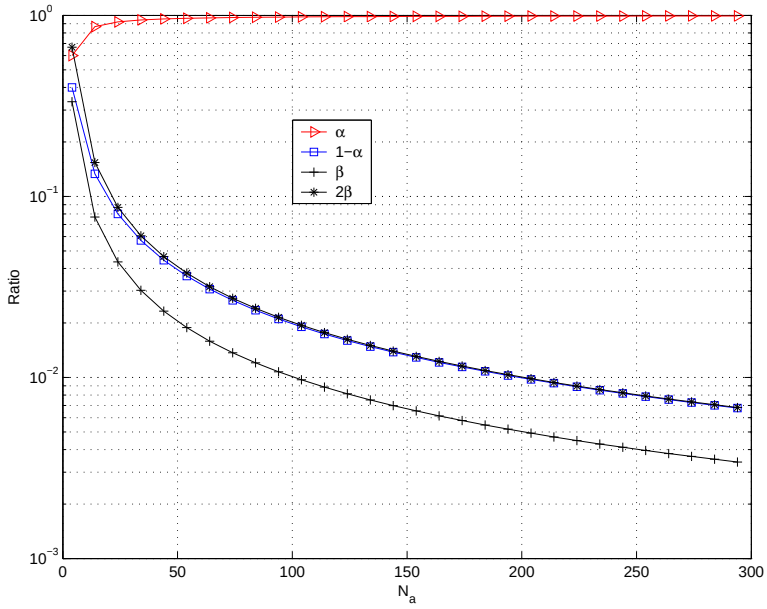

(a)

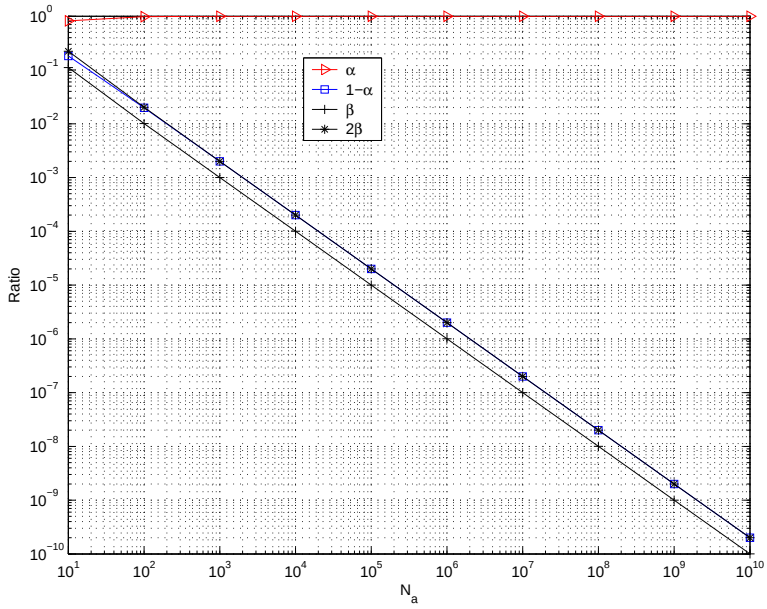

(b)

Figure 9.2. α, $1-\alpha$, β, and 2β versus component LDC codebook size N_a, (a) for small N_a and (b) for large N_a

systems, is shown in Figure 9.2. When N_a becomes large in Figure 9.2(b), the curves of $1-\alpha$ and 2β are quite close and are approximately an exponential relation to N_a. When N_a is small in Figure 9.2(a), the curve of $1-\alpha$ and 2β is notably different, and $1-\alpha$ and 2β can be large. From Table 9.1, where D denotes the constellation size of source data symbols, one may observe the relation among system configurations versus N_a for several examples. The above discussion will be partly verified through simulation in Section 9.4.2.

Note that except for the trivial extra computational load of coordinate interleaving, for the same size of LDC encoding matrices, the complexity per LDC codeword of the ST-CILDC system is almost the same as that of conventional LDC systems. However, the upper bound achievable average diversity order of a ST-CILDC system may be almost twice that of conventional block-based space-time code (BSTC) systems if the component LDC in the ST-CILDC are of similar diversity features. It is worth mentioning that using nonlinear sphere or ML decoding, the conventional BSTC systems need much higher complexity to reach an average diversity order comparable to ST-CILDC, since the size of the BSTC block would be double the size of the component LDC used in ST-CILDC and the worst case complexity is exponential in relation to the codebook size of the BSTC.

We remark the scope of this approach is not limited to LDC. Other block-based space-time code designs also may be improved using the proposed space-time inter-LDC coordinate interleaving approach. Further, the pair of LDC codewords used in ST-CILDC could be viewed as a single specially designed LDC codeword of size $2T \times N_T$. ST-CILDC systems could thus be viewed as an extension of LDC systems using different design criteria.

9.4 Performance

9.4.1 Simulation setup

Perfect channel knowledge (amplitude and phase) is assumed at the receiver but not at the transmitter. Assume the number of receive antennas is not less than the number of transmit antennas. Channel symbols are estimated using MMSE estimation. Data symbols use QPSK modulation in all simulations. The signal-to-noise-ratio (SNR) reported in all figures is the average symbol SNR per receive antenna.

Three space-time block codes, Code HH1, Code MG, and Code HH2, are used as component LDC coding matrices of ST-CILDC systems in the simulations. Code HH1 chosen is a class of rate-one square shown in (3.10). Code MG, proposed by Hassibi and Hochwald, is chosen from Design A of full diversity full rate (FDFR) codes proposed by Ma and Giannakis [76]. Code HH2 is a non-rate-one high rate codes for the configuration of $N_T = 4$,$T = 6$,$Q = 12$, proposed by Hassibi and Hochwald [42].

9.4.2 Performance comparison

The performance comparison of Code HH1 is shown in Figures 9.3, 9.4, and 9.5. The performance comparison of Code MG is shown in Figure 9.6. The performance comparison of Code HH2 is shown in Figure 9.7.

In block fading channels, i.e., when the 4×4 MIMO channels are constant over the pair of ST-LDC codewords and Code HH1 is used, ST-CILDC obtains the same performance as that of ST-LDC as shown in Figure 9.4.

However, as shown in Figures 9.3, 9.5 9.6, , and 9.7, which are results in rapid fading channels, ST-CILDC significantly outperforms ST-LDC at high SNRs. Thus, the ST-CILDC procedure may be applied to both rate-one and slightly lower rate codes.

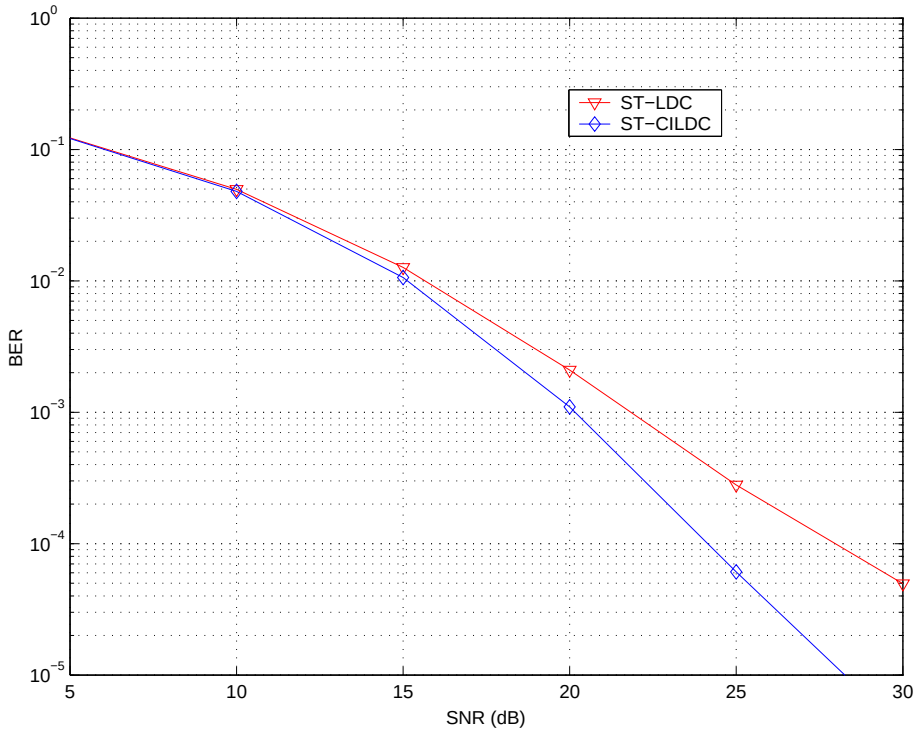

Figure 9.3. BER performance comparison of ST-CILDC vs. LDC using Code HH1, $CCR = 1$, $N_T = 4$, $N_R = 4$, $T = 4$, $Q = 16$

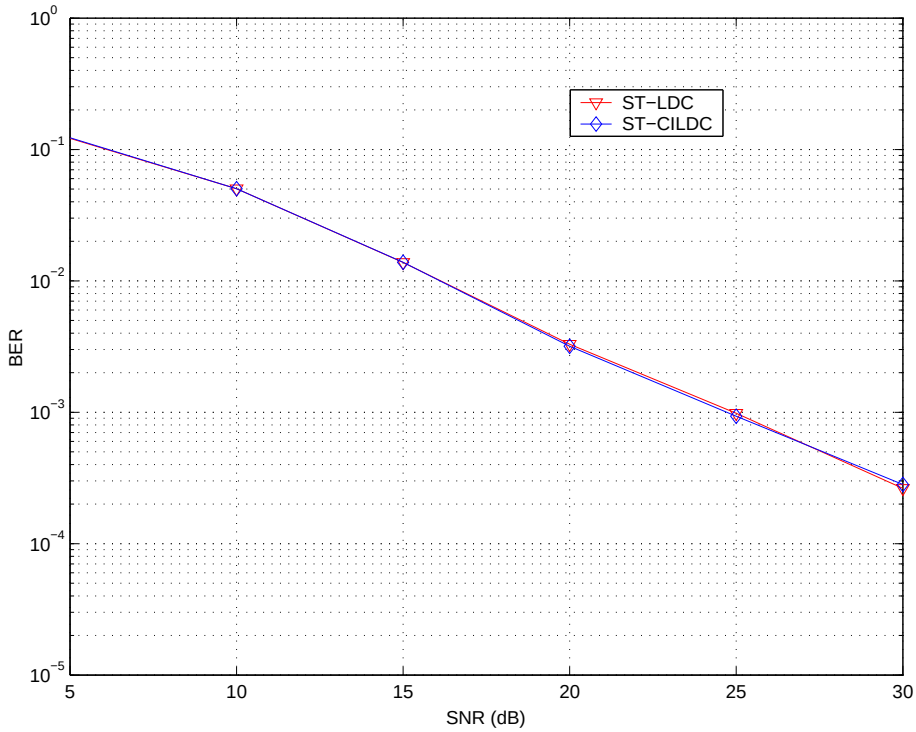

Figure 9.4. BER performance comparison of ST-CILDC vs. LDC using Code HH1, $CCR = 8$, $N_T = 4$, $N_R = 4$, $T = 4$, $Q = 16$

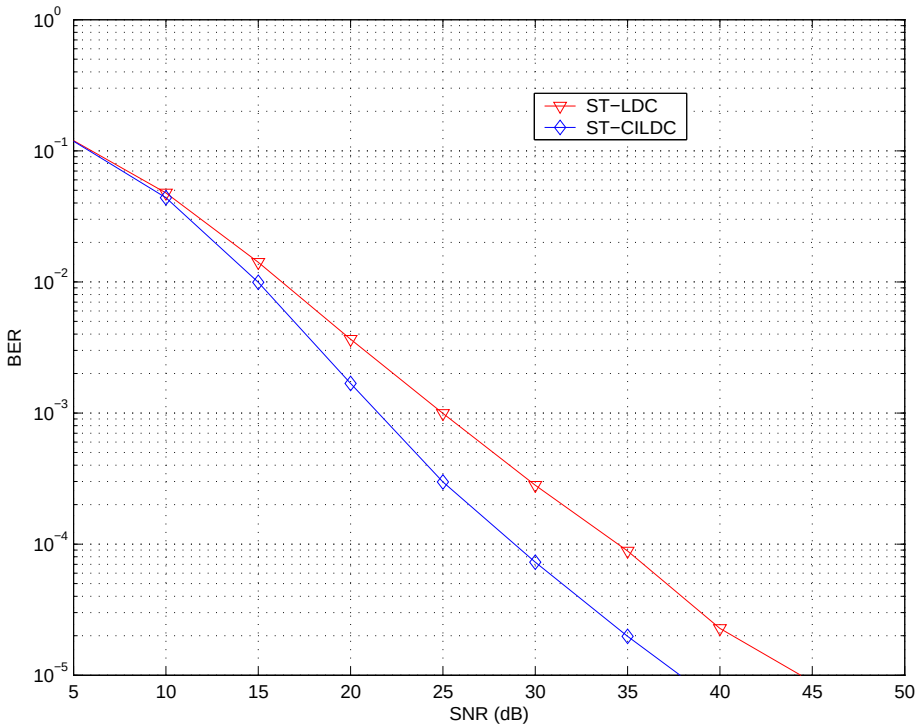

Figure 9.5. BER performance comparison of ST-CILDC vs. LDC using Code HH1, $CCR = 1$, $N_T = 2$, $N_R = 2$, $T = 2$, $Q = 4$

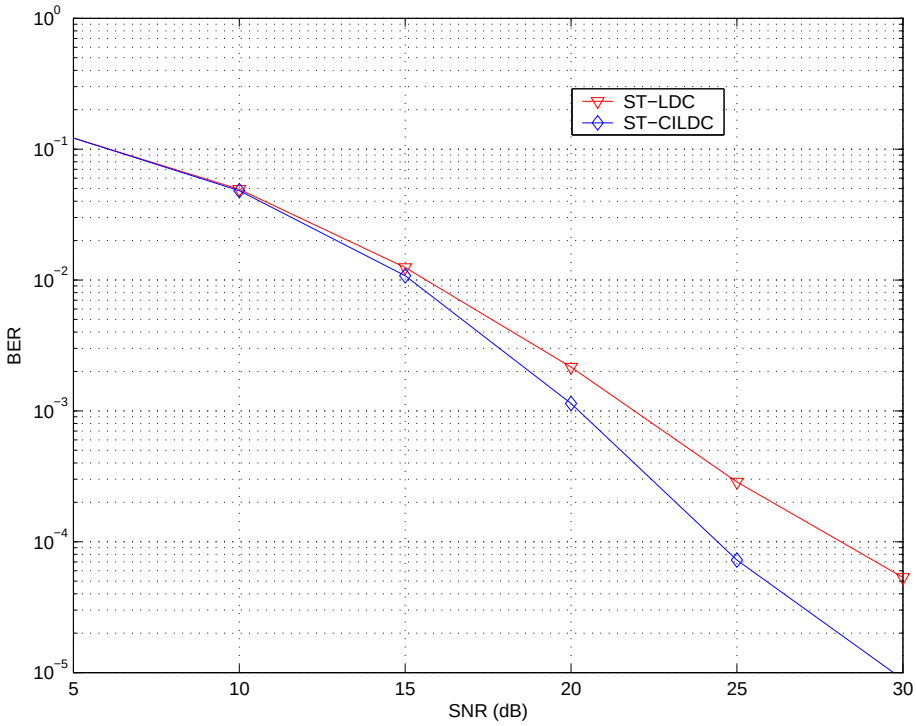

Figure 9.6. BER performance comparison of ST-CILDC vs. LDC using Code MG, $CCR = 1$, $N_T = 4$, $N_R = 4$, $T = 4$, $Q = 16$

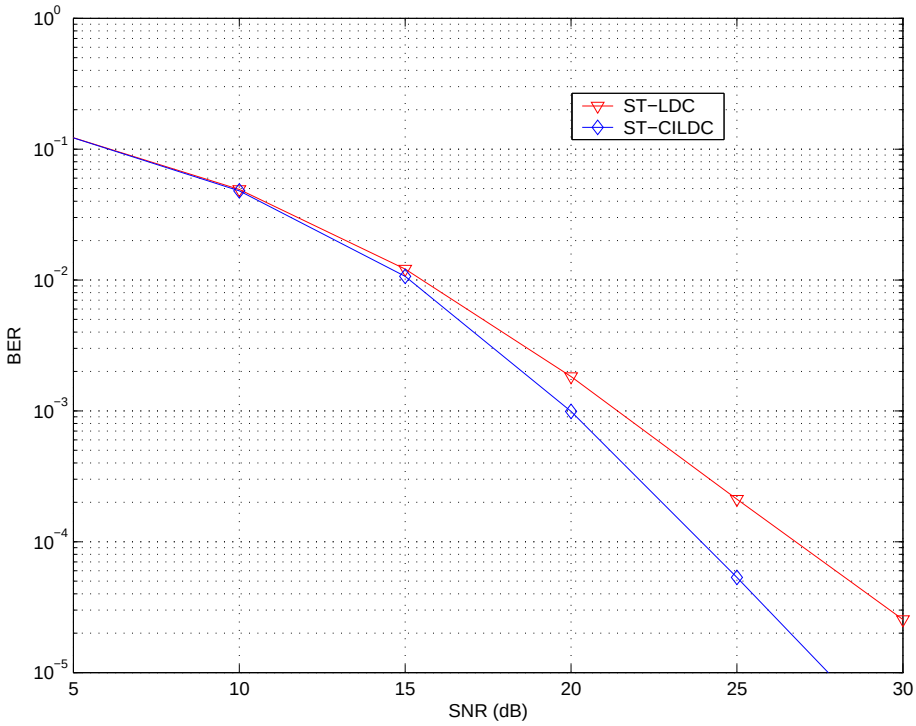

Figure 9.7. BER performance comparison of ST-CILDC vs. LDC using Code HH2, $CCR = 1$, $N_T = 4$, $N_R = 4$, $T = 6$, $Q = 12$

Observing Figures 9.3 and 9.6, the performances of Code HH1 and Code MG are similar in rapid fading channels. Thus, even though Code HH1 is not designed under a diversity criterion, Code HH1 appears to possess desirable diversity properties.

Note that Figure 9.5 shows the ST-CILDC performance in a 2×2 MIMO systems, and the codebook size of the corresponding component LDCs, N_a, is much smaller than those in Figures 9.3, 9.6, and 9.7. In the SNR region from 10 to 25 dB in Figure 9.5, the slopes of performance curves of ST-CILDC and ST-LDC are notably different, while in the SNR region higher than 25 dB, the slope of performance curves of ST-CILDC and ST-LDC are almost the same. This observation agrees with the discussion of average diversity order in Section 9.3, since ST-CILDC shows either much higher average diversity order or extra coding advantage over ST-LDC, the choice of which depends on the value of SNR ρ and the codebook size N_a.

9.5 Conclusion

This chapter has proposed a general space-time inter-LDC coordinate interleaving procedure, ST-CILDC, which may be applied to either rate-one (information lossless) or slightly lower rate block-based space-time coding systems. This enables not only symbol-level diversity but also coordinate-level diversity. The upper bound diversity order and statistical diversity order of ST-CILDC are analyzed. Although a ST-CILDC system does not obtain an increased diversity order over the corresponding conventional ST-LDC system, the ST-CILDC system show either much higher average diversity order or extra coding advantage compared with the corresponding conventional ST-LDC system in time varying channels. Compared with conventional block-based STC, ST-CILDC systems maintain diversity performance in quasi-static

block fading channels, and significantly improve the diversity performance in the high SNR regions of rapid fading channels.

Chapter 10

Summary and Future Directions

10.1 Summary

Newly proposed fundamental high-rate diversity approaches are the central concerns of this thesis, which are motivated by the requirements of high spectral efficiency and high reliability in new generation SISO and MIMO digital communications systems. In Chapter 4, a new class of rate-one rectangular LDC dispersion codes of arbitrary size are proposed and analyzed. In Chapters 5 and 6, LDC are proposed for application in multicarrier and single carrier SISO communications, respectively, and their diversity features are analyzed. In Chapters 7 and 8, LDC based high-rate space-time-frequency codes are proposed and analyzed. In Chapter 9, coordinate-interleaving or component interleaving are applied to space time LDC to achieve high performance in rapid fading channels.

This thesis primarily consider linear LDC decoding in the simulation studies, which can be justified as follows.

1) The proposed diversity systems, such as LDC-OFDM, are quite new, in other words, other comparable designs do not exist. Although linear decoding is

used and the system possibly does not fully exploit available diversity, such as time diversity, in the channels, the performance improvement demonstrates the diversity advantages of the new systems.

2) Clearly, maximum likelihood decoding (MLD) and MLD-like approaches may be needed to reach maximal achievable diversity and coding gains. However, it is shown that properly designed linear decoding for complex diversity coding system is able to realize a significant amount of the maximally achievable diversity order of the codes [13, 85, 104, 105].

3) Although pairwise error probability (PEP) based diversity analysis is best suitable for MLD and MLD-like approaches, existing research investigations have utilized PEP diversity analysis for linear decoding based diversity approaches [104, 105]. Even if linear decoding based diversity approaches cannot exploit maximal available diversity of the codes, PEP-based analysis captures, at least asymptotically, the significant diversity features of properly designed linear decoding based systems. PEP based analysis provides the upper bound diversity order of the proposed systems. The most important performance metric this thesis concerns is diversity order, which is related to the slope of the logarithm of the error probability or pairwise error probability. Even if linear decoding is used, the general trends of of the slopes of the error performance curves due to diversity effects introduced can be clearly observed in this thesis.

4) Linear decoding leads to much lower complexity, which makes proposed designs more practical.

As proof of concepts, linear dispersion codes under constraints (3.10) are primarily considered in simulations throughout this thesis, although more general linear

dispersion codes which do not satisfy constraints (3.10) are used in the simulations of Chapter 9. Actually, general linear dispersion codes which do not satisfy constraints (3.10) can be also applied in all the proposed diversity approaches in this thesis.

Instead of analyzing exact error probability, this thesis has analyzed the fundamental diversity properties, the upper bound diversity orders of proposed approaches. The main diversity dimensions discussed in this thesis are space, time, and frequency, which arise from the statistical nature of the environment in the real world. This thesis studies diversity approaches over not only spatial domain MIMO but also frequency domain MIMO. In general, statistical fading channels may have detrimental effects in communication systems. However, this thesis describes how to take advantage of the statistical fluctuation through efficiently exploiting diversity over physical dimensions.

10.2 Future Directions

10.2.1 Design of slightly-lower-rate codes

Although linear dispersion codes allow an arbitrary coding rate, this thesis primarily designs and utilizes rate-one codes. However, slightly lower-rate codes, which may have higher diversity order per data source symbols, have not been sufficiently addressed in the literature. We refer to the term slightly lower-rate codes to denote those as having rates higher than $1/\min\{N_T, N_R\}$ in space-time or frequency-time channels. The rate of those codes is generally higher than the rate of OSTBC.

10.2.2 Exact error performance of proposed diversity approaches

This thesis analyzes the proposed diversity approaches primarily through diversity order. However, exact error performance of proposed diversity approaches has not been analyzed. Instead using simulations, the analysis of exact error probability may help further confirm and quantify the performance of diversity systems.

10.2.3 New receiver designs of proposed diversity approaches

Although this thesis has proposed several receiver designs arising from diversity considerations, new receiver designs may be needed to obtain higher performance at lower complexity for different applications.

10.2.4 Proposed diversity approaches in more realistic channels

Although this thesis has utilized channel models with considerations to several realistic factors in the channels, more realistic channel models may be needed to apply proposed diversity approaches to actual physical channels.

Bibliography

[1] "Air interface for fixed broadband wireless access systems part A: systems between 2 and 11 GHz," *IEEE Std.802.16ab-01/01*, 2001.

[2] N. A1-Dhahir and J.M.Cioffi, "MMSE decision-feedback equalizers: finite-length results," *IEEE Trans.Inform.Theory*, pp. 961–975, July 1995.

[3] S. Alamouti, "A simple transmitter diversity scheme for wireless communications," *IEEE J.Select.Areas Commun.*, pp. 1451–1458, Oct. 1998.

[4] K. Azarian and H. Gamal, "The throughput-reliability tradeoff in MIMO channels," *submitted to IEEE Trans.Inform.Theory*, Aug. 2005.

[5] J. Bingham, "Multicarrier modulation for data transmission: an idea whose time has come," *IEEE Commun.Mag.*, vol. 28, pp. 5–14, May 1990.

[6] H. Blcskei, D.Gesbert, and A. and, "On the capacity of OFDM-based spatial multiplexing systems," *IEEE Trans.Commun.*, vol. 50, no. 2, pp. 225–234, Feb. 2002.

[7] H. Bolcskei and A. J. Paulraj, "Space-frequency coded broadband OFDM systems," in *Proc. IEEE Wireless Commun. and Networking Conference (WCNC) 2000*, vol. 1, 2000, pp. 1–6.

[8] K. Boulle and J.C.Belfiore, "Modulation schemes designed for the Rayleigh channel," in *Proc. Conference on Information Sciences and Systems (CISS) 1992*, 1992, pp. 288–293.

[9] D. G. Brennan, "Linear diversity combining techniques," *Proc.IRE*, vol. 47, June 1959.

[10] T. Buzid, S.Reinhardt, and M.Huemer, "A comparision of OFDM and non-linear SC/FDE signals: Non-linear SC/FDE signals: non-linear amplification," in *Proc. European Wireless Conf. 2005*, Apr. 2005.

[11] Q. Chen and J. Yin, "Impact of spatial temporal correlated and symbol-to-symbol variant fading on performance of MISO system," in *Proc. the IEEE 6th Circuits and Systems Symposium on Emerging Technologies: Frontiers of Mobile and Wireless Commun.*, vol. 1, 2004, pp. 161–164.

[12] L. J. Cimini, "Analysis and simulation of digital mobile channel using orthogonal frequency division multiplexing," *IEEE Trans.Commun.*, vol. 33, no. 7, pp. 665–675, July 1985.

[13] J. Conan and C. Lefebvre, "Linear equalization of frequency selective channels using space diversity," in *Proc. Fourth IEEE Int. Conf. on Universal Personal Commun.*, Nov. 1995, pp. 909–913.

[14] T. Couasnon, R.Monnier, and J.B.Rault, "OFDM for digital TV broadcasting," *Signal Processing*, vol. 39, pp. 1–32, Sept. 1994.

[15] T. M. Cover and J.A.Thomas, *Elements of Information Theory.* John Wiley & Sons, Inc., 1991.

[16] M. O. Damen, H. Gamal, and N.C.Beaulieu, "Linear threaded algebraic space-time constellation," *IEEE Trans.Inform.Theory*, pp. 2372–2388, Oct. 2003.

[17] O. Damen, A.Chkeif, and J.-C.Belfiore, "Lattice code decoder for space-time codes," *IEEE Commun.Lett.*, vol. 4, no. 5, pp. 161–163, May 2000.

[18] P. Dayal and M.K.Varanasi, "Maximal diversity algebraic space-time codes with low peak-to-mean power ratio," *IEEE Trans.Inform.Theory*, vol. 51, no. 5, pp. 1691–1708, May 2005.

[19] S. N. DIGGAVI, N. AL-DHAHIR, A. STAMOULIS, and A. R. CALDERBANK, "Great expectations: the value of spatial diversity in wireless networks," *Proc.of the IEEE*, vol. 92, no. 2, pp. 219–270, Feb. 2004.

[20] M. L. Doelz, E.T.Heald, and D.L.Martin, "Binary data transmission techniques for linear systems," *Proc.IRE*, vol. 45, pp. 656–661, May 1957.

[21] G. Durgin, *Space-time wireless channels.* Prentice Hall, 2003.

[22] O. Edfors, M.Sandell, J.-J. de Beek, S.K.Wilson, and P.O.Borjesson, "OFDM channel estimation by singular value decomposition," *IEEE Trans.Commun.*, vol. 46, no. 7, pp. 931–939, July 1998.

[23] C. Eklund, R.B.Marks, K.L.Stanwood, and S.Wang, "IEEE standard 802.16a: a technical overview of the wirelessman^{TM} the air interface for broadband wireless access," *IEEE Commun.Mag.*, vol. 40, no. 6, pp. 98–107, June 2002.

[24] T. Eng, N. Kong, and L.B.Milstein, "Comparison of diversity combining techniques for Rayleigh-fading channels," *IEEE Trans.Commun.*, pp. 1117–1129, Sept. 1996.

[25] B. G. Evans and K.Baughan, "Vision of 4G," *Electronics & Commun.Engineering Journal*, vol. 12, no. 6, pp. 293–303, Dec. 2000.

[26] D. Falconer, S.L.Ariyavisitakul, A.Benyamin-Seeyar, and B.Eidson, "Frequency domain equalization for single-carrier broadband wireless systems," *IEEE Commun.Mag.*, pp. 58–66, Apr. 2002.

[27] G. Femenias and I. Furio, "A new, simple, and exact union bound for reference-based predetection and postdetection diversity TCM-MPSK systems in rayleigh fading," *IEEE Trans.on Vehicular Technology*, vol. 49, no. 2, pp. 540–549, 2006.

[28] U. Fincke and M.Pohst, "Improved methods for calculating vectors of short length in lattice, including a complexity analysis," *Math.Comput.*, vol. 44, no. 170, pp. 463–471, Apr. 1985.

[29] G. D. Forney and G.Ungerboeck, "Modulation and coding for linear gaussian channels," *IEEE Trans.Inform.Theory*, vol. 44, pp. 2384–2415, Oct. 1998.

[30] G. J. Foschini, "Layered space-time architecture for wireless communication in a fading environment when using multi-element antennas," *Bell Labs Tech.J.*, vol. 1, no. 2, pp. 41–49, 1996.

[31] G. J. Foschini and M.J.Gans, "On limits of wireless communications in a fading environment when using multiple antennas," *Wireless Personal Commun.*, vol. 6, pp. 311–335, 1998.

[32] D. Gesbert, M.Shafi, D. shan Shiu, P.J.Smith, and A.Naguib, "From theory to practice: an overview of MIMO space-time coded wireless systems," *IEEE J.Select.Areas Commun.*, vol. 21, no. 3, pp. 281–302, Apr. 2003.

[33] G. B. Giannakis and S. Zhou, "Space-time coding using estimated channel information," *United States Patent Application Publication, Pub No.US2004/0066761 A1*, Apr. 2004.

[34] R. H. Gohary and T.N.Davidson, "Design of linear dispersion codes: Some asymptotic guidelines and their implementation," *IEEE Trans.Wireless Commun.*, vol. 4, no. 6, pp. 2892–2906, Nov. 2005.

[35] G. D. Golden, G.J.Foschini, R.A.Valenzuela, and P.W.Wolniansky, "Detection algorithm and initial laboratory results using the V-BLAST space-time communication architecture," *Electronics Letters*, vol. 35, no. 1, pp. 14–15, 1999.

[36] A. Goldsmith, S.A.Jafar, N.Jindal, and S.Vishwanath, "Capacity limits of MIMO channels," *IEEE J.Select.Areas Commun.*, vol. 21, no. 5, pp. 684–702, June 2003.

[37] Y. Gong and K. B. Letaief, "Space-frequency-time coded OFDM for broadband wireless communications," in *Proc. IEEE Global Telecommun. Conference (GLOBECOM) 2001*, vol. 1, Nov. 2001, pp. 519–523.

[38] J. Gruber, E.Abdou, P.Richards, and G.Williams, "Quality-of-service in evolving telecommunications networks," *IEEE J.Select.Areas Commun.*, vol. 4, no. 7, pp. 1084–1089, Oct. 1986.

[39] J. C. Guey, M. P. Fitz, M. R. Bell, and W.-Y. Kuo, "Signal designs for transmitter diversity wireless communication system over rayleigh fading channels," in *Proc. IEEE Vehicular Technology Conference 1996*, 1996, pp. 136–140.

[40] M. Guillaud and D.T.M.Slock, "Multi-stream coding for MIMO OFDM systems with space-time-frequency spreading," in *Proc. The Int. Symposium on Wireless Personal Multimedia Commun.*, vol. 1, Oct. 2002, pp. 120–124.

[41] S. H. Han and J. H. Lee, "An overview of peak-to-average power ratio reduction techniques for multicarrier transmission," *IEEE Wireless Commun.*, vol. 12, no. 2, pp. 56–65, Apr. 2005.

[42] B. Hassibi and B. M. Hochwald, "High-rate codes that are linear in space and time," *IEEE Trans.Inform.Theory*, vol. 48, no. 7, pp. 1804–1824, July 2002.

[43] B. Hassibi and H.Vikalo, "On the sphere-decoding algorithm I. Expected complexity," *IEEE Trans.Sig.Proc.*, vol. 53, no. 8, pp. 2806–2818, Aug. 2005.

[44] ——, "On the expected complexity of integer least-squares problems," in *Proc. IEEE Int. Conference on Acoustics, Speech, and Signal Proc. (ICASSP) 2002*, May 2002, pp. 1497–1500.

[45] R. Hayes and J. Caffery, "Dispersive covariance codes for MIMO precoding," in *Proc. IEEE Global Telecommun. Conference (Globecom) 2005*, vol. 3, Nov. 2005, pp. 1466–1470.

[46] L. He and H. Ge, "A new full-rate full-diversity orthogonal space-time block coding scheme," *IEEE Commun.Lett.*, vol. 7, no. 12, pp. 590–592, Dec. 2003.

[47] R. W. Heath and A. J.Paulraj, "Linear dispersion codes for MIMO systems based on frame theory," *IEEE Trans.Sig.Proc.*, vol. 50, no. 10, pp. 2429–2441, Oct. 2002.

[48] J. Heiskala and J. Terry, *OFDM wireless LANs: a theoretical and practical guide*. SAMS, 2002.

[49] J. F. Helard and B. Floch, "Trellis coded orthogonal frequency division multiplexing for digital video transmission," in *Proc. IEEE Global Telecommun. Conference (GLOBECOM) 1991*, vol. 2, Dec. 1991, pp. 785–791.

[50] D. Hutchison, A.Mauthe, and N.Yeadon, "Quality-of-service architecture: monitoring and control of multimedia communications," *Electronics & Commun.Engineering Journal*, vol. 9, no. 3, pp. 100–106, June 1997.

[51] D. M. Ionescu, "New results on space time code design criteria," in *Proc. IEEE Wireless Commun. and Networking Conference (WCNC) 1999*, Sept. 1999, pp. 684–687.

[52] K. Ishll and R. Kohno, "Space-time-frequency turbo code over time-varying and frequency-selective fading channel," *IEICE Trans.on Fundamentals of Electronics, Commun.and Computer Sciences*, vol. E88-A, no. 10, pp. 2885–2895, 2005.

[53] J. Jalden and B.Ottersten, "On the complexity of sphere decoding in digital communications," *IEEE Trans.Sig.Proc.*, vol. 53, no. 4, pp. 1474–1484, Apr. 2005.

[54] B. Jelicic and S.Roy, "Coordinate interleaving TCM for flat fading and AWGN channels," in *Proc. IEEE Global Telecommun. Conference (Globecom) 1994*, vol. 1, Nov. 1994, pp. 368–373.

[55] B. D. Jelicic and S.Roy, "Cutoff rates for coordinate interleaved QAM over Rayleigh fading channels," *IEEE Trans.Commun.*, vol. 44, no. 10, pp. 1231–1233, Oct. 1996.

[56] E. A. Jorswieck and H.Boche, "Optimal transmission strategies and impact of correlation in multiantenna systems with different types of channel state information," *IEEE Trans.Sig.Proc.*, vol. 52, no. 12, pp. 3440–3453, Dec. 2004.

[57] T. Kailath and H.V.Poor, "Detection of stochastic processes," *IEEE Trans.Inform.Theory*, vol. 44, no. 6, pp. 2230–2231, Oct. 1998.

[58] M. Z. A. Khan and B.S.Rajan, "Space-time block codes from co-ordinate interleaved orthogonal designs," in *Proc. IEEE Int. Symposium on Inform. Theory (ISIT) 2002*, 2002, pp. 275–275.

[59] M. Z. A. Khan, B.S.Rajan, and M. H. Lee, "Rectangular co-ordinate interleaved orthogonal designs," in *Proc. IEEE Global Telecommun. Conference (Globecom) 2003*, vol. 4, Dec. 2003, pp. 2003–2009.

[60] H. Kim, "Turbo coded orthogonal frequency division multiplexing for digital audio broadcasting," in *Proc. IEEE Int. Conference on Commun. (ICC) 2000*, vol. 1, 2000, pp. 420–424.

[61] J. Kim, I. Kim, S. Ro, D.Hong, and C. Kang, "Effects of multipath diversity on adaptive QAM in frequency selective Rayleigh fading channels," *IEEE Commun.Lett.*, vol. 6, no. 9, pp. 364–366, Sept. 2002.

[62] Y.-H. Kim and M.Kaveh, "Coordinate-interleaved space-time coding with rotated constellation," in *Proc. IEEE Vehicular Technology Conference (VTC) 2003*, vol. 1, Apr. 2003, pp. 732–735.

[63] Y. Kondo and T.Tanaka, "Adaptive time diversity for TDMA vs TDD personal communication systems," in *Proc. the Fourth IEEE Int. Conf. on Universal Personal Commun.*, Nov. 1995, pp. 973–976.

[64] S. K. Lai, R.S.Cheng, K.B.Letaief, and R.D.Murch, "Adaptive trellis coded MQAM and power optimization for OFDM transmission," in *Proc. IEEE Vehicular Technology Conference (VTC) 1999*, vol. 1, May 1999, pp. 290–294.

[65] W. C. Y. Lee, *Mobile communications design fundamentals*. SAMS, 1986.

[66] S. W. Lei and V.K.N.Lau, "Performance analysis of adaptive interleaving for OFDM systems," *IEEE Trans.Vehicular Technology*, vol. 51, no. 3, May 2002.

[67] J. J. A. Lempiainen and J.K.Laiho-Steffens, "the performance of polarization diversity schemes at a base station in smallmicro cells at 1800 MHz," *IEEE Trans.on Vehicular Technology*, vol. 47, no. 3, pp. 1087–1092, Aug. 1998.

[68] Y. Li, J.C.Chuang, and N.R.Sollenberger, "Transmitter diversity for OFDM systems and its impact on high-rate data wireless networks," *IEEE J.Select.Areas Commun.*, pp. 1233–1243, July 1999.

[69] L. Lin, L. Jr., and J.C.-I.Chuang, "Turbo codes for OFDM with antenna diversity," in *Proc. IEEE Vehicular Technology Conference (VTC) 1999*, vol. 2, May 1999, pp. 1664–1668.

[70] S. Lin and D. J.Costello, *Error control coding*. Prentice Hall, Apr..2004.

[71] Y.-P. Lin and S.-M. Phoong, "BER minimized OFDM systems with channel independent precoders," *IEEE Trans.on Sig.Proc.*, vol. 51, no. 9, Sept. 2003.

[72] Z. Liu, Y.Xin, and G.B.Giannakis, "Linear constellation precoded OFDM with maximum multipath diversity and coding gains," *IEEE Trans.Commun.*, vol. 51, no. 3, pp. 416–427, Mar. 2003.

[73] Z. Liu, "Maximum diversity in single-carrier frequency-domain equalization," *IEEE Trans.Inform.Theory*, vol. 51, no. 8, pp. 2937–2940, Aug. 2005.

[74] Z. Liu and G. B. Giannakis, "Space-time-frequency coded OFDM over frequency-selective fading channels," *IEEE Trans.Sig.Proc.*, vol. 50, no. 10, pp. 2465–2476, Oct. 2002.

[75] W. Luo and S. Wu, "Space-time-frequency block coding over Rayleigh fading channels for OFDM systems," in *Proc. Int. Conf. on Commun. Tech.*, vol. 2, Apr. 2003, p. 1012.

[76] X. Ma and G.B.Giannakis, "Full-diversity full-rate complex-field space-time coding," *IEEE Trans.Sig.Proc.*, vol. 51, no. 11, pp. 2917–2930, Nov. 2003.

[77] W. Mo and Z.Wang, "Average symbol error probability and outage probability analysis for general cooperative diversity system at high signal to noise ratio," in *Proc. Conference on Information Sciences and Systems 2004*, Mar. 2004.

[78] S. H. Muller and J. Huber, "OFDM with reduced peak to average power ratio by optimum combination of partial transmit sequences," *IEE Electronics Letters*, vol. 33, no. 5, pp. 368–369, Feb. 1997.

[79] A. F. Naguib, *Adaptive Antenna CDMA Wireless Network*. PhD thesis, Standford University, Palo Alto, CA, USA, Aug..1996.

[80] R. Newman, *Broadband communications*. Prentice Hall, Jan..2002.

[81] M. K. Ozdemir, E.Arvas, and H.Arslan, "Dynamics of spatial correlation and implications on MIMO systems," *IEEE Commun.Mag.*, vol. 42, no. 42, pp. S14–S19, June 2004.

[82] S.-M. Phoong and K.-Y. Chang, "Antipodal paraunitary matrices and their application to OFDM systems," *IEEE Trans.Sig.Proc.*, vol. 53, no. 4, pp. 1374–1386, Apr. 2005.

[83] H. V. Poor, *An introduction to signal detection and estimation.* Springer Verlag, Mar..1994.

[84] J. Proakis, *Digital communications*, 3rd ed. McGraw-Hill, 2000.

[85] D. Qu, G. Zhu, and Z. Chen, "Low complexity LMMSE turbo equalization for linearly precoded OFDM," in *Proc. IEEE PIMRC 2003*, vol. 1, Sept. 2003, pp. 819–823.

[86] T. S. Rappaport, *Wireless communications: Principles & practice.* Prentice Hall, 1996.

[87] U. Reimers, "DVB-T: the COFDM-based system for terrestrial television," *Electronics & Commun.Engineering Journal*, vol. 9, no. 1, pp. 28–32, Feb. 1997.

[88] S. Sandhu and A.Paulraj, "Union bound on error probability of linear space-time block codes," in *Proc. IEEE Int. Conference on Acoustics, Speech, and Signal Proc. (ICASSP) 2001*, vol. 4, May 2001, pp. 2473–2476.

[89] S. Sandhu and A. Paulraj, "Unified design of linear space-time block codes," in *Proc. IEEE Global Telecommun. Conference (Globecom) 2001*, vol. 2, Nov. 2001, pp. 1073–1077.

[90] S. Sandhu, R.Heath, and A.Paulraj, "Union bound for linear space-time codes," in *Proc. 38th Annual Allerton Conference on Commun., Control and Computing*, 2000.

[91] A. M. Sayeed, J. H. Kotecha, and Z. Hong, "Capacity-optimal structured linear dispersion codes for correlated MIMO channels," in *Proc. IEEE Vehicular Technology Conference (VTC) 2004 Fall*, vol. 3, Sept. 2004, pp. 1623–1627.

[92] L. Scharf, *Statistical signal processing: detection, estimation, and time series analysis*. Addison-Wesley, 1991.

[93] C. E. Shannon, "A mathematical theory of communication," *Bell Sys.Tech.Journal*, vol. 27, pp. 379–423, 1948.

[94] V. Shashidhar, B. S. Rajan, and P. V. Kumar, "Asymptotic-information-lossless designs and diversity-multiplexing tradeoff," in *Proc. IEEE Global Telecommun. Conference (Globecom) 2004*, vol. 1, Nov. 2004, pp. 366–370.

[95] P. Shelswell, "The COFDM modulation system: the heart of digital audio broadcasting," *Electronics & Commun.Engineering Journal*, vol. 127, no. 136, June 1995.

[96] S. Siwamogsatham, M.P.Fitz, and J.H.Grimm, "A new view of performance analysis of transmit diversity schemes in correlated Rayleigh fading," *IEEE Trans.Inform.Theory*, vol. 48, no. 4, pp. 950–956, Apr. 2002.

[97] W. Su, Z.Safar, and K.J.R.Liu, "Diversity analysis of space-time-frequency coded broadband OFDM systems," in *Proc. European Wireless 2004*, Feb. 2004.

[98] ——, "Full-rate full-diversity space-frequency codes with optimum coding advantage," *IEEE Trans.Inform.Theory*, vol. 51, no. 1, pp. 229–249, Jan. 2005.

[99] ——, "Towards maximum achievable diversity in space, time, and frequency: performance analysis and code design 128," *IEEE Trans.Wireless Commun.*, vol. 4, no. 4, pp. 1847–1857, July 2005.

[100] ——, "Diversity analysis of space-time modulation over time-correlated Rayleigh-fading channels," *IEEE Trans.Inform.Theory*, vol. 50, no. 8, pp. 1832–1840, Aug. 2004.

[101] V. Tarokh, H.Jafarkhani, and A.R.Calderbank, "Space-time block code from orthogonal designs," *IEEE Trans.Inform.Theory*, vol. 45, pp. 1456–1467, July 1999.

[102] V. Tarokh, N.Seshadri, and A.Calderbank, "Space-time codes for high data rate wireless communications: performance criterion and code construction," *IEEE Trans.Inform.Theory*, vol. 44, pp. 744–765, Mar. 1998.

[103] I. E. Telatar, "Capacity of multi-antenna gaussian channels," *European Trans.on Telecommun.*, vol. 10, no. 6, pp. 585–595, Nov. 1999.

[104] C. Tepedelenlioglu, "Maximum multipath diversity with linear equalization in precoded OFDM systems," *IEEE Trans.Inform.Theory*, vol. 50, no. 1, pp. 232–235, Jan. 2004.

[105] C. Tepedelenlioglu and Q. Ma, "On the performance of linear equalizers for block transmission systems," in *Proc. IEEE Global Telecommun. Conference (Globecom) 2005*, vol. 6, Nov. 2005.

[106] L. Thibault and M. T. Le, "Performance evaluation of COFDM for digital audio broadcasting. i. parametric study," *IEEE Trans.Broadcasting*, vol. 43, no. 1, pp. 64–75, Mar. 1997.

[107] O. Tirkkonen, A.Boariu, and A.Hottinen, "Minimal non-orthogonality rate 1 space-time block code for 3+ Tx antennas," in *Proc. IEEE Int. Symposium on Spread Spectrum Techniques (ISSSTA) 2000*, vol. 2, Sept. 2000, pp. 429–432.

[108] O. Tirkkonen and A.Hottinen, "Maximal symbolwise diversity in non-orthogonal space-time block codes," in *Proc. IEEE Int. Symposium on Inform. Theory (ISIT) 2001*, June 2001, pp. 197–197.

[109] ——, "Improved MIMO performance with non-orthogonal space-time block codes," in *Proc. IEEE Global Telecommun. Conference (Globecom) 2001*, vol. 2, Nov. 2001, pp. 1122–1126.

[110] O. Tirkkonen and M.Kokkonen, "Interference, information and performance in linear matrix modulation," in *Proc. IEEE Int. Symposium on Personal, Indoor and Mobile Radio Commun. (PIMRC) 2004*, vol. 1, Sept. 2004, pp. 27–32.

[111] U. Tureli, P.J.Honan, and H. Liu, "Low-complexity nonlinear least squares carrier offset estimator for OFDM: identifiability, diversity and performance," *IEEE Trans.Sig.Proc.*, vol. 52, no. 9, pp. 2441–2452, Sept. 2004.

[112] S. Verdu, *Multiuser detection.* Cambridge University Press, 1998.

[113] E. Viterbo and J.Boutros, "A universal lattice code decoder for fading channels," *IEEE Trans.Inform.Theory*, vol. 45, pp. 1639–1642, July 1999.

[114] Z. Wang and G.B.Giannakis, "Linearly precoded or coded OFDM against wireless channel fades ?" in *Proc. the 3rd Workshop on Signal Processing Advances in Wireless Commun.*, Mar. 2001, pp. 267–270.

[115] ——, "Wireless multicarrier communications: where Fourier meets Shannon," *IEEE Signal Proc.Mag.*, May 2000.

[116] Z. Wang, X.Ma, and G.B.Giannakis, "OFDM or single-carrier zero padded block transmissions," in *Proc. IEEE Wireless Commun. and Networking Conference (WCNC)*, vol. 2, Orlando, FL, Mar. 2002, pp. 660–664.

[117] Z. Wang and G. B. Giannakis, "A simple and general parameterization quantifying performance in fading channels," *IEEE Trans.Commun.*, vol. 51, no. 8, pp. 1389–1398, Aug. 2003.

[118] S. Wicker, *Error control systems for digital communication and storage.* Prentice-Hall, July.1994.

[119] J. H. Winters, J.Salz, and R.D.Gitlin, "The impact of antenna diversity on the capacity of wireless communication systems," *IEEE Trans.Commun.*, vol. 42, pp. 1740–1751, Feb. 1994.

[120] P. J. Wolniansky, C.J.Foschini, G.D.Golden, and R.A.Valenzuela, "V-BLAST: An architecture for realizing very high data rates over the rich-scattering wireless channel," in *Proc. IEEE ISSSE-98*, 1998, pp. 295–300.

[121] J. Wu and J.Ilow, "Integrated packet loss and error control schemes in wireless multimedia data links," in *Proc. IEEE Global Telecommun. Conference (Globecom) 2001*, vol. 1, Jan. 2001, pp. 685–689.

[122] J. Wu and S.D.Blostein, "Linear dispersion over time and frequency," in *Proc. IEEE Int. Conference on Commun. (ICC) 2004*, vol. 1, June 2004, pp. 254–258.

[123] J. Wu and S. D.Blostein, "High-rate codes over space, time, and frequency," in *Proc. IEEE Global Telecommun. Conference (Globecom) 2005*, vol. 6, Nov. 2005, pp. 3602–3607.

[124] ——, "Linear dispersion over space, time, and frequency," *submitted IEEE Trans.Inform.Theory*, Oct. 2005.

[125] Y. Xie, C.N.Georghiades, and K.Rohani, "Optimal bandwidth allocation for the data and feedback channels in MISO-FDD systems," *IEEE Trans.Commun.*, vol. 54, no. 2, pp. 197–203, Feb. 2006.

[126] Y. Xin, Z.Wang, and G.B.Giannakis, "Space-time diversity systems based on linear constellation precoding," *IEEE Trans.on Wireless Commun.*, vol. 2, pp. 294–309, Mar. 2003.

[127] J. Yuan, Z. Chen, B.Vucetic, and W.Firmanto, "Performance and design of space-time coding in fading channels," *IEEE Trans.Commun.*, vol. 51, no. 12, pp. 1991–1996, Dec. 2003.

[128] K. C. Zangi and L.G.Krasny, "Capacity-achieving transmitter and receiver pairs for dispersive MISO channels," *IEEE Trans.Wireless Commun.*, vol. 2, no. 6, pp. 1204–1216, Nov. 2003.

[129] J.-K. Zhang, K. M. Wong, and T. N. Davidson, "Information lossless full rate full diversity cyclotomic linear dispersion codes," in *Proc. IEEE Int. Conference on Acoustics, Speech, and Signal Proc. (ICASSP) 2004*, vol. 4, May 2004, pp. 465–468.

[130] W. Zhang, X.G.Xia, and P.C.Ching, "High-rate full-diversity space-time-frequency codes for MIMO multipath block fading channels," in *Proc. IEEE Global Telecommun. Conference (Globecom) 2005*, vol. III, Nov. 2005, pp. 1587–1591.

[131] W. Zhang, "Comments on "Maximum diversity in single-carrier frequency-domain equalization"," *IEEE Trans.Inform.Theory*, vol. 52, no. 3, pp. 1275–1277, Mar. 2006.

[132] L. Zheng and D.Tse, "Diversity and multiplexing: A fundamental tradeoff in multiple antenna channels," *IEEE Trans.Inform.Theory*, vol. 49, no. 5, pp. 1073–1096, May 2003.

[133] S. Zhou and G.B.Giannakis, "Optimal transmitter eigen-beamforming and space-time block coding based on channel correlations," *IEEE Trans.Inform.Theory*, vol. 49, no. 7, pp. 1673–1690, July 2003.

[134] W. Y. Zou and Y. Wu, "COFDM: an overview," *IEEE Trans.Broadcasting*, vol. 41, no. 1, pp. 1–8, Mar. 1995.

Appendix A

Derivations and proofs of U-LDC properties

A.1 Element expression of U-LDC dispersion matrices

Denote the (m,p) element of $\mathbf{A}^{(k,l)}$ as $\left[\mathbf{A}^{(k,l)}\right]_{m,p}$, where $\mathbf{A}^{(k,l)}$ stands for dispersion matrix $\mathbf{A}_q$, where $q = M(k-1)+l$, i.e. $\mathbf{A}^{(k,l)} = \mathbf{A}_{M(k-1)+l}$.

The elements of U-LDC matrices could be calculated as follows.

a) The case of $T \leq M$:

$$\left[\mathbf{\Pi}^a\right]_{v,p} = \delta\left(\left[v-p-a\right]\left(\mathrm{mod}M\right)\right), \tag{A.1}$$

$$\left[\mathbf{D}^b\right]_{m,u} = \delta\left(m-u\right)\exp\left(j\frac{2\pi}{T}b(m-1)\right), \tag{A.2}$$

$$\left[\mathbf{\Gamma}\right]_{u,v} = \delta\left(u-v\right), \tag{A.3}$$

$$
\begin{aligned}
&\left[\mathbf{A}^{(k,l)}\right]_{m,p} = \left[\mathbf{A}_{M(k-1)+l}\right]_{m,p} \\
&= \left[\tfrac{1}{\sqrt{T}}\mathbf{D}^{k-1}\mathbf{\Gamma}\mathbf{\Pi}^{l-1}\right]_{m,p} \\
&= \tfrac{1}{\sqrt{T}} \sum_{u=1}^{T} \sum_{v=1}^{M} \left[\begin{array}{l} \delta\left(m-u\right) \times \\ \exp\left(j\tfrac{2\pi}{T}(k-1)(m-1)\right) \times \\ \delta\left(u-v\right) \times \\ \delta\left(\left[v-p-(l-1)\right]\left(\mathrm{mod}M\right)\right) \end{array}\right] \\
&= \begin{cases} \frac{1}{\sqrt{T}}\delta\left(\left[m-p-(l-1)\right] \bmod M\right) \times \\ \exp\left(j\frac{2\pi}{T}(k-1)(m-1)\right), \\ \qquad \text{if } m=u=v \quad \text{and} \\ \left[m-p-(l-1)\right] \bmod M = 0; \\ \qquad 0, \text{otherwise.} \end{cases}
\end{aligned}
\tag{A.4}
$$

b) The case of $T > M$:

Through a similar derivation to that in (A.4),

$$
\begin{aligned}
&\left[\mathbf{A}^{(k,l)}\right]_{m,p} = \\
&= \begin{cases} \qquad \text{if } u=v=p \quad \text{and} \\ \left[m-p-(k-1)\right]\left(\mathrm{mod}T\right)=0, \\ \frac{1}{\sqrt{M}}\delta\left(\left[m-p-(k-1)\right]\left(\mathrm{mod}T\right)\right)\exp\left(j\frac{2\pi}{M}(l-1)(p-1)\right), \\ \qquad \text{otherwise}, 0 \end{cases}
\end{aligned}
\tag{A.5}
$$

A.2 Proof of Property 1

Proof: Denote $[\mathbf{G}_{LDC}]_{r,q}$ as the (r,q) element of $\mathbf{G}_{LDC}$, where $r,q = 1,\cdots,TM$. Further, r can be determined by the pair (m,p) , and q is determined by the pair (k,l). Thus we also denote $[\mathbf{G}_{LDC}]_{(m,p),(k,l)} = [\mathbf{G}_{LDC}]_{r,q}$. We know $\mathbf{G}_{LDC} = [vec(\mathbf{A}_1), ..., vec(\mathbf{A}_Q)]$. Note that q is also the index of $\mathbf{A}_q$.

We have the following relations,

$$r = T(m-1) + p, q = M(k-1) + l,$$

$$\begin{aligned}
l &= [[q-1]\,(\mathrm{mod}M)] + 1, \\
k &= [[q - [[q-1]\,(\mathrm{mod}M)] - 1]\,(\mathrm{mod}M)] + 1, \\
p &= [[r-1]\,(\mathrm{mod}T)] + 1, \\
m &= [[r - [[r-1]\,(\mathrm{mod}T)] - 1]\,(\mathrm{mod}T)] + 1.
\end{aligned}$$

Now we are ready to calculate $\left[\mathbf{G}_{LDC}\left[\mathbf{G}_{LDC}\right]^{\mathcal{H}}\right]_{r,q}$. In the calculation, the elements of $\mathbf{G}_{LDC}$ have index pair $(m_1, p_1), (k, l)$, and the elements of $[\mathbf{G}_{LDC}]^{\mathcal{H}}$ have index pair $(m_2, p_2), (k, l)$.

a) the case of $T \leq M$: From (A.4),

$$\begin{aligned}
&\left[\mathbf{G}_{LDC}\left[\mathbf{G}_{LDC}\right]^{\mathcal{H}}\right]_{r,q} = \\
&\frac{1}{T}\sum_{\substack{(m_1,p_1),\\(m_2,p_2),\\(k,l)}} \left[\begin{array}{l}
\delta\left([m_1 - p_1 - (l-1)]\,(\mathrm{mod}M)\right) \times \\
\exp\left(j\frac{2\pi}{T}(k-1)(m_1-1)\right) \times \\
\delta\left([m_2 - p_2 - (l-1)]\,(\mathrm{mod}M)\right) \times \\
\exp\left(-j\frac{2\pi}{T}(k-1)(m_2-1)\right)
\end{array}\right] \\
&= \begin{cases}
\frac{1}{T}\delta\left([m_1 - p_1 - (l-1)]\,(\mathrm{mod}M)\right) \times \\
\delta\left([m_2 - p_2 - (l-1)]\,(\mathrm{mod}M)\right) \times \\
\sum_{k=1}^{T}\left[\exp\left(j\frac{2\pi}{T}(m_1 - m_2)\,[k-1]\right)\right], \\
\text{if } [m_1 - p_1 - (l-1)]\,(\mathrm{mod}M) = 0 \\
\text{and} \\
[m_2 - p_2 - (l-1)]\,(\mathrm{mod}M) = 0; \\
0, \text{otherwise.}
\end{cases}
\end{aligned} \tag{A.6}$$

The above expression (A.6) tells us that $\left[\mathbf{G}_{LDC}\left[\mathbf{G}_{LDC}\right]^{\mathcal{H}}\right]_{r,q} \neq 0$, more clearly

$\left[\mathbf{G}_{LDC}\left[\mathbf{G}_{LDC}\right]^{\mathcal{H}}\right]_{r,q} = 1$, if and only if $(m_1, p_1) = (m_2, p_2)$, in other words, $r = q$. Thus $\mathbf{G}_{LDC}\left[\mathbf{G}_{LDC}\right]^{\mathcal{H}} = \mathbf{I}_{TM}$. Similarly, we could obtain $\left[\mathbf{G}_{LDC}\right]^{\mathcal{H}}\mathbf{G}_{LDC} = \mathbf{I}_{TM}$.

b) The proof of the case of $T > M$ is similar, and details are omitted.

Thus, $\mathbf{G}_{LDC}$ is unitary for arbitrary T and M. ■

A.3 Derivation of $\mathbf{A}_{q_1}\left[\mathbf{A}_{q_2}\right]^{\mathcal{H}}$ and $\left[\left[\mathbf{A}_{q_1}\right]^{\mathcal{H}}\mathbf{A}_{q_2}\right]$

To derive $\mathbf{A}_{q_1}\left[\mathbf{A}_{q_2}\right]^{\mathcal{H}}$, denote the (m,p) element of $\mathbf{A}_{q_1}$ as $\left[\mathbf{A}_{q_1}\right]_{m,p}$, and denote the (p,r) element of $\left[\mathbf{A}_{q_2}\right]^{\mathcal{H}}$ as $\left[\left[\mathbf{A}_{q_2}\right]^{\mathcal{H}}\right]_{p,r}$,

a) the case of $T \leq M$:

$$\begin{aligned}
&\left[\mathbf{A}_{q_1}\left[\mathbf{A}_{q_2}\right]^{\mathcal{H}}\right]_{m,r} = \left[\mathbf{A}^{(k_1,l_1)}\left[\mathbf{A}^{(k_2,l_2)}\right]^{\mathcal{H}}\right]_{m,r} = \\
&\frac{1}{T}\sum_{p=1}^{M}\begin{bmatrix}
\delta\left(\left[m-p-(l_1-1)\right](\mathrm{mod}M)\right)\times \\
\exp\left(j\frac{2\pi}{T}(k_1-1)(m-1)\right)\times \\
\delta\left(\left[r-p-(l_2-1)\right](\mathrm{mod}M)\right)\times \\
\exp\left(-j\frac{2\pi}{T}(k_2-1)(r-1)\right)
\end{bmatrix} \\
&= \begin{cases}
\frac{1}{T}\delta\left(\left[m-p-(l_1-1)\right](\mathrm{mod}M)\right)\times \\
\delta\left(\left[r-p-(l_2-1)\right](\mathrm{mod}M)\right)\times \\
\exp\left(j\frac{2\pi}{T}\left[(k_1-1)(m-1)-(k_2-1)(r-1)\right]\right), \\
\text{if } \left[m-p-(l_1-1)\right](\mathrm{mod}M)=0 \\
\text{and} \\
\left[r-p-(l_2-1)\right](\mathrm{mod}M)=0; \\
0, \text{otherwise.}
\end{cases}
\end{aligned} \tag{A.7}$$

b) the case of $T > M$:

The derivation of of the case of $T > M$ is similar to that of the case of $T \leq M$, thus details are omitted.

To calculate $\left[\left[\mathbf{A}_{q_1}\right]^{\mathcal{H}} \mathbf{A}_{q_2}\right]$, denote the (s,m) element of $\mathbf{A}_{q_1}$ as $\left[\left[\mathbf{A}_{q_1}\right]^{\mathcal{H}}\right]_{s,m}$, and denote the (m,t) element of $\left[\mathbf{A}_{q_2}\right]^{\mathcal{H}}$ as $\left[\mathbf{A}_{q_2}\right]_{m,t}$.

a) the case of $T \leq M$:

$$\begin{aligned}
&\left[\left[\mathbf{A}_{q_1}\right]^{\mathcal{H}} \mathbf{A}_{q_2}\right]_{s,t} = \left[\left[\mathbf{A}^{(k_1,l_1)}\right]^{\mathcal{H}} \mathbf{A}^{(k_2,l_2)}\right]_{s,t} = \\
&\frac{1}{T}\sum_{m=1}^{T}\left[\begin{array}{l}
\delta\left(\left[m-s-(l_1-1)\right](\mathrm{mod}M)\right)\times \\
\exp\left(-j\frac{2\pi}{T}(k_1-1)(m-1)\right)\times \\
\delta\left(\left[m-t-(l_2-1)\right](\mathrm{mod}M)\right)\times \\
\exp\left(j\frac{2\pi}{T}(k_2-1)(m-1)\right)
\end{array}\right] \\
&= \left\{\begin{array}{l}
\frac{1}{T}\delta\left(\left[m-s-(l_1-1)\right](\mathrm{mod}M)\right)\times \\
\delta\left(\left[m-t-(l_2-1)\right](\mathrm{mod}M)\right)\times \\
\exp\left(j\frac{2\pi}{T}\left[(k_2-k_1)(m-1)\right]\right), \\
\text{if } \left[m-s-(l_1-1)\right](\mathrm{mod}M)=0 \\
\text{and} \\
\left[m-t-(l_2-1)\right](\mathrm{mod}M)=0; \\
0, \text{otherwise.}
\end{array}\right.
\end{aligned} \tag{A.8}$$

b) the case of $T > M$:

The derivation of of the case of $T > M$ is similar, and details are omitted.

A.4 Proof of Property 2

Proof: We know if $q_1 = q_2 = q$, then $k_1 = k_2, l_1 = l_2$. From (A.8), we know that, if $T \leq M$, the diagonal elements of $\left[\mathbf{A}_q\right]^{\mathcal{H}} \mathbf{A}_q$ consist of T entries of $\frac{1}{T}$ and

$M-T$ entries of zero. Thus, if $T \leq M$, $Tr\left[\left[\mathbf{A}_q\right]^{\mathcal{H}} \mathbf{A}_q\right] = \frac{TM}{Q} = 1$ holds. If $T = M$, $\left[\mathbf{A}_q\right]^{\mathcal{H}} \mathbf{A}_q = \frac{1}{M}\mathbf{I}_M$.

Similarly, we can prove the case of $T > M$. Thus both (4.3) and (4.4) hold.

■

A.5 Proof of Property 3

Proof: We know

$$Tr\left[vec(\mathbf{A}_p)\left[vec(\mathbf{A}_q)\right]^{\mathcal{H}}\right] = \left[vec(\mathbf{A}_q)\right]^{\mathcal{H}} vec(\mathbf{A}_p). \tag{A.9}$$

In Property 1, we have already proven that $\mathbf{G}_{LDC} = [vec(\mathbf{A}_1), ..., vec(\mathbf{A}_{TM})]$ is unitary. Thus the different columns of $\mathbf{G}_{LDC}$ are orthogonal, thus $\left[vec(\mathbf{A}_q)\right]^{\mathcal{H}} vec(\mathbf{A}_p) = 0$ for any $1 \leq p \neq q \leq TM$.

Then we have $Tr\left[vec(\mathbf{A}_p)\left[vec(\mathbf{A}_q)\right]^{\mathcal{H}}\right] = 0$ for any $1 \leq p \neq q \leq TM$. ■

A.6 Proof of Property 4

Proof: We know $q_1 \neq q_2$, then $(k_1, l_1) \neq (k_1, l_1)$. Now we derive $Tr\left[\left[\mathbf{A}_{q_1}\right]^{\mathcal{H}} \mathbf{A}_{q_2}\right] = \sum_{s=1}^{M}\left[\left[\mathbf{A}_{q_1}\right]^{\mathcal{H}} \mathbf{A}_{q_2}\right]_{s,s}$.

a) the case of $T \leq M$: From (A.8), we get

$$\left[\left[\mathbf{A}_{q_1}\right]^{\mathcal{H}} \mathbf{A}_{q_2}\right]_{s,s} = \frac{1}{T}\sum_{m=1}^{T}\begin{bmatrix} \delta\left(\left[m-s-(l_1-1)\right](\mathrm{mod}\, M)\right) \times \\ \delta\left(\left[m-s-(l_2-1)\right](\mathrm{mod}\, M)\right) \times \\ \exp\left(j\frac{2\pi}{T}\left[(k_2-k_1)(m-1)\right]\right) \end{bmatrix}.$$

a. If $l_1 \neq l_2$, obviously

$$\delta\left(\left[m-s-(l_1-1)\right]\left(\mathrm{mod}M\right)\right)\times$$
$$\delta\left(\left[m-s-(l_2-1)\right]\left(\mathrm{mod}M\right)\right)=0$$

then

$$\left[\left[\mathbf{A}_{q_1}\right]^{\mathcal{H}}\mathbf{A}_{q_2}\right]_{s,s}=0.$$

Thus

$$Tr\left[\left[\mathbf{A}_{q_1}\right]^{\mathcal{H}}\mathbf{A}_{q_2}\right]=0.$$

b. If $l_1 = l_2$, then $k_1 \neq k_2$, only T terms of $\left[\left[\mathbf{A}_{q_1}\right]^{\mathcal{H}}\mathbf{A}_{q_2}\right]_{s,s}$ are non-zero. $Tr\left[\left[\mathbf{A}_{q_1}\right]^{\mathcal{H}}\mathbf{A}_{q_2}\right]$ could be written as

$$Tr\left[\left[\mathbf{A}_{q_1}\right]^{\mathcal{H}}\mathbf{A}_{q_2}\right]=\frac{1}{T}\sum_{u=a}^{a+T-1}\exp\left(j\frac{2\pi}{T}\left[(k_2-k_1)u\right]\right)=0$$

where a is a positive integer.

b) the case of $T > M$:

The proof of the case of $T > M$ is similar, and details are omitted.

Similarly, $Tr\left(\mathbf{A}_{q_1}\left[\mathbf{A}_{q_2}\right]^{\mathcal{H}}\right)=0.$ ■

A.7 Proof of Property 5

Proof:

Assume two different U-LDC codewords $\mathbf{S}_{LDC}$ and $\widetilde{\mathbf{S}}_{LDC}$ encode the same $(Q-1)$ data source symbols and one different data source symbol s_g and $\widetilde{s_g}$ respectively, where $s_g - \widetilde{s_g} \neq 0$ and $g = 1, ..., Q$

Thus, the difference of $\mathbf{S}_{LDC}$ and $\widetilde{\mathbf{S}_{LDC}}$ is

$$\Delta_g = \mathbf{S}_{LDC} - \widetilde{\mathbf{S}}_{LDC} = \left\{ \left[\sum_{q=1, q\neq g}^{Q} s_q \mathbf{A}_q \right] + s_g \mathbf{A}_g \right\} - \left\{ \left[\sum_{q=1, q\neq g}^{Q} s_q \mathbf{A}_q \right] + \widetilde{s_g} \mathbf{A}_g \right\}$$

$$= (s_g - \widetilde{s_g})\, \mathbf{A}_g.$$

The symbolwise diversity order is

$$r = \min \{ rank(\Delta_g), g = 1, ..., Q \} = \min \{ rank(\mathbf{A}_g), g = 1, ..., Q \}.$$

Thus, the proof is completed if all the $rank(\mathbf{A}_g)$ are computed for $g = 1, ..., Q$.

a) the case of $T \leq M$: From the proof of Property 2, we know that the diagonal elements of $[\mathbf{A}_g]^{\mathcal{H}} \mathbf{A}_g$ consist of T entries of $\frac{1}{T}$ and $M - T$ entries of zero. From (A.8), it is easy to determine that all non-diagonal elements of $[\mathbf{A}_g]^{\mathcal{H}} \mathbf{A}_g$ are zero. Thus,

$$rank([\mathbf{A}_g]^{\mathcal{H}} \mathbf{A}_g) = T.$$

Hence,

$$rank(\mathbf{A}_g) = rank([\mathbf{A}_g]^{\mathcal{H}} \mathbf{A}_g) = T,$$

where $g = 1, ..., Q$.

b) the case of $T > M$:

Similarly to the case of $T \leq M$, we can prove

$$rank(\mathbf{A}_g) = rank([\mathbf{A}_g]^{\mathcal{H}} \mathbf{A}_g) = M,$$

where $g = 1, ..., Q$.

Finally, The symbolwise diversity order is obtained as

$$r = \min \{ rank(\mathbf{A}_g), g = 1, ..., Q \} = \min \{ T, M \}.$$

■

Appendix B

Proof of Theorem 3

Proof:

(1) of Theorem 3 has been discussed in previous parts of Section 5.5. (4) of Theorem 3 is a straightforward result if (2) or (3) is given. Hence, only the proofs of (2) and (3) of Theorem 3 are given.

Note that $\left(\mathbf{M}^{(i)} - \tilde{\mathbf{M}}^{(i)}\right)$ is of size $TN_{F(i)} \times TN_{F(i)}$. Therefore the condition (5.54) ensures

$$rank\left(\left[\left(\mathbf{M}^{(i)} - \tilde{\mathbf{M}}^{(i)}\right)\right]\right) = TN_{F(i)}.$$

Accordingly,

$$\begin{aligned} rank(\mathbf{\Lambda}_{(i)}) &= rank\left(\left(\mathbf{M}^{(i)} - \tilde{\mathbf{M}}^{(i)}\right)\mathbf{R}_{\mathbf{H}^{(i)}}\left(\mathbf{M}^{(i)} - \tilde{\mathbf{M}}^{(i)}\right)^{\mathcal{H}}\right) \\ &= rank\left(\mathbf{R}_{\mathbf{H}^{(i)}}\left(\mathbf{M}^{(i)} - \tilde{\mathbf{M}}^{(i)}\right)^{\mathcal{H}}\right) \\ &= rank\left(\mathbf{R}_{\mathbf{H}^{(i)}}\right). \end{aligned} \tag{B.1}$$

So (2) of Theorem is proved.

If both $N_{F(i)} = L + 1$ and $rank(\mathbf{R}_{\mathbf{H}^{(i)}}) = T(L+1)$ hold, to achieve $rank(\mathbf{\Lambda}_{(i)}) = T(L+1)$, it is necessary to have

$$\begin{aligned} T(L+1) &= rank\left(\left(\mathbf{M}^{(i)} - \tilde{\mathbf{M}}^{(i)}\right)\mathbf{R}_{\mathbf{H}^{(i)}}\left(\mathbf{M}^{(i)} - \tilde{\mathbf{M}}^{(i)}\right)^{\mathcal{H}}\right) \\ &\leq rank\left(\left(\mathbf{M}^{(i)} - \tilde{\mathbf{M}}^{(i)}\right)\right). \end{aligned}$$

However, $\left(\mathbf{M}^{(i)} - \tilde{\mathbf{M}}^{(i)}\right)$ is of size $T(L+1) \times T(L+1)$ in this case. Hence, (5.54) is a necessary condition. Conversely, using the result of (2) of Theorem 3, $rank(\mathbf{\Lambda}_{(i)}) = rank\left(\mathbf{R}_{\mathbf{H}^{(i)}}\right) = T(L+1)$. So (3) of Theorem 3 is proven. ■

Appendix C

Proof of Theorem 4

Proof:

1) Note that $\mathbf{M}-\tilde{\mathbf{M}}$ is a diagonal matrix. Thus, to maximize rank of $\mathbf{M}-\tilde{\mathbf{M}}$, the necessary and sufficient condition is that all the diagonal elements are non-zero. Thus, to ensure $rank\left(\mathbf{M}-\tilde{\mathbf{M}}\right)=N_CT$, it is necessary and sufficient to have $c_p^{(k)}-\widetilde{c_p^{(k)}}\neq 0, p=1,...,N_C, k=1,...,T$.

   Recall $c_p^{(k)}=\left[\mathbf{z}_{CP-SC}^{(k)}\right]_{p,1}$ and $\mathbf{z}_{CP-SC}^{(k)}=\mathbf{F}_{Nc}\mathbf{x}_{SC}^{(k)}$, where $p=1,...,N_C$ and $k=1,...T$.

   Hence, the necessary and sufficient condition is

$$\left[\mathbf{z}_{CP-SC}^{(k)}-\widetilde{\mathbf{z}}_{CP-SC}^{(k)}\right]_{p,1}=\left[\mathbf{F}_{Nc}\left(\mathbf{x}_{SC}^{(k)}-\widetilde{\mathbf{x}}_{SC}^{(k)}\right)\right]_{p,1}\neq 0,$$

   where $p=1,...,N_C$ and $k=1,...T$.

2) Note that the condition is that the rank of frequency domain matrix satisfies $rank\left(\mathbf{M}-\tilde{\mathbf{M}}\right)=N_CT$.

Using the same strategy in the derivation of (B.1) and (5.49), we get

$$\begin{aligned} rank(\mathbf{\Lambda}) &= rank\left(\left(\mathbf{M}-\tilde{\mathbf{M}}\right)\mathbf{R_H}\left(\mathbf{M}-\tilde{\mathbf{M}}\right)^{\mathcal{H}}\right) \\ &= rank\left(\mathbf{R_H}\left(\mathbf{M}-\tilde{\mathbf{M}}\right)^{\mathcal{H}}\right) \\ &= rank\left(\mathbf{R_H}\right) \end{aligned} \tag{C.1}$$

where

$$\begin{aligned} \mathbf{R_H} &= E\left\{\left(\mathbf{I}_T\otimes\mathbf{W}\right)\mathbf{h}\left[\left(\mathbf{I}_T\otimes\mathbf{W}\right)\mathbf{h}\right]^{\mathcal{H}}\right\} \\ &= \left[\mathbf{I}_T\otimes\mathbf{W}\right]\mathbf{\Phi}\left[\mathbf{I}_T\otimes\left[\mathbf{W}\right]^{\mathcal{H}}\right] \qquad , \end{aligned} \tag{C.2}$$

where $\mathbf{\Phi} = E\left\{\mathbf{h}\left[\mathbf{h}\right]^{\mathcal{H}}\right\}$, $\mathbf{W} = \left[\mathbf{w}_1,\cdots,\mathbf{w}_{N_C}\right]^{\mathcal{T}}$, and $\mathbf{h} = \left[\left[\mathbf{h}^{(1)}\right]^{\mathcal{T}},\cdots,\left[\mathbf{h}^{(T)}\right]^{\mathcal{T}}\right]^{\mathcal{T}}$. Note that (B.1) and (5.49) have similar forms as (C.1) and (C.2). However, their matrix sizes are different. The frequency domain symbols in LDC-SCM are the results of size N_C Fourier transformation of source symbols, and thus the size of $\mathbf{M}$ must be $N_CT\times N_CT$. Note that the size of frequency-time block $\mathbf{M}^{(i)}$ of LDC-OFDM is $TN_{F(i)}\times TN_{F(i)}$, where $N_{F(i)}$ is usually much less than N_C.

Further, the product design criterion for CP-SCCB is that the minimum of products,

$$\begin{aligned} \Delta &= \prod_{k=1}^{T}\prod_{p=1}^{N_C}\left(\left|c_p^{(k)}-\widetilde{c_p^{(k)}}\right|^2\right) \\ &= \prod_{k=1}^{T}\prod_{p=1}^{N_C}\left|\left[\mathbf{F}_{Nc}\mathbf{x}_{SC}^{(k)}\right]_{p,1}-\left[\mathbf{F}_{Nc}\widetilde{\mathbf{x}}_{SC}^{(k)}\right]_{p,1}\right|^2, \end{aligned}$$

taken over distinct codewords must be maximized.

■

Appendix D

Proofs of results related to error union bound

D.1 Outline of the proof of Lemma 1

When two complex source symbol sequences differ in positions $\{q_1, ..., q_{K+1}\}$, the squared pairwise Euclidean distance is

$$\begin{aligned}\mathcal{D}_{a,b}^{(K+1)} &= \sum_{u=1}^{K+1}\left[\Omega_{q_u,q_u}\left|e_{q_u}^{(a,b)}\right|^2\right] + 2\,\mathrm{Re}\left\{\sum_{u=1}^{K+1}\sum_{u<v}^{K+1}\left[\Omega_{q_u,q_v}\left[e_{q_u}^{(a,b)}\right]^* e_{q_v}^{(a,b)}\right]\right\} \\ &= \mathcal{D}_{a,b}^{(K)} + \Omega_{q_{K+1},q_{K+1}}\left|e_{q_{K+1}}^{(a,b)}\right|^2 + 2\,\mathrm{Re}\left\{e_{q_{K+1}}^{(a,b)}\sum_{u=1}^{K}\left(\Omega_{q_u,q_{K+1}}\left[e_{q_u}^{(a,b)}\right]^*\right)\right\}.\end{aligned} \tag{D.1}$$

There are two possible $e_{q_{K+1}}^{(a,b)}$, either $e_{q_{K+1}}^{(a,b)} = x_{K+1} + jy_{K+1}$ or $e_{q_{K+1}}^{(a,b)} = -x_{K+1} - jy_{K+1}$. Note that if there is a pair of complex source symbols, $s_{q_{K+1}}^{(a)} = \alpha_{q_{K+1}}^{(a)} + j\beta_{q_{K+1}}^{(a)}$ and $s_{q_{K+1}}^{(b)} = \alpha_{q_{K+1}}^{(b)} + j\beta_{q_{K+1}}^{b)}$, the differences $e_{q_{K+1}}^{(a,b)}$ and $e_{q_{K+1}}^{(b,a)}$ are $e_{q_{K+1}}^{(a,b)} = \left(\alpha_{q_{K+1}}^{(a)} - \alpha_{q_{K+1}}^{(b)}\right) + j\left(\beta_{q_{K+1}}^{(a)} - \beta_{q_{K+1}}^{(b)}\right)$ and $e_{q_{K+1}}^{(b,a)} = -\left(\alpha_{q_{K+1}}^{(a)} - \alpha_{q_{K+1}}^{(b)}\right) - j\left(\beta_{q_{K+1}}^{(a)} - \beta_{q_{K+1}}^{(b)}\right)$, respectively. By symmetry, the number of different sequences with $e_{q_{K+1}}^{(a,b)} = x_{K+1} + jy_{K+1}$ is the same as the number of different sequences with $e_{q_{K+1}}^{(a,b)} = -x_{K+1} - jy_{K+1}$. Denote this number as n_{K+1}.

Let $\sum_{u=1}^{K}\left(\Omega_{q_u,q_{K+1}}\left[e_{q_u}^{(a,b)}\right]^*\right)=x_{1\leftrightarrow K}+jy_{1\leftrightarrow K}$. Note that

$$\tau_{K+1}\big|_{e_{q_{K+1}}^{(a,b)}=x_{K+1}+jy_{K+1}}=\left[e_{q_{K+1}}^{(a,b)}\sum_{u=1}^{K}\left(\Omega_{q_u,q_{K+1}}\left[e_{q_u}^{(a,b)}\right]^*\right)\right]\Bigg|_{e_{q_{K+1}}^{(a,b)}=x_{K+1}+jy_{K+1}}$$

$$=(x_{K+1}+jy_{K+1})(x_{1\leftrightarrow K}+jy_{1\leftrightarrow K})$$

$$=x_{K+1}x_{1\leftrightarrow K}-y_{K+1}y_{1\leftrightarrow K}+j(x_{1\leftrightarrow K}y_{K+1}+x_{K+1}y_{1\leftrightarrow K})$$

and

$$\Delta_2=\left[\frac{\rho}{2}\operatorname{Re}\left\{e_{q_{K+1}}^{(a,b)}\sum_{u=1}^{K}\left(\Omega_{q_u,q_{K+1}}\left[e_{q_u}^{(a,b)}\right]^*\right)\right\}\right]\Bigg|_{e_{q_{K+1}}^{(a,b)}=x_{K+1}+jy_{K+1}}.$$

Denote $\Delta_1=\frac{\rho}{2}\left[\mathcal{D}_{a,b}^{(K)}+\Omega_{q_{K+1},q_{K+1}}\left|e_{q_{K+1}}^{(a,b)}\right|^2\right]$ and

$$\Delta_2=\left[\frac{\rho}{2}\operatorname{Re}\left\{e_{q_{K+1}}^{(a,b)}\sum_{u=1}^{K}\left(\Omega_{q_u,q_{K+1}}\left[e_{q_u}^{(a,b)}\right]^*\right)\right\}\right]\Bigg|_{e_{q_u}^{(a,b)}=x_{K+1}+jy_{K+1}}.$$

Thus,

$$\left[\frac{2}{\rho}\mathcal{D}_{a,b}^{(K+1)}\right]\Bigg|_{e_{q_{K+1}}^{(a,b)}=x_{K+1}+jy_{K+1}}=\Delta_1+\Delta_2 \tag{D.2}$$

and

$$\left[\frac{2}{\rho}\mathcal{D}_{a,b}^{(K+1)}\right]\Bigg|_{e_{q_{K+1}}^{(a,b)}=-x_{K+1}-jy_{K+1}}=\Delta_1-\Delta_2. \tag{D.3}$$

The contribution to the error union bound from the $2n_{K+1}$ sequences with $e_{q_u}^{(a,b)}=\pm(x_{K+1}+jy_{K+1})$ at the position q_{K+1} can be written as

$$g=\frac{n_{K+1}}{N_B}\left[Q\left(\Delta_1+\Delta_2\right)+Q\left(\Delta_1-\Delta_2\right)\right]. \tag{D.4}$$

Since this holds for any $e_{q_u}^{(a,b)}$, q_u, $1\leqslant u\leqslant K$ and K, Lemma 1 holds.

D.2 Proof of Theorem 5

Proof: From Proposition 1, to minimize the union bound conditioned on $\mathbf{H}_U$, the optimality condition is $\Omega_{p,q} = 0$ for any $1 \leq p \neq q \leq Q$. We calculate the expectation of $\Omega_{p,q}$ over $\mathbf{H}_U$. The suboptimal condition is to try to make $E_{\mathbf{H}_U}[\Omega_{p,q}]$ as small as possible, although it may not be zero.

Denote $\psi^{(p,q)} = vec(\mathbf{A}_p)[vec(\mathbf{A}_q)]^{\mathcal{H}}$, and $\left[\psi^{(p,q)}\right]_{u,v}, u, v = 1, \cdots, TM$, is the (u,v)-th element of $\psi^{(p,q)}$. Note that, observing the structure of $\mathbf{H}_U$, we know that the number of rows of $\mathbf{H}_U$ is a multiple of T. Denote $[\mathbf{H}_U]_{(u,v)}, u, = 1, ..., KT, v = 1, ..., TM$ as the (u,v) element of $\mathbf{H}_U$, where K is a positive integer.

Now we calculate channel average $\Omega_{p,q}$ as

$$\begin{aligned}
&\mathbb{E}_{\mathbf{H}_U}\{\Omega_{p,q}\} = \mathbb{E}_{\mathbf{H}_U}\left\{\left[Tr\left(\mathbf{H}_U vec(\mathbf{A}_p)[vec(\mathbf{A}_q)]^{\mathcal{H}}[\mathbf{H}_U]^{\mathcal{H}}\right)\right]\right\} \\
&= \mathbb{E}_{\mathbf{H}_U}\left\{\left[Tr\left(\mathbf{H}_U \psi^{(p,q)}[\mathbf{H}_U]^{\mathcal{H}}\right)\right]\right\} \\
&= \mathbb{E}_{\mathbf{H}_U}\left\{\left[Tr\left(\sum_{r=1}^{K}\sum_{u=1}^{TM}\sum_{v=1}^{TM}\left[[\mathbf{H}_U]_{r,v}\right]^{*}[\mathbf{H}_U]_{r,u}\left[\psi^{(p,q)}\right]_{u,v}\right)\right]\right\} \\
&= \Lambda_{uu} + \Lambda_{uv},
\end{aligned} \tag{D.5}$$

where

$$\Lambda_{uu} = \sum_{r=1}^{KT}\sum_{u=1}^{TM}\left[\mathbb{E}_{[\mathbf{H}_U]_{r,u}}\left\{\left[[\mathbf{H}_U]_{r,u}\right]^{*}[\mathbf{H}_U]_{r,u}\right\}\left[\psi^{(p,q)}\right]_{u,u}\right]$$

and

$$\Lambda_{uv} = \sum_{r=1}^{KT}\sum_{u=1}^{TM}\sum_{v\neq u}^{TM}\left[\mathbb{E}_{[\mathbf{H}_U]_{r,u}}\left\{\left[[\mathbf{H}_U]_{r,v}\right]^{*}[\mathbf{H}_U]_{r,u}\right\}\left[\psi^{(p,q)}\right]_{u,v}\right].$$

Since the term Λ_{uu} with self-correlation or variance of subcarriers dominates the summation, Λ_{uu} dominates Λ_{uv}. We try to make $\Lambda_{uu} = 0$. Assume the auto correlation of any channel element $[\mathbf{H}_U]_{r,u}$ are the same. Assume $\mathbb{E}_{[\mathbf{H}_U]_{r,u}}\left\{\left[[\mathbf{H}_U]_{r,u}\right]^{*}[\mathbf{H}_U]_{r,u}\right\} = \sigma$ if $\mathbb{E}_{[\mathbf{H}_U]_{r,u}}\left\{\left[[\mathbf{H}_U]_{r,u}\right]^{*}[\mathbf{H}_U]_{r,u}\right\} \neq 0$, We expect $\Lambda_{uu} = 0$. Denote $\mathbf{J} = \mathbb{E}_{\mathbf{H}_U}\{[\mathbf{H}_U]^{*}\mathbf{H}_U\}$,

and $[\mathbf{J}]_{r,u}$ is the (r,u) element of $\mathbf{J}$, then

$$[\mathbf{J}]_{r,u} = \begin{cases} \sigma, \text{ if } u = r(\text{mod}T) + mT; \\ 0, \text{ if } u \neq r(\text{mod}T) + mT. \end{cases}$$

We obtain

$$\begin{aligned} \Lambda_{uu} &= \sum_{r=1}^{KT} \sum_{\substack{u=r(\bmod T)+mT \\ m=1,\ldots,M}} [\mathbf{J}]_{r,u} \left[\psi^{(p,q)}\right]_{u,u} \\ &= \sigma \sum_{r=1}^{KT} \sum_{\substack{u=r(\bmod T)+(m-1)T \\ m=1,\ldots,M}} \left[\psi^{(p,q)}\right]_{u,u} \\ &= K\left[Tr\left(\psi^{(p,q)}\right)\right] = 0. \end{aligned}$$

Thus we have the condition for minimizing the part of the union bound P_U related to the auto-correlation of the parallel channels based on averaged channel realizations

$$Tr\left[vec(\mathbf{A}_p)\left[vec(\mathbf{A}_q)\right]^{\mathcal{H}}\right] = 0.$$

■

Appendix E

Proof of Proposition 2

Proof:

1) Since

   a. all-zero data source vectors are allowed for the first stage LDC encoding,

   b. the first LDC encoding procedure enables full diversity in their 2-dimensions,

   c. $N_X < N_Y = T$,

   except for the all-zero first stage LDC codewords, each column of first stage LDC codewords of size $T \times N_X$ must have at least one non-zero element. Note that the source symbols of the corresponding a-th second LDC codeword consists of all n_Y-th X dimension columns of N_Y first LDC codewords, where $1 \leqslant n_Y \leqslant N_Y$. Thus the number of non-zero source symbols of each second LDC codeword is not less than N_Y unless all-zero first stage LDC codewords are involved as source symbols for the second stage LDC encoding.

   Using the condition that the first LDC encoding procedure enables full diversity in their 2-dimensions, the per dimension diversity orders of Y and time

dimensions satisfy

$$r_{d(Time)} = r_{d(Y)} = T = N_Y.$$

2) In this case, there is only one source symbol difference between a pair of 3-D codewords. Note that the whole DLD procedure can be considered as a single linear transformation, i.e., a multiplication between a matrix $\mathbf{G}_{STF}$ of size $N_X N_Y T \times Q N_Y$ and a source symbol vector of size $1 \times Q N_Y$. Assume that the pair of source symbol vectors of size $1 \times Q N_Y$ with only one symbol difference are $\mathbf{s}_{STF}$ and $\widetilde{\mathbf{s}_{STF}}$. The pairwise difference of two DLD codewords can be calculated by

$$\begin{aligned} \Psi &= \mathbf{G}_{STF}\mathbf{s}_{STF} - \mathbf{G}_{STF}\widetilde{\mathbf{s}_{STF}} \\ &= \mathbf{G}_{STF}\left(\mathbf{s}_{STF} - \widetilde{\mathbf{s}_{STF}}\right) \\ &= \mathbf{G}_{STF}\theta_{sw}, \end{aligned} \tag{E.1}$$

where θ_{sw} is the same as an all-zero vector except in the a single b-th position, where $1 \leqslant b \leqslant Q N_Y$. Since full symbol-wise diversity is determined by rank properties of difference of pairwise codewords, the rest of the discussion will only consider the coded STF block which is encoded using an all-zero source vector except a single non-zero source element, and the rank properties of this coded STF block is similar to the rank properties of the difference of a pair of STF blocks with only a single source element difference.

Without loss of generality, assume that all the source symbols for the N_Y first stage LDC codewords except the only non-zero element at the q-th position of source symbol vector $\mathbf{s}_{n_{Y(NZ)}}$ of size $1 \times Q$ for the $n_{Y(NZ)}$-th first stage LDC codeword are zero elements, where $1 \leqslant q \leqslant Q$ and $1 \leqslant n_{Y(NZ)} \leqslant N_Y$.

Note that

a. The case considered is either $N_X < N_Y = T$ or $N_X = T > N_Y$,

b. All the encoding matrices of the second stage LDCs are the same. The dispersion matrices of the second stage LDC is $\mathbf{A}_q^{(2)}$, where $q = 1, ..., N_Y T$. The LDC encoding matrices is denoted as

$$\mathbf{G}_{LDC}^{(2)} = \left[vec(\mathbf{A}_1^{(2)}), ..., vec(\mathbf{A}_{N_Y T}^{(2)}) \right], \tag{E.2}$$

which is also can be expressed as

$$\mathbf{G}_{LDC}^{(2)} = \begin{bmatrix} \mathbf{J}_{(1,1)} & \cdots & \mathbf{J}_{(1,N_Y)} \\ \vdots & \ddots & \vdots \\ \mathbf{J}_{(N_Y,1)} & \cdots & \mathbf{J}_{(N_Y,N_Y)} \end{bmatrix}, \tag{E.3}$$

where $\mathbf{J}_{(a,b)}$ is defined in (8.3).

Denote the n_X-th time dimension vector of size $1 \times T$ in the n_Y-th X-time plane after the i-th stage LDC encoding as $\mathbf{s}_{(n_Y)}^{(i,n_X)}$, where $i = 1, 2$.

Denote the coded symbol vector in the n_X-th Y-time plane after the i-th stage LDC encoding in the case that

i. $\mathbf{s}_{(n_{Y(NZ)})}^{(1,n_X)}$ is with at least one non-zero entry,

ii. the vectors $\mathbf{s}_{(n_Y(Z))}^{(1,n_X)}$ of size $1 \times T$, where $n_{Y(Z)} = 1, ..., N_Y$ and $n_{Y(Z)} \neq n_{Y(NZ)}$, are all-zero vectors,

as

$$\mathcal{S}_{n_X}^{Y(i,n_{Y(NZ)})} = \left[\left[\mathbf{s}_{(1)}^{(i,n_X)} \right]^{\mathcal{T}}, ..., \left[\mathbf{s}_{(n_{Y(NZ)})}^{(i,n_X)} \right]^{\mathcal{T}}, ..., \left[\mathbf{s}_{(N_Y)}^{(i,n_X)} \right]^{\mathcal{T}} \right]^{\mathcal{T}},$$

where $i = 1, 2$, and

$$\mathcal{S}_{n_X}^{Y(2,n_{Y(NZ)})} = \mathbf{G}_{LDC}^{(2)} \mathcal{S}_{n_X}^{Y(1,n_{Y(NZ)})}. \tag{E.4}$$

$\mathcal{S}_{n_X}^{Y(2,n_{Y(NZ)})}$ can be further derived as

$$\begin{aligned}\mathcal{S}_{n_X}^{Y(2,n_{Y(NZ)})} &= \mathbf{G}_{LDC}^{(2)}\mathcal{S}_{n_X}^{Y(1,n_{Y(NZ)})} \\ &= \begin{bmatrix} \left[\mathbf{J}_{(1,n_{Y(NZ)})}\mathbf{s}_{(n_{Y(NZ)})}^{(1,n_X)}\right]^{\mathcal{T}}, ..., \\ \left[\mathbf{J}_{(g,n_{Y(NZ)})}\mathbf{s}_{(n_{Y(NZ)})}^{(1,n_X)}\right]^{\mathcal{T}}, ..., \\ \left[\mathbf{J}_{(N_Y,n_{Y(NZ)})}\mathbf{s}_{(n_{Y(NZ)})}^{(1,n_X)}\right]^{\mathcal{T}} \end{bmatrix}^{\mathcal{T}}.\end{aligned} \tag{E.5}$$

Thus,

$$\mathbf{s}_{(n_Y)}^{(2,n_X)} = \mathbf{J}_{(n_Y,n_{Y(NZ)})}\mathbf{s}_{(n_{Y(NZ)})}^{(1,n_X)}, \tag{E.6}$$

where $n_Y = 1, ..., N_Y$ and $1 \leqslant n_{Y(NZ)} \leqslant N_Y$.

Denote the coded symbol vector in the n_Y-th X-time plane after the senond stage LDC encoding in the case that

i. $\mathbf{s}_{(n_{Y(NZ)})}^{(1,n_X)}$ is with at least one non-zero entry,

ii. the vectors $\mathbf{s}_{(n_Y(Z))}^{(1,n_X)}$ of size $1 \times T$, where $n_{Y(Z)} = 1, ..., N_Y$ and $n_{Y(Z)} \neq n_{Y(NZ)}$, are all-zero vectors,

as

$$\mathcal{K}_{n_Y}^{X(2,n_{Y(NZ)})} = \left[\mathbf{s}_{(n_Y)}^{(2,1)}, ..., \mathbf{s}_{(n_Y)}^{(2,N_X)}\right].$$

Using (E.6), $\mathcal{S}_{n_Y}^{X(2,n_{Y(NZ)})}$ can be derived as

$$\begin{aligned}\mathcal{K}_{n_Y}^{X(2,n_{Y(NZ)})} &= \left[\mathbf{s}_{(n_Y)}^{(2,1)}, ..., \mathbf{s}_{(n_Y)}^{(2,N_X)}\right] \\ &= \mathbf{J}_{(n_Y,n_{Y(NZ)})}\left[\mathbf{s}_{(n_{Y(NZ)})}^{(1,1)}, ..., \mathbf{s}_{(n_{Y(NZ)})}^{(1,N_X)}\right],\end{aligned} \tag{E.7}$$

According to (E.7), if both $\left[\mathbf{s}_{(n_{Y(NZ)})}^{(1,1)}, ..., \mathbf{s}_{(n_{Y(NZ)})}^{(1,N_X)}\right]$ and $\mathbf{J}_{(n_Y,n_{Y(NZ)})}$ are full rank, $\left[\mathbf{s}_{(n_Y)}^{(2,1)}, ..., \mathbf{s}_{(n_Y)}^{(2,N_X)}\right]$ is full rank. Since the first stage LDC encoding procedure enables full symbol-wise diversity in its 2-dimensions, $\left[\mathbf{s}_{(n_{Y(NZ)})}^{(1,1)}, ..., \mathbf{s}_{(n_{Y(NZ)})}^{(1,N_X)}\right]$ is guaranteed to be full rank. Thus, in both cases of $N_X < N_Y = T$ and $N_X =$

$T > N_Y$, $rank\left(\left[\mathbf{s}_{(n_{Y(NZ)})}^{(1,1)}, ..., \mathbf{s}_{(n_{Y(NZ)})}^{(1,N_X)}\right]\right) = N_X$ holds. Since $\mathbf{J}_{(a,b)}$ is assumed to be full rank for $a = 1, ..., N_Y$ and $b = 1, ..., N_Y$, and $rank\left(\left[\mathbf{s}_{(n_Y)}^{(2,1)}, ..., \mathbf{s}_{(n_Y)}^{(2,N_X)}\right]\right) = N_X$ holds. Hence,

a. $r_{sd(X)} = N_X$ holds for both cases of $N_X < N_Y = T$ and $N_X = T > N_Y$,

b. $r_{sd(Time)} = N_X$ holds for the case of $N_X = T > N_Y$.

Each X dimension column of the $n_{Y(NZ)}$-th first stage LDC codewords of size $T \times N_X$ must have at least one non-zero element, where $1 \leqslant n_{Y(NZ)} \leqslant N_Y$. Note that the source symbols for the corresponding n_X-th second stage LDC codeword consists of all n_Y-th time dimension columns of N_Y first stage LDC codewords, where $1 \leqslant n_X \leqslant N_X$ and $n_Y = 1, ..., N_Y$. Further, due to the all-zero source elements used, all the N_X time dimension columns of the $n_{Y(Z)}$-th first stage LDC codeword of size $T \times N_X$ are zero columns, where $n_{Y(Z)} \neq n_{Y(NZ)}, 1 \leqslant n_{Y(Z)} \leqslant N_Y$. Thus the number of non-zero source symbols of each second LDC codeword, N_{NZ}, is in the range of $1 \leqslant N_{NZ} \leqslant K$ for the $n_{Y(NZ)}$-th first stage LDC codeword, unless all-zero first stage LDC codewords are involved as source symbols for the second stage LDC encoding. Note that the second stage LDC encoding procedure enables full K-symbol-wise diversity in its 2-dimensions, where K is the maximum number of non-zero symbols of all the n_X-th time dimensions after the first stage LDC encoding procedure, where $n_X = 1, ..., N_X$. Thus,

a. $r_{sd(Y)} = N_Y$ holds for both cases of $N_X < N_Y = T$ and $N_X = T > N_Y$,

b. $r_{sd(Time)} = T$ holds for the case of $N_X < N_Y = T$.

Finally, the conclusion is that in the cases of both $N_X < N_Y = T$ and $N_X = T >$

N_Y, the STF block, constructed using DLD procedure, achieves full symbol-wise diversity order.

■

Appendix F

Proof of theorem and lemma related to ST-CILDC

F.1 Proof of Theorem 6

Proof:

1) This is a straightforward result of the previous discussion in Section 6.4.

2) The number of all possible directional pairs of $\mathbf{M}$ and $\widetilde{\mathbf{M}}$ in $\Upsilon^{(1)}$ and $\Upsilon^{(2)}$ are the same value $N_1 = 2N_a \begin{pmatrix} N_a \\ 2 \end{pmatrix}$. The number of all possible directional pairs of $\mathbf{M}$ and $\widetilde{\mathbf{M}}$ in $\Upsilon^{(3)}$ is $N_2 = 4 \begin{pmatrix} N_a \\ 2 \end{pmatrix} \begin{pmatrix} N_a \\ 2 \end{pmatrix}$.

The number of all possible pairs of $\mathbf{M}$ and $\widetilde{\mathbf{M}}$ is $2N_1 + N_2$.

Providing that that all different directional pairs of $\mathbf{M}$ and $\widetilde{\mathbf{M}}$ are equally probable, the probability of $\Upsilon^{(3)}$ is given by

$$\alpha = \frac{\begin{pmatrix} N_a \\ 2 \end{pmatrix} \begin{pmatrix} N_a \\ 2 \end{pmatrix}}{\begin{pmatrix} N_a \\ 2 \end{pmatrix} \begin{pmatrix} N_a \\ 2 \end{pmatrix} + N_a \begin{pmatrix} N_a \\ 2 \end{pmatrix}}.$$

Note that $\mathbf{R_H}$ is of full rank. Thus,

$$rank \begin{pmatrix} \mathbf{\Lambda}, \\ \left\{ \left(\mathbf{M}, \widetilde{\mathbf{M}} \right) \right\} \in \Upsilon^{(3)} \end{pmatrix} = rank \left(\mathbf{\Psi}_3 \right)$$
$$\leqslant r_d^{(1)} + r_d^{(2)}.$$

■

F.2 Proof of Theorem 7

Proof: $q_i(x)$, where $i = 1, ..., L$, can be derived as

$$q_i(x) = -\frac{\partial \left(\log_a p_i(x) \right)}{\partial \left(\log_a x \right)}$$
$$= -\frac{x}{p_i(x)} \frac{\partial \left(p_i(x) \right)}{\partial x},$$

Thus, $\frac{\partial (p_i(x))}{\partial x} = -\frac{p_i(x) q_i(x)}{x}$.

$w(x)$ can be derived as

$$w(x) = -\frac{\partial \left(\log_a \left(\sum_{i=1}^{L} p_i(x) \right) \right)}{\partial \left(\log_a (x) \right)}$$
$$= -\frac{x}{\sum_{i=1}^{L} p_i(x)} \sum_{i=1}^{L} \frac{\partial \left(p_i(x) \right)}{\partial x} = -\frac{x}{\sum_{i=1}^{L} p_i(x)} \sum_{k=1}^{L} \left(\frac{p_k(x) q_k(x)}{x} \right).$$

Now we derive

$$\begin{aligned}
&\tau_1(x) = w(x) - q_1(x) \\
&= \left(\frac{x}{\sum_{i=1}^{L} p_i(x)} \sum_{k=1}^{L} \left(\frac{p_k(x) q_k(x)}{x} \right) \right) - q_1(x) \\
&= \frac{\sum_{k=2}^{L} \left(p_k(x) \left(q_k(x) - q_1(x) \right) \right)}{\sum_{i=1}^{L} p_i(x)}.
\end{aligned}$$

Note that $p_i(x) > 0$, where $i = 1, ..., L$, and $0 < q_1(x) \leqslant ... \leqslant q_L(x) < +\infty$.

1) If $q_1(x) \neq q_L(x)$, $\tau_1(x) = w(x) - q_1(x) > 0$, and thus $w(x) > q_1(x)$.

2) If $q_1(x) = q_L(x)$, $\tau_1(x) = w(x) - q_1(x) = 0$, and thus $w(x) = q_1(x)$.

Similarly, we may also derive $\tau_L(x) = w(x) - q_L(x)$.

1) If $q_1(x) \neq q_L(x)$, $\tau_1(x) = w(x) - q_L(x) < 0$, and thus $w(x) < q_L(x)$.

2) If $q_1(x) = q_L(x)$, $\tau_1(x) = w(x) - q_1(x) = 0$, and thus $w(x) = q_L(x)$.

Hence,

1) If $q_1(x) \neq q_L(x)$,

$$q_1(x) < w(x) < q_L(x). \tag{F.1}$$

2) If $q_1(x) = q_L(x)$, $q_1(x) = w(x) = q_L(x)$.

It is the time to determine the closeness of $w(x)$ to $q_1(x)$ and $q_2(x)$ in the case of

$q_1(x) \neq q_2(x)$. The closeness between $q_1(x)$ and $w(x)$ is quantified by

$$\begin{aligned}\left|\frac{\tau_1(x)}{q_1(x)}\right| &= \left|\frac{w(x)-q_1(x)}{q_1(x)}\right| \\ &= \left|\frac{\sum_{k=2}^{L}\left(p_k(x)\left(q_k(x)-q_1(x)\right)\right)}{q_1(x)\left(\sum_{i=1}^{L}p_i(x)\right)}\right| \\ &= \left|\sum_{k=2}^{L}\left(\frac{1-\frac{q_k(x)}{q_1(x)}}{\frac{1}{p_k(x)}\sum_{i=1}^{L}p_i(x)}\right)\right|.\end{aligned} \tag{F.2}$$

Similarly, the closeness between $q_L(x)$ and $w(x)$ is quantified by

$$\left|\frac{\tau_L(x)}{q_L(x)}\right| = \left|\frac{w(x)-q_L(x)}{q_L(x)}\right| = \left|\sum_{k=1}^{L-1}\left(\frac{1-\frac{q_k(x)}{q_L(x)}}{\frac{1}{p_k(x)}\sum_{i=1}^{L}p_i(x)}\right)\right|.$$

Now, we can examine the closeness between $q_1(x)$ and $w(x)$ in the case of $x \to +\infty$. Note that $\lim_{x\to+\infty}\left(\frac{p_k(x)}{p_1(x)}\right) = 0$, thus $\lim_{x\to+\infty}\left(\frac{p_1(x)}{p_k(x)}\right) = +\infty$, where $k = 2, ..., L$. We obtain

$$\begin{aligned}&\lim_{x\to+\infty}\left(\frac{1}{p_k(x)}\sum_{i=1}^{L}p_i(x)\right) \\ &= 1 + \lim_{x\to+\infty}\left(\frac{1}{p_k(x)}\sum_{i=2,i\neq k}^{L}p_i(x)\right) + \lim_{x\to+\infty}\left(\frac{p_1(x)}{p_k(x)}\right) \\ &= +\infty,\end{aligned}$$

where $k = 2, ..., L$. Also note that $\exists k, 1 < \lim_{x\to+\infty}\frac{q_k(x)}{q_1(x)} < +\infty$, where $k = 2, ..., L$. Hence,

$$\lim_{x\to+\infty}\left|\frac{w(x)-q_1(x)}{q_1(x)}\right| = \lim_{x\to+\infty}\left|\sum_{k=2}^{L}\left(\frac{1-\frac{q_k(x)}{q_1(x)}}{\frac{1}{p_k(x)}\sum_{i=1}^{L}p_i(x)}\right)\right| = 0.$$

■

Appendix G

A construction of rate-one joint full frequency-time diversity LDC-OFDM

In this section, a joint full frequency-time diversity OFDM design is proposed as the following proposition,

Proposition 3 *The frequency selective channel order is L. Consider a vector with $Q = N_F T$ source symbols of QAM (or PAM, or BPSK, or QPSK) constellation, where $N_F \geqslant L+1$. Assume that the frequency-time LDC codeword is of size $T \times N_F$, where time dimension is of size T, frequency dimension is of size N_F. Assume that there exists a LCP (either LCP-A or LCP-B) encoding matrix Θ of size $Q \times Q$,*

$$\Theta = \begin{bmatrix} 1 & \alpha_1 & \cdots & \alpha_1^{Q-1} \\ 1 & \alpha_2 & \cdots & \alpha_1^{Q-1} \\ \vdots & \vdots & \ddots & \vdots \\ 1 & \alpha_Q & \cdots & \alpha_Q^{Q-1} \end{bmatrix},$$

where α_q, $q = 1, ..., Q$, is defined in [72, 126]. Define LDC encoding matrix as $\mathbf{G}_{LDC} = \Theta$. Then this FT-LDC design achieves full joint frequency-time diversity under arbitrary frequency-time correlation. The maximal achievable diversity order

is $T(L+1)$.

Proof:

Denote the set with all the possible symbol vectors of QAM (or PAM, or BPSK, or QPSK) constellation as $\mathcal{C}$.

Denote

$$\Theta = \left[\theta_1^{\mathcal{T}}, ..., \theta_Q^{\mathcal{T}}\right]^{\mathcal{T}},$$

where θ_q is the q-th row of Θ.

Since LCP encoding matrix Θ is able to support that

$$\left[\mathbf{G}_{LDC}\left(\mathbf{s}-\widetilde{\mathbf{s}}\right)\right]_{q,1} \neq 0,$$

where $q = 1, ..., Q$, $(\mathbf{s}-\widetilde{\mathbf{s}}) \neq \mathbf{0}$, $\{\mathbf{s}, \widetilde{\mathbf{s}}\} \in \mathcal{C}$

Thus, for any $(\mathbf{s}-\widetilde{\mathbf{s}}) \neq \mathbf{0}$, $\{\mathbf{s}, \widetilde{\mathbf{s}}\} \in \mathcal{C}$, the following holds

$$\left[\mathbf{G}_{LDC}(\mathbf{s}-\widetilde{\mathbf{s}})\right]_{q,1} \neq 0$$

for any $q = 1, ..., Q$.

According to Theorem 3, this LDC-OFDM achieves full joint frequency-time diversity under arbitrary frequency-time correlation. If the joint frequency-time channel is full rank, this LDC-OFDM achieves diversity order $T(L+1)$. ■